

**SYNTHESIS, PHOTOCHEMICAL AND
PHOTOPHYSICAL PROPERTIES OF A SERIES OF
FREE BASE AND METALLOPORPHYRIN METAL
PENTCARBONYL COMPLEXES**

By

Karl McDonnell, B.Sc

**A Thesis presented to Dublin City University for the degree of Doctor of
Philosophy**

Supervisor: Prof. Conor Long and Dr. Mary Pryce

School of Chemical Sciences

Dublin City University

August 2004

To my parents

I hereby certify that this material, which I now submit for assessment on the programme of study leading to award of Doctor of Philosophy by research thesis, is entirely my own work and has not been taken from the work of others, save and extent that such work has been cited and acknowledged with the text of my work

Signed Karl McDonnell

Karl McDonnell

I D number 99145308

Date 25/09/06

Acknowledgements

I would like to thank my supervisors Prof. Conor Long and Dr. Mary Pryce for all their help and advice throughout the course of my research. Without the constant support and help from them, this thesis might not have come about. I appreciate the amount of time and effort that went into reading and correcting this work.

A huge thank you must go to all the technicians at DCU: Mick, Damien, Maurice, Veronica, Ann, Ambrose, Vinny, John, and Mary. Thank you for all your help. Special thanks to Vinny and Damien for organising all the social events during my time there. It made it all the more enjoyable.

From the first year of my Ph.D., the group was always easing going and very friendly. From the people who were there before me to those who joined after, life on our side of the lab was always interesting. Thanks to Peter, Kieran, Davnat, Jennifer, Kevin, Jonathon, Claire, and Mohammad. A special thanks to Peter and Jonathon for opening my mind to the joys of reggae and Celtic, and Kieran for the games of golf. Thanks to all the other students who were there: Ray, Rob, Declan, Cathal, Ger, Marco, Stefania, Adrian, Wes, Bill, Noel, Noel B, Shaneo, Tommy, Eimear, Eadaoin, Kathleen, Colm, Michaela, Ian, Bernhard, and Andy.

Thank you to Amanda, whom has given so much help in finishing this write-up, which was harder than I could have imagined. Thank you.

Finally, a huge thanks to my family, I now have a job so you can stop making fun of me and especially my parents who have been so patient and understanding throughout all of this.

Abstract

This thesis contains details of a study of the synthesis, characterisation, photochemical and photophysical properties of a series of novel free base porphyrins, metalloporphyrins and their complexes with metal carbonyl fragments. The systems employed in this study have potential use in energy/electron transfer processes.

Chapter 1 contains an introduction to the chemistry of porphyrins, metalloporphyrins and their excited states as well as highlighting the main principles of photochemistry and the bonding in metal carbonyl complexes.

In chapter 2 the photochemistry of free base porphyrins and metalloporphyrins, when complexed to metal centres, is discussed along with literature relevant to this topic.

The photochemistry (both time-resolved and steady state) and photophysics (lifetimes, fluorescence spectra and quantum yield) measurements of *mono* 4-pyridyl-10,15,20-triphenyl porphyrin (MPyTPP) and its $W(CO)_5$ and $Cr(CO)_5$ complexes are discussed in chapter 3. In each case the triplet and singlet excited state photochemistry is found to be located on the porphyrin moiety. The presence of the $M(CO)_5$ group altered the electronic characteristics of the complexes when compared to the uncomplexed free base porphyrin.

Chapter 4 describes the photochemistry and photophysics of porphyrins when di-substituted with $W(CO)_5$ and $Cr(CO)_5$ moieties, which were produced from *cis*-5,10-di-4-pyridyl-15,20-diphenyl porphyrin (*cis*-D₁PyD₁PP). Similarly to the *mono*-complexed analogues the results obtained suggest that the excited state photochemistry was again centred on the porphyrin component. Changes observed for the di-complexed porphyrins are similar to those of the *mono*-complexed porphyrins except that the shifts are increased due to the presence of the two metal carbonyl units.

The work presented in chapter 5 concerns the metalloporphyrins, $ZnMPyTPPW(CO)_5$ and $ZnMPyTPPCr(CO)_5$. Complexation of Zn to the centre of a porphyrin dramatically alters the electronic properties of the porphyrin. The effect of the $M(CO)_5$ unit on the zinc porphyrin complexes was investigated using photochemical and photophysical techniques. The results are compared to zinc tetraphenyl porphyrin (ZnTPP) and ZnMPyTPP because ZnMPyTPP polymerises through co-ordination of the N atom of the pyridine to the Zn(II) centre.

In chapter 6 the various characterisation methods and experimental conditions for the synthesis and analysis of all complexes are described. Complexes and ligands were characterised by a range of spectroscopic methods such as NMR, IR and UV/Vis.

Table of Contents:

1.	Introduction to porphyrins, metalloporphyrins and bonding in organometallic compounds	
1.1	Photosynthesis	2
1.2	Photochemical and photophysical pathways	6
1.3	Porphyrins	9
1.3.1	Introduction to porphyrins and metalloporphyrin	9
1.3.2	Excited states of porphyrins	13
1.3.3	Porphyrins as light harvesters in an antenna unit	15
1.4	Bonding in organometallic compounds	17
1.4.1	Stability of organometallic compounds	17
1.4.2	The nature of bonding in metal-carbonyl complexes	18
1.5	Bibliography	20
2.	Literature Survey on the Photochemistry and Photophysics of Porphyrin and Metalloporphyrin Complexes and Arrays	
2.1	Introduction	23
2.2	Introduction to the photophysical and photochemical properties of tetra aryl porphyrins and metalloporphyrins	24
2.3	The photophysical and photochemical effects of porphyrins due to co-ordination of peripherally linked transition metal centers	33
2.4	Supramolecular assemblies of porphyrins incorporating metal and organic linkages	45
2.5	Conclusion	54
2.6	Bibliography	55

3.	5-<i>mono</i> 4-pyridyl 10, 15, 20 triphenyl porphyrin and its tungsten and chromium pentacarbonyl complexes	
	- Results and discussion	
3 1	Introduction	62
3 2	UV-vis studies of 5-<i>mono</i>-4-pyridyl 10,15,20-triphenyl porphyrin and its pentacarbonyl complexes	
	M(CO)₅ (M = Cr or W)	64
3.2	Infrared studies of 5-<i>mono</i>-4-pyridyl 10,15,20-triphenyl porphyrin and its pentacarbonyl complexes	
	M(CO)₅ (M = Cr or W)	67
3 3	¹H NMR spectrum of 5-<i>mono</i>-4-pyridyl 10,15,20-triphenyl porphyrin and its pentacarbonyl complexes	
	M(CO)₅ (M = Cr or W)	69
3.5	Steady state photolysis experiments monitored in the UV-vis	70
	3 5 1 SSP of MPyTPPW(CO) ₅ under 1 atm of CO	70
	3 5 2 SSP of MPyTPPW(CO) ₅ under 1 atm of Ar	72
	3 5 3 SSP of MPyTPPCr(CO) ₅ under 1 atm of CO	74
	3 5 4 SSP of MPyTPPCr(CO) ₅ under 1 atm of Ar	76
	3 5 5 Discussion of results	77
3.6	Steady State photolysis monitored in by Infrared spectroscopy	80
	3 6 1 Steady state photolysis of Cr(CO) ₆ in the presence of triphenylphosphine	81
	3 6 2 Steady state photolysis of MPyTPPM(CO) ₅ with PPh ₃	82
3.7	Fluorescence studies of 5-<i>mono</i>-4-pyridyl 10,15,20-triphenyl porphyrin and its M(CO)₅ complexes M = W or Cr	84
	3 7 1 Emission spectra and quantum yields of MPyTPP and its M(CO) ₅ complexes M = W or Cr	84
	3 7 2 Fluorescence lifetimes of MPyTPPW(CO) ₅ and MPyTPPCr(CO) ₅	86
	3 7 3 Discussion of results	88
3 8	Laser Flash Photolysis of MPyTPP and its M(CO)₅ complexes M = W or Cr	91
	3 8 1 Laser flash photolysis of MPyTPPW(CO) ₅ at 532 nm under 1 atmosphere of CO/Ar	91
	3 8 2 Laser flash photolysis of MPyTPPCr(CO) ₅ at 532 nm under 1 atmosphere of CO/Ar	96
	3 8 3 Discussion of results	101

3.9	Conclusion	107
3.10	Bibliography	111
4.	(5-<i>mono</i>-4-pyridyl 10, 15, 20-triphenyl porphyrinato) zinc(II) tungsten and chromium pentacarbonyl complexes - Results and discussion	
4.1	Introduction	115
4.2	UV-vis studies of (5- <i>mono</i> -4-pyridyl 10,15,20-triphenyl porphyrinato) zinc(II) and its pentacarbonyl complexes $M(CO)_5$ (M = Cr or W)	117
4.3	Infrared studies of (5- <i>mono</i> -4-pyridyl 10,15,20-triphenyl porphyrinato) zinc(II) and its pentacarbonyl complexes $M(CO)_5$ (M = Cr or W)	121
4.4	1H NMR spectrum of 5- <i>mono</i> -4-pyridyl 10,15,20-triphenyl porphyrinato) zinc(II) and its pentacarbonyl complexes $M(CO)_5$ (M = Cr or W)	123
4 5	Steady state photolysis experiments monitored in the UV-vis	125
4 5 1	Steady state photolysis of $ZnMPyTPPW(CO)_5$ under 1 atm of CO	125
4 5 2	Steady state photolysis of $ZnMPyTPPW(CO)_5$ under 1 atm of Ar	127
4 5 3	Steady state photolysis of $ZnMPyTPPCr(CO)_5$ under 1 atm of CO	129
4 5 4	Steady state photolysis of $ZnMPyTPPCr(CO)_5$ under 1 atm of Ar	131
4 5 5	Discussion of results	133
4.6	Fluorescence studies of (5- <i>mono</i> -4-pyridyl 10,15,20-triphenyl porphyrinato) zinc(II) and its pentacarbonyl complexes $M(CO)_5$ (M = Cr or W)	136
4 6 1	Emission spectra and quantum yields of $ZnMPyTPP$ and its $M(CO)_5$ complexes (M = W or Cr)	136
4 6 2	Fluorescence lifetimes of $ZnMPyTPPW(CO)_5$ and $ZnMPyTPPCr(CO)_5$	139
4 6 3	Discussion of results	141

4 7	Laser Flash Photolysis of ZnMPyTPP M(CO)₅ complexes (M = Cr or W)	143
4 7 2	Laser flash photolysis of ZnMPyTPPW(CO) ₅ at 532 nm under 1 atmosphere of CO/Ar	143
4 7 3	Laser flash photolysis of ZnMPyTPPCr(CO) ₅ at 532 nm under 1 atmosphere of CO/Ar	148
4 7 4	Discussion of results	153
4 8	Conclusion	158
4.9	Bibliography	162
5.	5, 10 - cis 4 – Dipyriddy - 15, 20 - diphenylporphyrin and its tungsten and chromium pentacarbonyl complexes - Results and discussion	
5 1	Introduction	166
5.2	UV-vis studies of 5, 10-dt-4, pyridyl 15, 20-diphenyl porphyrin and its pentacarbonyl complexes M(CO)₅ (M = Cr or W)	168
5.3	Infrared studies of 5, 10-dt-4, pyridyl 15, 20-diphenyl porphyrin and its pentacarbonyl complexes M(CO)₅ (M = Cr or W)	170
5 4	¹H NMR spectrum of 5, 10-dt-4, pyridyl 15, 20-diphenyl porphyrin and its pentacarbonyl complexes M(CO)₅ (M = Cr or W)	171
5 5	Steady state photolysis experiments monitored in the UV-vis	172
5 5 1	Steady state photolysis of <i>cis</i> -D ₁ PyD ₁ PP(W(CO) ₅) ₂ under 1 atm of CO	172
5 5 2	Steady state photolysis of <i>cis</i> -D ₁ PyD ₁ PP(W(CO) ₅) ₂ under 1 atm of Ar	174
5 5 3	Steady state photolysis of <i>cis</i> -D ₁ PyD ₁ PP(Cr(CO) ₅) ₂ under 1 atm of CO	175
5 5 4	Steady state photolysis of <i>cis</i> -D ₁ PyD ₁ PP(Cr(CO) ₅) ₂ under 1 atm of Ar	176
5 5 5	Discussion of results	177
5.6	Fluorescence studies of 5, 10 cis 4-dipyriddy 15, 20-diphenyl porphyrin and its M(CO)₅ complexes M = W or Cr	179

5 6 1	Emission spectra and quantum yields of 5, 10 <i>cis</i> 4-dipyridyl 15, 20-diphenyl porphyrin and its $M(\text{CO})_5$ complexes ($M = \text{W}$ or Cr)	179
5 6 2	Fluorescence lifetimes of <i>cis</i> -D ₁ PyD ₁ PP($\text{W}(\text{CO})_5$) ₂ and <i>cis</i> -D ₁ PyD ₁ PP($\text{Cr}(\text{CO})_5$) ₂	181
5 6 3	Discussion of results	183
5 7	Laser Flash Photolysis of 5, 10 <i>cis</i> 4-dipyridyl 15, 20-diphenyl porphyrin and its $M(\text{CO})_5$ complexes $M = \text{W}$ or Cr	185
5 7 1	Laser flash photolysis of <i>cis</i> -D ₁ PyD ₁ PP($\text{W}(\text{CO})_5$) ₂ at 532 nm under 1 atmosphere of CO/Ar	185
5 7 2	Laser flash photolysis of <i>cis</i> -D ₁ PyD ₁ PP($\text{Cr}(\text{CO})_5$) ₂ at 532 nm under 1 atmosphere of CO/Ar	189
5 7 3	Discussion of results	193
5 8	Conclusion	196
5.9	Bibliography	198

6. Experimental

6 1	Reagents	201
6.2	Equipment	202
6 2 1	Infrared spectroscopy	202
6 2 2	Absorption spectroscopy	202
6 2 3	Nuclear Magnetic Resonance spectroscopy	202
6 2 4	Emission spectroscopy	202
6.3	Determination of extinction coefficients	204
6.4	Time Correlated Single Photon counting (TCSPC) techniques nanosecond time resolved emissions spectroscopy	205
6.5	Laser flash photolysis	207
6 5 1	Preparation of degassed samples for laser flash photolysis	207
6 5 2	Laser Flash Photolysis with UV-Vis Detector Apparatus	207

6 6	Synthesis	210
6 6 1	Synthesis of free base porphyrins	215
6 6 2	Synthesis of ZnTPP	216
6 5 3	Synthesis of ZnMPyTPP	217
6 6 4	Synthesis of MPyTPPW(CO) ₅	218
6 6 5	Synthesis of MPyTPPCr(CO) ₅	219
6 6 6	Synthesis of <i>cis</i> -D ₁ PyD ₁ PP(W(CO) ₅) ₂	220
6 6 7	Synthesis of <i>cis</i> -D ₁ PyD ₁ PP(Cr(CO) ₅) ₂	221
6 6 8	Synthesis of ZnMPyTPPW(CO) ₅	222
6 6 9	Synthesis of ZnMPyTPPCr(CO) ₅	223
6 6 10	Synthesis of <i>trans</i> -D ₁ PyD ₁ PP(W(CO) ₅) ₂	224
6 6 11	Synthesis of 3-pyridyl porphyrin	225
6 6 12	Synthesis of ferrocene-pyridine porphyrin	226
6 6 13	Synthesis of tetra-phenyl porphyrin Cr(CO) ₃	226
6 6 14	Synthesis of zinc tetraphenyl Cr(CO) ₃ porphyrin	227
6.7	Bibliography	228
Appendix A: Extinction Coefficients		229

Abbreviations

ATP	Adenosine triphosphate
bipy	bipyridyl
Chl	Chlorophyll
<i>cis</i> -DiPyDiPP	<i>cis-di</i> -pyridyl <i>di</i> -phenyl porphyrin
CT	Charge transfer
FNR	Ferredoxin NADP ²⁺ Reductase
HOMO	Highest occupied molecular orbital
ISC	Intersystem crossing
LF	Ligand field
LMCT	Ligand to metal charge transfer
MLCT	Metal to ligand charge transfer
MPyTPP	<i>Mono</i> pyridyl triphenyl porphyrin
NADP ²⁺	Nicotinamide adenine dinucleotide phosphate
PQ	Palisade parenchyma
PS	Photosystems
Q	Quinone
STE _N	Singlet – Triplet energy transfer
TPP	Tetra phenyl porphyrin
TPyMPP	<i>tri</i> -phenyl <i>mono</i> pyridyl porphyrin
TPyP	Tetra pyridyl porphyrin
TTE _N	Triplet – Triplet energy transfer
ttpy	4 – tolyl 2, 2, 6, 2,terpyridyl
Z	Tyrosine residue
TMPyP	Tetra methyl pyridyl porphyrin
ZnMPyTPP	Zinc <i>mono</i> pyridyl triphenyl porphyrin
ZnOEP	Zinc octa ethyl porphyrin
ZnTPP	Zinc tetra phenyl porphyrin

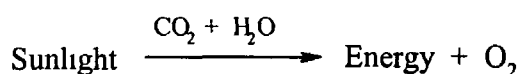
Chapter 1

Introduction to Porphyrins, Metalloporphyrins and Bonding in Organometallic Chemistry

1.1 Photosynthesis

Photosynthesis is one of the most important fundamental photochemical processes affecting all life on earth. This process involves the conversion of sunlight, water and CO₂ to energy and O₂ (see Eqn 1.1). The harvesting and conversion of sunlight to energy in plants and photosynthetic bacteria is carried out in a complex sequence of events in which porphyrins and porphyrin related molecules play an important role.

Eqn 1.1



Photochemists and photobiologists have been studying photosynthesis for over 150 years. This work began with the investigation of the luminescence of chlorophyll (a porphyrin light harvester in plants) in 1834.¹ Since then photochemical and photophysical studies of porphyrins and metalloporphyrins have sought to understand how chlorophyll performs this complex task of harvesting and converting sunlight into plant energy.

In addition to being a source of energy, photosynthesis also regulates the composition of our atmosphere. During photosynthesis CO₂ is removed from the atmosphere and O₂ is added (Eqn 1.1). The CO₂ in the atmosphere is recycled every 300 years while O₂ is recycled every 2000 years.

The organisms, which carry out photosynthesis, can be classified into two distinct groups: (i) those that reduce CO₂ to carbohydrates but cannot oxidise water to O₂ and (ii) those that primarily reduce O₂ to water. Photosynthetic units consist of distinct regions. The first is the region where light harvesting occurs. This is known as the antenna and consists of an array of chlorophyll molecules and accessory pigments that capture the solar irradiation. The second region is the reaction centre where the excitation energy is processed.

The primary photoprocess can occur in two distinct photochemical reaction centres namely photosystems I and photosystems II (PS_I and PS_{II}). An electron transport chain links these reaction centres. In 1960 Hill and Bendall proposed a scheme known as the 'Z Scheme' (see Figure 1.1) which indicated the manner by which these two processes operate²

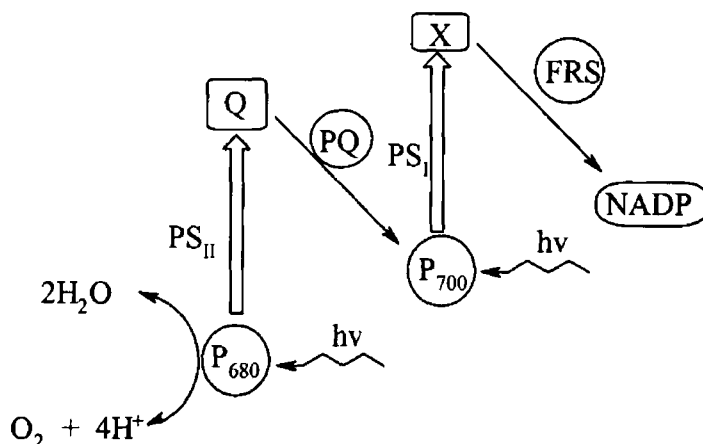


Figure 1.1 Z Scheme for photosynthesis

This remains the accepted scheme for photosynthesis. In Figure 1.1 the photochemical reaction centres I and II are shown as P₇₀₀ and P₆₈₀, where the subscripts indicate the longest wavelength absorption maxima for each centre. Each system contains an array of antenna pigments of which chlorophyll is the principal component, usually 300 molecules of chlorophyll are present for each reaction centre. The two components are linked via a series of electron acceptors and carriers indicated as Q and X in Figure 1.1. The identity of these components is still unknown.

The dihydroporphyrins (Chl) are the main photoactive component of the reaction centres. They contain Mg(II) ions at the centre and a hydrophobic phytyl chain in one of the pyrrole rings (see Figure 1.2). There are two types of chlorophyll present at the reaction centre: Chl-a and Chl-b. Chl-a is the major pigment and is present in all photosynthetic organisms that evolve O₂.

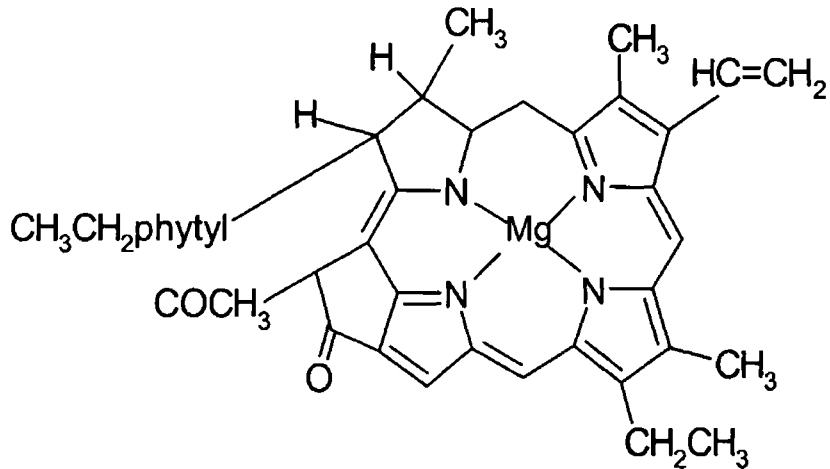


Figure 1 2 Structure of chlorophyll a

The following is the proposed sequence of reactions in photosynthesis

- (i) light is harvested by the chlorophyll antennae,
- (ii) primary charge separation in photosystems I and II,
- (iii) charge transfer/electron flow between photosystems I and II,
- (iv) water oxidation in the reaction centre of photosystem II,
- (v) fuel formation in the reaction centres of photosystems I

The overall reaction can be summarised as follows Upon illumination of the chloroplast the chlorophyll and carotenoid antennae absorb the light The excitation energy migrates efficiently through an array of chlorophyll and pigment molecules until it reaches a low energy trap site where it is converted into chemical energy (Figure 1 3) This movement of excitation energy is known as exciton migration

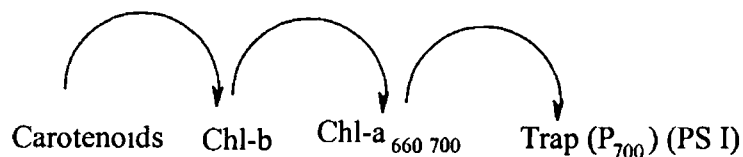


Figure 1 3 Heterogeneous energy transfer between different types of pigments

Initially the photoexcited electron is channelled to P₆₈₀ of PS_{II}. A one-electron transfer to a molecule of chlorophyll from the reaction centre then occurs (special pair). This electron subsequently migrates to P₇₀₀, and PS_I NADP²⁺ is oxidised to NADPH₂. ATP formed from the reactions of PS_I and PS_{II} reduces CO₂ to carbohydrate.

At the PS_{II} reaction centre O₂ is produced from the reduction of CO₂. The energy of the photon produced is sufficient to achieve a charge separation to yield Z⁺, which is reduced by Mn. Mn clusters act as a store for the positive charge. After four cycles the Mn cluster possesses a +4 charge. By receiving 4 electrons from water it returns to the neutral state and two water molecules are oxidised to a molecule of O₂. No definite structure is known for the Mn cluster but it is a powerful oxidising agent capable of oxidising two molecules of water.

In 1984 Deisenhofer *et al* reported the isolation and crystal structure of part of the bacteria involved in photosynthesis, which led to a greater possibility in understanding the photosynthetic process.^{3 4} Currently the structure of PS_I and PS_{II} are poorly defined and hence it is impossible to determine the precise orientation of each component in the overall system.

1.2 Photochemical and photophysical pathways in metal complexes

As discussed in the previous section, photosynthesis involves the absorbance of light and the excitation of electrons. The excited electron follows a reaction pathway in the conversion of sunlight to energy, which has been extensively investigated^{3,4}. Scientists have been attempting to mimic this process for many years and in doing so, have designed a schematic representation of possible excited state pathways which can occur upon absorption of a photon by certain metal complexes. These excited states, and their possible interconversion pathways, are shown in the modified Jablonski diagram (Figure 1.4)

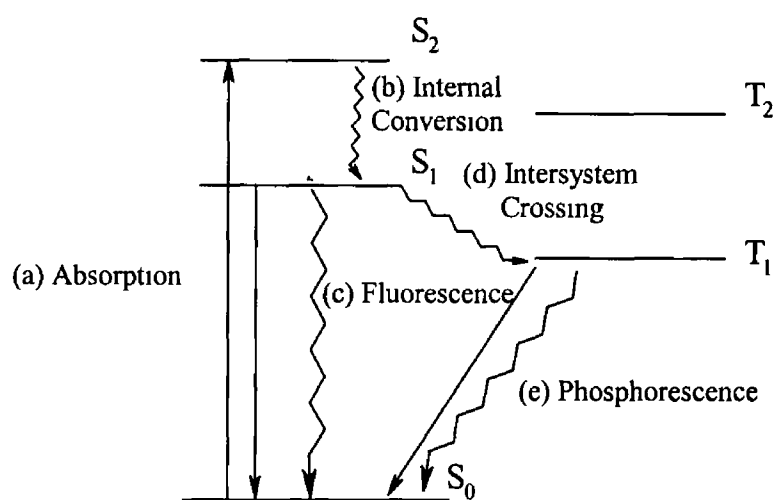


Fig 1.4 Jablonski energy level diagram — radiative transition
~~~~ radiationless transitions

Electronic excited states in metal complexes dissipate energy through a combination of two processes, (i) radiative transitions and (ii) non-radiative transitions. By measuring the quantum yield of these transitions, the relative importance of the two processes can be determined.

The absorption of light by the molecule is the first step, (a) in the Jablonski diagram. This causes excitation from the ground state to an upper singlet excited state  $S_2$ , if the ground state is singlet in character. This is followed by rapid non-radiative transition to the lowest singlet excited state,  $S_1$ , in a process known as internal conversion, step (b). Internal conversion is a radiationless transition from a higher excited state to the lowest energy excited state of the same multiplicity, i.e.  $S_n \rightarrow S_1$  or  $T_n \rightarrow T_1$ . From the lowest energy singlet excited state two decay pathways are possible, the molecule can undergo non-radiative or alternatively radiative decay. Non-radiative relaxation can occur by means of vibrational relaxation of the excited species through collisional interaction with the surrounding medium or by intersystem crossing with states of different multiplicity, step (d). Intersystem crossing is a transition from singlet to triplet states or vice versa and is possible because of spin inversion, i.e.  $S_1 \rightarrow T_1$  or  $T_1 \rightarrow S_0$ . Intersystem crossing must adhere to certain selection rules, which depend on the magnitude of the spin orbit coupling.  $S_1 \rightarrow T_1$  takes place either by direct spin orbit coupling of  $S_1$  to higher vibrational levels of  $T_1$  or by spin orbit coupling to a higher state  $T_n$  followed by rapid internal conversion to  $T_1$ . The rate of intersystem crossing is increased as the magnitude of spin orbit coupling increases. Spin orbit coupling increases in going down a group and this effect is known as the heavy atom effect (see Section 1.3).

In contrast to internal conversion and intersystem crossing, fluorescence (step c) and phosphorescence (step e) are radiative processes, i.e. they result in the emission of a photon of light. These processes are commonly referred to as luminescence. From Figure 1.4, fluorescence is deactivation from a singlet excited state while phosphorescence is deactivation from a triplet excited state. Because a portion of the energy acquired in the absorption process is dissipated via radiationless deactivation, the energy of the emitted radiation is always lower than that of the absorbed radiation, i.e. the emission occurs at a longer wavelength, than the wavelength of the absorbed photon.

The shift in the  $\lambda_{\max}$  of the emission spectra with respect to the  $\lambda_{\max}$  of the absorption spectra is known as Stoke's shift (see Figure 1.5). In general the Stoke's shift is large when the geometry of the excited state is significantly different to that of the ground

state. The shift in absorption increases with emission differences between the geometries of the ground and excited states. The energy of the excited state molecule decreases and fluorescence is shifted to longer wavelengths. The fluorescence spectrum is frequently a mirror image of the absorption spectrum and this is because the shape of the potential energy surface for the excited state vibrational frequencies and the ground state vibrational frequencies are similar.

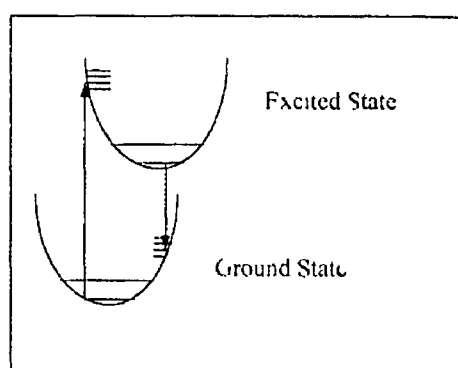


**Figure 1.5** Diagrammatic representation of the Stokes' shift<sup>5</sup>

The triplet state of a complex is populated *via* intersystem crossing, and phosphorescence corresponds to a transition from the lowest excited triplet state  $T_1$  to the ground state,  $S_0$ . It is the reverse of the  $S_0 \rightarrow T_1$  absorption spectrum, which of course is spin forbidden and therefore has low intensity. The  $T_1$  state is below the  $S_1$  state and phosphorescence occurs at longer wavelengths than fluorescence due to the low energy spin parallel nature of the triplet state. The lifetime of the phosphorescence state is quite long and therefore radiationless transitions are important in its deactivation.

## 1.3 Porphyrins

### 1.3.1 Introduction to porphyrins and metalloporphyrins

The basic structure of porphyrins is known as a porphine (Figure 1.6), it consists of four pyrrole rings linked by four methine bridges (the carbon atom at the centre of this bridge is said to be in the *meso* position). Kuster first proposed the structure in 1912 but porphyrins were not isolated or structurally characterised until 1928.<sup>6</sup> The macrocycle consists of twenty carbon atoms and four nitrogen atoms and because of conjugation of the double bonds produce an intensely coloured compound (see Figure 1.6). The porphyrin macrocycle is an aromatic system consisting of 22  $\pi$  electrons, however only eighteen of these are involved in the delocalisation pathway and so obeying Huckel's rule for aromaticity ( $4n + 2 \pi$  electrons).<sup>7</sup>

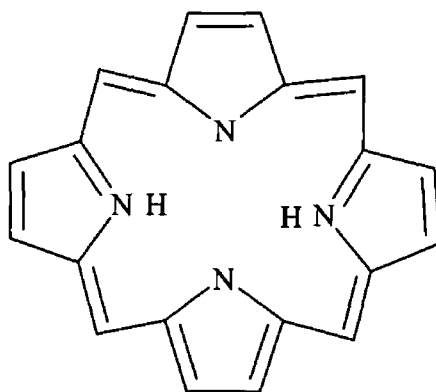


**Figure 1.6 Structure of the porphine parent ligand**

As a result of these features porphyrins have unique spectral properties such as the ability to absorb light in the visible region of the spectrum and the ability to convert this light to physical or chemical energy (photosynthesis). Substitution at the *meso* position forms porphyrins known as *meso*-substituted porphyrins. These are generally aryl porphyrins and are usually synthetically made, the most common examples being tetraphenylporphyrins (TPP) and tetrapyrrolylporphyrins (TPyP).<sup>8</sup>

Free base porphyrins contain two weakly acidic protons on the central nitrogens ( $pK_a \approx 16$ ) These are readily displaced by treatment with various metals such as Zn, Mg, Fe, forming metalloporphyrins (Reaction 1.2)

**Reaction 1.2**



The  $^1H$  NMR signal for these inner N-H protons are diamagnetically shifted to high field below that of TMS from  $-2$  to  $-4$  ppm because of the aromatic ring current which shields them when inside the macrocycle Upon metallation these signals are no longer observed

The most distinctive characteristic of porphyrins are their UV-vis spectral features UV-vis spectra also demonstrate the second major difference between free base porphyrins and metalloporphyrins Both types of porphyrins have two distinct regions in the UV-vis spectrum The first region occurs between  $410 - 430$  nm and is known as the Soret band or B band It is the origin of the lowest excited singlet state and has a molar extinction coefficient of  $\epsilon = 10^5 \text{ dm}^3 \text{ mol}^{-1} \text{ cm}^{-1}$

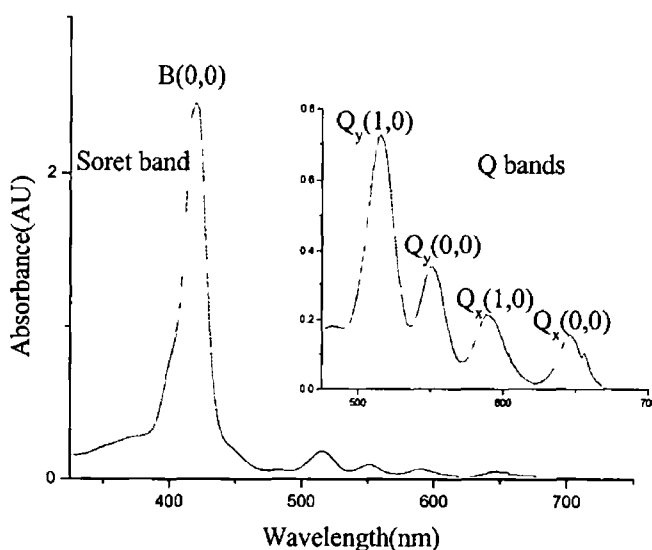


**Figure 1.7 UV-vis spectrum showing the Soret band and Q bands ( $\times 10$ ) of free base porphyrin, (TPP)**

At lower energy, i.e. at wavelengths greater than 470 nm the Q bands are observed. They appear between 470 – 660 nm for free base porphyrins (see Figure 1.7) and between 500 – 600 nm for metalloporphyrins. Free base porphyrins have four Q bands because they possess  $D_{2h}$  symmetry. Upon formation of the metalloporphyrin the symmetry changes to  $D_{4h}$  and the number of Q bands is reduced from four to two (see Figure 1.8).

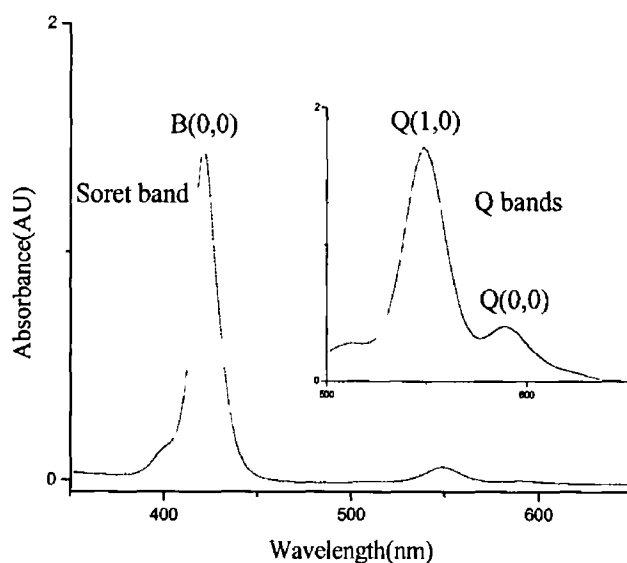


**Figure 1.8 UV-vis spectrum of the Soret and Q bands ( $\times 10$ ) of a typical metalloporphyrin (ZnTPP)**

In the case of a metalloporphyrin the lowest energy band is the electronic origin  $Q(0,0)$  of the lowest energy excited singlet state. The higher energy band is  $Q(1,0)$  and is a vibrational satellite of  $Q(0,0)$ . When the metal is removed the  $Q(0,0)$  band is split into  $Q_x(0,0)$  and  $Q_y(0,0)$  which also have vibrational satellites of their own i.e.  $Q_x(1,0)$  and  $Q_y(1,0)$ .

The four orbital model as developed by Gouterman *et al* is used to describe the formation of the UV-vis bands<sup>9,10,11</sup>. Using this model for the porphine ring the ground state configuration of  ${}^1A_{1g}$  is the highest occupied molecular orbital (HOMO). The

lowest unoccupied molecular orbital  $e_g(\pi^*)$  is degenerate. The lowest singlet excited state configuration from this is  ${}^1(a_{2u}, e_g)$  and  ${}^1(a_{1u}, e_g)$ , see Figure 1.9. In metalloporphyrins the symmetry of the molecule is such that  ${}^1(a_{2u}, e_g)$  and  ${}^1(a_{1u}, e_g)$  transitions are degenerate and this causes strong interaction between them. When the transition dipoles of the two configurations nearly cancel, the resulting resonance yields the weak  $Q(0,0)$  band, when the transition dipoles of the two configurations add, they form the intense Soret or  $B(0,0)$  band. Soret bands are strongly allowed excited states while  $Q$  bands are quasi-forbidden. In free base porphyrins the presence of the central protons lift the degeneracy of the  $e_g(\pi^*)$  orbitals, which causes the  $Q(0,0)$  band to split into  $Q_x(0,0)$  and  $Q_y(0,0)$ .

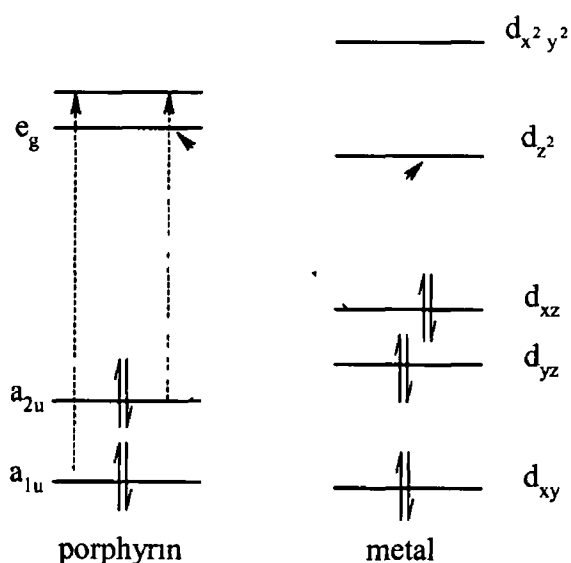


**Figure 1.9 Energy diagram of the porphyrin ring and metal  $d$  orbitals**

### 1.3.2 Excited states of porphyrins

Regular porphyrins are defined as those whose absorption and emission spectra are determined primarily by the  $\pi$  electrons of the porphyrin ring. Emission of regular free base porphyrins and closed shell metalloporphyrins are typically  $\pi^*-\pi$  in origin i.e. porphyrin based excited states, (fluorescence occurs from  $^1S(\pi-\pi^*)$  while phosphorescence occurs from  $^3T(\pi-\pi^*)$ ). Irregular porphyrins are porphyrins, which contain metals with an opened shell of valence electrons, thereby allowing the metal to interact with the porphyrin in the excited state (see Figure 1.9) <sup>2</sup>

The various transitions in the time resolved spectra possible for metalloporphyrins are (i)  $\pi-\pi^*$ , (ii) d-d, (iii)  $\pi^*-\text{d}$  CT and (iv)  $\text{d}-\pi^*$  CT <sup>12</sup>. Only the  $\pi-\pi^*$  transitions are possible for free base porphyrins as they do not contain a central metal ion. These transitions show distinct spectral features, which can be used to help explain the photophysical and photochemical behaviour of porphyrins or metalloporphyrins.

- (i)  $\pi-\pi^*$  transitions - these transitions result from the delocalised  $\pi$  system in free base and closed shell metalloporphyrins. They are identifiable by the following features, <sup>13,14</sup> (a) net bleaching in the Soret band, (b) net bleaching of the Q bands with TPP complexes showing a new absorption band between 450 and 650 nm, (c) some complexes show the presence of two absorption peaks between 700 and 900 nm that may differ for triplet and singlet states.
- (ii)  $\text{d}-\pi^*$  or MLCT transitions (see Figure 1.7) - these are transitions that can occur between the highest occupied d-orbital on the metal and the lowest unoccupied orbital,  $e_g(\pi^*)$  on the porphyrin. Once more they are recognisable by the following features, <sup>13,14</sup> (a) possible new absorption lying between the bleedings in the Soret and the visible bands, (b) broad absorption to the low energy side of the Q - bleaching.
- (iii)  $\pi^*-\text{d}$  or LMCT transitions (see Figure 1.9) - where the transition are now from the highest occupied orbital,  $^1A_{1g}$ , on the porphyrin and the lowest unoccupied d-orbital on the metal.

- (iv) d-d transitions – promotion of d electrons between the d-orbital manifold. These transitions are formed by deactivation of higher energy states and are similar in appearance but red shifted from that of  $\pi$ - $\pi^*$  transitions because the porphyrin is in the ground state  $((a_{1u})^2(a_{2u})^2)$  and the d-d excited state will be the normal four orbital  $\pi$ - $\pi^*$  transition.

These transitions are allowed in metalloporphyrins while in free base porphyrins the  $\pi$ - $\pi^*$  transitions only, are allowed.

The singlet and triplet states formed following irradiation are sufficiently long-lived to permit bimolecular reactions with quenching species, which can be present in solution.<sup>15</sup> Fluorescence lifetimes are typically  $\leq 10$  ns and quenchers must be present at high concentrations to effectively quench this state.<sup>16</sup> The quenching of the excited states of porphyrins can occur by one of the following mechanisms:

- (a) Electron transfer       $MP^* + Q \longrightarrow MP^{+/-} + Q^{+/-}$
- (b) Energy transfer         $MP^* + Q \longrightarrow MP + Q^*$
- (c) Accelerated deactivation     $MP^* + Q \longrightarrow MP + Q + \text{heat}$

MP in the above reaction pathways represents either the metalloporphyrin or the free base porphyrin. Light induced electron transfer reactions represent an important reaction of porphyrin molecules.

### 1 3 3 Porphyrins as light harvesters in an antenna unit

In nature, photons are exploited by living organisms as energy sources in photosynthetic processes. Part of the photosynthetic system concerns the optimisation of light harvesting, that is, the efficient absorption and conversion of incident sunlight into chemical energy (see Figure 1 10). This process depends on the nature and organisation of the receiving matter<sup>17</sup>. Much research has gone into the design of structurally organised systems capable of utilising the energy of photons to perform photosynthesis without actually succeeding replicate it<sup>18 19</sup>.

In photosynthesis, light harvesters make use of antenna systems, which contain a large number of chromophores, such as porphyrins. They have a larger cross section for the absorption of light (see Figure 1 8). They absorb a photon of energy from the light and this photon then migrates efficiently through the system to the reaction centres of PSI or PSII (see Section 1 1).

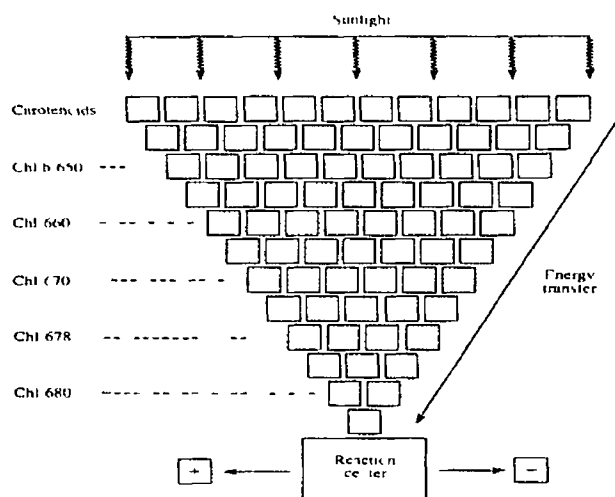


*Figure 1 10 Schematic representation of the antenna unit of a photosynthetic system (see ref 17)*

Light harvesting systems must satisfy a number of requirements,

- (i) capable of absorbing light,

- (ii) stability towards photodecomposition,
- (iii) populated with high efficiency from the excited state obtained by light absorption,
- (iv) be reasonably long lived

The excited states involved as donors in energy transfer satisfy the final two requirements. Extensive investigations have shown that porphyrins satisfy most of these requirements as is also evident from their use in nature<sup>20,21,22</sup>

These characteristics make porphyrins excellent candidates in the design of synthetic systems capable of exploiting light in a route towards artificial photosynthesis

## 1 4 Bonding in organometallic compounds

### 1 4.1 Stability of organometallic compounds

In order to discuss the photochemical properties of the compounds in this work it is necessary to describe the general bonding and electronic structure of organometallic compounds. Organometallic chemistry is concerned with the chemistry of the M-C bond and unlike co-ordination compounds, organometallic compounds show a high tendency to achieve the inert gas electron configuration around a metal. Electron counting has been very useful in helping to predict the structures and reactivity of these complexes.

Organometallic compounds tend to react so as to achieve the favoured 18-electron configuration, which is known as the 18-electron rule. To explain this rule, a first row transition metal has 9 valence orbitals  $1s_2$ ,  $3p_6$ ,  $5d_{10}$  and each can hold a maximum of two electrons. Therefore a metal in a complex needs 18 valence electrons to obey the 18-electron rule.

Complexes such as  $\text{Cr}(\text{CO})_6$  and  $\text{Ni}(\text{CO})_4$  obey this rule. In the case of  $\text{Cr}(\text{CO})_6$  chromium is in the zero oxidation state and therefore has a  $d^6$  configuration. The six carbonyl ligands donate two electrons each giving a total of twelve. Some electrons come from the metal and the ligand must provide the rest to give it the stable 18-electron configuration ( $\pi$  back bonding makes no difference when counting the electrons). This rule does have some limitations but works best for sterically small ligands like CO.

## 1.4.2 The nature of bonding in the metal-carbonyl bond

A carbonyl ligand (carbon monoxide) is an example of a good  $\pi$ -acceptor ligand for electron rich metal atoms in transition chemistry. The bonding between CO and a metal consists of two components, (i) ligand to metal  $\sigma$  bonds which results from the transfer of electron density from the C atom lone pair to an empty  $d\pi$  orbital on the metal and (ii) back donation from the  $d\pi$  orbital to an empty  $\pi^*$  orbital on the C atom.

- (i) Figure 1.11 is a molecular orbital diagram for carbon monoxide (CO). The atomic orbitals of the O atom are lower in energy than those of the C atom because of the higher effective nuclear charge on the O atom compared to carbon. The O-based atomic orbitals contribute more to the bonding molecular orbitals in CO whereas the  $\pi^*$  orbitals have more C character. The metal binds to CO via a M-C  $\sigma$  bond through the interaction of the C based HOMO with an empty  $d\pi$  orbital on the metal. The HOMO is mainly centred on the C atom as the O atom is more electronegative and the orbitals are lower in energy.

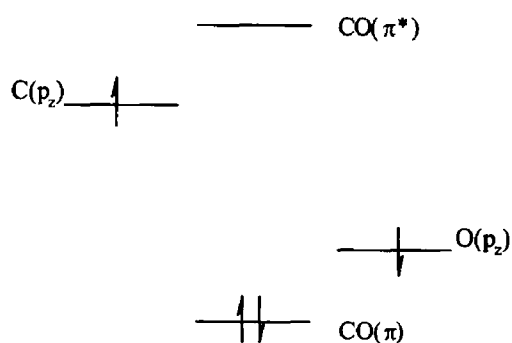


**Figure 1.11 Molecular orbital diagram of a  $\pi$  bond of CO**

- (ii) The M-C  $\sigma$  bond increases the electron density on the metal. This is offset by back donation from the metal  $d\pi$  orbitals to the  $\pi^*$  orbitals on CO (see Figure 1.12). As the O atom is more electronegative than the C atom, the filled  $\pi$  orbitals of the C-O are localised on the O atom, hence the  $\pi^*$  orbitals are localised on the C. This form of bonding is known as back bonding.

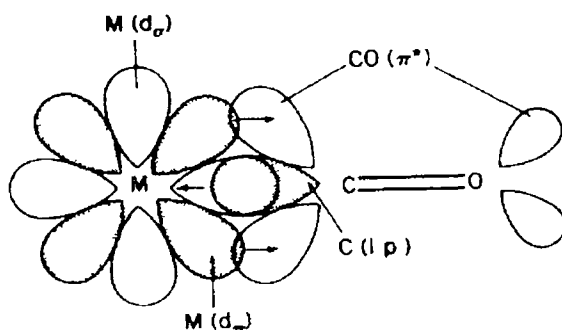


**Figure 1 12 Molecular orbital diagram of M-CO showing (i)  $\sigma$  bonding and (ii)  $\pi$  back bonding**

These  $\pi^*$  antibonding orbitals are high in energy but they do have the effect of stabilising the  $d_{\pi}$  orbitals which has important consequences,

- (a) The ligand field splitting parameter,  $\Delta$ , increases
- (b) M-L back donation allows zero and low valent metals to form stable complexes

This type of bonding is synergistic, that is the  $\sigma$  donation of the carbonyl group to the metal is accompanied by back donation from the metal to the carbonyl  $\pi^*$  orbitals. It has the overall effect of decreasing the M-C  $\sigma$  bond and also lengthening and weakening the C-O double bond due to population of its  $\pi^*$  orbitals.

## 1 5 Bibliography

---

- 1 E I Rabinowitch, *Photosynthesis*, 1951, vol II, part 1, Chapter 23, Wiley, New York
- 2 K Kalyanasundaram, *Photochemistry and Photophysics of Polypyridine and Porphyrin complexes*, 1992, Academic Press, London
- 3 J Deisenhofer, O Epp, K Miki, R Huber, H Michel, *J Mol Biol* , 1984, 180, 385
- 4 J Deisenhofer, H Michel, *Angew Chem , Int Ed Engl* , 1989, 28, 829
- 5 M Klessinger, J Michl, *Excited states and photochemistry of organic molecules*, 1995, Chapter 5, VCH Publishers Ltd , Cambridge
- 6 L R Milgrom, *The Colours of Life*, 1997, Oxford University Press, New York
- 7 J R Darwent, P Douglas, A Harriman, G Porter, *Coord Chem Rev* , 1982, 47, 43
- 8 K Kalyanasundaram, *Inorg Chem* , 1984, 23, 2453
- 9 A Antipas, J W Buchler, M Gouterman, P D Smith, *J Am Chem Soc* , 1978, 100, 3015
- 10 P J Spellane, M Gouterman, A Antipas, S Kim, Y C Liu, *Inorg Chem* , 1981, 19, 386
- 11 A Antipas, M Gouterman, *J Am Chem Soc* , 1983, 105, 4896
- 12 J Roderuez, C Kirmaier, D Holten, *J Am Chem Soc* , 1989, 111, 6500
- 13 H Linschitz, K Sarkanen, *J Am Chem Soc* , 1958, 80, 4826, H Linschitz, L Pekkarinen, *J Am Chem Soc* , 1960, 82, 2407
- 14 A Harriman, *J Chem Soc , Faraday Trans 2*, 1981, 77, 1281
- 15 J R Darwent, P Douglas, A Harriman, G Porter, M C Richoux, *Coord Chem Rev* , 1982, 44, 83
- 16 G R Seely, *Photochem Photobiol* , 1978, 27, 639
- 17 V Balzani, F Scandola, *Supramolecular photochemistry*, 1991, Ellis Horwood, Chichester
- 18 J M Lehn, *Angew Chem , Int Ed Engl* , 1990, 29, 1304
- 19 V Balzani, *Tetrahedron*, 1992, 48, 10443

- 
- 20 A Harriman, *Supramolecular Photochemistry*, **1987**, Reidel, Holland
- 21 S Anderson, H L Anderson, J K M Sanders, *Angew Chem, Int Ed Engl*,  
**1992**, *31*, 907
- 22 S Prathapan, T E Johnson J S Lindsey, *J Am Chem Soc*, **1993**, *115*, 7519

## **Chapter 2**

# **Literature Survey on the Photochemistry and Photophysics of Porphyrin and Metalloporphyrin Complexes and Arrays**

## 2.1 Introduction

Porphyrins belong to one of the most important classes of organic compounds due to their role in biological processes, intense visible light absorption and interesting excited state properties<sup>1</sup> Photosynthesis is a complex photochemical reaction on which all life depends and the possibility of mimicking this process *in vitro* depends largely on being able to understand its key component namely chlorophyll, which contains metalloporphyrin units

From the initial work on the photochemical properties of chlorophyll and the first man made porphyrins, to the huge supramolecular arrays of today, porphyrins and related macrocycles have been studied for their electron transfer and energy transfer potential<sup>2,3</sup> Covalently linked porphyrins as well as porphyrin metal complexes have been extensively used in this photosynthetic research In the following section an overview of the many studies carried out on porphyrins from the simplest free base porphyrins and metalloporphyrins to metal complexed supramolecular systems, will be presented

The section begins with the first photochemical studies carried out on free base porphyrins and concludes with a study of metalloporphyrins<sup>1</sup> The following section deals with the peripheral linkage of metals and other electron acceptors to porphyrins These systems are used to study photoinduced energy transfer or electron transfer in molecular dyads<sup>4,5</sup> The final section of the literature survey deals with the next step, the formation of triads, which allows for porphyrin-to-porphyrin electron transfer *via* a non-covalent metal bridge as well as covalently linked multiporphyrinic arrays<sup>6,7</sup>

The following pages give an overview of the development of both the photochemical and photophysical properties of porphyrins and porphyrin arrays

## 2.2 Introduction to the photochemical and photophysical properties of tetra aryl porphyrins and metalloporphyrins

Since the pioneering work of Becher and Kasha which probed the photophysical properties of porphyrins and Krasnoviskii's reversible photochemical reduction of chlorophyll, many studies investigated the photochemical and photophysical properties of free base porphyrins and metalloporphyrins <sup>1</sup>

A general method for the preparation of free base porphyrins and metalloporphyrins was established between 1941 and 1951 <sup>8 9 10</sup> Before this the decay kinetics of the triplet excited state of chlorophyll a and chlorophyll b had been extensively investigated <sup>11</sup> However the first "flash illumination" measurements on man made porphyrins were not conducted until later on tetra phenyl porphyrins and zinc tetra phenyl porphyrins <sup>12</sup> Some work had been done earlier by Livingston and Fujimori on chlorins and phthalocyanines using photographic flash experiments <sup>13</sup> Even using these simple techniques researchers had noted certain trends in the triplet state absorption of porphyrins, the strongest band lies to low energy of the Soret band and also there was a second band to the high energy side of the Soret band <sup>12 13 14</sup> These experiments suffered from scattered signals under the main red band of the bacteriochlorophyll which is now known to be the result of fluorescence <sup>14</sup>

Linshitz and Pekkarinen were also the first to explore the effect of heavy metal ions on the triplet lifetimes of porphyrins <sup>14</sup> They used the recognised photochemistry of anthracene as a model for their results because of the similarities between the photochemistry of porphyrins and aromatic hydrocarbons <sup>15</sup> These workers found the triplet states of porphyrins were quenched in the presence of heavy metal salts such as NiCl<sub>2</sub> These metal quenchers were not as effective as those previously reported for anthracene <sup>14</sup> They found that the lighter metals had little or no effect on the triplet excited states but heavier metals were efficient quenchers (see Table 2.1 for quenching constants of TPP, ZnTPP and anthracene) This was explained at the time by using the

heavy atom affect, and subsequently led to the development of the interaction of porphyrins and external substituents <sup>14</sup>

| <i>Quencher</i>   | <i>Solvent</i> | <i>Anthracene</i> | <i>TPP</i> | <i>ZnTPP</i> |
|-------------------|----------------|-------------------|------------|--------------|
| NiCl <sub>2</sub> | Pyridine       | 12                | 1 0        | 0 98         |
| CuCl <sub>2</sub> | Pyridine       | 46                |            | 12           |
| CoCl <sub>2</sub> | Pyridine       | 6 2               |            | 0 14         |
| MnCl <sub>2</sub> | Pyridine       | 0 43              | <0 05      |              |

**Table 2 1** *The quenching constants for anthracene, TPP and ZnTPP in the presence of various metal salts (ref. 14)*

Understanding the changes in the excited states of porphyrins and shifts in their UV-vis spectrum are important in developing a method to mimic the natural process of photosynthesis. Tetra aryl porphyrins such as TPP and TPyP became the main porphyrins of interest due to the wide range of synthetic possibilities available <sup>16</sup>. Despite the non coplanar configuration of the aryl substituents and the porphine, <sup>17,18</sup> resonance-type substituent effects are dominant <sup>19</sup>. *Para* substituents on free base porphyrins and metalloporphyrins, which have been widely studied, caused slight spectral changes in the UV-vis spectrum.

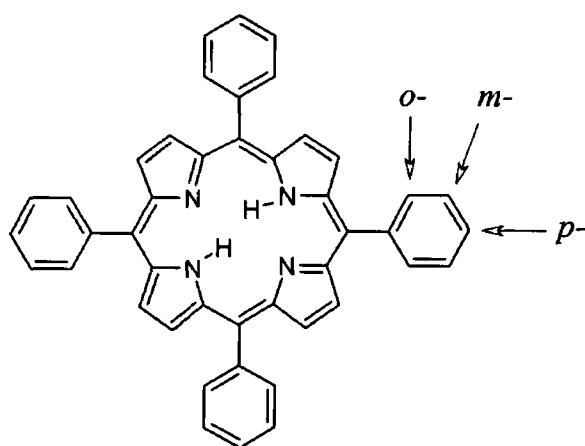


**Figure 2.1** *m-, o- and p- substituents as would be found on a porphyrin*

The Soret band and Q bands shifted to longer wavelength (2-4 nm) and the ratio of the Q(1,0) to Q(0,0) in metalloporphyrins is increased (see Table 2.2)<sup>20</sup> Although the effect on the porphyrin by *para* substituents was slight, the effect of *ortho* substituents was more significant<sup>20</sup>

Figure 2.1 outlines the possible position of the *m*-, *o*-, and *p*- substituents in relation to a porphyrin and Table 2.2 shows the effect on the relative Q band intensity of *p*-, *o*- substituents on porphyrins. Similar changes observed for *para* substituents also occurred for substituents in the *ortho* position however the shifts in the Soret and Q bands increased up to 10 nm and the reduction in intensity of the Q(0,0) band were dramatically increased relative to the Q(1,0) band (see eqn, 3.1)

| <i>Porphyrin</i>   | $Q_x(0,0)$ | $Q_y(1,0)$ | $Q(1,0)/Q(0,0)$ |
|--------------------|------------|------------|-----------------|
| TPP                | 0.0162     | 0.0180     | 1.11            |
| <i>o</i> -Cl-TPP   | 0.0640     | 0.0192     | 0.30            |
| <i>p</i> -Cl-TPP   | 0.0179     | 0.0197     | 1.10            |
| ZnTPP              | 0.4350     | 0.2350     | 0.54            |
| <i>o</i> -Cl-ZnTPP | 0.7777     | 0.1400     | 0.18            |
| <i>p</i> -Cl-ZnTPP | 0.0810     | 0.0470     | 0.58            |

**Table 2.2 Effect of *ortho* and *para* chloro-substitution on the relative intensities of  $Q_y(0,0)$  and  $Q_x(0,0)$  absorption bands (see ref. 20)**

Longo *et al* discovered that electron withdrawing substituents such as iodine in the *para* or *ortho* position caused the greatest shifts in the UV-vis spectrum with fluorine causing the smallest changes. Zn porphyrins showed the same spectral changes as those of the free base porphyrin although the nature of the halogen did not affect the magnitude of the reduction in intensity<sup>20</sup>. The red shift in the porphyrin bands and the relative reduction in the intensity of the Q bands, which was common throughout is typical of most aryl substituted porphyrins studied<sup>21,22,23</sup>

Some of the most important results of porphyrin metal interactions are seen in the emission spectra, singlet lifetimes and also the triplet excited states of the complexes. Since the calculation of the fluorescence quantum yield of 0.2 for tetraphenylporphyrin by Gouterman *et al.*,<sup>24</sup> researchers have used this value to compare the effect of a range of substituents on the fluorescence quantum yield.<sup>25,26,27,28</sup>

| <i>Porphyrin</i>   | <i>Medium</i>                 | $\Phi_{fl}$ | $\tau_{fl}$ , ns |
|--------------------|-------------------------------|-------------|------------------|
| TPP                | C <sub>6</sub> H <sub>6</sub> | 0.11        | 13.6             |
| <i>o</i> -Cl-TPP   | C <sub>6</sub> H <sub>6</sub> | 0.02        |                  |
| <i>p</i> -Cl-TPP   | C <sub>6</sub> H <sub>6</sub> | 0.09        |                  |
| ZnTPP              | C <sub>6</sub> H <sub>6</sub> | 0.03        | 2.3              |
| <i>o</i> -Cl-ZnTPP | C <sub>6</sub> H <sub>6</sub> | 0.038       |                  |
| <i>p</i> -Cl-ZnTPP | C <sub>6</sub> H <sub>6</sub> | 0.02        |                  |

**Table 2.3** The differences observed in fluorescence quantum yields and lifetimes for a series of ortho and para chloro-substituted tetraphenylporphyrins (ref. 29)

Researchers have found that the presence of substituents on the aryl groups can affect the fluorescence yield and singlet lifetimes of porphyrins. It was noted that the fluorescence measurements followed a pattern similar to that of the absorption spectrum with *p*-substituted aryl groups having smaller effects than the *o*-aryl groups. This pattern was observed for free base porphyrins with reductions in the singlet quantum yields of the *p*-substituted complexes being greater than that of the *o*-substituted complexes (see Table 2.3).<sup>20,29</sup> The fluorescence yield was high in the case of the substituted metalloporphyrins but could not be explained by the author.<sup>20</sup>

The singlet state lifetimes and quantum yields are reduced following the introduction of zinc or other metals into the centre of the porphyrin ring (see Table 2.3).<sup>20</sup> A study of the substituent effect was then carried out on the fluorescence properties of a number of *p*-substituted tetraphenylporphyrins.<sup>30</sup> Substituents ranging from good electron donors

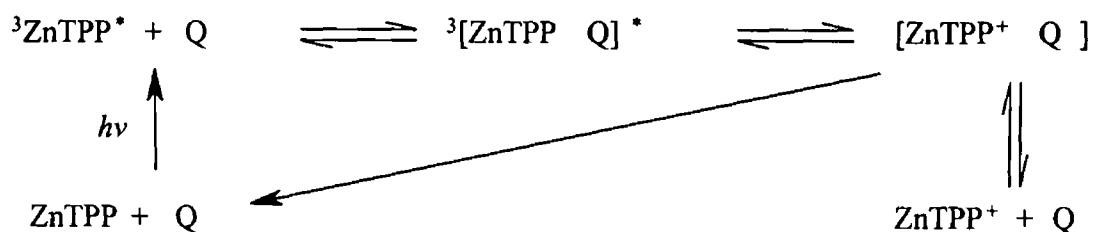
(NMe<sub>2</sub>) to good electron acceptors (p-benzoquinone) were used. Results indicated that electron acceptors cause a substantial reduction in the fluorescence quantum yield and the singlet lifetimes while electron donors such as nitro groups increased the rate of radiationless decay in a process known as intramolecular quenching. With the increase in radiationless decay the sum of the fluorescence yield and the triplet quantum yield was significantly less than one (see Table 2.4)

| <i>Porphyrin</i>                                                       | $\Phi_{fl}$ | $\Phi_{trip}$ | $\Phi_{fl} + \Phi_{trip}$ |
|------------------------------------------------------------------------|-------------|---------------|---------------------------|
| H <sub>2</sub> -OEP                                                    | 0.14        | 0.86          | 1.00                      |
| H <sub>2</sub> - $\alpha$ -NO <sub>2</sub> -OEP                        | 0.02        | 0.65          | 0.67                      |
| H <sub>2</sub> - $\alpha,\gamma$ -(NO <sub>2</sub> ) <sub>2</sub> -OEP | 0.02        | 0.44          | 0.46                      |
| Zn-OEP                                                                 | 0.04        | 0.96          | 1.00                      |
| Zn- $\alpha$ -NO <sub>2</sub> -OEP                                     | 0.005       | 0.84          | 0.85                      |
| Zn- $\alpha,\gamma$ -(NO <sub>2</sub> ) <sub>2</sub> -OEP              | 0.005       | 0.40          | 0.41                      |

**Table 2.4 Differences observed in the quantum yields for both triplet and singlet following substitution of a nitro group to an octa ethyl porphyrins**

Since the early work of Linschitz and Pekkarinen on the triplet state absorption spectrum of chlorophyll, the triplet state absorption spectra of regular porphyrins have been studied by conventional flash photolysis in order to understand the mechanism of photosynthesis<sup>13,26,31,32,33</sup>. The  $\pi$ - $\pi^*$  excited states of both porphyrins and metalloporphyrins are characterised by strong absorption between 420 nm and 490 nm (i.e. between the Soret band and Q(1,0) band)<sup>1,2,3</sup>. In addition the triplet excited states contain a broad featureless absorption extending into the infrared region of the spectrum. The quantum yield for the triplet state in TPP is 0.87 and as with the studies on the fluorescence quantum yields, the triplet state quantum yield was used to estimate the interaction between porphyrins and substituents in the triplet excited state<sup>34</sup>. This work demonstrated that singlet to triplet intersystem crossing was the dominant route for radiationless deactivation of the S<sub>1</sub> excited state in porphyrins<sup>20</sup>.

One of the first attempts to mimic covalently linked electron transfer or charge separation witnessed in nature, involved the quenching of the excited states of porphyrins and metalloporphyrins by quinones<sup>35,36,37,38</sup> A review by Connolly and Bolton in 1987 revealed hundreds of porphyrin-quinone studies in the literature<sup>39</sup> Since then the number of these systems has grown quite considerably but recently interests have shifted to metal based porphyrin complexes Linschitz *et al* showed that chlorophyll undergoes reversible photo bleaching in the presence of benzoquinone<sup>40</sup> and this was found to be typical of ZnTPP<sup>41</sup> Following excitation to the singlet excited state in a porphyrin an electron can be transferred to the quinone moiety forming a radical and a porphyrin  $\pi$ -cation radical, which reforms the neutral species on the nanosecond range<sup>42</sup> Laser flash photolysis of free base porphyrins and metalloporphyrins in the presence of a quinone leads to the formation of a long lived transient species identified as a triplet complex or exciplex followed by electron transfer within the complex In polar solvents the primary radical pair may undergo complete separation to yield the products of full electron transfer, ZnTPP<sup>+</sup> and Q In non-polar solvents charge recombination dominates (see Scheme 2 1)



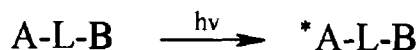
**Scheme 2 1 Quenching of porphyrin excited states by quinones (Q)**

This complex decays with a rate constant of  $\approx 3 \times 10^3 \text{ s}^{-1}$ , and based on the dependence of the lifetime on the quinone concentration, the complex is formed in a 1:1 ratio<sup>43,44</sup> Emission from the triplet state is completely quenched by the quinone even at 77 K Wasielewski *et al* carried out work on a number of systems involving porphyrins linked to quinones *via* an organic bridge<sup>45</sup> Excitation into the excited singlet state of the complex resulted in charge separation and charge recombination processes (see Reaction 2 1 - 2 3) The lifetime of the charge recombination process was longer than that of the charge separation process, which was consistent with the short bridge used Wasielewski also looked at the effect of the bridge length on the rate of electron transfer and

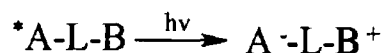
discovered that the charge separation and recombination rate constants decrease exponentially with distance <sup>42</sup>

Insertion of rigid spacers and polyene chains between the porphyrins and quinones has also been investigated <sup>46,47</sup> It was discovered that rigid bicyclooctane bridges reduced the efficiency of the electron transfer process between the porphyrin and the quinone. This caused inefficient quenching of the porphyrin singlet excited state. Fluorescence intensity decreased sharply as the number of bicyclooctane linkers was increased. The use of polyene chains as linkers between the porphyrin and the quinones was more effective at increasing the efficiency of the electron transfer process. The polyene bridges behave as conducting molecular wires and are capable of carrying electrons over considerable distances in a few picoseconds. Charge separation took place in about 3 ps while charge recombination took 10 ps to be completed. The decrease in electron transfer rates with increasing length of the polyene chain was very small i.e. the system had a very low distance-dependence for polyene bridges.

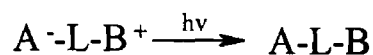
**Reaction 2.1**



**Reaction 2.2**



**Reaction 2.3**



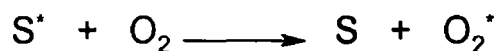
Molecular oxygen plays a major role in the photodamage in various sensitised biological systems. It is also an efficient quencher of the triplet states of porphyrins and other organic dyes <sup>48 49 50</sup>

Two types of mechanisms were proposed for this photooxidation process

**Reaction 2.4 Type I**



**Reaction 2.5 Type II**



For the free radical mechanism, or Type I the triplet excited sensitizer  $S^*$  reduces molecular  $O_2$  to the superoxide anion  $O_2^{\cdot -}$  or related species. Type II reactions allow the porphyrin triplet excited state to transfer energy to  $O_2$  to generate singlet oxygen (see Reaction 2.4 and 2.5). Measurement of singlet oxygen formation is a good indicator of the quenching ability of  $O_2$  for the triplet states of porphyrins (see table 2.5).

| <i>Porphyrin</i>   | $\Phi(^1O_2)$ |
|--------------------|---------------|
| TPP                | 0.2           |
| $H_2TMPyP^{4+}$    | 0.74          |
| $Zn(II)TMPyP^{4+}$ | 0.88          |
| $Cd(II)TMPyP^{4+}$ | 0.75          |

**Table 2.5 Quantum yield for singlet oxygen formation during the quenching of the triplet excited state (ref 50) (TMPy – tetra methyl porphyrin)**

The significant reductions in the triplet and singlet excited states lifetimes and quantum yields of porphyrins because of the intramolecular electron transfer between the porphyrins and  $O_2$  or organic acceptors such as quinones and methyl viologens led researchers to investigate the possibility of developing systems consisting of porphyrins covalently linked to transition metal redox centres.

The first reported example of such a system was by Schmidt *et al* and involved a combination of tetra phenyl porphyrin and ferrocene (see Figure 2.2)<sup>51</sup>. Although Schmidt *et al* did not experience the desired reduction in fluorescence yield of the complex or change in lifetimes, a new step had been taken towards the design of electron

transfer systems involving porphyrins. Examples of porphyrins linked to transition metal centres did not appear in the literature until the 1990s, and this with the discovery of coordination polymers of metalloporphyrins increased the interest in the synthesis of complex porphyrin macrocycles.

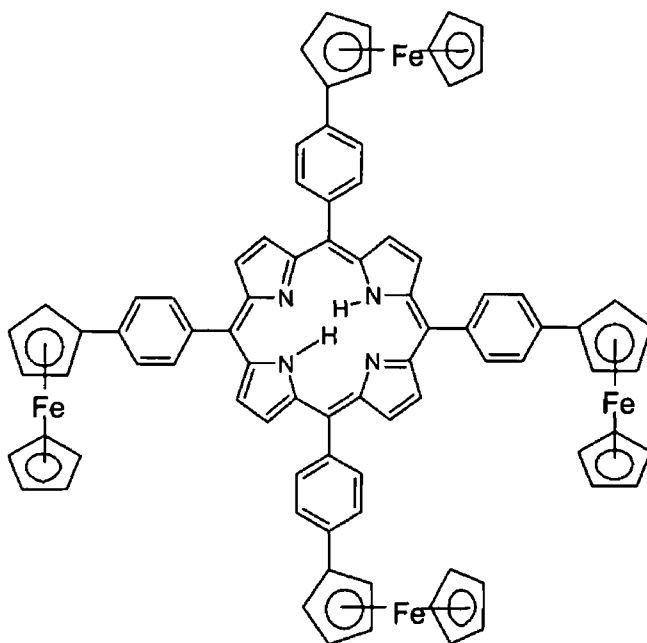
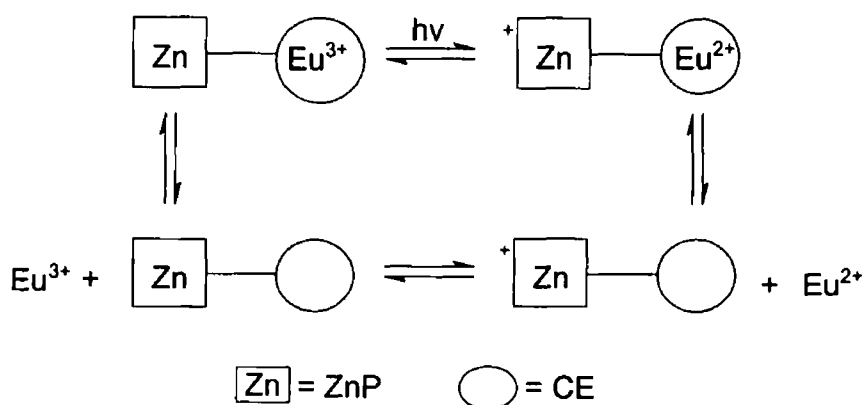


**Figure 2.2 Tetra ferrocenyl phenyl porphyrin**

### 2.3 Coordination to peripherally linked transition metal centres

As shown in the previous section, there are many examples of systems that undergo intramolecular electron transfer from porphyrins to organic receptors<sup>52</sup>. Systems that undergo electron transfer processes from porphyrins to externally but covalently linked transition metal complexes were rare until the mid nineties. At this time only four examples of such systems had been explored so as to investigate the possibility of photoinduced electron transfer from the porphyrin moiety to the peripheral metal centre<sup>53</sup>.

The first of such systems to be investigated was those containing  $\text{Eu}^{3+}$  cations in the cavities of crown ethers attached to the *meso* position of a zinc porphyrin (ZnPCE)<sup>54,55</sup>. Effective intramolecular electron transfer from the triplet state of the metalloporphyrins to the  $\text{Eu}^{3+}$  cation was observed. However the reduction of the Eu ion resulted in it being displaced from the crown ether cavity, thus rendering the reaction irreversible (see Scheme 2.2). The singlet lifetimes and corresponding quantum yields varied upon changing the metal of the crown ether (see Table 2.6).



**Scheme 2.2** Proposed sequence for intramolecular transfer from ZnTPP to a covalently linked crown ether (CE)

A similar scheme involving two porphyrins linked *via* a crown ether containing no metal centre showed results typical of organic linkages between porphyrins with singlet state

lifetimes typical of porphyrin monomers. Hence it was concluded that metal centres were required in the crown ether to alter the lifetimes and quantum yields of the porphyrin, and even then the effects were small (see Table 2.6)<sup>56</sup>

| <i>Porphyrins</i> | <i>Cation</i>    | $\Phi_{fl}$ | $\tau_s/ns$ |
|-------------------|------------------|-------------|-------------|
| ZnTPP             |                  | 0.040       | 1.9         |
| ZnPCE             |                  | 0.038       | 1.7         |
| ZnPCE             | Na <sup>+</sup>  | 0.038       | 1.7         |
| ZnPCE             | Eu <sup>3+</sup> | 0.029       | 1.3         |

**Table 2.6 Photophysical properties of various cation complexes of ZnPCE compared to ZnTPP (PCE-porphyrin crown ether) (ref. 56)**

Another attempt to mimic the electron transfer process involved using the oxidised form of 5, 10, 15, 20 tetra ferrocenyl phenyl porphyrin (see Figure 2.2)<sup>51</sup>. As electron transfer from the porphyrin to the ferrocene centres could not compete with the rate of decay of the porphyrin excited state, the ferrocenium centres proved to be an ineffective acceptor for an electron from the excited singlet state of the porphyrin. Two reasons were given for this, firstly lack of electron transfer could be because of its high exothermicity as in the case of porphyrin quinone zwitterions,<sup>57</sup> and secondly electron transfer can be slow when the acceptor is metal centred. A system consisting of a porphyrin and a d<sup>10</sup> metal proved to be more successful in the electron transfer process, but again they are somewhat inefficient.<sup>58</sup> The latter system consisted of two [18]-N<sub>2</sub>O<sub>4</sub> receptor molecules covalently bound to opposite sides of a porphyrin and connected together *via* a biphenyl strap (see Figure 2.3). Each of these receptors contained an Ag<sup>+</sup> ion. It had previously been shown that the organic spacer (biphenyl strap) had no bearing on the properties of the porphyrin, as was the case for the crown ether.<sup>59</sup>



Researchers investigating the electron transfer potential of a peripherally molybdenated tetra phenyl porphyrin complex discovered similar charge separation and charge recombination properties <sup>4 5 53</sup>

Yet again the fluorescence quantum yield and the singlet lifetime of the porphyrin were reduced from 10 ns to 30 ps. Once more formation of the  $\pi$ -radical of the porphyrin occurred quickly ( $k > 3 \times 10^{12} \text{ s}^{-1}$ ), which was followed by a slower charge recombination ( $k > 4.6 - 8.5 \times 10^9 \text{ s}^{-1}$ )

These investigations were the first involving electron transfer from the excited states of porphyrins to transition metals. In all but one of the cases initial charge separation was rapid but charge recombination was relatively slow. A number of reasons have been put forward to explain, including slow solvent reorganisation,<sup>60</sup> or the possibility of structural changes upon oxidation of the peripheral redox centre may occur. In the case of the molybdenated porphyrin, precursor molecules have shown geometric rearrangement that would effect electron transfer <sup>61 62 63</sup>

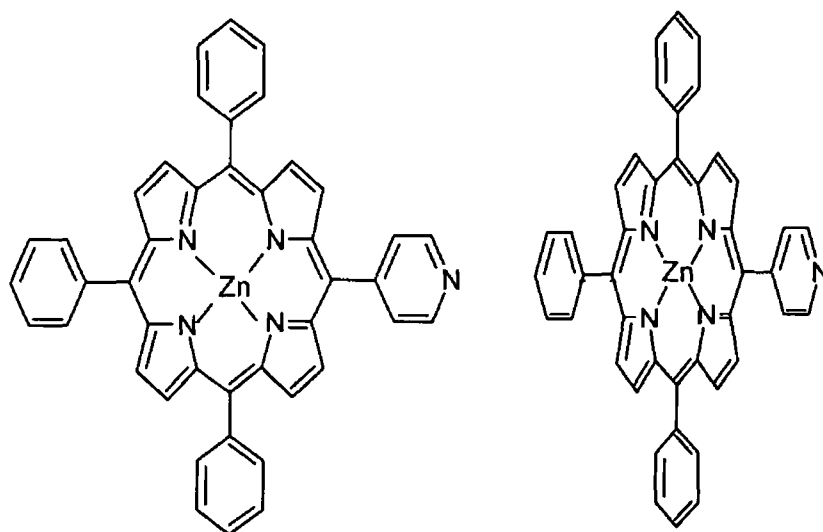


**Figure 2.4 Structure of ZnMPyTPP dimer**

Another discovery, reported recently, which greatly increased the interest in porphyrins and their electron transfer potential to metal centres, is the co-ordination potential of

pyridyl porphyrins and the formation of ZnMPyTPP polymers (see Figure 2.4) <sup>64,65</sup> This is the earliest example of a co-ordination polymer reported using pyridyl porphyrins, although a linkage polymer of an Fe porphyrin had previously been reported <sup>66</sup> Pyridine commonly binds to zinc at the centre of porphyrins and ZnMPyTPP was formed by the co-ordination of pyridine on the porphyrin periphery to an adjacent zinc metal centre <sup>65</sup> The discovery of this led to the synthesis of a large number of complexes bound to a porphyrin *via* a pyridyl linker

The peripheral co-ordination of singly unsaturated metal centres to pyridyl porphyrins produced species with new and interesting photochemical and photophysical properties <sup>67,68</sup> Of particular interest to researchers were pyridyl porphyrins co-ordinated to ruthenium(II) centres <sup>69,70</sup> Porphyrins have long been used as electron donors while Ru(II) metal centres such as Ru(bipy)<sub>2</sub>Cl<sup>+</sup> and Ru(tpy) have low energy excited states and hence the Ru centres are readily reduced <sup>71</sup> Such a combination could potentially lead to the development of an artificial photosynthetic model

Toma *et al* investigated a number of these systems by co-ordinating [Ru(bipy)<sub>2</sub>Cl]<sup>+</sup> to a *mono-, di-, tri- or tetra* pyridyl porphyrin and investigating the effects of the metal centre on the porphyrin singlet lifetimes and fluorescence quantum yields <sup>67,72</sup> These workers observed a reduction in singlet state lifetimes which was linear relative to the number of Ru(II) centres co-ordinated to the porphyrin through the pyridyl moiety i.e. the reduction caused by four Ru(II) centres was four times greater than that of one Ru(II) centre. A reduction in the quantum yields was also found to be dependent on the number of Ru(II) centres attached, and this was attributed to the heavy atom effect which had been observed as early as 1960 <sup>14</sup> Upon complexation of the porphyrins with the Ru centres, shifts in the UV-vis spectrum of the porphyrins of 2-3 nm to lower energy were also observed. These shifts are typical of peripheral complexation of metals to porphyrins <sup>67</sup>

The emission observed was from the lowest excited singlet state on the porphyrin and was assigned to Q<sub>x</sub>(0,0) and Q<sub>x</sub>(1,0) transitions. The fluorescence quantum yields decreased with increasing pyridyl groups and co-ordinated metal subunits (see Table

2.7) <sup>72</sup> Ruthenium centres have been thought to induce the heavy atom effect, which in turn reduces the fluorescence quantum yields by up to 100 times. The quantum yields of the uncomplexed porphyrins are inversely proportional to the number of pyridyl groups attached because of the interactions of the pyridyl groups with the solvent molecules through the N atom lone pair and non-specific dipole-dipole interactions <sup>73</sup>. These interactions should enhance the vibronic coupling with the solvent molecules and increase the rate of the non-radiative decay to the ground state <sup>72</sup>.

| <i>Porphyrin</i>                                                                          | $\Phi_f(512\text{ nm})$ | $\lambda_{em}/\text{nm}$ |
|-------------------------------------------------------------------------------------------|-------------------------|--------------------------|
| MPyTrPP                                                                                   | $9.9 \times 10^{-2}$    | 651, 715                 |
| <i>Cis</i> -DiPyDiPP                                                                      | $9.1 \times 10^{-2}$    | 650, 714                 |
| TrPPyMPP                                                                                  | $8.4 \times 10^{-2}$    | 650, 714                 |
| [MPyTrPPRu(bipy) <sub>2</sub> Cl] <sup>+</sup>                                            | $2.9 \times 10^{-3}$    | 653, 715                 |
| [ <i>cis</i> -DiPyDiPPRu <sub>2</sub> (bipy) <sub>4</sub> Cl <sub>2</sub> ] <sup>2+</sup> | $8.6 \times 10^{-4}$    | 656, 717                 |
| [TrPPyMPPRu <sub>3</sub> (bipy) <sub>6</sub> Cl <sub>3</sub> ] <sup>3+</sup>              | $3.2 \times 10^{-4}$    | 654, 716                 |

**Table 2.7 Fluorescence quantum yields and emission maxima for a series of free base porphyrins and their ruthenium analogues (ref 72)**

Prodi and co-workers reported similar results when they investigated the effect of RuCl<sub>2</sub>(DMSO)<sub>2</sub>(CO) on the photophysical and photochemical lifetimes of *mono*-, *di* and *tri*- pyridyl porphyrin <sup>70</sup>. Again the reduction in singlet lifetimes was paralleled by a similar reduction in fluorescence quantum yield with the  $\pi$ - $\pi^*$  transient absorption spectrum of the complexes having a profile characteristic of an uncomplexed free base porphyrin (see Table 2.8)

| <i>Porphyrin</i>                                                      | <i>(<math>\tau_s</math>, ns)</i> |
|-----------------------------------------------------------------------|----------------------------------|
| MPyTPP                                                                | 8.1                              |
| cis-D1PyD1PP                                                          | 8.0                              |
| TriPyMonoPP                                                           | 7.5                              |
| MPyTPP[RuCl <sub>2</sub> (DMSO) <sub>2</sub> (CO)]                    | 6.3                              |
| cis-D1PyD1PP[RuCl <sub>2</sub> (DMSO) <sub>2</sub> (CO)] <sub>2</sub> | 4.4                              |
| TriPyMPP[RuCl <sub>2</sub> (DMSO) <sub>2</sub> (CO)] <sub>3</sub>     | 3.3                              |

**Table 2.8 Fluorescence lifetimes of pyridyl porphyrins and Ru(II) adducts (see ref 70)**

Winnischifer *et al* synthesised and carried out spectral studies on tetra pyridyl porphyrin linked to four pentacyanoferrate(II) groups and found that the pyridyl porphyrin acted as an electron withdrawing group<sup>74</sup> The group induces a significant increase in the basicity of the porphyrin ring in comparison to free base porphyrin complexed to four Ru(II) centres as shown by a  $pK_a$  shift from 2.2 for the ruthenium and porphyrin to 4.7 for the ferrate porphyrin<sup>75,76</sup> For the cyano ferrate porphyrin the substituent is in the 2 - position on the pyridyl ring which allows for more orbital overlap than is the case in for substitution at the four position<sup>74</sup> Also the cyano group increases the electron density on the Fe(II) ion as it is a better  $\sigma$ -donor than  $\pi$ -acceptor, while 2,2 bipyridine is a strong  $\pi$ -acceptor and a weak  $\sigma$ -donor<sup>77</sup>

The study of non-covalent assemblies has led to some interesting results for electron and energy transfer<sup>78,79</sup> Solution studies have shown that electron transfer can occur between zinc metalloporphyrins and Ru(bpy)<sub>3</sub><sup>2+</sup> through fluorescence quenching<sup>80</sup> Quenching was not efficient for free base porphyrins as quenching only occurs through co-ordination of the Ru(II) unit to the porphyrin centre *via* the zinc atom The pathway for fluorescence quenching in these systems is photoinduced electron transfer from the excited singlet state of the porphyrin to the Ru(bpy)<sub>3</sub><sup>2+</sup> moiety Other multicomponent complexes containing porphyrins and Ru(II) metal centres have been developed but excited state quenching occurs by energy transfer rather than electron transfer<sup>71,81</sup> Recently systems

containing porphyrin dyads and  $\text{Ru}(\text{bpy})_3^{2+}$  have been prepared in which fluorescence quenching was observed through electron transfer processes<sup>82</sup> All examples of electron transfer or energy transfer, mentioned so far involve the quenching of the singlet excited states of porphyrins<sup>71 76 80</sup> However none deal with the excited state expulsion of a ligand at sites remote from the porphyrin chromophore as a quenching mechanism

Co-ordination of a metal carbonyl fragment to a porphyrin leads to a system, which can be readily investigated to determine the extent of electron or energy transfer between the two by using the extensive data for the excited states of porphyrins and metal carbonyl compounds<sup>1</sup> A number of metal carbonyl centres porphyrins have appeared in the literature but surprisingly few have actually been studied photochemically

Aspley *et al* synthesised a porphyrin metal carbonyl complex in order to investigate the intramolecular photochemical interaction between the chromophore and the metal unit<sup>83</sup> The porphyrin was linked to the metal pentacarbonyl moiety *via* a phenyl ring adjoined to a nicotinamide or an isonicotinamide ligand Metal carbonyl compounds have their own photochemistry which can be analysed in the IR This can be useful in indicating changes at a site remote from the porphyrin A series of metalloporphyrin and free base porphyrins linked to a tungsten pentacarbonyl moiety *via* a nicotinamide and a isonicotinamide linker were synthesised Excited state spectra were dominated by the presence of intense porphyrin transitions with no evidence of tungsten based MLCT bands<sup>1,21,84</sup> Nevertheless photodissociation of  $\text{W}(\text{CO})_5$  was reported upon irradiation of the complex in a solution of THF at  $\lambda_{\text{exc}} > 495 \text{ nm}$  At this wavelength the porphyrin absorption dominates Evidence for loss of the  $\text{W}(\text{CO})_5$  fragment and formation of  $\text{W}(\text{CO})_5\text{THF}$  was seen in the IR as new absorptions were recorded at 2075, 1929 and 1890  $\text{cm}^{-1}$  for  $\text{W}(\text{CO})_5\text{THF}$ , (the porphyrin tungsten pentacarbonyl complex has IR stretches at 2071, 1930 and 1901  $\text{cm}^{-1}$ ) The only other example of a reported metal pentacarbonyl porphyrin complex is where  $\text{W}(\text{CO})_5$  co-ordinated *via* a phosphorus atom, but no photochemistry was carried out<sup>85</sup>

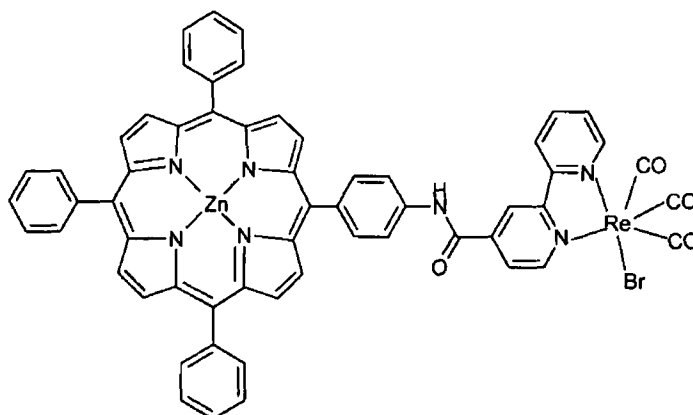


**Fig 2.5 Zinc 5[4-(4-methyl-2, 2-bipyridyl-4-carboxamidyl) phenyl]-Re(CO)<sub>3</sub>Br-10-15-20-triphenylporphyrin**

A more interesting system involved the low energy excitation of a Re(CO)<sub>3</sub>bpy porphyrin (see Figure 2.5). Excitation of this complex resulted in the loss of a ligand on the Re metal at a site remote from the chromophore.<sup>86</sup> Initial results showed a 50% reduction in the fluorescence intensity for this compound with respect to the porphyrin but no change in the structure of the complex.<sup>87</sup> However, conversion of the complex to a salt of OFT resulted in the desired photosubstitution at irradiation  $\lambda_{exc} > 495$  nm due to photoinduced electron transfer from the porphyrin to the Re metal centre. Again excitation occurs through absorption by the porphyrin moiety. Results were confirmed by changes in the IR spectra. Irradiation of the isolated Re(CO)<sub>3</sub>bpy ligand, at  $\lambda_{exc} > 495$  nm yielded no evidence of CO loss.<sup>88</sup>

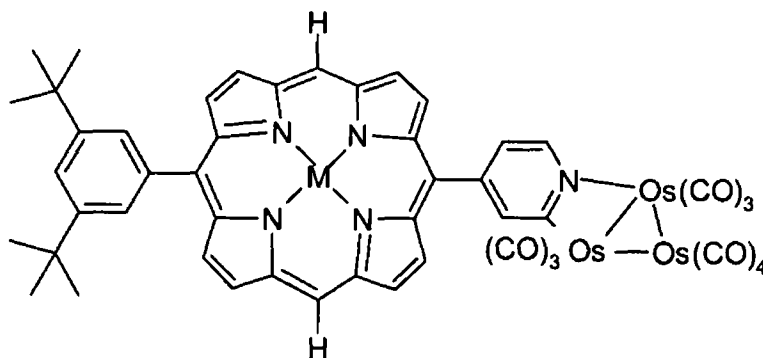


**Fig. 2.6 Triosmium cluster zinc porphyrin derivative**

Gogan *et al* were the first to synthesise carbonyl porphyrins containing the Zn(II)TPP and Cr(CO)<sub>3</sub> fragments<sup>89</sup> Comparison of the infrared spectrum of the porphyrin complexes with that of C<sub>6</sub>H<sub>6</sub>Cr(CO)<sub>3</sub> led the author to the conclusion that the product was a mixture of mono- and di-substituted porphyrin i.e C<sub>6</sub>H<sub>6</sub>Cr(CO)<sub>3</sub> and C<sub>6</sub>H<sub>6</sub>Cr((CO)<sub>3</sub>)<sub>2</sub> Crystal structures were not obtained because the samples decomposed readily in solution to form Zn(II)TPP<sup>89</sup>

Complexation of triosmium clusters containing carbonyl ligands to pyridyl metalloporphyrin gives heterometallic derivatives that contain the overall spectroscopic properties of the porphyrin fragment while incorporating the electronic and structural characteristics of the osmium cluster (see Figure 2.6)<sup>90</sup>

Interest in multi-porphyrin assemblies that can mimic the naturally occurring multichromophore aggregates in photosynthesis have recently led to the formation of porphyrin squares such as that shown in Figure 2.7 The use of metal carbonyl centres to form porphyrin squares has also been investigated (see Figure 2.7) Re(CO)<sub>3</sub> was used as the corner unit in a tetra *trans* pyridyl porphyrin array<sup>91</sup> The formation of the square introduced a bathochromic shift in the UV-vis spectrum of ca 6 nm, typical of a net removal of electron density from the  $\pi$  system of the porphyrin ring<sup>53</sup> The fluorescence spectrum of the assembly had the profile of the uncomplexed porphyrin, however formation of the square assembly resulted in a 90% reduction in emission intensity

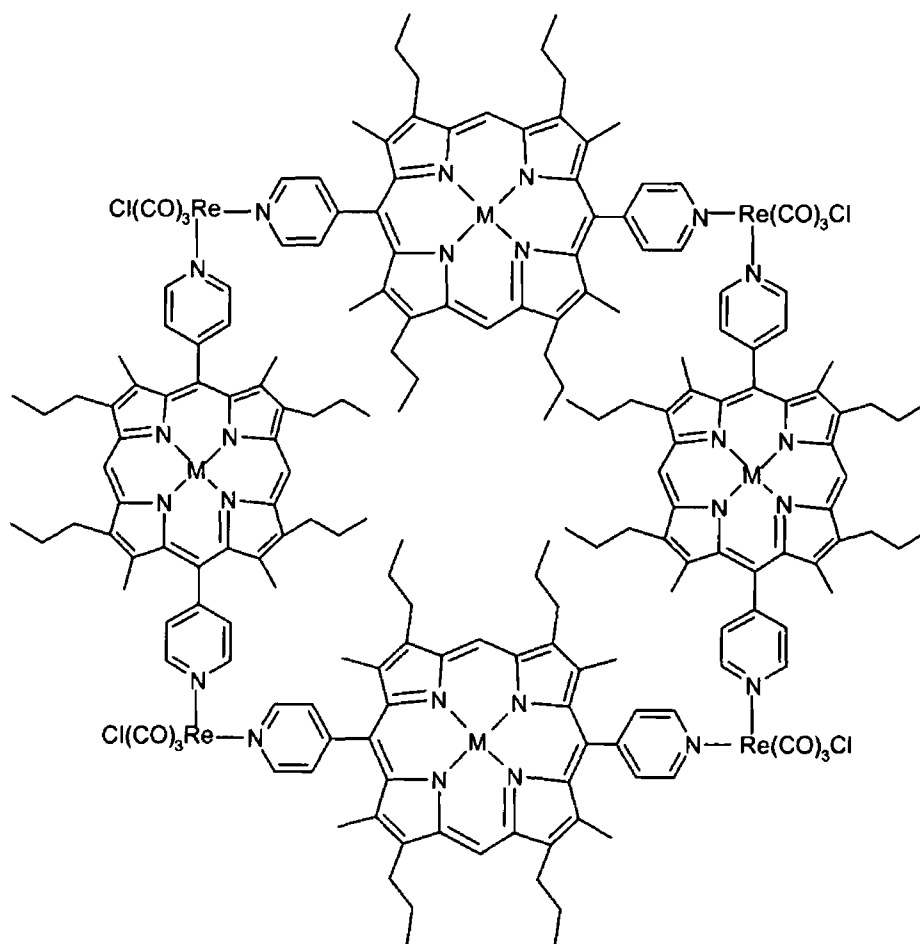


**Figure 2.7 (2, 8, 12, 18)-tetra butyl-3, 7, 13, 17-tetra methyl-5, 15-bis-(4-pyridyl) porphyrin  $[Re(CO)_3Cl]_4$**

Stang *et al* formed porphyrin squares similar to that in Figure 2.7 however instead of using Re as the corner unit they used Pt(II) and Pd(II) linkages<sup>92-93</sup> Palladium(II) dichloride units and *cis*- and *trans*-pyridyl porphyrins were used by Dram and co-workers to produce a 21 member array consisting of twelve Pd(II)Cl<sub>2</sub> components and nine porphyrin rings<sup>94</sup> While Stang found a 30-60% drop in fluorescence intensity the twenty one member array produced a 90% reduction in the fluorescence quantum yield. The singlet excited state lifetime was reduced from 12 ns in the free porphyrin to 1 ns for the array. Other porphyrin squares have been synthesised but the aims were purely structural and no photochemistry was carried out<sup>95</sup> Yuan *et al* found that Pd(II) and Pt(II) were excellent co-ordination points in the design of multi-porphyrin squares. Re(CO)<sub>3</sub>Cl has

been used as a bridging ligand between two *cis*-pyridyl porphyrins in order to investigate the energy transfer between the porphyrin dimers<sup>96</sup> Complexation of Re(I) to the porphyrin showed no changes in the intensities of the Q bands indicating little electronic effect<sup>21</sup> Absorption and emission bands were shifted by 6 nm which is consistent with net removal of electron density from the porphyrin  $\pi$  system upon rhenium-pyridine bond formation<sup>91</sup> Quantum yields and singlet state lifetimes are reduced (a typical reduction in singlet lifetime is from 8.7 ns for the free base porphyrin to 4.1 ns for an equivalent dimer) These are consistent with fluorescence emission from free base and metalloporphyrins<sup>1</sup> The use of metals as linkages is beneficial, as unlike organic components they remain rigid, although metal centres can result in the porphyrins becoming weakly or non-fluorescent (ferrocene porphyrins), as discussed

As the photophysical and photochemical properties of porphyrins were better understood more elaborate and complex systems were needed and designed to develop a model closer in structure to that involved in photochemistry in nature

## 2.4 Supramolecular assemblies incorporating multiporphyrinic arrays

Covalently linked multifunctional porphyrin arrays are important in the design of systems capable of mimicking photosynthesis.<sup>2</sup> Covalent bonds between a donor and acceptor can provide an efficient pathway for electron transfer interactions over a long distance. In order to mimic the charge separation process of photosynthesis, numerous dyads involving porphyrins have been synthesised and their properties investigated.<sup>5, 51, 54</sup> These systems have been further developed and have led to the formation of more complex arrays such as triads, which consist of a primary electron donor in the excited state ( $D_1^*$ ), a second electron donor ( $D_2$ ) and an electron acceptor (A), (see Scheme 2.4)<sup>97</sup>

### Scheme 2.4



Rotaxanes are one of the most studied systems in this area of porphyrin chemistry. Porphyrin containing rotaxanes consist of two porphyrins covalently linked *via* a phenanthroline spacer and the components of the macrocycle can move relative to each other even though they are mechanically interlocked (see Figure 2.8). Sauvage *et al.* have undertaken extensive studies in this area.<sup>6, 98</sup> Initial studies carried out involved an array consisting of a zinc/free base porphyrin connected *via* a phenanthroline spacer to a gold porphyrin.<sup>99</sup> Selective excitation of the individual porphyrins and comparison with porphyrin monomers provides information on the electron transfer process in the system.<sup>25, 26</sup> Excitation of the systems through the zinc/free base porphyrin resulted in significant quenching of their singlet states, 97% and 80% respectively. Both systems showed large reductions in intersystem crossing efficiently leading to a reduction in triplet excited state formation. This can be explained by the formation of a charge transfer species consisting of a  $\pi$  radical cation for the zinc porphyrin and a neutral gold porphyrin subunit formed by electron transfer from the excited porphyrin. This has the effect of reducing the lifetime of the singlet excited states. The presence of a heavy atom in the gold porphyrin subunit allowed for efficient intersystem crossing to the triplet

excited state upon excitation of the complex. Very little fluorescence was observed, even at room temperature when intersystem crossing was not as prominent<sup>100</sup>

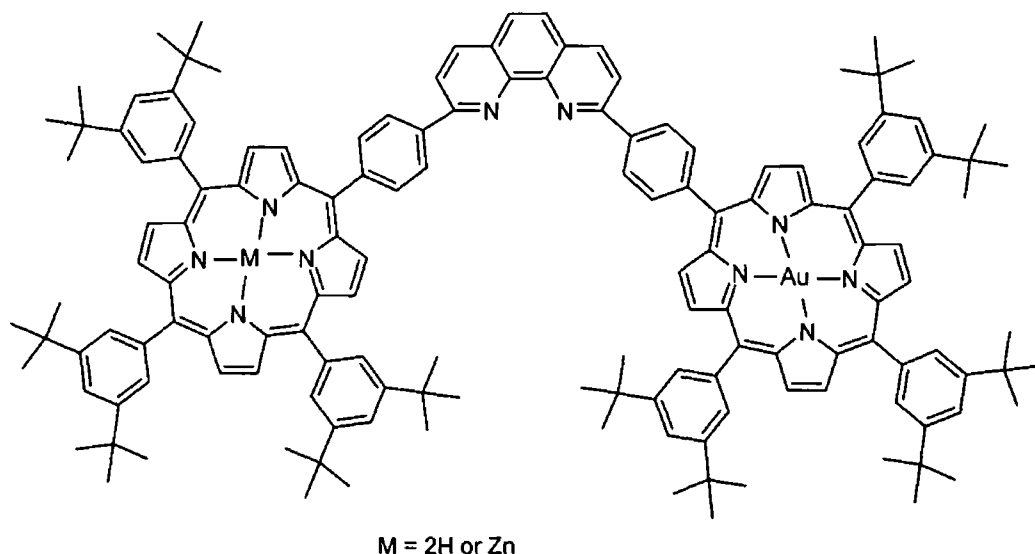


**Figure 2.8 Porphyrin rotaxane consisting of a free base porphyrin and gold porphyrin linked via a phenanthroline thread**

Synthesis of the porphyrin in Figure 2.8 with a central copper atom coordinated to the phenanthroline unit (Copper(I) bis(1,10)-phenanthroline) gave rise to a complex whose rate of forward electron transfer from the free base/zinc porphyrin to the gold porphyrin was dramatically increased. Given in Table 2.9 are the different lifetimes for the individual electron transfer steps<sup>101</sup>. The rate of the reverse reaction was unaffected by the presence of the copper atom.

The diphenyl phenanthroline linker acts as a superexchange medium and is a good conducting medium for electron transfer *via* a through bond pathway. Co-ordination of a Cu(I) metal into the ligand centre has the effect of decreasing the energy gap between the zinc porphyrin and diphenyl phenanthroline by reducing the energy of the LUMO of the diphenyl phenanthroline while keeping it above the HOMO of the zinc porphyrin unit. The reverse electron transfer reaction was unaffected as the energy gap between the HOMO of the gold porphyrin and the LUMO of diphenyl phenanthroline was too high in energy to be affected to a large extent by the co-ordination of a Cu(I) metal<sup>101,102</sup>

| <i>Porphyrin complex</i>                                                  | <i>k/10<sup>8</sup>(s<sup>-1</sup>)</i> |
|---------------------------------------------------------------------------|-----------------------------------------|
| $(^*ZnP)-(AuP^+) \rightarrow (^*ZnP)-(AuP^{\bullet})$                     | 178                                     |
| $(^*ZnP)-(AuP^{\bullet}) \rightarrow (ZnP)-(AuP^+)$                       | 17                                      |
| $(^*ZnP)-(AuP^+)^{\bullet} \rightarrow (^*ZnP)-(AuP^{\bullet})$           | 76                                      |
| $(^*ZnP)-Cu^+-(AuP^+) \rightarrow (^*ZnP)-Cu^+-(AuP^{\bullet})$           | >10000                                  |
| $(^*ZnP)-Cu^+-(AuP^{\bullet}) \rightarrow (ZnP)-Cu^+-(AuP^+)$             | 20                                      |
| $(^*ZnP)-Cu^+-(AuP^+)^{\bullet} \rightarrow (^*ZnP)-Cu^+-(AuP^{\bullet})$ | 530                                     |

**Table 2.9 Rate constants for the various electron transfer steps for multicomponent systems (ref. 100 and 101)**

Covalently linked donor-acceptor *meso* porphyrins systems have been designed in an effort to promote electron transfer<sup>103</sup> Unlike the systems discussed in the previous section this series of multiporphyrinic arrays have been linked by a series of non-metallic aromatic hydrocarbons and unsaturated chains including substituted benzene and polyenes i.e. they do not contain a metal centred linkage Bridging porphyrins using only  $\pi$ -conjugated linkers are used to determine the effect of covalent electron exchange interactions more closely by using different chain lengths Porphyrin chains containing up to 128 porphyrin subunits have been designed<sup>7</sup> Unlike the UV-vis spectrum of metal linked porphyrins the UV-vis spectrum of these covalently linked porphyrins are a sum of the individual subunits, which allows for selective excitation of individual components A sequence of zinc porphyrins linked to an iron porphyrin *via* a number of substituted phenyl and diphenyl rings showed distance dependence charge separation constants while the charge recombination rate constants were independent of distance<sup>104</sup> This was expected as the interaction of the porphyrins in the S<sub>1</sub> state was weak, indicated by their UV-vis spectra, which could be described in terms of a superposition of the individual spectra of the monomers However when Strachan *et al* studied the electron transfer process between a free base porphyrin and a zinc porphyrin linked by diphenylpolyene and diphenylpolyne bridges, the distance dependency of the systems was quite small and could be explained by the Dexter mechanism, which was the dominant mechanism

involved in the electron exchange interaction across the  $\pi$ -bridges<sup>105</sup> The geometries of the systems had a large effect on the extent of the interaction between the porphyrins with an enforced face-to-face geometry having the strongest electron interactions (using phenyl linkers substituted at the *meta/ortho* position)

In each of the bridged porphyrins discussed, fluorescence emission was observed from the free base porphyrin Trimeric porphyrin systems consisting of zinc porphyrins linked by phenyl and phenylpolyene spacers exhibited singlet-to-singlet electron transfer across the spacer showing an interaction similar to that of the zinc/free base porphyrin dimers<sup>101,102</sup> The geometry of porphyrin chains has expanded considerably in recent years because of developments in synthetic techniques, which have been used to produce arrays consisting of six porphyrin units These porphyrins in turn can be coupled directly to each other<sup>106</sup> These *meso* linked porphyrins show properties similar to that of the individual component because of the poor communication through the orthogonal geometry of the array The arrangement of the array prevents the formation of a “stacked energy sink” and this should allow for high efficient energy transfer over a long distance<sup>108</sup> The Z1 (Z = Zn(II)-5,15-diarylporphyrin) monomer exhibits a fluorescence spectrum typical of Zn(II) porphyrins while increasing the length of the chain (i.e. di(Zn(II)-5,15-diarylporphyrin), Z3-tri(Zn(II)-5,15-diarylporphyrin) and tetra(Zn(II)-5,15-diarylporphyrin)) causes a red shift in the emission maxima The shift increases with the number of porphyrin groups attached The fluorescence quantum yield for these systems was determined and compared to that of Zn(II)TPP ( $\Phi_f$  of 0.03)<sup>107</sup> The fluorescence quantum yield increased up to arrays of 16 porphyrins but was reduced when the array was extended further Singlet state lifetimes also decreased as the number of porphyrin subunits in the array increased (see Table 2.10)<sup>108</sup>

An array up to a length of 128 porphyrin units has been synthesised The singlet lifetime of this rod like structure was 0.12 ns with a fluorescence quantum yield of 0.008<sup>108</sup> These directly linked porphyrin arrays are similar in structure to the natural occurring photosynthetic reaction centre and therefore are the most useful artificial light harvesting

molecular modules. However the use of self co-ordinating pyridyl porphyrins has also been investigated due to their relatively simple synthetic pathways

| <i>Compound</i> | $\Phi_f$ | $\tau$ (ns) |
|-----------------|----------|-------------|
| Z1              | 0.022    | 2.64        |
| Z2              | 0.029    | 1.94        |
| Z3              | 0.045    | 1.83        |
| Z4              | 0.060    | 1.75        |

**Table 2.10 Singlet excited state lifetimes and relative fluorescence quantum yield. Z1-Zn(II) 5,15 diarylporphyrin, Z2-di(Zn(II) 5,15 diarylporphyrin), Z3-tri(Zn(II) 5,15 diarylporphyrin) and Z4-tetra(Zn(II) 5,15 diarylporphyrin) (ref 107)**

As mentioned previously self co-ordination of pyridyl porphyrins increased the interest in porphyrin chemistry and provided a new synthetic route to form non-covalently linked multiporphyrinic oligomers.<sup>65</sup> The use of pyridyl groups as linkages has been discussed briefly in relation to the formation of porphyrin squares.<sup>93</sup> Pyridyl groups and other nitrogen containing groups have been used as linkages between porphyrins to produce side to face arrays and linear arrays, which have been investigated in relation to photoinduced electron transfer.<sup>109</sup> Co-ordination porphyrins allow for the formation of multiporphyrinic systems, which are highly flexible and allow for easy preparation of the multicomponent array while permitting good geometrical control.

One of the most thoroughly studied systems consists of a free base/zinc porphyrin covalently linked to a gold porphyrin via a ruthenium(II) bis terpyridyl unit (see Figure 2.9).<sup>110</sup> This is an extension of the system mentioned previously and allows for comparison of the covalent system (porphyrins linked via covalent bonds) to the co-ordination system (porphyrins linked via a co-ordination metal centre).<sup>98</sup> In such systems zinc porphyrins in the excited state act as the electron donor and the gold porphyrin acts as the acceptor much like the system of Zn(II) porphyrin and the crown ether with a Au<sup>3+</sup>

centre<sup>54,55</sup> In this case the porphyrin macrocycle is large enough to contain the reduced gold metal and the charge recombination process can take place relatively easily

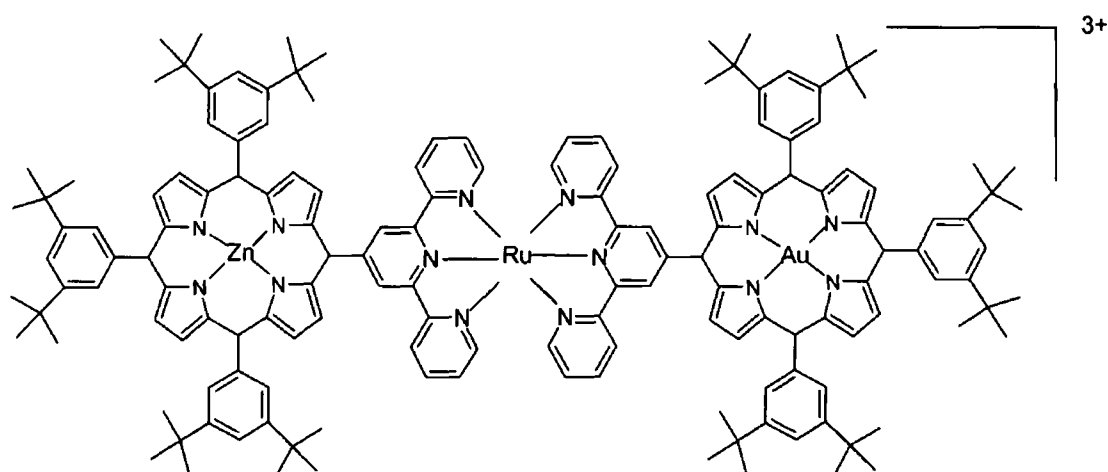


**Figure 2.9 Free base porphyrin linked to a gold porphyrin via a ruthenium(II)bis(terpyridyl) unit (see ref 109)**

This triad is a crude model for the primary interporphyrin electron transfer step in bacterial photosynthesis. Porphyrin dyads have been constructed but these triads provide a system where the terminal porphyrins and cations can be changed to allow a synthetic pathway to a family of complexes with distinctive electronic properties<sup>51,53,58</sup>. Such systems allow for excitation into any of the three subunits and prior knowledge of the individual components allows elucidation of electronic pathways in the triads.

Excitation at the ruthenium(II) MLCT absorption band (440 nm) gave rise to a weakly fluorescent signal at 640 nm (containing spectral features) due to the ruthenium(II) bis(terpyridyl) complex. The singlet state lifetime was also reduced to 220 ps from 565 ps for the ruthenium(II)bis(terpyridyl), and this is due to quenching of the triplet state of the Ru(II) centre by triplet energy transfer to the porphyrins<sup>111</sup>.

Extensive studies into the formation of the triplet state of the gold porphyrin component have been completed by laser flash photolysis where the gold porphyrin chromophore dominates<sup>99</sup>. Excitation into the gold component for all triad complexes gave triplet

lifetimes, which were comparable with the gold porphyrin monomer. Therefore triplet energy transfer from the gold porphyrin to the Ru(II) centre or terminal porphyrin component is inefficient. Energy transfer from gold porphyrins to free base and zinc porphyrins is favourable,<sup>98</sup> however the insertion of a Ru(II) metal centred ligand is ineffective in promoting electronic coupling between the two porphyrins. The Ru based excited state fails to compete with the non-radiative deactivation of the gold(III) porphyrin ( $k \approx 6.7 \times 10^8 \text{ s}^{-1}$ )

The last component of the triad is the free base or zinc metallated porphyrin. Fluorescence measurements where only the free base porphyrin absorbs gave rise to a fluorescent spectrum typical of the free base porphyrin,<sup>21</sup> the quantum yield was quenched by *ca* 15%. Upon excitation and formation of the singlet excited state of the free base porphyrin an electron is transferred to the Ru(II) complex.<sup>71</sup> Secondary electron transfer resulted in the formation of a long lived species with a lifetime of 77 ns which was attributed to the charge transfer state in which an electron was transferred from the Ru(II) centre to the appended gold(III) porphyrin (see Figure 2.10)

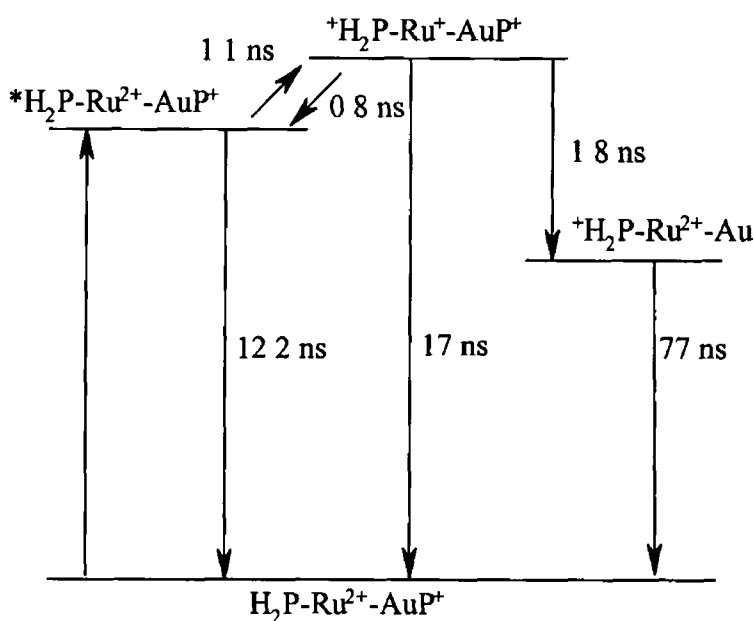


**Figure 2.10** Electron transfer processes and excited state lifetimes following excitation of free base porphyrin subunit in a bisporphyrin linked Ru(II)bis(terpyridyl) complex

Excitation of the zinc complex leads to electron transfer similar to that for the free base porphyrins (see Figure 2.11). The lifetimes of the charge transfer state were shorter than that of the free base porphyrin due to the smaller energy gap for the zinc porphyrin system.<sup>110,112</sup>

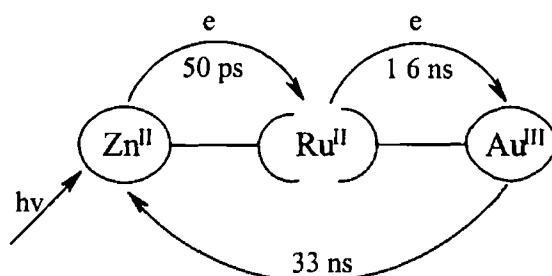


**Figure 2.11** Electron transfer process and excited state lifetimes after excitation of the zinc porphyrin subunit in bisporphyrin linked Ru(II)bis(terpyridyl) complex

Flamigni *et al* carried out extensive studies on similar complexes and found that, even in these multicomponent arrays, the photophysical properties can be described in terms of intramolecular processes between states localised on the individual components, as they retain their properties with very small perturbations.<sup>113</sup> Prodi *et al* devised a system consisting of a *tetra meso* pyridyl porphyrin adjoined to four ruthenium carbonyl porphyrins in a pentameric structure (see Figure 2.12).<sup>69</sup> They were assembled by axial co-ordination of the *meso* pyridyl groups of the free base porphyrin to the metal centre of the Ru(II) porphyrin. Again interactions were weak i.e. the energy levels of each molecular component was relatively unperturbed by intercomponent interactions.<sup>2</sup> Fluorescence originating from excitation of the free base porphyrin, was substantially weaker than that of the corresponding monomer. It was accompanied by a parallel decrease in the fluorescence lifetimes from 9.7 ns for the monomer to  $\approx 0.5$  ns for the pentameric complex.

One explanation for the decrease in singlet lifetimes was interporphyrin electron transfer. This was thought unlikely as there is a large energy gap between the electron transfer states of Ru complexes.<sup>114</sup> Another and more probable explanation is spin-orbit

perturbation (heavy atom effect) caused by the ruthenium centres, which results in intersystem crossing to the axial porphyrin<sup>115</sup> The transient absorption spectrum of the complex had none of the ruthenium porphyrin characteristics and was typical of free base porphyrins<sup>1</sup> Lifetimes of the triplet state were not significantly shorter than those of the free base monomer demonstrating once again the dominance of the free base porphyrin on the photochemistry and photophysics of multiporphyrinic structures

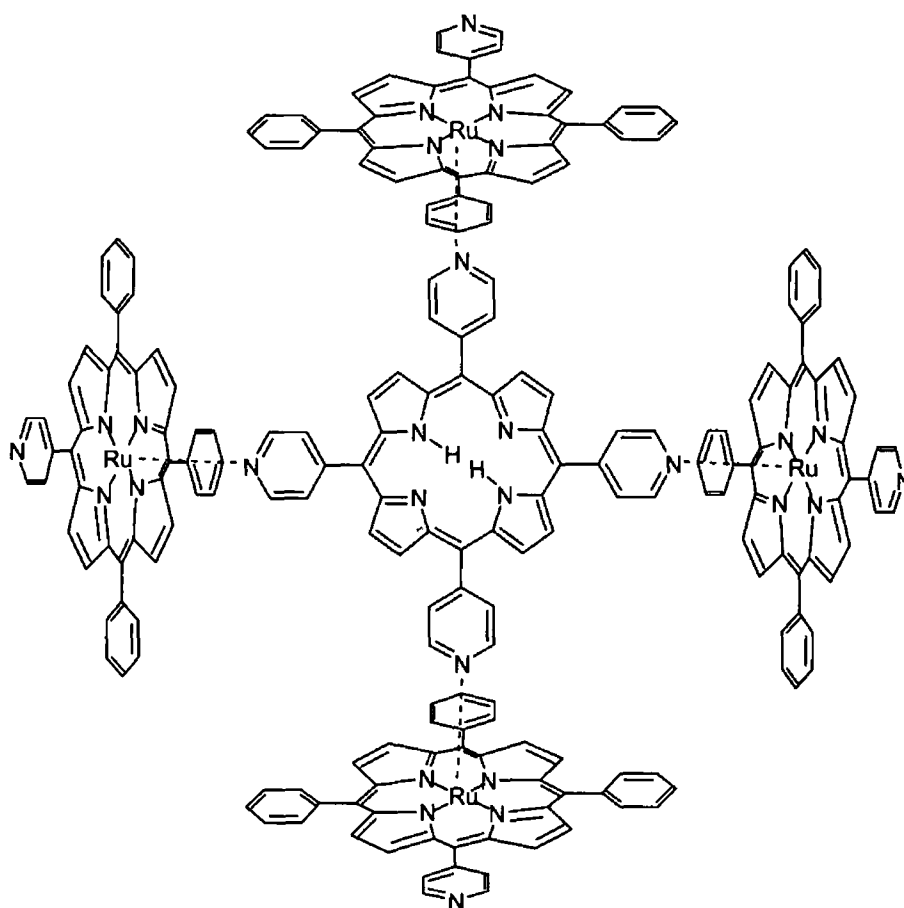


**Figure 2.12 Schematic structure of pentameric free base ruthenium porphyrin complex**

## 2.6 Conclusion

For the last fifty years the photochemistry and photophysics of porphyrins have been extensively studied in an attempt to understand the photosynthetic process in more detail. From the earliest of these experiments dealing with the effects on the UV-vis spectrum and fluorescence spectrum of the monomer due to substituents on the phenyl ring in the *meso* position to electron transfer pathways in multiporphyrinic, developments in the study of porphyrins has been rapid, in particular over the last 15 years. Before 1990 only a few examples of porphyrin systems bound to an external covalently linked transition metal based redox centre were known. The number and variety of this type of complex has increased dramatically since then with more and more researchers becoming interested in the photoinduced charge separation process used in the conversion of light energy into chemical energy. The PS<sub>I</sub> structure of cyanobacterial photosystems has been found to contain 90 chlorophylls and 22 carotenoids by which light energy is efficiently harvested and guided to the photosynthetic reaction centre. It uses well-organised supramolecular systems in which components are held at fixed positions and orientations to each other. As can be seen from the examples mentioned both covalent and non-covalent multiporphyrinic arrays provide us with systems, which have these geometries that are crucial for efficient electron transfer necessary for mimicking the photosynthetic process. Linked porphyrin arrays are examples of light harvesters, which are closest in properties to natural photosynthetic organisms and is an area which will continue to develop until the photosynthetic process has been unravelled and reproduced.

## 2 7 Bibliography

---

- 1 K Kalyanasundaram, *Photochemistry of Polypyridyl and Porphyrin Complexes*, 1992, Academic Press, London
- 2 V Balzani, F Scandola, *Supramolecular photochemistry*, 1991, Ellis Horwood, Chichester
- 3 I I Dilung, E I Kapinus, *Russian Chemical Review*, 1978, 47, 43
- 4 N M Rowley, S S Kurek, M W George, S M Hubig, P D Beer, C J Jones, J M Kelly, J A McCleverty, *J Chem Soc , Chem Commun* , 1992, 497
- 5 N M Rowley, S S Kurek, P R Ashton, T A Hamor, C J Jones, N Spencer, J A McCleverty, G S Beddard, T E Feehan, N T H White, E J L McInnes, N N Paynes, L J Yellowlees, *Inorg Chem* , 1996, 35, 7526
- 6 M J Blanco, M C Jimenez, J C Cambron, V Heitz, M Linke, J P Sauvage, *Chem Soc Rev* , 1999, 28, 293
- 7 Y H Kim, D H Jeong, D Kim, S C Jeoung, H S Cho, S K Kim, N Aratani, A Osuka, *J Am Chem Soc* , 2001, 123, 76
- 8 P Rothemund, *J Am Chem Soc* , 1941, 63, 267
- 9 P Rothemund, *J Am Chem Soc* , 1948, 70, 1808
- 10 G D Dorough, J R Miller, F M Heunneken, *J Am Chem Soc* , 1951, 73, 4315
- 11 H Lmschitz, K Sarkanen, *J Am Chem Soc* , 1958, 80, 4826
- 12 H Linschitz, L Pekkarinen, *J Am Chem Soc* , 1960, 82, 2407
- 13 R Livingston, E Fujimori, *J Am Chem Soc* , 1958, 80, 5610
- 14 H Lmschitz, L Pekkarinen, *J Am Chem Soc* , 1960, 82, 2411
- 15 E Livingston, D W Tanner, *Trans Faraday Soc* , 1958, 54, 765
- 16 J R Darwent, P Douglas, A Harriman, G Porter, M C Richoux, *Coord Chem Rev* , 1982, 44, 83
- 17 E B Fleicher, *J Am Chem Soc* , 1963, 85, 1353
- 18 A D Alder, F R Longo, J D Finarelli, *J Org Chem* , 1967, 32, 476
- 19 M Moet-Ner, A D Alder, *J Am Chem Soc* , 1975, 97, 5107
- 20 D J Qumby, F R Longo, *J Am Chem Soc* , 1975, 97, 5111

- 
- 21 K Kalyanasundaram, *Inorg Chem* , 1984, 23, 2453
  - 22 R A Freitag, D G Whitten, *J Phys Chem* , 1983, 87, 3918
  - 23 R A Freitag, J A Mercer-Smith, D G Whitten, *J Am Chem Soc* , 1981, 103, 1981
  - 24 P G Seybold, M Gouterman, *J Mol Spectrosc* , 1969, 31, 1
  - 25 A Harriman, *J Chem Soc , Faradays Trans 1* , 1980, 76, 1978
  - 26 A Harriman, *J Chem Soc , Faradays Trans 2* , 1981, 77, 1281
  - 27 A Harriman, *J Chem Soc , Faradays Trans 2* , 1981, 78, 2727
  - 28 M Gouterman, L K Hanson, G E Khalil, J W Buchler, K Rohbock, D Dolphin, *J Am Chem Soc* , 1975, 97, 3142
  - 29 K Kalyanasundaram, *J Chem Soc , Faraday Trans 2* , 1983, 79, 1365
  - 30 A Harriman, R J Hosie, *J Chem Soc , Faraday Trans 2* , 1982, 77, 1695
  - 31 R Livingston, V A Ryan, *J Am Chem Soc* , 1958, 75, 2176
  - 32 K Kalyanasundaram, M Neumann-Spallart, *J Phys Chem* , 1982, 86, 5163
  - 33 K Kalyanasundaram, *Chem Phys Lett* , 1984, 104, 357
  - 34 N Nappa, J S Valentine, *J Am, Chem Soc* , 1978, 100, 5075
  - 35 D F Rohrbach, E Deustsch, W R Heinman, R F Pasternack, *Inorg Chem* , 1977, 16, 2650
  - 36 R D Chapman, E B Fleischer, *J Am Chem Soc* , 1982, 104, 1575
  - 37 A Harriman, G Porter, A Wilowska, *J Chem Soc , Faradays Trans 2* , 1983, 79, 807
  - 38 M A Bergkamp, J Dalton, T Netzel, *J Am Chem Soc* , 1982, 104, 253
  - 39 J S Connolly, J R Bolton in *Photoinduced electron transfer, Part D*, 1988, Elsevier, Amsterdam
  - 40 H Linschitz, J Renner, *Nature*, 1952, 169, 193
  - 41 A Harriman, G Porter, N Searle, *J Chem Soc , Faradays Trans , 2* , 1979, 75, 1515
  - 42 M R Wasielewski, M P Niemczyk, W A Svec, E P Pewitt, *J Am Chem Soc* , 1985, 55, 2327
  - 43 J K Ray, F A Carroll, D G Whitten, *J Am Chem Soc* , 1974, 96, 6349

- 
- 44 D G Whitten, J C Yau, F A Carroll, *J Am Chem Soc* , 1971, 92, 2291
- 45 M R Wasielewski, M P Niemczyk, W A Svec, E P Pewitt, *J Am Chem Soc* , 1985, 107, 1080
- 46 A D Joran, B A Leland, G G Geller, J L Hopfield, P B Dervan, *J Am Chem Soc* , 1984, 106, 6090
- 47 M R Wasielewski, D G Johnson, W A Svec, K M Kersey, D E Cragg, D W Minsek, in *Photochemical energy conversion*, 1989, Elsevier, pg 135
- 48 G S Cox, D G Whitten, *J Am Chem Soc* , 1982, 104, 516
- 49 G S Cox, C Bobillier, D G Whitten, *Photochem Photobiol* , 1982, 36, 401
- 50 J P Keene, D Kessel, E J Land, R W Redmond, T G Truscott, *Photochem Photobiol* , 1986, 43, 118
- 51 E S Schmidt, T S Calderwood, T C Bruce, *Inorg Chem* , 1986, 25, 3718
- 52 A D Hamilton, H D Rubin, A B Bocarsly, *J Am Chem Soc* , 1984, 106, 7255
- 53 N M Rowley, S S Kurek, J-D Foulon, T A Hamor, C J Jones, J A McCleverty, S M Hubig, E J L McInnes, N N Paynes, L J Yellowlees, *Inorg Chem* , 1995, 34, 4414
- 54 G Blondeel, A Harriman, G Porter, A Wilowska, *J Chem Soc , Faradays Trans* , 1984, 80, 867
- 55 T Lyoda, M Morimoto, N Kawasaki, T Shimidzu, *J Chem Soc , Chem Commun* , 1991, 1480
- 56 J Martensson, K Sandros, O Wennerstrom, *J Phys Org Chem* , 1994, 7, 534
- 57 M R Wasielewski, M P Niemczyk, W A Svec, E P Pewitt, *J Am Chem Soc* , 1985, 107, 1080
- 58 M Gubelmann, A Harriman, J M Lehn, J L Sessler, *J Phys Chem* , 1990, 94, 208
- 59 M Gubelmann, A Harriman, J M Lehn, J L Sessler, *J Chem Soc , Chem Commun* , 1988, 77
- 60 R J Harrison, B Pearce, G S Beddard, J A Cowan, J K M Sanders, *Chem Phys* , 1987, 116, 429

- 
- 61 J A McCleverty, *Chem Soc Rev* , **1983**, *12*, 331
- 62 J A McCleverty, G Denti, S J Reynolds, A S Drane, N El Murr, A E Rae, N A Bailey, H Adams, J M A Smith, *J Chem Soc , Dalton Trans* , **1983**, 81
- 63 S L W McWhinnie, C J Jones, J A McCleverty, T A Hamor, J D Foulon, *Polyhedron*, **1993**, *12*, 37
- 64 A M Shachter, F B Fleischer, R C Haltiwanger, *J Chem Soc , Chem Commun* , **1988**, 960
- 65 F B Fleischer, A M Shachter, *Inorg Chem* , **1991**, *30*, 3763
- 66 M J Ginter, G M McLaughlin, K J Berry, K S Murray, M Irvimg, P E Clark, *Inorg Chem* , **1984**, *23*, 283
- 67 H E Toma, K Araki, *J Photochem Photobiol , A*, **1994**, *83*, 245
- 68 E Alessio, M Macchi, S Heath, L G Marzilli, *Inorg Chem* , **1997**, *36*, 5614
- 69 A Prodi, M T Indelli, C J Kleverlaan, F Scandola, E Alessio, L G Marzilli, *Chem Eur J* , **1999**, *5*, 2668
- 70 A Prodi, C J Kleverlaan, M T Indelli, F Scandola, *Inorg Chem* , **2001**, *40*, 3498
- 71 L Flamigni, N Armaroli, F , V Balzani, J P Collins, J O Dalbavie, V Heitz, J P Sauvage, *J Phys Chem* , **1997**, *101*, 5936
- 72 F M Engelmann, P Losco, H Winnischofer, K Araki, H E Toma, *J Porph and Phthalo* , **2002**, *6*, 33
- 73 J M Zaleski, C K Chang, G E Leroi, R I Cukier, D G Nocera, *J Am Chem Soc* , **1992**, *114*, 3564
- 74 H Winnischofer, F M Engelmann, H E Toma, K Araki, H R Rechenberg, *Inorg Chim Acta* , **2002**, *190*, 1
- 75 P Hambright, E B Fleischer, *Inorg Chem* , **1970**, *9*, 1757
- 76 K Araki, H E Toma, *J Coord Chem* , **1993**, *30*, 9
- 77 H E Toma, E Stradler, *Inorg Chem* , **1985**, *24*, 3085
- 78 J L Sessler, B Wang, A Harriman, *J Am Chem Soc* , **1995**, *117*, 704
- 79 C A Hunter, R K Hyde, *Angew Chem , Int Ed Engl* , **1996**, *35*, 1936
- 80 E J Shin, D Kim, *J of Photochem and Photobiol A* , **2002**, *91*, 1

- 
- 81 A Harriman, M Hissler, O Trompete, R Ziessel, *J Am Chem Soc* , 1999, 121, 2516
- 82 D LeGourrieree, M Anderson, J Davidson, E Mukhtar, L Sun, L Hammarstrom, *J Phys Chem A*, 1999, 103, 557
- 83 C J Aspley, J R Lindsay Smith, R N Perutz, D Pursche, *J Chem Soc , Dalton Trans* , 2002, 170
- 84 J S Lindsey, J K Delaney, D C, Mauzerall, H Linschitz, *J Am Chem Soc* , 1988, 110, 3610
- 85 G Markl, M Reiss, P Kreitmeier, H Noth, *Angew Chem Int Ed Engl* , 1995, 34, 2230
- 86 A Gabrielsson, F Hartl, J R Lindsey Smith, R N Perutz, *J Chem Soc , Chem Commun* , 2002, 950
- 87 C J Aspley, J R Lindsey, R N Perutz, *J Chem Soc , Dalton Trans* , 1999, 2269
- 88 W Kaim, S Kohlmann, *Inorg Chem* , 1990, 29, 2909
- 89 N J Gogan, Z U Siddiqui, *Can J Chem* , 1972, 50, 720
- 90 S L Darling, P K Y Goh, N Bampos, N Feeder, M Montalti, L Prodi, B F G Johnson, J K M Sanders, *Chem Commun*, 1998, 2031
- 91 R V Slone, J T Hupp, *Inorg Chem* , 1997, 36, 5422
- 92 P J Stang, J Fan, B Olenyuk, *Chem Commun* , 1997, 1453
- 93 J Fan, J A Whiteford, B Olenyuk, M D Levin, P J Stang, E B Fleischer, *J Am Chem Soc* , 1999, 121, 2741
- 94 C Drain, J M Lehn, *J Chem Soc , Chem Commun* , 1994, 2313
- 95 H Yuan, L Thomas, L K Woo, *Inorg Chem* , 1996, 35, 2808
- 96 K E Splan, M H Keefe, A M Massari, K A Walters, J T Hupp, *Inorg Chem* , 2002, 41, 619
- 97 S Chardon-Noblat, J P Sauvage, P Mathis, *Angew Chem Int Ed Eng* , 1989, 593
- 98 J C Chambron, J P Collin, J O Dalbavie, C O Dietrich-Buchecker, V Heitz, F Odobel, N Solladie, J P Sauvage, *Coord Chem Rev* , 1998, 178, 1299

- 
- 99 A M Brun, A Harriman, V Heitz, J P Sauvage, *J Am Chem Soc* , 1991, 113, 8657
- 100 A Antipas, D Dolphin, M Goutermann, E C Johnson, *J Am Chem Soc* , 1978, 100, 7705
- 101 J C Chambron, A Harriman, V Heitz, J P Sauvage, *J Am Chem Soc* , 1993, 115, 6109
- 102 J C Chambron, A Harriman, V Heitz, J P Sauvage, *J Am Chem Soc* , 1993, 115, 7419
- 103 A Osuka, , G Noya, S Tamguchi, T Okada, Y Nishimura, I Yamazaki, N Mataga, *Chem Eur J* , 2000, 6, 33
- 104 A Osuka, K Maruyama, N Mataga, T Asahi, I Yamazaki, N Tmai, *J Am Chem Soc* , 1990, 112, 4958
- 105 J P Strachan, S Gentemann, J Seth, W A Kalsbeck, J S Lindsey, D Holten, D F Bocian, *Inorg Chem* , 1998, 37, 1191
- 106 A Nakano, A Osuka, T Yamazaki, Y Nishimura, S Akimoto, I Yamazaki, A Itaya, M Murakami, H Miyasaka, *Chem Eur J* , 2001, 7, 3134
- 107 P G Seybold, M Goutermann, *J Mol Spectrom*, 1969, 31, 1
- 108 N Aratani, A Osuka, H S Cho, D Kim, *J of Photochem And Photobiol* , C *Photochem Rev* , 2002, 3, 25
- 109 T Imamura, K Fukushima, *Coord Chem Rev* , 2000, 198, 133
- 110 A Harriman, F Obodel, J P Sauvage, *J Am Chem Soc* , 1995, 117, 9461
- 111 J P Collins, A Harriman, V Heitz, F Odobel, J P Sauvage, *J Am Chem Soc* , 1994, 116, 5679
- 112 F Obodel, J P Sauvage, *New J Chem* , 1994, 18, 1139
- 113 L Flamigni, F Barigelletti, N Armaroli, J P Collin, J P Sauvage, J A Gareth Williams, *Chem Eur J* , 1998, 4, 1744
- 114 S Anderson, H L Anderson, A Bashall, M McPartlin, J K M Sanders, *Angew Chem* , 1995, 106, 1196
- 115 C M Drain, F Nifiatis, A Vasenko, J D Batteas, *Angew Chem Int Ed* , 1998, 37, 2344

## **Chapter 3**

### ***5-Mono 4-pyridyl 10, 15, 20-triphenyl* porphyrin and its tungsten and chromium pentacarbonyl complexes - Results and discussion**

### 3 1 Introduction

Porphyrin type components have been studied widely in multicomponent systems in which photoinduced electron or energy transfer occurs, as porphyrins are efficient light absorbing molecules that absorb strongly in the visible spectral region. Porphyrins are an important tool in the understanding and development of more advanced artificial photochemical systems capable of converting solar energy into electricity or fuels<sup>1,2,3</sup>. Previous studies have investigated the photochemistry and photophysics of metalloporphyrins (porphyrins co-ordinated at the centre by transition metals)<sup>4</sup>. Porphyrins have also been used as electron donors in many multicomponent systems containing transition metal fragments<sup>5</sup>. These studies also investigate the communication between the porphyrin and the metal centre. What is less known is the effect that a metal carbonyl has upon the photochemical and photophysical properties when bound directly to the peripheral part of the porphyrin.

Within the development of metal carbonyl porphyrins, pyridyl porphyrins are considered to be particularly attractive as a building block due to the co-ordination ability of the nitrogen atom<sup>6,7,8</sup>. In this chapter the use of *meso* substituted *mono* substituted pyridyl porphyrins as a model for electron or energy transfer process is discussed. The available nitrogen donor atom on the pyridyl group provides a convenient route to the co-ordination of a metal containing fragment to the porphyrin macrocycle while maintaining the useful spectroscopic, photophysical and photochemical properties of a *tetra* aryl porphyrin. Adducts obtained by peripheral co-ordination of a metal fragment to a porphyrin have potentially interesting photochemical and photophysical properties of the porphyrin, however as yet there have only been a few reports on the co-ordination of metal carbonyl fragments to a porphyrin of this type<sup>9</sup>.

These studies are primarily concerned with profiling the photophysics and photochemistry of electron and/or energy transfer processes between the absorbing site (porphyrin) and the actual centre acting as an electron acceptor or energy site. Less well studied are systems, which use the absorbed energy to perform a chemical transformation

such as a bond breaking or isomerisation. In this work the ability of a porphyrin to transfer energy to a metal carbonyl fragment (i.e.  $M(CO)_5$  where  $M = W/Cr$ ) is investigated. The metal carbonyl moiety was attached *via* a pyridyl linker and it was hoped to monitor the efficiency at which electron or energy transfer occurs across  $\pi$ -substituents, such substituents are orthogonal to the *meso* position of the porphyrin ring (see Fig 3.1). Another important feature of the metal carbonyl porphyrin system is the availability of intense  $\nu_{CO}$  absorption in the IR spectrum that provides a useful additional spectroscopic handle. The interaction between the porphyrin chromophore and the metal carbonyl moiety was investigated in the ground state by UV-vis,  $^1H$  NMR and IR spectroscopies as well as in the excited state by using photochemical studies, fluorescence spectroscopy, singlet and triplet lifetimes and quantum yield determinations.

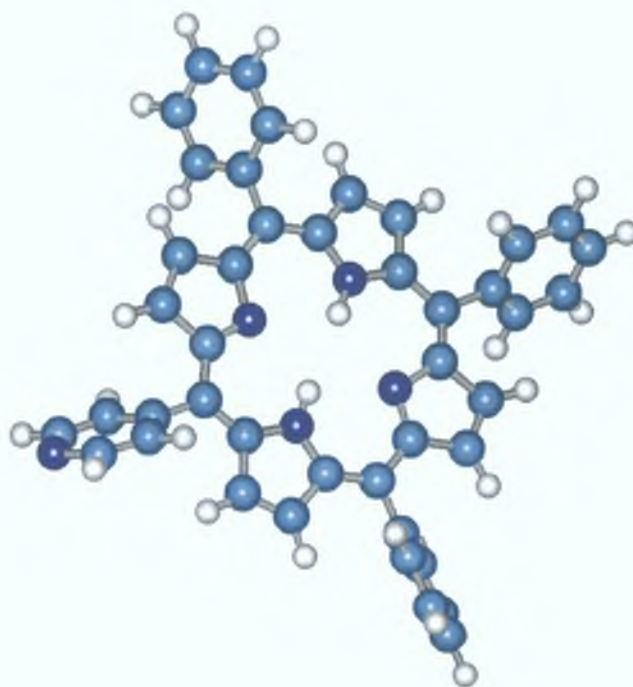


***Fig 3.1 Diagram of 5-mono 4-pyridyl 10,15,20-triphenyl porphyrin (MPyTPP) demonstrating that the plane of the aryl groups in the meso position are orthogonal to the plane of the porphyrin ring (dark blue atoms are nitrogen atoms while the lightest are hydrogen)***

### 3.2 UV-vis studies of 5-*mono*-4-pyridyl 10,15,20-triphenyl porphyrin and its pentacarbonyl complexes $M(CO)_5$ ( $M = Cr$ or $W$ )

**Table 3 1 UV bands of free base porphyrin and pentacarbonyl complexes (nm)**

| <i>Porphyrin</i>          | <i>B(0,0)</i> | <i>Q<sub>y</sub>(1,0)</i> | <i>Q<sub>y</sub>(0,0)</i> | <i>Q<sub>x</sub>(1,0)</i> | <i>Q<sub>x</sub>(0,0)</i> | $A[Q(0,0)]/A[Q(1,0)]$ |
|---------------------------|---------------|---------------------------|---------------------------|---------------------------|---------------------------|-----------------------|
| MPyTPP                    | 418           | 514(1 0)                  | 548(0 39)                 | 588(0 39)                 | 644(0 20)                 | 0 45                  |
| MPyTPPCr(CO) <sub>5</sub> | 420           | 516(1 0)                  | 552(0 48)                 | 590(0 30)                 | 646(0 22)                 | 0 54                  |
| MPyTPPW(CO) <sub>5</sub>  | 422           | 516(1 0)                  | 552(0 51)                 | 590(0 30)                 | 646(0 24)                 | 0 58                  |

\*See equation 3.1 for calculation of values

Table 3 1 summarises the electronic absorption spectral features of *mono*-pyridyl triphenyl porphyrin (MPyTPP), MPyTPPW(CO)<sub>5</sub> and MPyTPPCr(CO)<sub>5</sub>. The absorption spectrum of the uncomplexed free base porphyrin (MPyTPP) has been reported previously in the literature<sup>10</sup>. The absorption spectra of these metal carbonyl complexes are similar to those of uncomplexed free base porphyrins. The UV-vis absorption spectra are characterised by a strong Soret band at 420 nm and four Q bands of decreasing absorption between 510 nm and 650 nm (see Fig 3 2)<sup>11</sup>.

The spectra of both the complexes and the free base porphyrins are similar except for a noticeable red shift of 2 - 4 nm when compared to those of the uncomplexed free base porphyrin<sup>12</sup>. Pyridyl metal carbonyl complexes such as  $M(CO)_5(C_5H_4N)$  usually have a MLCT band at  $\approx 340$  nm (see Figure 3 8, pg 78), however in the complexes synthesised in this study there is no evidence for such a transition. Furthermore, the LF transition for  $M(CO)_5(C_5H_4N)$  has been reported to occur at 382 nm<sup>13, 14</sup> and again in the porphyrin metal carbonyl complexes there is no evidence from the UV-vis spectra of the porphyrin complexes for such a transition. However it is possible that this transition may be masked by the strongly absorbing Soret band of the porphyrin (see Fig 3 8)<sup>15</sup>. The masking of the N-M LF and the MLCT band of the porphyrin metal carbonyl complex can be explained

by the intensity of the absorption spectrum of the porphyrin when compared to that of  $M(CO)_5(C_5H_4N)$

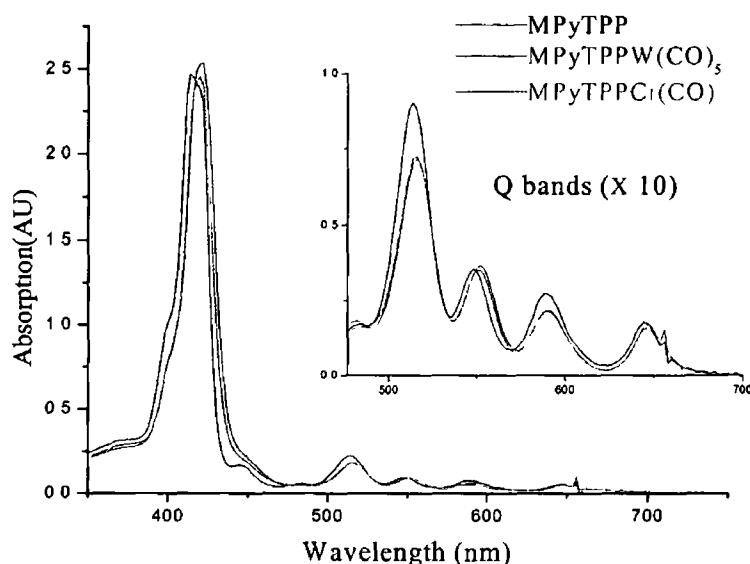


**Fig 3 2 UV-vis spectra of MPyTPP, MPyTPPW(CO)<sub>5</sub> and MPyTPPCr(CO)<sub>5</sub> ( $1.6 \times 10^5 \text{ mol dm}^{-3}$ ) showing strong Soret bands and Q bands ( $\times 10$ ) in dichloromethane**

Between the wavelengths of 380-430 nm, the extinction coefficient of MPyTPP is in the range  $40,000$  to  $80,000 \text{ dm}^3 \text{ mol}^{-1} \text{ cm}^{-1}$ , compared to just  $7000 \text{ dm}^3 \text{ mol}^{-1} \text{ cm}^{-1}$  for the  $W(CO)_5(C_5H_4N)$  complex at its  $\lambda_{\text{max}}$  ( $\sim 400 \text{ nm}$ ),<sup>10</sup> the band intensity is even less at 340 nm for the  $W(CO)_5(C_5H_4N)$  MLCT band. Although there is no presence of a MLCT band for the complexed porphyrin, the small but consistent red shift of 2-4 nm of the Soret and the Q bands indicates a weak electronic interaction between the metal centre and the porphyrin macrocycle.<sup>5</sup>

There is also a change in the absorption intensities of the Q bands normalised with respect to Q(1,0). The Q(1,0) band is insensitive to the electronic effects that the substituents in the *meso* position have on the porphyrin macrocycle. Therefore the absorbance ratio of Q(0,0) (this band is sensitive to substituents in the *meso* position)

with respect to Q(1,0) can be shown to determine the effect, if any, a substituent has on a porphyrin<sup>16</sup> and is given by the equation<sup>17</sup>

*Eqn 3.1*

$$Q(0,0)/Q(1,0) = [Q_x(0,0) + Q_y(0,0)]/[Q_x(1,0) + Q_y(1,0)]$$

An increase in this ratio is observed after complexation to the peripheral position of the porphyrin<sup>16</sup>

A number of points can be highlighted from the data given in Table 3 1

(i) The changes in the overall appearance of the UV-vis spectrum of the free base porphyrin and the metal complexed porphyrins are as expected for these *meso* substituted macrocycles<sup>18</sup> These similarities suggest that there is little interaction between the metal carbonyl unit and the porphyrin macrocycle However, while small changes were observed in this study they were measurable and consistent with previous observations in the literature<sup>4</sup> (i.e. red shift of 2-4 nm in the absorption bands of the metal complexes compared to that of the free MPyTPP)<sup>12</sup>

(ii) The red shifts observed in the UV-vis spectra upon complexation were similar in a range of solvents so changes due to solvent-solute interactions can therefore be excluded as an explanation for this shift

(iii) The relative intensity of the Q<sub>y</sub>(0,0) and Q<sub>y</sub>(1,0) bands in the porphyrin metal carbonyl complexes is greater than for the uncomplexed free base porphyrin MPyTPP It has been shown that the electron donating character of a substituent in *meso*-tetraphenyl porphyrins increases the absorption intensities of the Q<sub>y</sub>(0,0) transitions while the presence of electron withdrawing substituents results in a decrease in the absorption intensities of the Q<sub>y</sub>(0,0) transitions<sup>18 19 20</sup> The presence of a Cr(CO)<sub>5</sub> or a W(CO)<sub>5</sub> moiety should therefore have the effect of decreasing the intensities of Q<sub>y</sub>(0,0) band relative to the Q<sub>y</sub>(1,0) band, but from Table 3 1, the opposite is observed

### 3.3 Infrared studies of 5-*mono*-4-pyridyl-10,15,20-triphenyl porphyrin and its pentacarbonyl complexes M(CO)<sub>5</sub> (M = Cr or W)

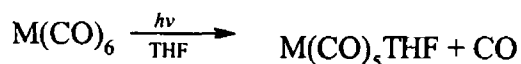
Table 3.2

| <i>Porphyrin</i>          | <i>IR Bands (cm<sup>-1</sup>)</i> |      |      |
|---------------------------|-----------------------------------|------|------|
| MPyTPPW(CO) <sub>5</sub>  | 2072                              | 1929 | 1895 |
| MPyTPPCr(CO) <sub>5</sub> | 2068                              | 1934 | 1899 |

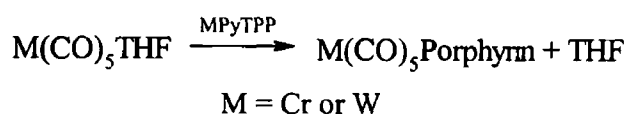
The IR spectroscopic data (metal carbonyl region only) for the MPyTPP complexes are presented in Table 3.2. The three carbonyl absorptions observed for each metal carbonyl complex is consistent with the local C<sub>4v</sub> symmetry of the pentacarbonyl unit (see Fig 3.3)<sup>21</sup>. According to Kolodziej *et al*<sup>22</sup>, the spectral data in Figure 3.3 confirms that the metal atom is bound to the nitrogen atom in the porphyrin complex. There is no evidence for the formation of disubstituted tetracarbonyl complexes due to co-ordination of two porphyrins to the metal. These complexes were synthesised by firstly forming the *mono*-substituted pentacarbonyl complex (THF)M(CO)<sub>5</sub> and subsequently carrying out an exchange reaction with (THF)M(CO)<sub>5</sub> and *mono*-pyridyl porphyrin ligand.

The reaction proceeded *via* the following pathway<sup>23</sup>

Eqn 3.2



Eqn 3.3



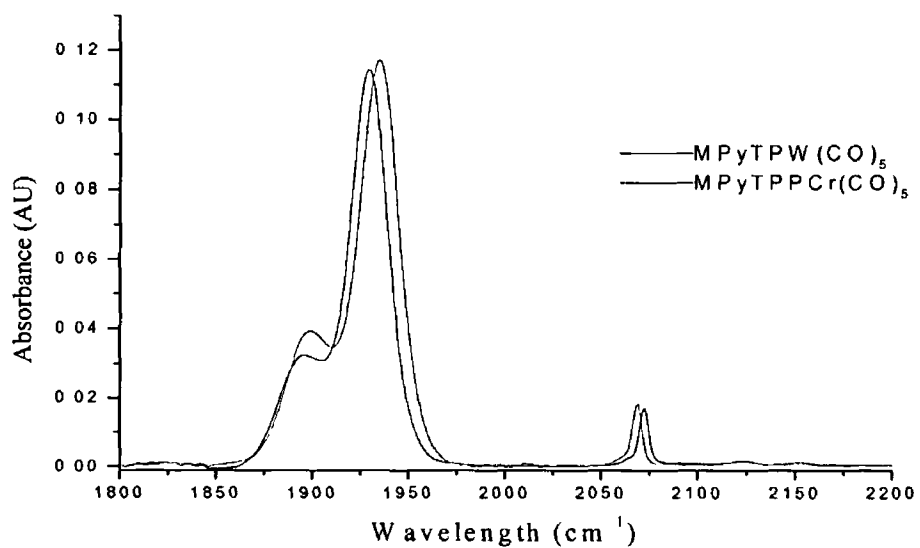


***Figure 3 3 IR spectra of MPyTPW(CO)<sub>5</sub> and MPyTPPCr(CO)<sub>5</sub> ( $1.6 \times 10^{-5} \text{ mol dm}^{-3}$ ), recorded in dichloromethane***

Removal of the uncomplexed free base porphyrin was achieved by column chromatography as outlined in Section 6.5 while unreacted hexacarbonyl was removed by sublimation under reduced pressure.

### 3.4 $^1\text{H}$ NMR spectrum of 5-*mono*-4-pyridyl 10,15,20-triphenyl porphyrin and its pentacarbonyl complexes $\text{M}(\text{CO})_5$ ( $\text{M} = \text{Cr}$ or $\text{W}$ )

*Table 3.3*

| <i>Porphyrin</i>          | <i>2 H, 2, 6 dipyridyl, <math>\delta</math> ppm</i> | <i>2 H, internal pyrrole, <math>\delta</math> ppm</i> |
|---------------------------|-----------------------------------------------------|-------------------------------------------------------|
| MPyTPP                    | 9.04                                                | -2.83                                                 |
| MPyTPPCr(CO) <sub>5</sub> | 9.17                                                | -2.84                                                 |
| MPyTPPW(CO) <sub>5</sub>  | 9.13                                                | -2.83                                                 |

Selected  $^1\text{H}$  NMR data of MPyTPP, MPyTPPCr(CO)<sub>5</sub> and MPyTPPW(CO)<sub>5</sub> are presented in Table 3.3. The presence of a singlet at -2.83 ppm arising from the internal pyrrole protons at the centre of the porphyrin molecule are only observed for free base porphyrins and these protons are displaced upon metallation. These internal protons experience a high field shift because of the internal ring current of the porphyrin molecule.<sup>24</sup> The presence of this proton signal confirms the absence of a metal ion at the centre of the porphyrin ring.

When comparing the  $^1\text{H}$  NMR spectra of the free base porphyrin to either the Cr or W adducts a small shift of  $\delta$  0.1 ppm in the position of the 2,6 pyridyl proton resonance is observed. The resonance shift confirms that the metal pentacarbonyl unit is co-ordinated through the N of the pyridine site. The protons are shifted downfield because of the donation of electron density from the pyridine nitrogen lone pair to the metal centre.<sup>25</sup> The remaining resonances are unaffected by complexation.

### 3.5 Steady state photolysis experiments monitored in the UV-vis region

#### 3.5.1 Steady state photolysis of MPyTPPW(CO)<sub>5</sub> under 1 atmosphere of CO

A solution of MPyTPPW(CO)<sub>5</sub> in dichloromethane (conc.  $2.3 \times 10^{-5}$  mol dm<sup>-3</sup>) was subjected to steady state photolysis ( $\lambda_{\text{exc}} > 400$  nm or 500 nm). The sample was degassed using the freeze pump thaw method before being placed under 1 atmosphere of CO. Initially the sample was irradiated at  $\lambda_{\text{exc}} > 500$  nm, and few changes were observed in the UV-vis spectrum other than a small grow-in at 290 nm (see Figure 3.4). This was attributed to the formation of W(CO)<sub>6</sub>. Isosbestic points were apparent at 315 and 275 nm. As the process was very inefficient under these conditions, the irradiation wavelength was changed to  $> 400$  nm.

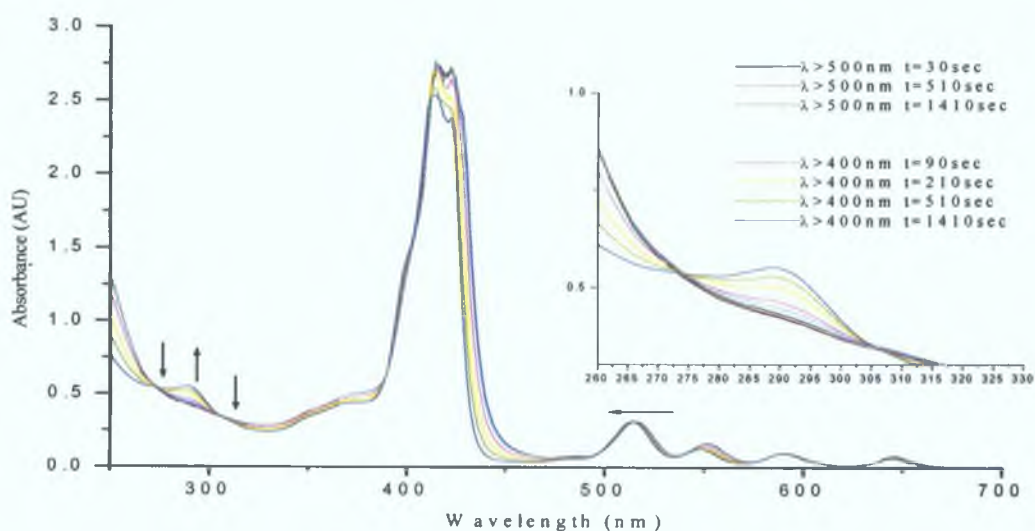


**Figure 3.4** UV-vis spectra of MPyTPPW(CO)<sub>5</sub> ( $2.3 \times 10^{-5}$  mol dm<sup>-3</sup>) recorded during steady state photolysis ( $\lambda > 400$  nm and 500 nm) under 1 atmosphere of CO in dichloromethane solution

Upon changing the irradiation wavelength to  $\lambda_{\text{exc}} > 400$  nm, the effects of photolysis were more evident. The grow-in at 290 nm was larger and the isosbestic points at 315 nm and 275 nm became clearer. In addition the Q bands were shifted to higher energy by 2-4 nm.

This blue shift can be attributed to the formation of uncomplexed free base porphyrin formed by loss of the  $W(CO)_5$  unit. Photolysis was allowed to continue for 20 mins until no further changes were observed.

It was shown earlier that the presence of a metal carbonyl unit at the peripheral region of a porphyrin causes a red shift in the UV-vis spectrum. The removal of this external moiety has the opposite effect, Rowley *et al*, recorded a red shift of 5 nm in a molybdenated tetra phenyl porphyrin in relation to the uncomplexed species.<sup>26</sup> Photolysis of a solution of the free base porphyrin did not change the UV-vis spectrum.

### 3.5.2 Steady state photolysis of MPyTPPW(CO)<sub>5</sub> under 1 atmosphere of Ar

A solution of MPyTPPW(CO)<sub>5</sub> in dichloromethane (conc.  $2.3 \times 10^{-5}$  mol dm<sup>-3</sup>) was subjected to steady state photolysis ( $\lambda_{\text{exc}} > 400$  nm or 500 nm). Samples were degassed using the freeze pump thaw method before being placed under 1 atmosphere of Ar. Again the sample was initially irradiated at  $\lambda_{\text{exc}} > 500$  nm. The changes observed in the UV-vis spectrum during photolysis were less obvious than those recorded under 1 atmosphere of CO for the same photolysis time. This was attributed to the absence of added CO with which the sixteen electron W(CO)<sub>5</sub> species can react, to form W(CO)<sub>6</sub>.

Obviously under these conditions the formation of W(CO)<sub>6</sub> would be less efficient than for experiments conducted in CO saturated solution. The yield of W(CO)<sub>6</sub> is limited by the ability of the W(CO)<sub>5</sub> fragment to scavenge CO *via* bimolecular reactions.

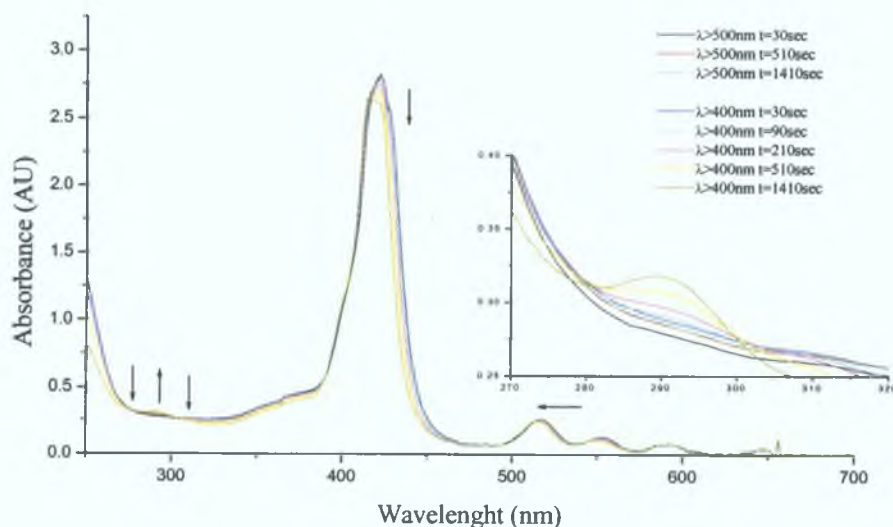


**Figure 3.5** UV-vis spectra of MPyTPPW(CO)<sub>5</sub> ( $2.3 \times 10^{-5}$  mol dm<sup>-3</sup>) recorded during steady state photolysis ( $\lambda > 400$  nm and 500 nm) under 1 atmosphere of Ar in dichloromethane

When the irradiation wavelength was increased to  $\lambda_{exc} > 400$  nm there was some evidence for the formation of  $W(CO)_6$  at 290 nm (see Figure 3.5). After prolonged photolysis (~ 20 mins) the photolysis was stopped as no further changes were observed in the UV-vis spectrum. Again a shift in the Q bands was noted, indicating the formation of the uncomplexed porphyrin. The formation of the isosbestic points was not observed under these conditions which would indicate that the formation of  $W(CO)_6$  was not quantitative.

### 3.5.3 Steady state photolysis of MPyTPPCr(CO)<sub>5</sub> under 1 atmosphere of CO

A solution of MPyTPPCr(CO)<sub>5</sub> in dichloromethane (conc.  $2.6 \times 10^{-5}$  mol dm<sup>-3</sup>) was subjected to steady state photolysis ( $\lambda_{\text{exc}} > 400$  nm or 500 nm). Again the sample was degassed using the freeze thaw method before being placed under 1 atmosphere of CO. The same conditions were employed as in the case of the tungsten analogue, the sample was initially irradiated at  $\lambda_{\text{exc}} > 500$  nm, where a slight increase in absorbance at 290 nm was observed (see Figure 3.6). This was attributed to the formation of Cr(CO)<sub>6</sub>, as subsequently confirmed by IR spectroscopy at the end of the photolysis experiment.

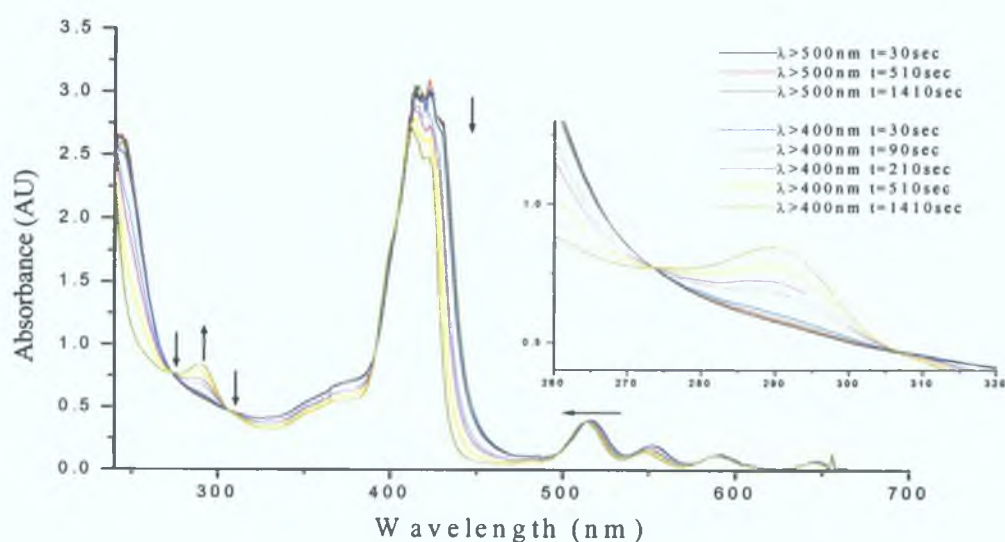


**Figure 3.6** UV-vis spectra of MPyTPPCr(CO)<sub>5</sub> ( $2.6 \times 10^{-5}$  mol dm<sup>-3</sup>) recorded during steady state photolysis ( $\lambda > 400$  nm and  $> 500$  nm) under 1 atmosphere of CO in dichloromethane

As was observed for the tungsten analogue when the energy of the irradiation was increased to  $\lambda_{\text{exc}} > 400$  nm the changes to the UV-vis spectrum became more significant. Photolysis was continued for a further 23.5 mins until no further changes were observed. Again formation of isosbestic points at 275 and 315 nm were observed in addition to the formation of a band at 290 nm assumed to be Cr(CO)<sub>6</sub>. The isosbestic points are evidence that the reaction to form Cr(CO)<sub>6</sub> and uncomplexed free base porphyrin was clean and

uncomplicated by the side or subsequent reactions. Further evidence of the formation of the uncomplexed free base porphyrin is the shift to lower wavelength of the Soret and Q bands in the UV-vis spectrum. Although the shift is of only 2-4 nm it is consistent with results obtained during photolysis of  $\text{MPyTPPW}(\text{CO})_5$  as discussed previously and similar to the effect observed by Rowley and co-workers i.e. a red shift of 5 nm in a molybdenated tetra phenyl porphyrin in relation to the uncomplexed species<sup>26</sup>

### 3.5.4 Steady state photolysis of MPyTPPCr(CO)<sub>5</sub> under 1 atmosphere of Ar

A solution of MPyTPPCr(CO)<sub>5</sub> in dichloromethane (conc.  $1.9 \times 10^{-5}$  mol dm<sup>-3</sup>) was subjected to steady state photolysis ( $\lambda_{\text{exc}} > 400$  nm or 500 nm). Again the sample was degassed using the freeze-pump thaw method before being placed under 1 atmosphere of Ar. As before, the sample was initially irradiated at  $\lambda_{\text{exc}} > 500$  nm. Again the changes during photolysis were smaller than those recorded under 1 atmosphere of CO under the same photolysis conditions. This was because in the absence of added CO the formation of Cr(CO)<sub>6</sub> was not quantitative and relied on the ability of the photogenerated Cr(CO)<sub>5</sub> unit to scavenge CO from parent molecules or photogenerated metal carbonyl fragments to form Cr(CO)<sub>6</sub>.

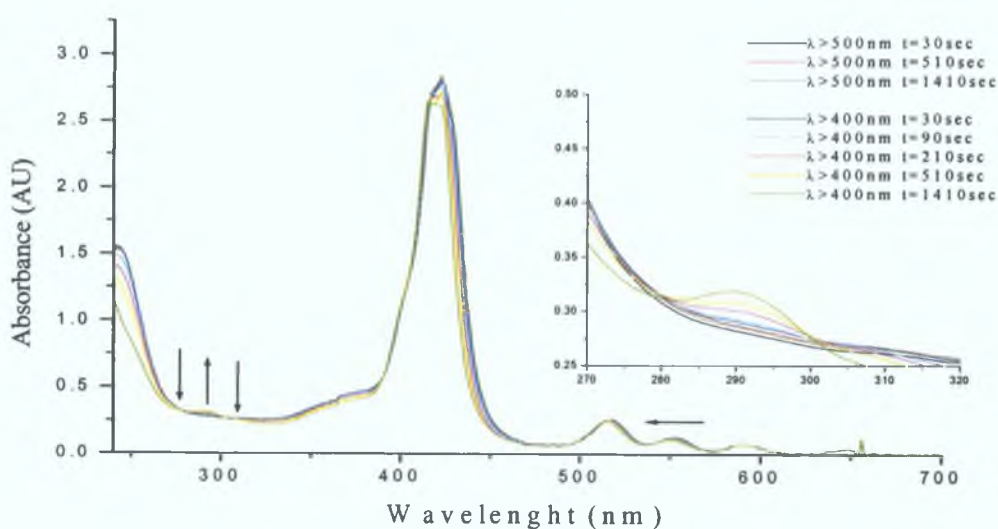


**Figure 3.7** UV-vis spectra of MPyTPPCr(CO)<sub>5</sub> ( $1.9 \times 10^{-5}$  mol dm<sup>-3</sup>) recorded during steady state photolysis ( $\lambda > 400$  nm and  $> 500$  nm) under 1 atmosphere of Ar in dichloromethane

When the irradiation wavelength was decreased in energy to  $\lambda_{\text{exc}} > 400$  nm some evidence for the formation of Cr(CO)<sub>6</sub> at 290 nm was obtained. After 23.5 mins the photolysis at  $\lambda_{\text{exc}} > 400$  nm was complete as no further changes were apparent. Again, a shift in the UV-vis bands was observed, indicating the formation of the free porphyrin. No isosbestic points were observed in this experiment (see Figure 3.7).

### 3 5 5 Discussion of results

Steady state photolysis was carried out in dichloromethane, as opposed to a hydrocarbon solution because of the limited solubility of the free base porphyrin and its metal carbonyl complexes (all samples were prepared as described in Section 6 5 1)

Photolysis of the uncomplexed free base porphyrin yielded no changes in the UV-vis spectrum The metal carbonyl complexes were irradiated with cut off filters with  $\lambda_{exc} > 400$  nm and  $\lambda_{exc} > 500$  nm Initially samples were irradiated with  $\lambda_{exc} > 500$  nm However, as described in the proceeding section only minor changes were observed in the UV-vis spectra of the complexes under these conditions A slight increase in the absorbance at 290 nm for each complex indicated the formation of the appropriate  $M(CO)_6$  compound When irradiating at  $\lambda_{exc} > 500$  nm the light is absorbed by the Q bands of the porphyrin (see Figure 3 2) Q bands are much less intense than the Soret band (430-480 nm) and therefore the changes brought about by irradiating at this excitation wavelength are less than those changes observed when irradiating the Soret band

When the cut off filter was changed to  $\lambda_{exc} > 400$  nm changes occurred much more rapidly, even under an atmosphere of Ar Changes around 290 nm are expected to be less obvious under an atmosphere of Ar At this irradiating wavelength the light is being absorbed into the highly intense Soret band of the porphyrin and there is greater quantum efficiency for the absorption of light through this band Shifts in the UV-vis spectra of the complexed porphyrin were also apparent, as the sample was photolysed at this wavelength The Q bands shifter to higher energy, a change of approximately 2-4 nm as the photolysis proceeded This is due to the formation of the uncomplexed free base porphyrin as the N-M bond breaks Despite most of the light being absorbed by the Soret band and the Q bands of the porphyrin, loss of the metal carbonyl moiety from the porphyrin complex is observed Cleavage of the N-M bond is thought to occur from population of a LF excited state<sup>13</sup> Therefore formation of  $M(CO)_6$  suggests some communication between the porphyrin macrocycle and the peripheral metal carbonyl

moiety by population of metal carbonyl based excited states following electron/energy transfer from the porphyrin<sup>9,27,28</sup>

It is possible that the porphyrin and  $M(CO)_5(C_5H_4N)$  entities of the complex can be treated as individual components in a supramolecular molecule. The shifts of 2-4 nm to lower energy upon formation of the pentacarbonyl complex in the UV-vis spectrum indicate that the interaction between the two molecular units is not particularly strong. The  $M(CO)_5(C_5H_4N)$  unit does not absorb into the  $\lambda > 500$  nm region (see Figure 3.8). In fact it only weakly absorbs out to 460 nm (see Figure 3.8), but excitation of this compound at  $\lambda_{exc} > 500$  nm leads to loss of the metal carbonyl moiety<sup>29,30</sup>. Therefore any photochemical changes observed during photolysis at this wavelength must be the result of light absorbed by the porphyrin. When photolysing the complexes at  $\lambda_{exc} > 400$  nm it is thought that cleavage of the N-M bond is caused by population of ligand field excited states on the  $M(CO)_5(C_5H_4N)$  component as the ligand field (LF) band of  $M(CO)_5(C_5H_4N)$  is the lowest lying excited state and is considerably reactive<sup>13</sup>. It could be argued that this may cause an increase in the quantum efficiency for the formation of  $M(CO)_6$ .

However due to the intense porphyrin Soret band overlapping the weakly absorbing MLCT band at 382 nm and the LF band at 440 nm, it is unlikely that the  $M(CO)_5(C_5H_4N)$  moiety will absorb a significant amount of light<sup>13</sup>. As mentioned previously the extinction coefficients of porphyrins between the wavelengths of 380-430 nm are in the range 40 000 to 80 000  $dm^3 mol^{-1} cm^{-1}$  compared to just 7000  $dm^3 mol^{-1} cm^{-1}$  for the  $W(CO)_5(C_5H_4N)$  complex at its  $\lambda_{max}$  (~ 400 nm). The  $M(CO)_5(C_5H_4N)$  moiety has an absorption maxima for the MLCT at 382 nm and this is very weak when compared to the intense Soret band of the porphyrin. There is no evidence of this MLCT or the lower energy LF band for  $M(CO)_5(C_5H_4N)$  in the UV-vis spectrum of the porphyrin<sup>13</sup>. Despite not being able to assign transitions as being either MLCT or LF in the UV-vis spectrum, cleavage of the N-M bonds with eventual formation of the  $M(CO)_6$  in the presence of CO occurs. The porphyrin absorbs practically all the light at  $\lambda_{exc} \geq 500$  nm which therefore

suggests that cleavage of the N-M bond is caused by electronic communication between the porphyrin and the  $M(CO)_5$  moiety

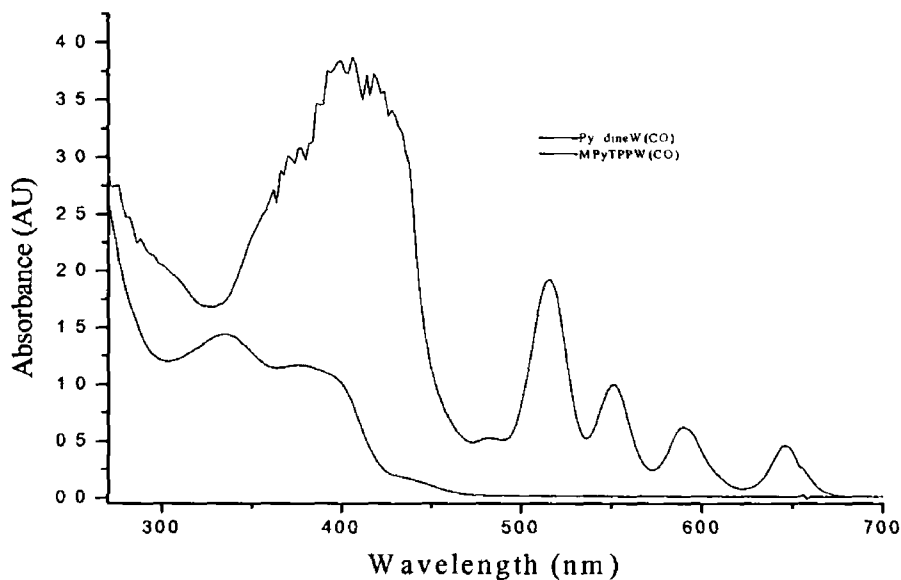


**Figure 3.8 UV-vis of  $MPyTPPW(CO)_5$  ( $1.5 \times 10^{-4} \text{ mol dm}^{-3}$ ) and  $C_5H_4NW(CO)_5$  ( $1.5 \times 10^{-4} \text{ mol dm}^{-3}$ ) in dichloromethane**

Further investigations into the photophysical and photochemical properties were carried out to try and elucidate the exact mechanism behind the cleavage of this bond, and this included fluorescence measurements, which will be discussed later

### 3.6 Steady State photolysis monitored in by Infrared spectroscopy

Photolysis of the porphyrin pentacarbonyl complex was also monitored by IR spectroscopy and the changes observed confirmed those found in the UV-vis experiments. Prior to photolysis all samples were saturated with CO by purging for 15 mins. Initially samples were irradiated at  $\lambda_{exc} > 500$  nm and subsequently with  $\lambda_{exc} > 400$  nm filter. Unlike the photolysis experiments which was monitored using UV-vis detection, changes in the  $\nu_{CO}$  region of the IR spectrum are not obscured by porphyrin based absorption bands. The only bands observed in the metal carbonyl region of the spectrum at the end of photolysis are those of the pentacarbonyl moiety and the hexacarbonyl product.

As expected, the greatest changes are observed when the sample is exposed to irradiation at  $\lambda_{exc} > 400$  nm. Once more, photosubstitution is greatly reduced using the  $\lambda_{exc} > 500$  nm filter. Again cleavage of the N-M bond is observed with subsequent formation of the metal hexacarbonyl complex (Figure 3.10).

### 3.6.1 Steady state photolysis of $\text{Cr}(\text{CO})_6$ in the presence of triphenylphosphine

To analyse the results of the photolysis of  $\text{MPyTPPM}(\text{CO})_5$  in the presence of  $\text{PPh}_3$ ,  $\text{M}(\text{CO})_6$  was photolysed in the presence of  $\text{PPh}_3$  and monitored in the IR. As  $\text{Cr}(\text{CO})_6$  does not absorb at 500 nm photolysis at this wavelength would show no changes in the IR spectrum, therefore the excitation wavelength used increased was  $\lambda_{\text{exc}} > 400$  nm changes were observed. Shown in Figure 3.9 are the difference spectra obtained following a total of two minutes irradiation at  $\lambda > 400$  nm of  $\text{Cr}(\text{CO})_6$  in pentane in the presence of  $\text{PPh}_3$ . The negative peak at  $1989\text{ cm}^{-1}$  indicates depletion of starting material  $\text{Cr}(\text{CO})_6$  with the peaks at  $1896$ ,  $1945$  and  $2065\text{ cm}^{-1}$  indicating formation of the photoproduct,  $\text{Cr}(\text{CO})_5\text{PPh}_3$ .

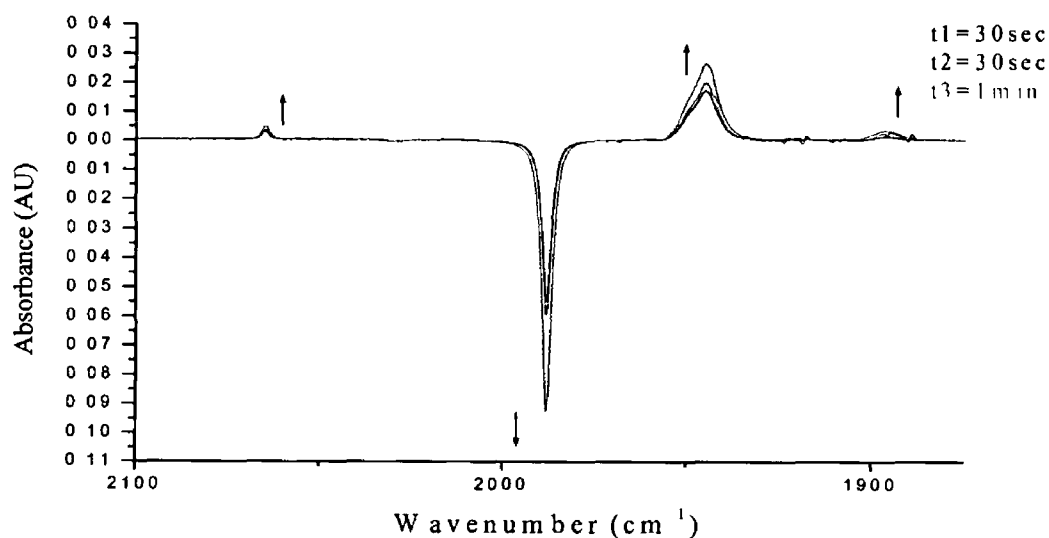


**Figure 3.9 IR spectral changes following steady state photolysis of  $\text{Cr}(\text{CO})_6$  in pentane the presence of excess  $\text{PPh}_3$  at 293 K**

Following photolysis one of the carbonyls is replaced by the  $\text{PPh}_3$  to form the pentacarbonyl complex  $(\text{CO})_5\text{Cr}(\text{PPh}_3)$ . Photolysis was not carried out at higher wavelength, as substitution of CO is more efficient and this would also give rise to the formation of  $\text{M}(\text{CO})_4(\text{PPh}_3)_2$ .

### 3.6.2 Steady state photolysis of MPyTPPM(CO)<sub>5</sub> with PPh<sub>3</sub>

MPyTPPM(CO)<sub>5</sub> was photolysed in the presence of an excess of PPh<sub>3</sub>, in dichloromethane. In Section 3.5 changes were observed in the UV-vis spectrum which suggested cleavage of the N-M bond of the porphyrin complex and formation of M(CO)<sub>6</sub> when CO is formed. Section 3.6.1 showed the formation of M(CO)<sub>5</sub>(PPh<sub>3</sub>) and the bands associated with the loss of CO, from M(CO)<sub>6</sub>. Assuming that the N-M bond of MPyTPPM(CO)<sub>5</sub> is cleaved the formation of IR bands associated with M(CO)<sub>5</sub>PPh<sub>3</sub> should be apparent from the IR spectrum.

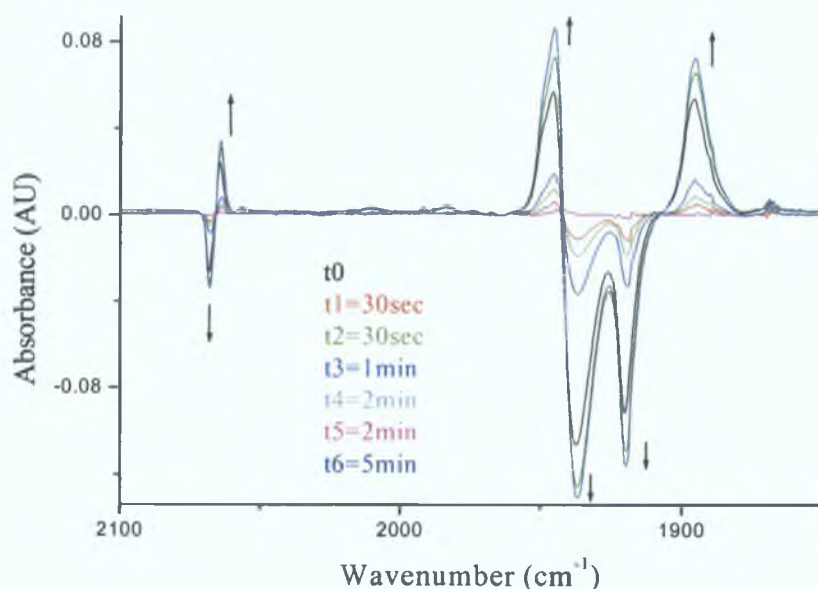


**Figure 3.10** Steady state photolysis of MPyTPPM(CO)<sub>5</sub> in pentane( the presence of excess PPh<sub>3</sub> at 293 K monitored in the IR

Initially the solution was irradiated with at  $\lambda_{\text{exc}} > 500$  nm, however the changes in the IR spectrum were small. Increasing the irradiation wavelength to  $\lambda_{\text{exc}} > 400$  nm increased the magnitude of the spectral changes. As before depletion of the parent pentacarbonyl bands at 1919, 1934 and 2069  $\text{cm}^{-1}$  was observed. This was accompanied by the grow in of bands at 1896, 1945 and 2065  $\text{cm}^{-1}$  assigned to Cr(CO)<sub>5</sub>PPh<sub>3</sub> (see Figure 3.10). Again the irradiation energy was not increased any further to prevent the formation of side

products such as  $M(CO)_4(PPh_3)_2$ . The changes were typical of that expected for  $M(CO)_5(C_5H_4N)$  in the presence of a coordinating ligand<sup>13</sup>. There is no evidence for the reformation of the  $MPyTPPM(CO)_5$  and only one metal carbonyl product was produced i.e.  $M(CO)_5(PPh_3)$ .

### 3.7 Fluorescence studies of 5-mono-4-pyridyl 10,15,20-triphenyl porphyrin and its $M(CO)_5$ complexes $M = W$ or $Cr$

#### 3.7.1 Emission spectra and quantum yields for MPyTPP and its $M(CO)_5$ complexes ( $M = W$ or $Cr$ )

Fluorescence spectra were obtained for both the metal carbonyl complexes and the uncomplexed free base porphyrin ligand. The spectra are strikingly similar as can be seen from Figure 3.11, thus indicating that the metal carbonyl porphyrins emit from the porphyrin unit of the molecule. There are slight shifts in the maxima of the complexes but the profiles are essentially identical.

**Table 3.4 Emission maxima and relative intensities of free base porphyrin and pentacarbonyl complexes**

| <i>Porphyrin</i>          | <i>Emission Maxima (nm)</i> |               | <i>Relative <math>\phi_f</math></i> | <i><math>\phi_f</math></i> |
|---------------------------|-----------------------------|---------------|-------------------------------------|----------------------------|
| MPyTPP                    | 654 nm (1.0)                | 714 nm (0.41) | 1.0                                 | 0.099                      |
| MPyTPPCr(CO) <sub>5</sub> | 655 nm (1.0)                | 716 nm (0.40) | 0.74                                | 0.073                      |
| MPyTPPW(CO) <sub>5</sub>  | 656 nm (1.0)                | 717 nm (0.35) | 0.86                                | 0.085                      |

The red shift of the bands by 2-4 nm is indicative of a metal entity attached to the periphery of the porphyrin ring (see Table 3.4).<sup>31</sup> Pyridyl porphyrins are more acidic than the tetraphenyl porphyrins and some reports have attributed the red shifts to the electron withdrawing character of the pyridine group. Such effects are usually only observed in tetrapyrrolyl porphyrins where the influence of the pyridine group are amplified.<sup>16</sup>

Fluorescence quantum yield was measured at  $\lambda_{exc} = 512$ . The fluorescence quantum yield of MPyTPP has been reported previously at this wavelength.<sup>32</sup> A series of solutions were made which had identical absorbances ( $Abs = 0.21$ ) at the  $\lambda = 532$  nm. Using isoabsorptive samples is a standard way of determining changes in fluorescence yield.<sup>33</sup> There is a reduction in the fluorescence yield of the complexes compared to the uncomplexed free base porphyrin (see Figure 3.11). This was calculated using equation

3.4 and the values obtained are for relative yields only. The reduction in  $\Phi_f$  is a real change. These reductions are because of the inefficient non-planar interaction of the porphyrine ring  $\pi$  system with the orthogonal pyridyl group to which the metal moiety is attached.<sup>34</sup> The heavy atom effect has previously been proposed as the reason for the reduction in the quantum yield of the fluorescence in Ru(II) and Pd porphyrin arrays,<sup>31</sup> however Cr is not considered a heavy atom, as the atomic mass is too low. Figure 3.26 (Section 3.9) explains how this reduction came about. There is also a reduction in the relative intensities of the emission peaks (Table 3.4) with the greatest decrease seen in the intensity of the Q(0,0) band of the W complex. The intensity of the Q(0,0) band falls in the order MPyTPP > MPyTPPCr(CO)<sub>5</sub> > MPyTPPW(CO)<sub>5</sub>.

Eqn 3.4

$$\frac{\Phi_c}{\Phi_L} = \frac{A_L I_c}{A_c I_L}$$

$\Phi_c$  = Fluorescence Quantum yield of complexed porphyrin

$A_c$  = Absorbance of complex at  $\lambda_{exc}$

$I_c$  = Area under the peak of the complex

$\Phi_L$  = Fluorescence Quantum yield of uncomplexed porphyrin

$A_L$  = Absorbance of porphyrin at  $\lambda_{exc}$

$I_L$  = Area under the peak of the porphyrin

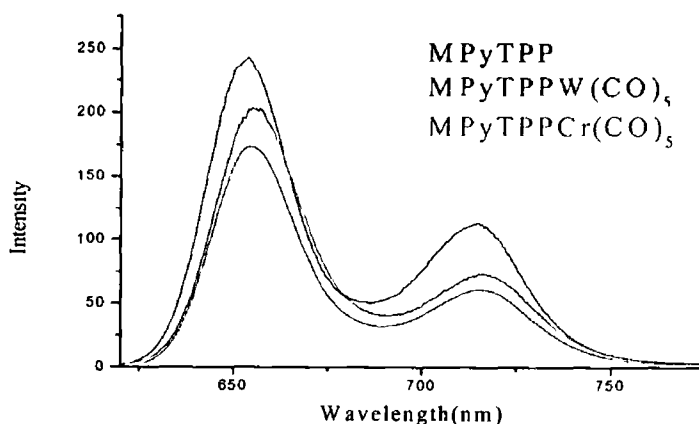


**Figure 3.11 Emission spectra of isoabsorptive samples of MPyTPP, MPyTPPW(CO)<sub>5</sub> and MPyTPPCr(CO)<sub>5</sub> at 293 K ( $\lambda_{exc}$  532 nm) in dichloromethane**

### 3.7.2 Fluorescence lifetimes of MPyTPPW(CO)<sub>5</sub> and MPyTPPCr(CO)<sub>5</sub>

The fluorescence lifetimes were measured for the MPyTPP uncomplexed free base porphyrin, MPyTPPW(CO)<sub>5</sub> and MPyTPPCr(CO)<sub>5</sub> complexes. From Table 3.5 it is clear that the decrease in the singlet state lifetimes correlates to the difference in emission intensities. The decrease in lifetimes is in the order MPyTPP > MPyTPPW(CO)<sub>5</sub> > MPyTPPCr(CO)<sub>5</sub>. The heavy atom effect is unlikely to explain the results obtained in this study as the lifetime of the W complex should be less than that of the Cr complex.

**Table 3.5**

| <i>Porphyrin</i>          | <i>(DCM) τ<sub>fl</sub>(ns)</i> | <i>RAL (DCM) τ<sub>fl</sub>(ns)*</i> | <i>RAL (EtOH) τ<sub>fl</sub>(ns)*</i> |
|---------------------------|---------------------------------|--------------------------------------|---------------------------------------|
| MPyTPP                    | 10.06                           |                                      |                                       |
| MPyTPPCr(CO) <sub>5</sub> | 6.13                            | 5.39                                 | 5.86                                  |
| MPyTPPW(CO) <sub>5</sub>  | 8.38                            | 6.70                                 | 7.36                                  |

\* Results obtained at RAL (Rutherford Appleton Laboratories) which were carried out by Jonathon Rochford using the experimental procedure referenced.<sup>35</sup>

Figure 3.26 (Section 3.9) is used to explain the differences observed in the free base porphyrins, MPyTPPCr(CO)<sub>5</sub> and MPyTPPW(CO)<sub>5</sub> complexes. Upon complexation the ground state absorbance and emission spectra are shifted to lower energy. There is a shift in energy of the order MPyTPP > MPyTPPW(CO)<sub>5</sub> > MPyTPPCr(CO)<sub>5</sub> and this follows the same order as the reduction in lifetimes observed. Complexation therefore has caused a reordering of the energy levels of the subunits of the complex compared to the individual component. This is contrary to the formation of a supramolecular system whose energy levels are simply the addition of the unperturbed energy levels of each molecular component (Figure 3.25, Section 3.9). The tungsten complex is longer lived than the chromium analogue. Even though the trend in lifetimes is the same the lifetimes differ but this could be explained by differences in equipment sensitivity and condition. From the results obtained it can be seen changing the solvent does not greatly affect the lifetimes.

Shown in Figure 3.12 is a typical transient signal observed following 438 nm excitation of  $\text{MPyTPPCr}(\text{CO})_5$  and represents a typical lifetime measurement. All samples were monitored at 655 nm as this is the  $\lambda_{\text{max}}$  of the emission spectrum. Samples were prepared as described in Section 6.1. It is clear from the transient signal that the instrument response function is shorter than the timescale of the lifetime of the complex and does not interfere in the measurement.

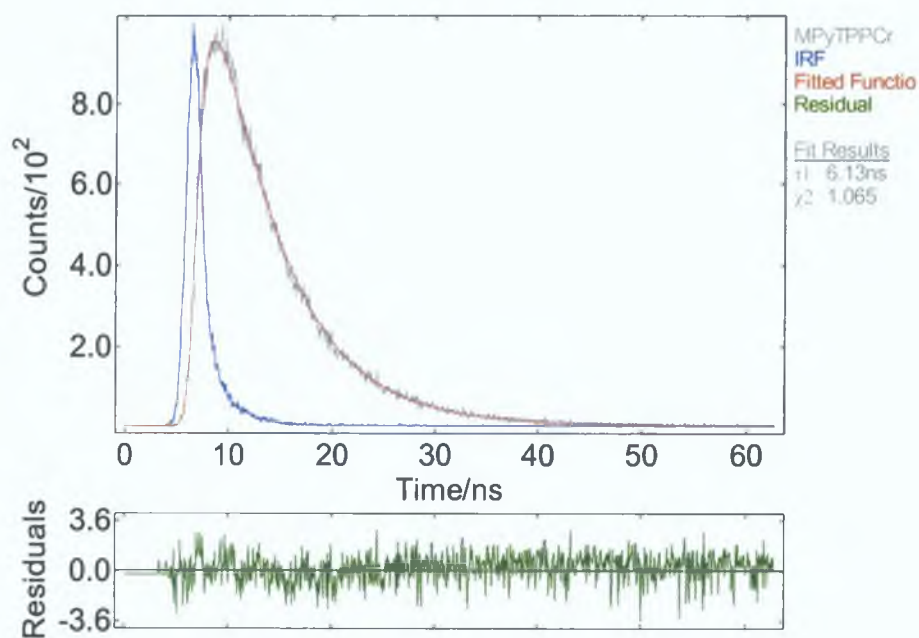


**Figure 3.12** A typical trace obtained at 655 nm following excitation of  $\text{MPyTPPCr}(\text{CO})_5$  at 293 K ( $\lambda_{\text{exc}}$  438 nm) in dichloromethane

### 3.7.3 Discussion of results

Porphyrins emit from the lowest excited singlet state ( $S^1 \rightarrow S^0$  relaxation), which is  $\pi^* - \pi$  in character. The dual emission of porphyrins is due to excitation centred on the lowest singlet excited state transition (0-0 and 0-1 transitions) and emits at 650 nm (Q(0,0)) and 715 nm (Q(0,1)). This type of emission is typical for all free base tetra aryl porphyrins and is independent of the substituent at the *meso* position. Changing the excitation wavelength from higher to lower energy leads only to a change in the relative intensity of the bands and does not affect the overall position of the  $\lambda_{\text{max}}$  or lead to the formation of new bands. The emission is also oxygen independent as oxygen exists in the triplet ground state and is a triplet state quencher. The singlet excited state of MPyTPP has a lifetime 10.06 ns (see Figure 3.13).

The quantum yield for fluorescence of MPyTPP is approximately 10% and varies slightly by changing the number of pyridine ligands in the *meso* position of the porphyrin. The decrease in quantum yield with extra pyridyl units is thought to be the result of interaction of the N on the pyridyl unit and the solvent.<sup>36</sup> As the complexed porphyrins do not have a free pyridyl unit (a metal unit is co-ordinated to the N) the quantum yield should increase relative to the uncomplexed porphyrin, which has a free pyridyl unit.

Upon complexation of the porphyrins with a  $W(CO)_5$  moiety little change is observed in the overall profile of the emission spectra of the complexes studied compared to the uncomplexed porphyrin (Section 3.7.1). The maxima of the complexes are consistently shifted by 2-4 nm to lower energy. There is however a reduction in the intensity of the emission. Again there is a reduction in the lifetime of the singlet excited state. This reduction is in the region of 4 ns (40% of lifetime of uncomplexed free base porphyrin), but it is outside experimental error of the equipment used. It has also been shown that temperature does not affect the lifetime of the excited state of the porphyrin. At 295 K lifetimes of uncomplexed free base porphyrin were 11.3 ns and at 77 K the lifetime was reported to be 11.8 ns.<sup>37</sup> Although the profile of the fluorescence spectra is typical of the

porphyrin the changes observed are evidence that the metal orbitals do interact with those of the porphyrin.

The decrease in emission intensity and accompanying decrease in fluorescence lifetime has previously been reported in porphyrin dyads and arrays containing heavy atoms and has been attributed, by some workers, to interporphyrin electron transfer processes.<sup>38,39,40</sup> However this is unlikely as in most cases it is energetically unallowed (the energy levels of the individual components are arranged in such a way that inhibits electron transfer between them) and the most probable cause of this reduced fluorescence is spin orbit perturbation caused by the metal.<sup>31</sup> This is known as the heavy atom effect. In other Ru-porphyrin systems, Prodi *et al.* have shown that an increase in the number of metal atoms leads to an equal reduction in the emission lifetimes, with the emission lifetime linearly dependent upon the number of metal atoms present and so agreeing with the heavy atom effect.<sup>41, 42, 43</sup>

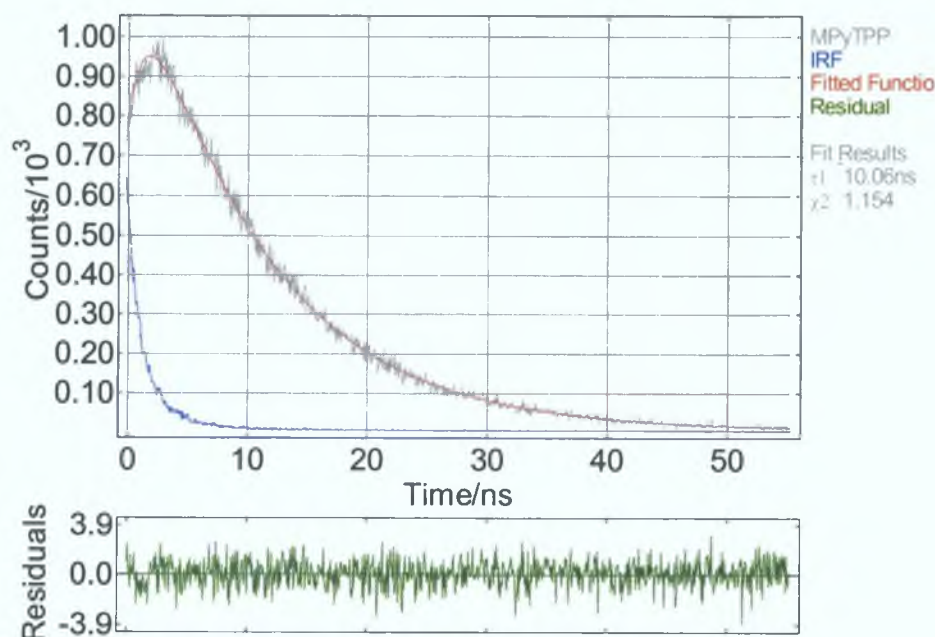


**Figure 3.13** A typical signal obtained at 655 nm following excitation of MPyTPP in dichloromethane at 293 K ( $\lambda_{exc}$  438 nm)

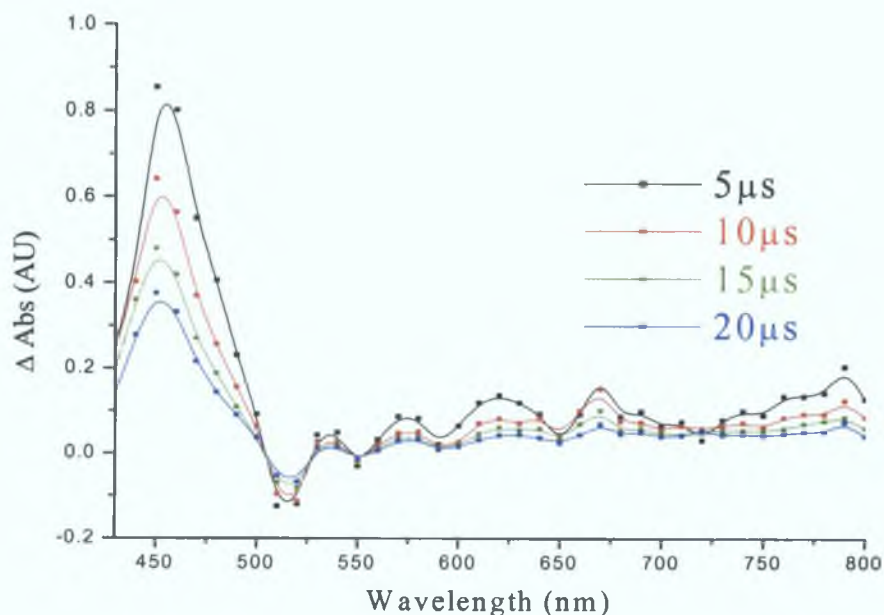
A similar argument cannot be used to explain the observed lifetimes for the chromium complex as the Cr lifetimes are shorter than that of the W complex. The fact that the spectrum of the complexes are shifted to longer wavelengths in both the emission spectrum and the absorbance spectrum suggests that there is interaction between the porphyrin macrocycle and the Cr(CO)<sub>5</sub> or W(CO)<sub>5</sub> moieties. This orbital interaction could lead to the formation of new orbitals at lower energy (see Scheme 3.1) and would therefore explain the spectral changes of the complexes. Previously in all published work a reduction in the singlet lifetimes and emission intensity of porphyrins upon complexation by peripheral fragments (different to dyads and arrays) has been attributed to the heavy atom effect.

Figure 3.25 suggests the reasoning proposed in Section 3.5 where population of S<sub>1</sub> on the porphyrin leads to population, *via* singlet-triplet energy transfer (STEN) to the <sup>3</sup>LF level on M(CO)<sub>5</sub>(C<sub>5</sub>H<sub>4</sub>N) if energetically favourable. This argument would seem logical given that cleavage of N-M bonds accompanies the reduction in lifetime and emission intensity.

### 3.8 Laser Flash Photolysis of MPyTPP and its $M(\text{CO})_5$ complexes $M = \text{W}$ or $\text{Cr}$

#### 3.8.1 Laser flash photolysis of $\text{MPyTPPW}(\text{CO})_5$ at 532 nm under 1 atmosphere of CO

The transient absorption spectrum of  $\text{MPyTPPW}(\text{CO})_5$  (Figure 3.14) was obtained between 430 and 800 nm. The transient absorption difference spectra obtained have similar characteristics to those assigned to the  $^3(\pi-\pi^*)$  excited state relaxation of the uncomplexed free base porphyrin. Similarly to the uncomplexed free base porphyrin,  $\text{MPyTPPW}(\text{CO})_5$  absorbs strongly between 440 nm and 490 nm with a maximum at approximately 450 nm. Uncomplexed and complexed systems contributed bleaching at ca. 520 nm and less intense transient absorption in the Q-band region.



**Figure 3.14** Transient absorption spectra of  $\text{MPyTPPW}(\text{CO})_5$  at  $\lambda_{\text{exc}} = 532$  nm under 1 atmosphere of CO in dichloromethane at 293 K

When the transient absorption spectrum of  $\text{MPyTPPW}(\text{CO})_5$  was directly compared with that of the uncomplexed free base porphyrin in the 430-490 nm region some differences were evident. The samples had identical absorbance at the excitation wavelength. The

complexed porphyrin exhibits a red shift of the  $\lambda_{\max}$  of *ca* 10 nm in addition to a reduction in intensity of this maximum (Figure 3 15)

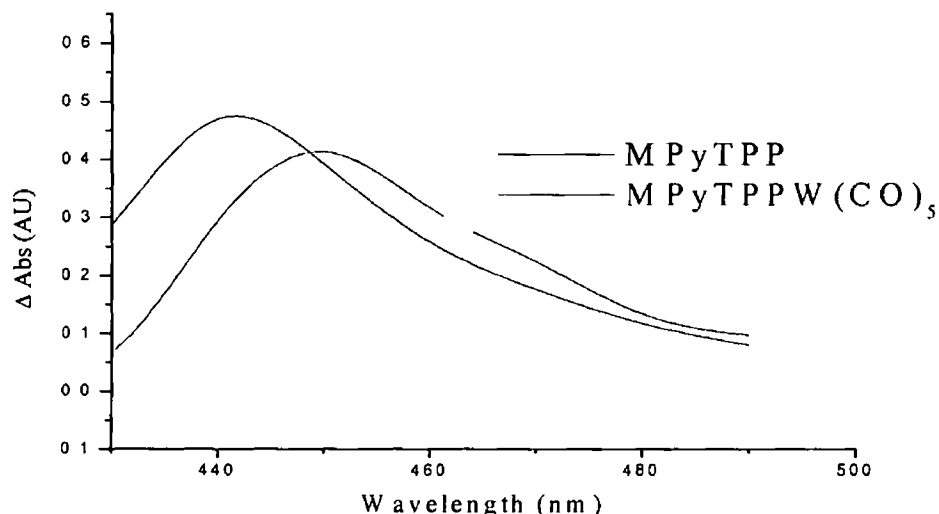


**Figure 3 15 Transient absorption spectra of MPyTPP and MPyTPPW(CO)<sub>5</sub> (identical absorbance at  $\lambda_{exc} = 532$  nm at 293 K)**

There are a number of possibilities to explain what could be involved upon excitation of the complex (see Figure 3 25 and 3 26, Section 3 9). It has been suggested that with the W(CO)<sub>5</sub> moiety co-ordinated in the *meso* position, an internal heavy atom effect could be expected. This should lead to a substantial decrease in the lifetime of the singlet and triplet states. In the complex being discussed the heavy atoms are remote from the porphyrin and would not readily affect intersystem crossing (ISC), as the W(CO)<sub>5</sub> unit is complexed to a pyridine ring which is orthogonal to the porphyrin ring. The reduced interaction caused by the orientation of the pyridyl ring is shown by the similarity of the triplet lifetimes between the complex and the uncomplexed porphyrin.

In Figure 3 26 it is suggested that the W(CO)<sub>5</sub> component is lost through population of the <sup>3</sup>LF state of the W(CO)<sub>5</sub>(C<sub>5</sub>H<sub>4</sub>N) entity. Population of this energy state should lead to a reduction in intensity of the transient absorption spectrum of the ground state complex. The spin forbidden process of singlet to triplet intersystem crossing is the predominant route for radiationless deactivation of S<sub>1</sub> in porphyrins with S→T formation is about

90%<sup>20</sup> This would make it difficult to observe any reduction or increase in intensity<sup>16</sup> There should be an accompanying reduction in the intensity of the transient of the complex compared to that of the porphyrin when measured at the same wavelength Figure 3.16 shows no appreciable differences in the transient signals for the triplet excited state of both the complex and the uncomplexed free base porphyrin The lifetime of both the complex and the uncomplexed free base porphyrin are similar (see Table 3.6) The triplet state decays with mixed first/second order kinetics (Figure 3.16), and this is attributed to competition between unimolecular decay and triplet-triplet annihilation processes and is typical for all porphyrins<sup>10,12</sup>

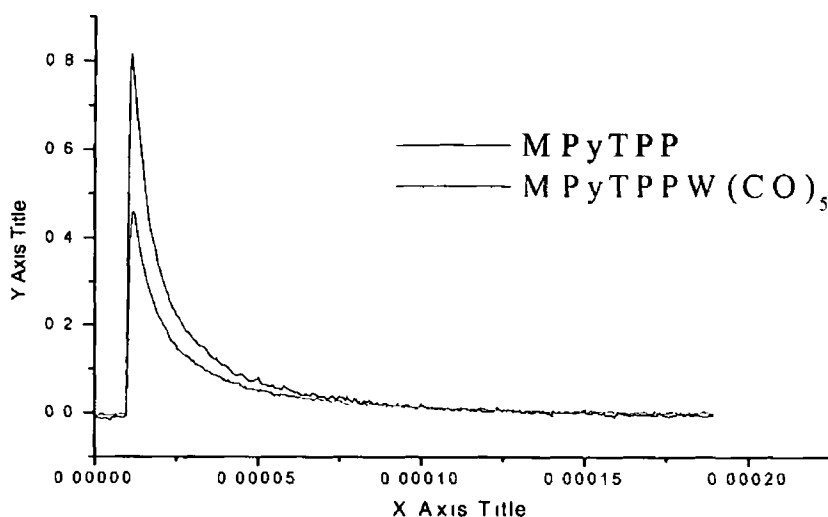


**Figure 3.16** Transient of *MPyTPP* compared to that of *MPyTPPW(CO)<sub>5</sub>*  $\lambda_{exc} = 532\text{nm}$  monitored at 440 nm in dichloromethane solution at 293 K

Scheme 3.1 suggests a different reaction mechanism for the formation of the triplet excited state in the complex. The fact that there is little change in the lifetime of the complex compared to that of the uncomplexed free base porphyrin suggests that the metal carbonyl moiety has no effect on the porphyrin excited state dynamics. However, changes were detected in the emission spectra and the fluorescence lifetime of the complexes.

**Table 3.6**

450 nm

| <i>Porphyrin</i>         | $\tau_{trip}(\mu s)$ | $k_{obs} (s^{-1})$ |
|--------------------------|----------------------|--------------------|
| MPyTPP                   | 30                   | $32748 \pm 3275$   |
| MPyTPPW(CO) <sub>5</sub> | 26                   | $37989 \pm 3799$   |

Figure 3 26 and Scheme 3 2 suggest that the interaction of the metal carbonyl fragment and the porphyrin reduces the energy of the lowest energy singlet state of the metal carbonyl fragment From the reaction Scheme, population of these singlet state orbitals results in loss of the M(CO)<sub>5</sub> fragment Therefore excitation of the porphyrin complex leads to formation of the triplet state of the uncomplexed free base porphyrin This explains why no significant changes in the triplet lifetimes during laser flash photolysis are observed

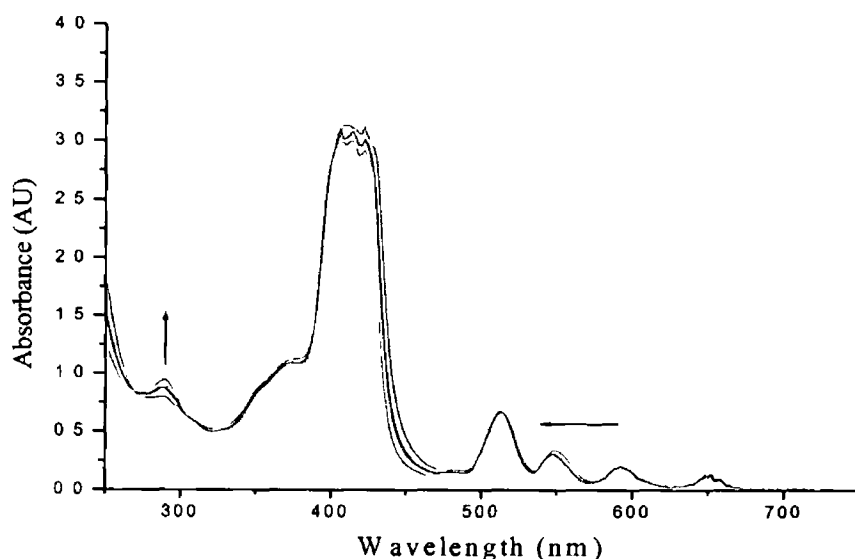


**Figure 3 17 UV-vis spectra of MPyTPPW(CO)<sub>5</sub> recorded during a laser flash photolysis experiment ( $\lambda_{exc} = 532$  nm) in dichloromethane under 1 atmosphere of CO**

Throughout each flash photolysis experiment, the UV-vis spectrum of the sample was continuously recorded, so as to monitor any changes As the experiment progressed a grow in at 290 nm was assigned in the UV-vis spectrum to the formation of W(CO)<sub>6</sub> (see

Figure 3 17) An IR spectrum of the photolysed solution indicated the formation of a band at  $1981\text{ cm}^{-1}$  which is assigned to  $\text{W}(\text{CO})_6$ . Once more the pentacarbonyl bands of the complex are present and have been accompanied by a grow in of the hexacarbonyl peak (see Figure 3 18). These changes have been attributed to the formation of the singlet excited state of the porphyrin pentacarbonyl complex which leads to cleavage of the N-M bond. Figure 3 18 shows an IR of  $\text{MPyTPPW}(\text{CO})_5$  after laser flash photolysis.

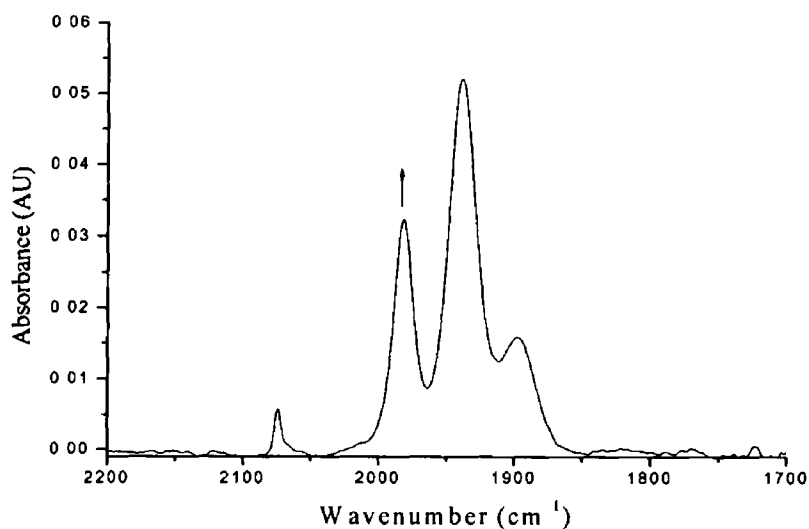


**Figure 3 18 IR of  $\text{MPyTPPW}(\text{CO})_5$  after laser flash photolysis ( $\lambda_{\text{exc}} = 532\text{ nm}$ ) in dichloromethane under 1 atmosphere of CO**

### 3.8.2 Laser flash photolysis of MPyTPPCr(CO)<sub>5</sub> at 532 nm under 1 atmosphere of CO

The transient absorption spectrum of MPyTPPCr(CO)<sub>5</sub> (Figure 3.19) was recorded between 430 and 800 nm, and as was found with MPyTPPW(CO)<sub>5</sub> had characteristics similar to the <sup>3</sup>(π-π\*) excited state of the uncomplexed free base porphyrin. Both the free base porphyrin and MPyTPPCr(CO)<sub>5</sub> absorbs strongly between 440 and 490 nm with the maxima again at *ca.* 460 nm for the latter. MPyTPPCr(CO)<sub>5</sub> showed bleaching at 520 nm and less intense absorption in the Q-band region which is typical of MPyTPP.

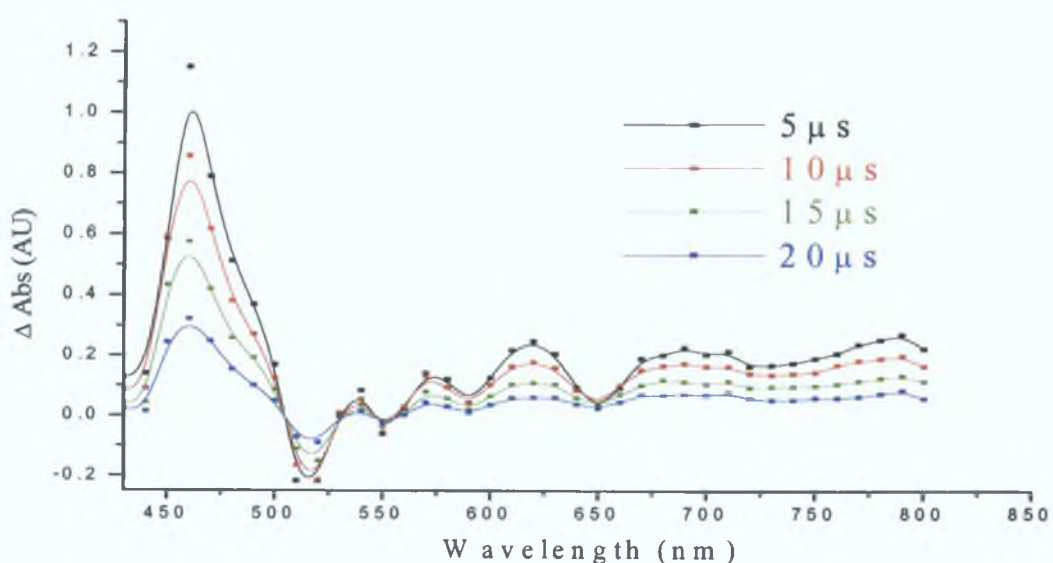


**Figure 3.19** Transient absorption spectrum of MPyTPPCr(CO)<sub>5</sub> at  $\lambda_{exc} = 532$  nm under 1 atmosphere of CO in dichloromethane at 293 K

Although the transient absorption spectrum of MPyTPPCr(CO)<sub>5</sub> had the same overall profile of the uncomplexed free base porphyrin, changes were evident when they were compared by studying solutions with identical absorbances at  $\lambda_{exc} = 532$  nm (Figure 3.20). A reduction in the intensity of the spectrum from 430-450 nm is apparent. This reduction is similar to that observed for MPYTPPW(CO)<sub>5</sub> and the red shift in the  $\lambda_{max}$  is  $\sim 10$  nm.

As outlined in Scheme 3.1, the formation of  $\text{Cr}(\text{CO})_6$  is due to population of the energetically favourable  $^3\text{LF}$  state on  $\text{C}_5\text{H}_4\text{NM}(\text{CO})_5$ . This could lead to a reduction in the lifetime of the triplet state of the complex as it could be a competing process with intersystem crossing. Although the transient absorption intensity was reduced for the Cr complex, 90% conversion from the  $\text{S} \rightarrow \text{T}$  usually recorded for the uncomplexed free base porphyrin is too large to allow detection of the small effect of the population of the  $^3\text{LF}$  state of the  $\text{C}_5\text{H}_4\text{NM}(\text{CO})_5$  unit.<sup>16</sup>

**Table 3.7**

| 450 nm                    |                                    |                                  |
|---------------------------|------------------------------------|----------------------------------|
| <i>Porphyrin</i>          | $\tau_{\text{trip}} (\mu\text{s})$ | $k_{\text{obs}} (\text{s}^{-1})$ |
| MPyTPP                    | 30                                 | $32748 \pm 3275$                 |
| MPyTPPCr(CO) <sub>5</sub> | 27                                 | $36797 \pm 3680$                 |

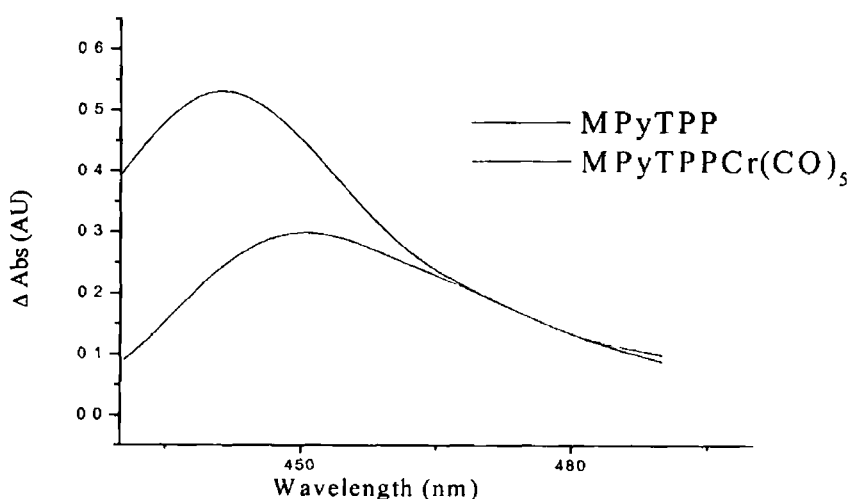


**Figure 3.20** Transient absorption spectrum (20  $\mu\text{s}$ ) of isoabsorptive samples of MPyTPP and MPyTPPCr(CO)<sub>5</sub> at  $\lambda_{\text{exc}} = 532 \text{ nm}$  at 293 K

For MPyTPPW(CO)<sub>5</sub> intersystem crossing due to the heavy atom effect was used to try and explain the reduction in the intensity of the emission spectra (see Section 3.8.1) and to predict changes that would have been expected in the transient absorption spectra i.e. a

similar reduction in the lifetime of the triplet state and a reduction in the intensity of the transient signals. If the system was affected by intersystem crossing changes due to the W atom would have been greater. They were not the case and Figure 3.26 was used to demonstrate what is happening.

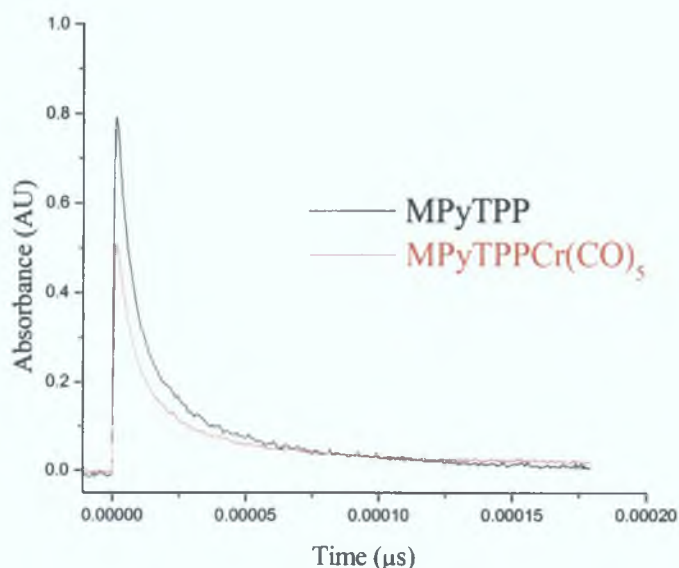


**Figure 3.21** Transient signals obtained at 440 nm following laser flash photolysis of both MPyTPP and MPyTPPCr(CO)<sub>5</sub> at 532nm dichloromethane at 293 K

If intersystem crossing was involved in these porphyrin complexes a greater change would have been expected for the triplet lifetimes of the W complex compared to that of the uncomplexed porphyrin. This is not the case and as Cr is not a heavy atom the spin orbit coupling is very small. The lifetimes of the triplet states were similar for both the chromium complex and the uncomplexed free base porphyrin (see Table 3.7). As can be seen, no changes in the triplet lifetime of the complex compared to the uncomplexed free base porphyrin the theory behind Scheme 3.2 can also be applied to the Cr complex. The triplet state decays with mixed first/second order kinetics (Figure 3.21). As previously stated this is attributed to competition between unimolecular decay and triplet-triplet annihilation processes and is typical for all porphyrins.<sup>10, 12</sup>

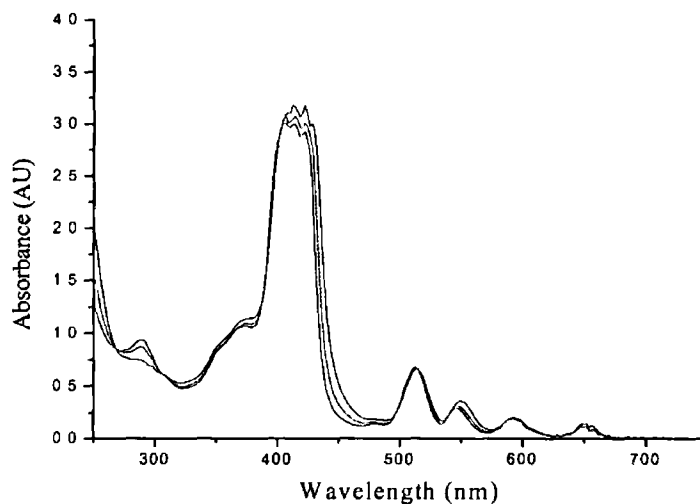


**Figure 3.22 UV-vis spectra of  $\text{MPyTPPCr(CO)}_5$  recorded during laser flash photolysis ( $\lambda_{\text{exc}} = 532 \text{ nm}$ ) in dichloromethane under 1 atmosphere of CO**

However formation of  $\text{Cr(CO)}_6$  is evident at 290 nm from the UV (see Figure 3.22) which suggests that loss of the  $\text{Cr(CO)}_5$  unit occurs

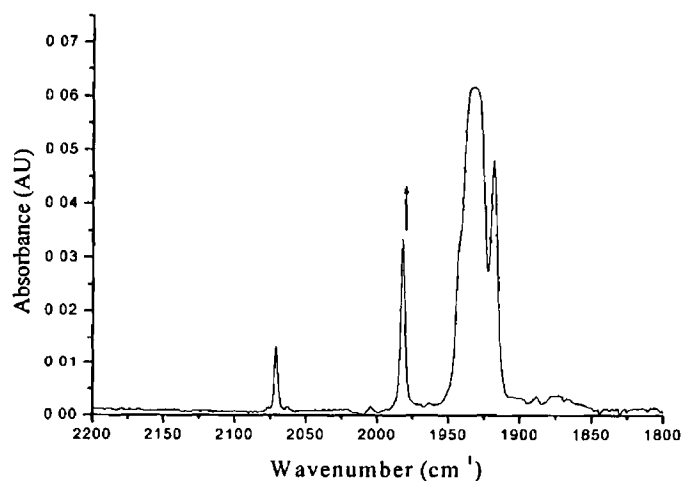


**Figure 3.23 IR of  $\text{MPyTPPCr(CO)}_5$  after laser flash photolysis ( $\lambda_{\text{exc}} = 532 \text{ nm}$ ) in dichloromethane under 1 atmosphere of CO**

The IR spectrum of the sample solution was measured after the transient absorption spectrum had been obtained. Once more the pentacarbonyl bands of the complex were depleted and the formation of  $\text{Cr}(\text{CO})_6$  is evident from the  $\nu_{\text{CO}}$  band at  $1991\text{ cm}^{-1}$  (see Figure 3.23)

### 3.8.3 Discussion of results

Laser flash photolysis was carried out on the uncomplexed free base aryl porphyrin (MPyTPP) and its metal carbonyl complexes (MPyTPP)M(CO)<sub>5</sub> in deoxygenated dichloromethane under one atmosphere of CO and also under one atmosphere of Ar (M = W or Cr).

The time-resolved absorbance of the triplet state of a typical tetraphenyl or tetrapyrrolyl porphyrins have a lifetime of *ca.* 29  $\mu$ s at room temperature.<sup>4</sup> Free base porphyrins exhibit strong transient signals from 430 nm to 480 nm and there is also bleaching at 520 nm with less intense absorption in the Q-band region extending into the IR region. The transient signals obtained in this study were typical of <sup>3</sup>( $\pi$ - $\pi^*$ ) excited states of aryl porphyrins (see Figure 3.24).<sup>44,45</sup>

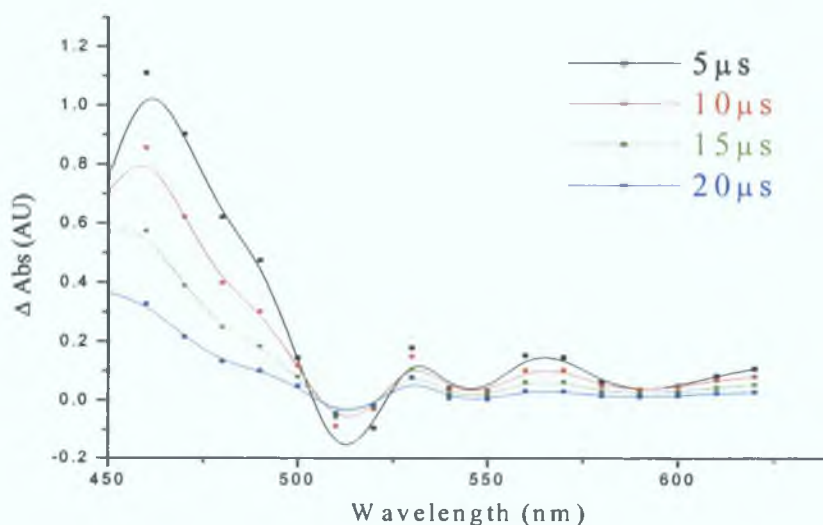


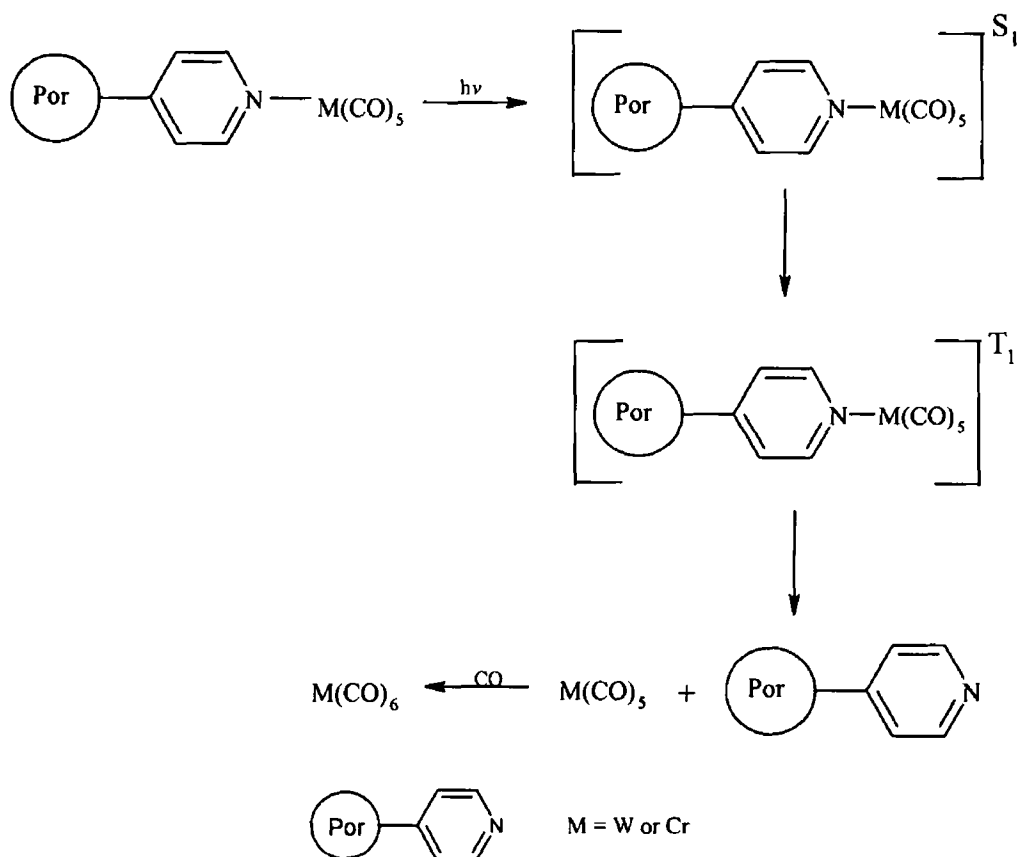
**Figure 3.24** Transient absorption spectrum of MPyTPP obtained following laser flash photolysis at 532 nm under 1 atmosphere of CO in dichloromethane at 293 K

These systems discussed here were chosen, with the aim of investigating the efficiency at which the electron or energy transfer process can occur across orthogonal  $\pi$ -substituents on the *meso* position of porphyrins. The UV-vis spectrum of W(CO)<sub>5</sub>(C<sub>5</sub>H<sub>4</sub>N) was

discussed in Section 3.2 and it was shown that this compound has no significant absorbance at wavelengths longer than 430 nm.  $M(CO)_5(C_5H_4N)$  experiences pyridine ligand loss with a quantum yield approaching 1.0 from the population of a metal-centred LF excited state.<sup>13,46</sup>

Laser flash photolysis ( $\lambda_{exc} = 532$  nm) of  $MPyTPPM(CO)_5$  in deoxygenated dichloromethane populates the excited states associated with the porphyrin moiety rather than the  $M(CO)_5$  pyridyl unit as the latter does not absorb at 532 nm. The transient absorption spectra for both metal carbonyl porphyrin complexes have similar features to that of triplet states of the uncoordinated porphyrin (see Figure 3.24), with strong absorbances from 430 nm to 480 nm and also bleaching at 520 nm. Less intense absorptions are observed in the Q-band region.

Scheme 3.1



For the complexed porphyrin the lifetimes of the triplet excited state were also similar to that of the uncoordinated porphyrin with differences of only 4  $\mu$ s between all three porphyrins. However the triplet state lifetimes of both complexes are less than that of the free base porphyrin. Measurements using different concentrations of CO and Ar confirmed that neither affects the lifetime of the triplet state. Throughout the laser flash photolysis the UV-vis spectra were continually recorded. A grow in of a new band at approximately 290 nm indicated the formation of  $M(CO)_6$  as the experiment proceeded. This was confirmed by obtaining an IR spectrum at the end of the experiment (see Figure 3.18 and 3.23).

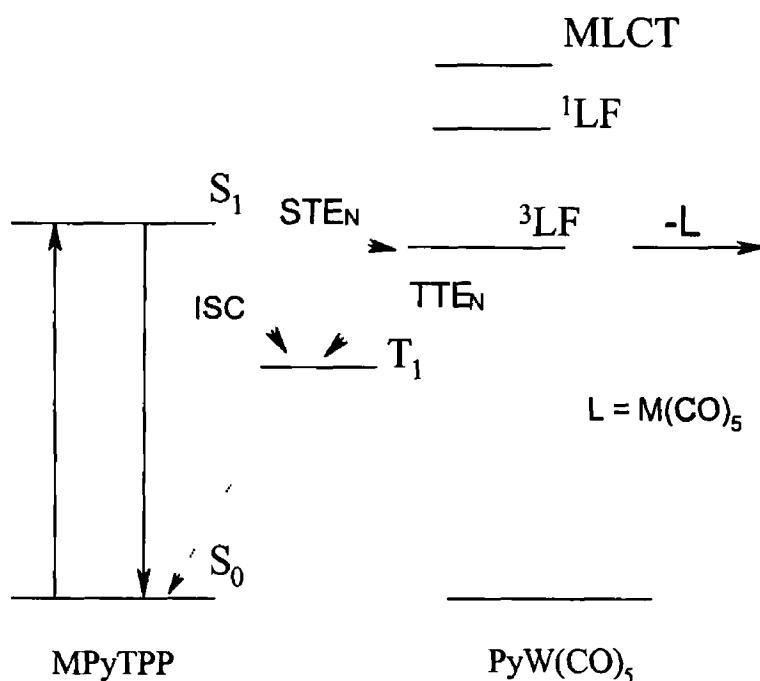


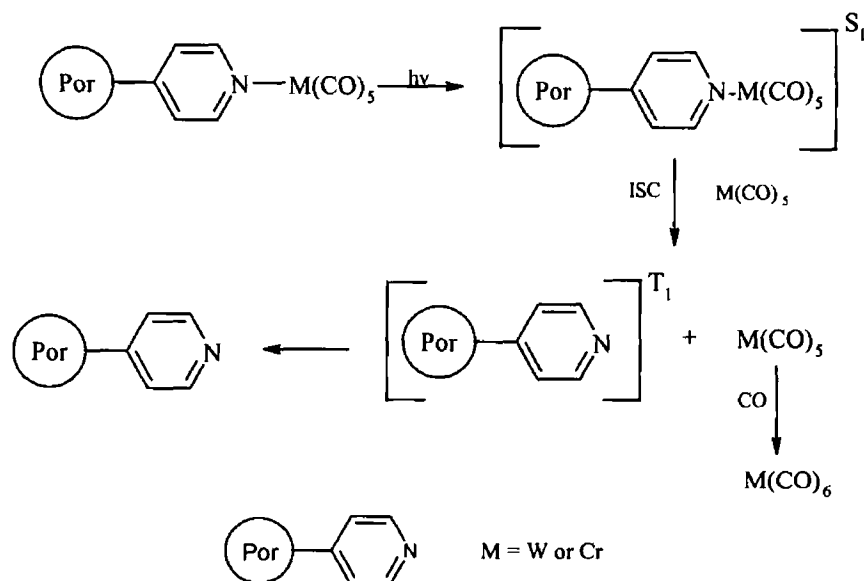
**Figure 3.25** Diagrammatical representation of the deactivation pathway following population of the singlet excited state in  $MPyTPPM(CO)_5$  ( $\lambda_{exc} = 532$  nm)

The spectroscopic changes in the UV-vis were consistent with the formation of the free porphyrin and the metal hexacarbonyl (see Scheme 3.1 and 3.2). The heavy atom effect has been ruled out due to similarity of the triplet lifetimes of the complexed and uncomplexed porphyrins. One possible explanation of the observed photochemistry is as follows, although other pathways are possible. Formation of a new band due to the

hexacarbonyl is observed. The cause of this could be due to loss of the carbonyl moiety from the triplet excited state of the porphyrin carbonyl complex. Scheme 3.1 shows formation of a triplet state associated with the complex and loss of the  $M(CO)_5$  moiety from this excited state. However, loss of this moiety should lead to a significant change in the lifetime of the triplet state of the complex relative to that of the uncomplexed porphyrin.

This is not the case and an alternative reaction mechanism is proposed in Scheme 3.2. Another possibility for explaining the photochemistry observed is given in the following Scheme.

Scheme 3.2



In this process, excitation of the complex causes population of the singlet state. Loss of the  $M(CO)_5$  component occurs from this excited state and ISC leads to population of the excited triplet state of the uncomplexed free base porphyrin (See figure 3.26). The transient absorption spectra of the W and Cr porphyrin complexes have the characteristics of the uncomplexed free base porphyrin. In Section 3.8 it was observed that the shift to

lower energy of the various transient absorption spectra of the complexes could be due to the formation of singlet energy levels, which are lower in energy than that of the uncomplexed free base porphyrin

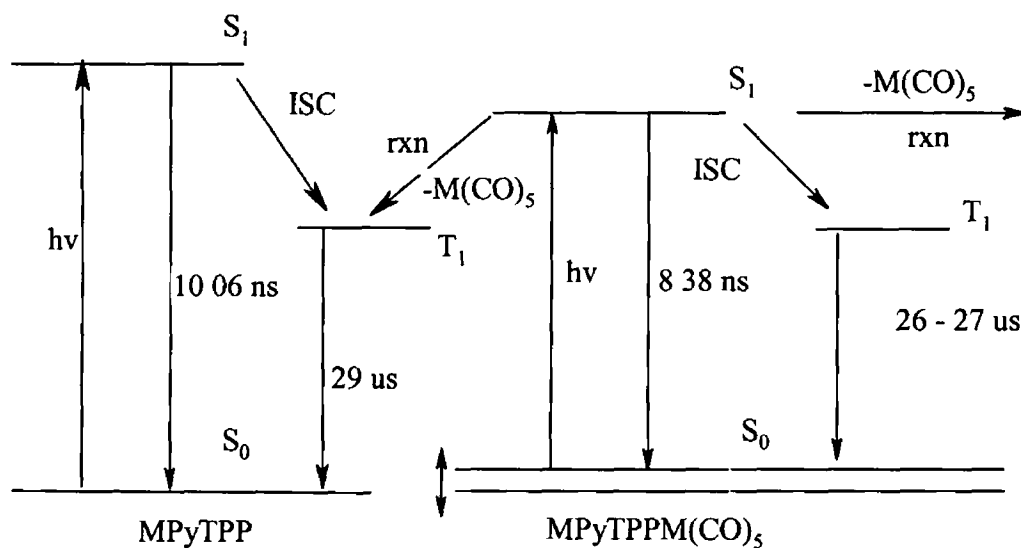


**Figure 3 26** Diagrammatical representation of the deactivation pathway from the singlet excited state in  $MPyTPPM(CO)_5$ . ( $\lambda_{exc} = 532 \text{ nm}$ )

Even when the photolysis was conducted in the absence of CO in a carefully deaerated solution of  $MPyTPPM(CO)_5$  in dichloromethane and placed under an atmosphere of Ar, formation of the triplet state due to the free base porphyrin was observed as indicated by the lifetimes of the transient signals. Under this inert atmosphere, recombination of the pentacarbonyl and the porphyrin was not evident from the IR spectra. When the solution was analysed in the IR depletion formation of the hexacarbonyl was evident. For pyridine metal pentacarbonyl photodissociation of the ligand and not CO is the most efficient photochemical process over the excitation region<sup>13 47</sup>

It could be stated that irradiation of the porphyrin metal carbonyl complex leads to population of the triplet excited state on the porphyrin ring yet loss of the metal carbonyl moiety anchored orthogonal to the ring in the *meso* position is observed. The loss of the  $M(CO)_5$  from pyridine complexes has only been observed photochemically ( $\lambda_{exc} = 355$

nm) following population of the  $^3\text{LF}$  of the  $\text{M}(\text{CO})_5(\text{C}_5\text{H}_4\text{N})$  unit. Therefore direct photolysis of the porphyrin leads to indirect population of this pyridyl unit and loss of the  $\text{M}(\text{CO})_5$  moiety. Electron/energy transfer from the porphyrin to the metal moiety results in cleavage of N-W bond. The photochemical product  $\text{M}(\text{CO})_5$  intermediate is then efficiently scavenged by CO to yield  $\text{M}(\text{CO})_6$  and uncoordinated porphyrin.

### 3 9 Conclusion

Synthesis of the uncomplexed free base porphyrins (*mono*-pyridyl triphenyl porphyrin) and two metal adduct complexes have been carried out. Investigation into the electronic communication (due to electron/energy transfer processes) between the porphyrin chromophore and the metal carbonyl moiety was carried out using an extensive array of techniques including photophysical (emission spectra and singlet lifetimes) and photochemical (time resolved and steady state spectroscopies). Complexation of a metal carbonyl group to the porphyrin macrocycle provides an extra means of characterisation, through the structure sensitive M-CO stretching mode. Furthermore metal carbonyl groups have their own characteristic signatures in the IR, which are highly sensitive to electron density at the metal centre. Given what is known of the photochemistry and photophysical properties of tetra aryl uncomplexed free base porphyrins, two possible reaction schemes have been proposed for the cleavage of the  $M(CO)_5$  fragment

In Scheme 3.1 because the metal carbonyl unit is linked to the porphyrin ring *via* a pyridyl linker which is orthogonal to the ring, and because the UV-vis spectrum of the porphyrin ligand changes on complexation, it can be assumed that the energy levels of each molecular component (free base porphyrin and  $M(CO)_5(C_5H_4N)$ ) are relatively unperturbed by intercomponent interaction<sup>12</sup>. Therefore energy level diagrams of the separate components can be added to obtain an overall energy level diagram for the complex system (figure 3.25). The porphyrin metal carbonyl complex may then be treated as a supramolecular species.

This excited state diagram forms the basis of the proposed energy pathway following excitation of the porphyrin centre at 532 nm. At this excitation wavelength the  $M(CO)_5(C_5H_4N)$  moiety does not absorb, and only the porphyrin unit is therefore excited. In the UV-vis spectra we observe consistent shifts of 2-4 nm upon complexation. The fluorescence spectra of the complexed porphyrins are also typical of the free porphyrin originating from the lowest excited singlet state on the porphyrin. Some factors are available to support the theory behind Figure 3.25, firstly the reduction in the singlet

lifetime of the W complex compared to the uncomplexed porphyrin supports the proposal that intersystem crossing has been enhanced by the presence of the heavy atom. Secondly, the loss of the  $M(CO)_5$  component supports the suggestion of singlet-triplet energy transfer from the  $S_1$  on the porphyrin to the  $^3LF$  on the  $C_5H_4NM(CO)_5$  unit. During laser flash photolysis it was clear that cleavage of the M-N bond occurred even if the sample was photolysed at 532 nm. At this wavelength only population of the excited states on the porphyrin occurs, i.e.  $M(CO)_5(C_5H_4N)$  does not absorb at this wavelength so all light is absorbed by the porphyrin macrocycle. Loss of the pyridyl ligand from  $M(CO)_5(C_5H_4N)$  occurs following population of the  $^3LF$  of this compound. According to Scheme 3.1 this energy level is populated following laser flash photolysis at 532 nm. From Figure 3.25 population of the  $^3LF$  energy level of  $M(CO)_5(C_5H_4N)$  would lead to a reduction in the singlet state lifetime. This would explain both the reduction in the lifetime of the singlet of the complex and the formation of  $M(CO)_6$  due to cleavage of the M-N bond. However, this interpretation fails for a number of reasons. Firstly the reduction in lifetime has previously been put down to the heavy atom effect, which has been discussed in Section 3.7. In the case of tungsten this explanation is acceptable, however this cannot be so for the chromium analogue. The heavy atom effect enhances ISC due to the spin orbit coupling effect, which is responsible for singlet to triplet transitions. With increasing atomic number the effect enhances. Therefore as tungsten is a heavier atom than chromium it would be expected that the singlet lifetime of the tungsten complex would be shorter lived than the chromium complex. This is not the case and even though the differences are small they are real and consistent. Secondly there is no significant reduction in the lifetime of the triplet state for either complex (see Section 3.8). The heavy atom effect would also have a major consequence on the triplet lifetime of the complex. The heavy atom effect reduces the value of the triplet lifetime of a ligand containing a heavy metal by causing the triplet to obtain some singlet character and reduce the amount of pure triplet present.

Another possible pathway, to explain the reduction in the singlet lifetimes other than that just described for the heavy atom effect, is shown in Figure 3.26.

Figure 3.26 indicates that the energy levels of the porphyrin and the  $M(CO)_5$  entity do not act as they should in a supramolecular system and the intercomponent interactions cannot be treated as negligible although an interaction in the triplet state is not apparent. This model helps to explain why we do not see a change in the triplet lifetime of the complex. In the ground state electronic absorbance spectra of the porphyrin complexes are shifted to lower energy when compared to the uncomplexed porphyrin. It has been reported that metallation of the porphyrin decreases the fluorescence quantum yield and lifetime of the porphyrin to a greater extent than that of substitution at the *meso* position.<sup>48</sup> The singlet lifetime of a porphyrin with Zn at the centre is  $\sim 2.0$  ns while that of the W complexes studied was 8.4 ns. The pyridine and phenyl rings of the porphyrin are twisted out of the molecular plane so that they are isolated from the conjugated system of the macro ring (see Figure 3.1). The reduction in singlet lifetime can be explained by the formation of a lower energy singlet state relative to the free porphyrin. This can be clarified by the red shift of the emission spectra and ground state spectra of the complexes relative to the uncomplexed free base porphyrin. From Figure 3.26, loss of the carbonyl moiety occurs from this excited state. When measuring the triplet excited state there are no substantial changes in the lifetimes related to population of a complex based triplet excited state, the lifetimes are very similar for all porphyrins, complexed or uncomplexed.

In conclusion two mechanisms were proposed, one which assumed the formation of a supramolecular complex upon complexation of the porphyrin with  $M(CO)_5$ . This allowed the separate entities of the molecule to be treated individually. This Scheme failed for a number of reasons (i) the lifetime of the triplet state of the complex was similar to that of the uncomplexed porphyrin, (ii) the reduction in the lifetime of the W complex was less than that of the Cr complex even though W was a heavier atom.

The other Scheme assumes that the separate entities interact to an extent that the energy levels are rearranged. This is supported by the fact that (i) the complexes show ground state absorption spectra and emission spectra at lower energy than the uncomplexed porphyrin, (ii) these lower energy spectra are accompanied by a reduction in lifetimes of

the complexes (iii) The triplet state of the complex shows no relative reduction in intensities and is strikingly similar to that of the uncomplexed free base porphyrin

### 3.9 Bibliography

---

- 1 V Balzani, F Scandola, *Supramolecular Photochemistry*, Horwood, Chichester, UK, 1991
- 2 A Harriman, J P Sauvage, *Chem Soc Rev* , **1996**, 41
- 3 A P de Silva, H Q N Gunaratne, T Gunnlaugsson, A J M Huxley, C P McCoy, J T Rademacher, T E Rice, *Chem Rev* , **1997**, 97, 1515
- 4 K Kalyanasundaram, *Photochemistry of Polypyridyl and Porphyrin Complexes*, Academic Press, London, **1992**
- 5 N M Rowley, S S Kurek, J-D Foulon, T A Hamor, C J Jones, J A McCleverty, S M Hubig, E J L McInnes, N N Paynes, L J Yellowlees, *Inorg Chem* , **1995**, 34, 4414
- 6 E Alessio, E Iengo, L G Marzilli, *Supramolecular Chemistry*, **2002**, 14, 103
- 7 N Aratani, A Osuka, H S Cho, D Kim, *J Photochem Photobiol C Photochem Rev* , **2002**, 3, 25
- 8 T Imamura, K Fukushima, *Coord Chem Rev* , **2000**, 198, 133
- 9 C J Aspley, J R Lindsay Smith, R N Perutz, D Pursche, *J Chem Soc , Dalton Trans* , **2002**, 170
- 10 K Kalyanasundaram, *Photochemistry of Polypyridyl and Porphyrin Complexes*, Academic Press, London, **1992**, chapt 12
- 11 E J Shin, D Kim, *J Photochem Photobiol A*, **2002**, no, 6084
- 12 A Prodi, M T Indelli, C J Kleverlaan, F Scandola, E Alessio, T Gianferrara, L G Marzilli, *Chem Eur J* , **1999**, 5, 2668
- 13 M S Wrighton, H B Abrahamson, D L Morse, *J Am Chem Soc* , **1976**, 98, 4105
- 14 C Maralejo, C H Langford, D K Sharma, *Inorg Chem*, **1989**, 28, 2205
- 15 C J Aspley, J R Lindsey Smith, R N Perutz, *J Chem Soc , Dalton Trans*, **1999**, 2269
- 16 K Kalyanasundaram, *Inorg Chem* , **1984**, 23, 2453

- 
- 17 P J Spellman, M Gouterman, A Antipas, S Kim, Y C Lin, *Inorg Chem*, **1980**, *19*, 386
- 18 M Moet-Ner, A D Alder, *J Am Chem Soc*, **1975**, *97*, 5107
- 19 J B Kim, J J Leonard, F R Longo, *J Am Chem Soc*, **1972**, *94*, 3986
- 20 D J Quimby, F R Longo, *J Am Chem Soc*, **1975**, *97*, 5111
- 21 P Glyn, F P A Johnson, M W George, A J Lees, J J Turner, *Inorg Chem*, **1991**, *30*, 3543
- 22 R M Kolodziej, A J Lees, *Organometallics*, **1986**, *5*, 450
- 23 A J Lees, A W Adamson, *J Am Chem Soc*, **1982**, *104*, 3804
- 24 E B Flecher, A M Shachter, *Inorg Chem*, **1991**, *30*, 3763
- 25 L T Cheng, W Tam, D F Eaton, *Organometallics*, **1990**, *9*, 2856
- 26 N M Rowley, S S Kurek, P R Ashton, T A Hamor, C J Jones, N Spencer, J A McCleverty, G S Beddard, T E Feehan, N T H White, E J L McInnes, N N Paynes, L J Yellowlees, *Inorg Chem*, **1996**, *35*, 7526
- 27 C J Aspley, J R Lindsay Smith, R N Perutz, D Pursche, *J Chem Soc, Dalton Trans*, **2002**, 170
- 28 A Prodi, C J Kleverlaan, M T Indelli, F Scandola, E Alessio, E Iengo, *Inorg Chem*, **2001**, *40*, 3498
- 29 M Wrighton, *Inorg Chem*, **1974**, *13*, 905
- 30 M S Wrighton, K R Pope, *Inorg Chem*, **1985**, *24*, 2792
- 31 C M Drain, F Nifiatis, A Vasenko, J D Batteas, *Angew Chem Int Ed*, **1998**, *37*, 2344
- 32
- 33 M Sirish, B G Maiya, *J Photochem Photobiol A Chem I*, **1994**, *77*, 189
- 34 K Kalyanasundaram, *J Chem Soc, Faraday Trans 2*, **1983**, *79*, 1365
- 35 R H Bisby, M Arvanitidis, S W Botchway, I R Clark, A W Parker, D Tobin, *Photochem and Photobiol Science 2*, **2003**, *2*, 157
- 36 J M Zaleski, C K Chang, G E Leroy, R I Cukier, D G Nocera, *J Am Chem Soc*, **1992**, *114*, 3564
- 37 L Flamigni, F Barigelletti, N Armaroli, J P Collin, J P Sauvage, J A G Williams, *Chem Eur J*, **1998**, *4*, 1744

- 
- 38 S Anderson, H L Anderson, A Bashall, M McPartlin, J K M Sanders, *Angew Chem* , **1995**, *106*, 1196
- 39 J S Hsiao, B P Krueger, R W Wagner, T E Johnson, J K Delaney, D C Mauzerall, G R Fleming, J S Lindsey, D F Bocian, R J Donohoe, *J Am Chem Soc* , **1996**, *118*, 11181
- 40 D Gust, T A Moore, A Moore, F Gao, D Luttrull, J M DeGraziano, X C Ma, L R Makings, S J Lee, R V Bensasson, M Rougee, F C De Schryver, M Vand der Auweraer, *J Am Chem Soc* , **1991**, *113*, 3638
- 41 C M Drain, J M Lehn, *J Chem Soc Chem Commun* , **1994**, 2313
- 42 H Yaun, L Thomas, L K Woo, *Inorg Chem* , **1996**, *35*, 2808
- 43 R V Slone, J T Hupp, *Inorg Chem* , **1997**, *36*, 5422
- 44 M Linke, N Fujita, J C Chambron, V Heitz, J P Sauvage, *New J Chem* , **2001**, *25*, 790
- 45 H Shiratori, T Ono, K Nozaki, A Osuka, *Chem Commun* , **1999**, 2181
- 46 G Malouf, P C Ford, *J Am Chem Soc* , **1974**, *96*, 601
- 47 R M Dahlgren, J I Zink, *J Am Chem Soc* , **1979**, *101*, 1448
- 48 K Kalyanasundaram, *Photochemistry of Polypyridyl and Porphyrin Complexes*, Academic Press, London, **1992**, chapt 13, pag 403

## **Chapter 4**

**(5-Mono 4-pyridyl 10, 15, 20- triphenyl porphyrinato) zinc(II) and its tungsten and chromium pentacarbonyl complexes - Results and discussion**

## 4.1 Introduction

Metalloporphyrins have been widely investigated for their potential application in artificial biological systems. Many metalloporphyrins have been synthesised and studied as models for light harvesting and reaction centre complexes found in green plants and photosynthetic bacteria.<sup>1</sup> Such species also occupy a relevant position in the rapidly developing field of supramolecular chemistry,<sup>2</sup> since they are also used as building blocks for the construction of supramolecular artificial systems with special built in properties and functions to carry out light induced reactions.<sup>3</sup>

This chapter expands on the work discussed in chapter three, on free base porphyrins and metal carbonyl complexes. The work described in this chapter concerns the photochemistry and photophysical properties of metalloporphyrins peripherally coordinated to a metal centre. These systems are models for electron/energy transfer process. There are many examples of metalloporphyrins linked to peripheral reaction centres,<sup>4</sup> but very few of these show any physical interaction between the electron donor chromophore and the peripheral unit. In this work metal carbonyl moieties are attached to the peripheral of the metalloporphyrin in order to investigate the communication between the two units. Metal carbonyl metalloporphyrin complexes are an area that is largely unexplored. In contrast the photochemistry of  $M(\text{CO})_5(\text{C}_5\text{H}_4\text{N})$  complexes ( $M = \text{Cr}$  or  $\text{W}$ ) has been extensively researched.<sup>5</sup> Another important feature of the metal carbonyl porphyrin system is the availability of intense  $\nu_{\text{CO}}$  absorptions in the IR spectrum that can provide useful spectroscopic information. The metal carbonyl moiety is attached to the porphyrin *via* a pyridyl linker and it is these pyridyl links that make pyridyl porphyrins useful in the synthesis of these complexes.

In addition insertion of the metal (zinc) into tetra phenyl porphyrin alters the emission and absorbance characteristics of the porphyrin as described in the following sections. Insertion of the metal induces change in the physical conformation of the porphyrin ring. The plane of the porphyrin displays some twisting of the pyrrole carbons with deviations in the plane of the central nitrogen atoms ranging from 0.0028 to 0.2273 Å.<sup>6</sup> In addition

the zinc atom is 0.2849 Å out of the plane of the porphyrin ring for ZnTPP.<sup>6</sup> This is comparable to other zinc porphyrins derivatives where the metal atom sits ~0.2 - 0.3 Å out of the plane of the porphyrin ring.<sup>7,8</sup> The phenyl and pyridyl rings in the *meso* position of the porphyrin remain orthogonal to the porphyrin ring after coordination of the metal.

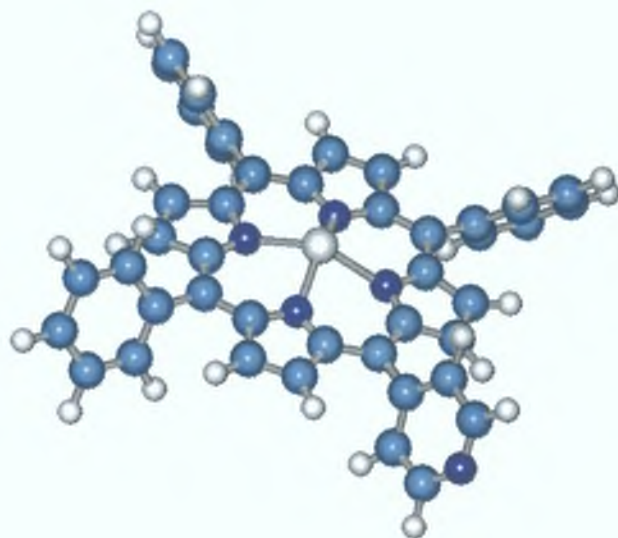


***Figure 4.1 A molecular model representation of 5-mono 4-pyridyl 10,15,20- triphenyl porphyrinato zinc(II) (ZnMPyTPP) which shows the plane of the aryl groups in the meso position are orthogonal to the plane of the porphyrin ring (dark blue atoms are nitrogen atoms while the white atoms are hydrogen and the central zinc atom)***

In this study the interaction between the porphyrin chromophore and the metal carbonyl moiety was investigated in the ground state using UV-vis, NMR and IR spectroscopy. The excited states of these systems was probed using a combination of laser flash photolysis, fluorescence spectroscopy and single photon-counting techniques.

**4.2 Electronic absorption spectra of (5-*mono*-4-pyridyl 10,15,20-triphenyl porphyrinato) zinc(II) and its metal pentacarbonyl complexes M(CO)<sub>5</sub> (M = Cr or W)**

**Table 4 1 UV bands of metalloporphyrin and pentacarbonyl complexes (nm)**

| <i>Porphyrin</i>            | <i>B(0,0)</i> | <i>Q(1,0)</i> | <i>Q(0,0)</i> | $A[Q(0,0)]/$<br>$A[Q(1,0)]$ |
|-----------------------------|---------------|---------------|---------------|-----------------------------|
| ZnMPyTPP polymer            | 418           | 562(1 0)      | 604(0 55)     | 0 55                        |
| ZnMPyTPPCr(CO) <sub>5</sub> | 420           | 548(1 0)      | 588(0 24)     | 0 24                        |
| ZnMPyTPPWCO) <sub>5</sub>   | 422           | 548(1 0)      | 588(0 29)     | 0 29                        |

Table 4 1 contains the electronic absorption spectral features of the *para* substituted *mono*-4-pyridyl 10,15,20-triphenyl porphyrinato zinc(II) polymer (ZnMPyTPP) and the metal carbonyl containing derivatives, ZnMPyTPPW(CO)<sub>5</sub> and ZnMPyTPPCr(CO)<sub>5</sub>. The absorption spectrum of the uncomplexed zinc porphyrin (ZnMPyTPP) has been reported previously.<sup>6</sup> The electronic absorption profile of both the chromium and tungsten pentacarbonyl complexes is similar to those of the uncomplexed zinc porphyrin. The UV-vis absorption spectrum of the uncomplexed zinc porphyrin is characterised by a strong Soret band at 420 nm and two Q bands of decreasing intensity at 562 nm and 606 nm (see Figure 4 2).<sup>9</sup> A substantial shift occurs upon complexation of the zinc porphyrins with the metal pentacarbonyl moiety. Unlike the shifts of 2 - 4 nm observed for the free base porphyrin (Section 3 2) the shifts for the zinc porphyrins are 14 - 16 nm in range. The reason for this large shift in the absorbance bands of the UV-vis spectrum is because the electronic environment of the pyridine in the *meso* position of the zinc porphyrin (metalloporphyrin) has changed more dramatically from that of the free base porphyrin (see Section 3 2). The pyridine ligand of the metalloporphyrin is now coordinated to the zinc atom at the centre of the porphyrin ring.

The Zn (II) ion has a strong affinity for a five coordinate environment, which favours axial ligation in the metalloporphyrin. In a zinc porphyrin, the zinc atom is co-ordinated

to four nitrogens at the centre of the porphyrin ring. The zinc atom will easily co-ordinate to a fifth ligand if one is available. It has been previously demonstrated that pyridine will bind to the metal centre of metalloporphyrins using zinc tetra phenyl porphyrin and pyridine.<sup>10</sup> Upon co-ordination of pyridine to the centre of a metalloporphyrin the Q(0,0) and Q(1,0) bands undergo a red shift. In the case of ZnMPyTPP the pyridine in the *meso* position is incorporated into the macrocycle and not present as a free reagent in solution. The N atom of the pyridine unit of the porphyrin co-ordinates to the Zn atom of another and this leads to the formation of a polymer linked through the N atom and the zinc atom (see Figure 4.3). Increasing the concentration of ZnMPyTPP in solution increased the red shift of the Q bands, which has been attributed to the formation of higher molar mass polymers.<sup>11</sup>

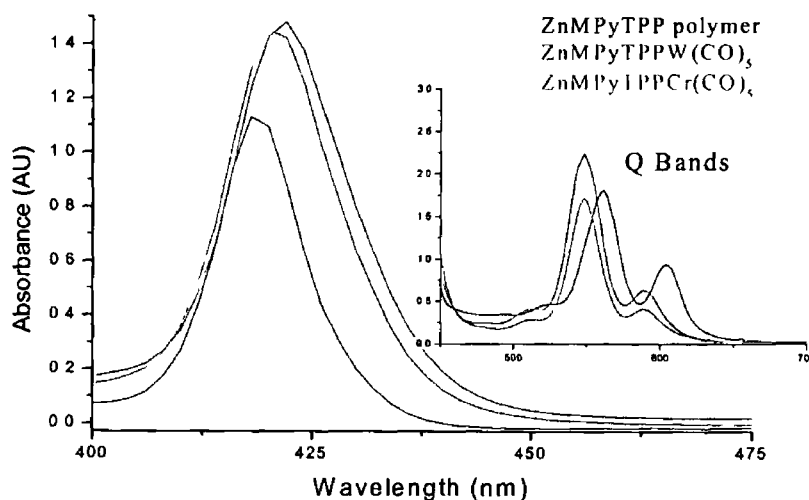


**Figure 4.2** UV-vis spectra of ZnMPyTPP polymer, ZnMPyTPPW(CO)<sub>5</sub> and ZnMPyTPPCr(CO)<sub>5</sub> ( $1.0 \times 10^{-6} \text{ mol dm}^{-3}$  at 532 nm) showing strong Soret bands and Q bands ( $\times 10$ ) in dichloromethane

There is also a change in the absorption intensities of the Q bands normalised with respect to the Q(1,0) band. The intensity of the Q(1,0) band is insensitive to the electronic effects that the substituents in the *meso* position have on the porphyrin macrocycle.

Therefore the absorbance ratio of the Q(0,0) band (this band is sensitive to substituents in the *meso* position) with respect to the Q(1,0) band can be shown to determine the interaction between zinc and the porphyrin (see Table 4.1)<sup>12</sup> The intensity of the Q(0,0) band relative to the Q(1,0) band in the porphyrin metal carbonyl complexes is significantly lower than for the uncomplexed metalloporphyrin, ZnMPyTPP. It has been shown that the electron donating character of a substituent in *meso*-tetraphenyl porphyrins increases the absorption intensities of the Q(0,0) transitions while the presence of electron withdrawing substituents results in a decrease in the absorption intensities of the Q(0,0) transitions<sup>9,13</sup> From Table 4.1 the intensity of the Q(0,0) band relative to the Q(1,0) band of the polymer is greater than that of the pentacarbonyl metalloporphyrin complex.

The dramatic changes in the UV-vis spectrum of the porphyrins are brought about by cleavage of the N-Zn bond, which occurs upon formation of the pentacarbonyl complex. The N-Zn is intrinsically weak and a complexing ligand such as  $M(CO)_5$  will break this bond. However, as was described in Section 4.5 the polymer can reform after the pentacarbonyl moiety has been removed. Once the polymer is formed the pyridine protons and pyrrole  $\beta$ -hydrogens of one porphyrin are inside the ring current of the porphyrin macrocycle to which it is bound (Figure 4.3) and this causes a large high field shift of these protons. The electron density at the *meso* position of the ring also increases hence the large shift in the UV-vis spectrum. Once the polymer chain is ruptured upon complexation with the pentacarbonyl fragment, the electron density at the *meso* position of the ring is reduced and the intensity of the Q(0,0) band relative to the Q(1,0) band is also reduced. This is in contrast to the effect described previously where there was no additional electron density at the *meso* position of the free base porphyrin before complexation with the pentacarbonyl moiety (Section 3.2). In this case the addition of the pentacarbonyl moiety tends to increase electron density at the porphyrin ring with respect to the free base porphyrin.

Another major difference in the UV-vis spectra of the metalloporphyrins with respect to the free base porphyrin is the change in the Q band region. Insertion of a metal into the

centre of the porphyrin reduces the symmetry of the macrocycle from  $D_{2h}$  to  $D_{4h}$  and as a consequence two of the bands ( $Q_y(0,0)$  and  $Q_x(0,0)$ ) are unresolved (see Section 1.2.1). This band has only one vibrational satellite at higher energy and hence only two Q bands are seen for the metalloporphyrin.

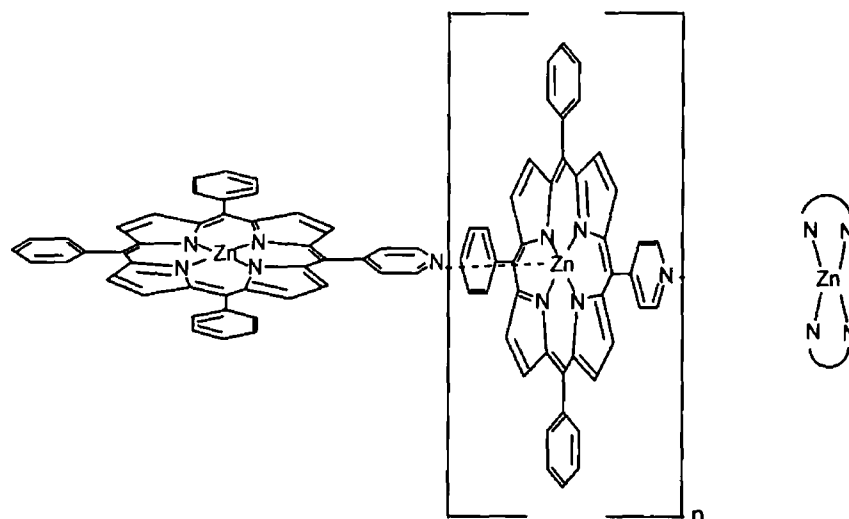


**Figure 4.3 Structure of ZnMPyTPP polymer**

The pentacarbonyl moiety is linked to the porphyrin *via* a pyridyl linker and as observed in Section 3.2, pyridyl metal carbonyl complexes usually have a MLCT band at approximately 340 nm (see Figure 3.4). However, the complexes synthesised in this study gave no evidence for such a transition. Furthermore, the LF transition for  $M(CO)_5(C_5H_4N)$  has been reported to occur at 382 nm,<sup>14,15</sup> but no evidence was obtained in this study from UV-vis spectra of the porphyrin complexes of such a transition. The absorbance of the metalloporphyrin at this wavelength is as intense as the free base porphyrin with extinction coefficients in the region 40 000 to 80 000  $dm^3 mol^{-1} cm^{-1}$  compared to just 7000  $dm^3 mol^{-1} cm^{-1}$  for the  $W(CO)_5(C_5H_4N)$  complex at its  $\lambda_{max}$  (~400 nm). It is possible that the strongly absorbing Soret band of the porphyrin masks the weak absorption features of the  $W(CO)_5(C_5H_4N)$  unit (see Figure 4.2).<sup>16</sup>

**4.3 Infrared spectra of (5-mono-4-pyridyl 10,15,20-triphenyl porphyrinato) zinc(II) and its metal pentacarbonyl complexes  $M(CO)_5$  ( $M = Cr$  or  $W$ )**

The spectroscopic IR data (in the  $\nu_{CO}$ ) for the two substituted ZnMPyTPP complexes are presented in Table 4.2. Three carbonyl absorptions were observed for each metal carbonyl complex in the IR spectrum, which is consistent with the local  $C_{4v}$  symmetry of the metal carbonyl centre (see Figure 4.3)<sup>17</sup>

**Table 4.2**

| <i>Porphyrin</i>            | <i>IR Bands (<math>cm^{-1}</math>)</i> |      |      |
|-----------------------------|----------------------------------------|------|------|
| ZnMPyTPPW(CO) <sub>5</sub>  | 2070                                   | 1931 | 1916 |
| ZnMPyTPPCr(CO) <sub>5</sub> | 2067                                   | 1937 | 1917 |

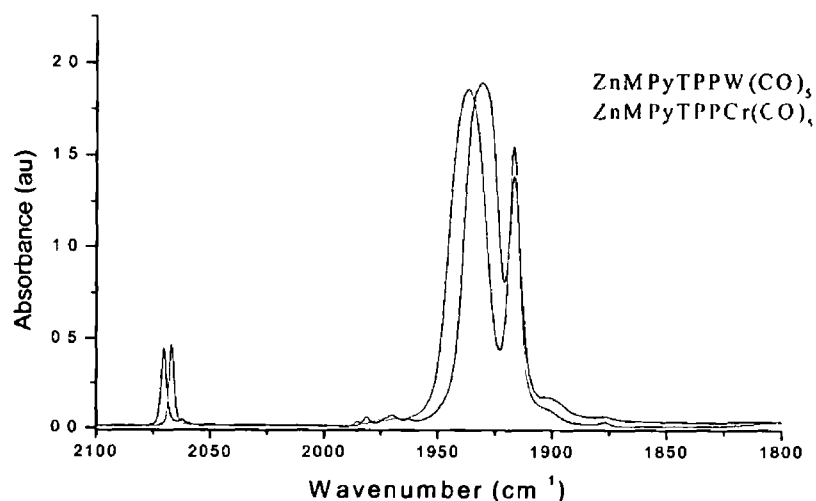


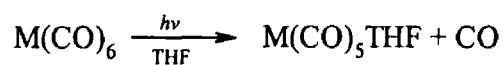
**Figure 4.3 IR spectra of ZnMPyTPPW(CO)<sub>5</sub> and ZnMPyTPPCr(CO)<sub>5</sub> recorded in dichloromethane**

Both complexes were formed by reacting ZnMPyTPP polymer with the photochemically produced  $M(CO)_5THF$  ( $M = W$  or  $Cr$ ) as described in Section 6.5. Removal of the

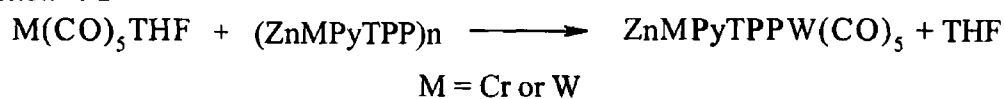
unreacted porphyrin was achieved by column chromatography as outlined in Section 6.3. Unreacted  $W(CO)_6$  or  $Cr(CO)_6$  (hexacarbonyl was in excess) was removed by sublimation under reduced pressure.

Synthesis of the metalloporphyrin metal pentacarbonyl complexes proceeds *via* the following reaction pathway<sup>18</sup>

**Reaction 4.1**



**Reaction 4.2**



4.4 <sup>1</sup>H NMR studies of 5-*mono*-4-pyridyl 10, 15, 20-triphenyl porphyrinato) zinc(II) and its pentacarbonyl complexes M(CO)<sub>5</sub> (M = Cr or W)

Table 4.3

| <i>Porphyrin</i>            | <i>4 H, 2, 6 dipyridyl, δ ppm</i> | <i>4 H, 3,5 dipyridyl, δ ppm</i> | <i>β-pyrrole, δ ppm</i> |
|-----------------------------|-----------------------------------|----------------------------------|-------------------------|
| ZnTPP                       | -                                 | -                                | 8 86                    |
| ZnMPyTPP                    | 2 60                              | 6 23                             | 8 86, 8 51, 7 41        |
| ZnMPyTPPCr(CO) <sub>5</sub> | 9 20                              | 8 19                             | 8 85                    |
| ZnMPyTPPW(CO) <sub>5</sub>  | 9 22                              | 8 18                             | 8 86                    |

The <sup>1</sup>H NMR data for ZnTPP, ZnMPyTPP polymer, ZnMPyTPPCr(CO)<sub>5</sub> and ZnMPyTPPW(CO)<sub>5</sub> are presented in Table 4.3. The absence of a singlet at ≈ -2.83 ppm arising from the internal pyrrole protons distinguishes metalloporphyrins from free base porphyrins. The removal of this singlet from the <sup>1</sup>H NMR and the formation of two Q bands in the UV-vis spectrum confirm that insertion of the zinc at the porphyrin centre has taken place.

Following formation of the zinc porphyrins and prior to formation of the metal pentacarbonyl analogues, the porphyrin forms a polymer, *via* linkages of the zinc atom with the nitrogen in the pyridine. This causes significant changes in the <sup>1</sup>H NMR besides the removal of the signal at ≈ -2.83 ppm. The bound pyrrole protons and pyridine protons are now in the porphyrin ring current and this causes them to experience a ring current effect and they are shifted up field. Complexation of the porphyrin with the pentacarbonyl moiety removes the ring current effect and the protons shift down field to their original position.

Formation of the polymer causes the pyrrole β-hydrogens to shift from a multiplet centred at 8.86 ppm for the free base porphyrin to a series of multiplets at 7.41, 8.51 and 8.86 ppm for the metalloporphyrin polymer. Formation of the pentacarbonyl metalloporphyrin complex results in the protons reforming a multiplet at ≈ 8.9 ppm. The pyridine protons shift upfield from 9.05 and 8.22 ppm for the free base porphyrin to 6.23

and 2.60 ppm for the metalloporphyrin polymer. Formation of the pentacarbonyl metalloporphyrin causes the protons to shift back to  $\approx 9.2$  and  $8.22$  ppm.

Complexation of the pentacarbonyl moiety to the metalloporphyrin shifts the 2,6 pyridyl protons relative to the free base porphyrin by  $\approx \delta 0.4$  ppm. The protons are shifted downfield because of the donation of electron density from the pyridine nitrogen lone pair to the metal centre.<sup>19</sup> The remaining resonances are unaffected by complexation.

## 4.5 Steady state photolysis experiments monitored with UV-vis spectroscopy

### 4.5.1 Steady state photolysis of $\text{ZnMPyTPPW}(\text{CO})_5$ under 1 atmosphere of CO

Solutions of  $\text{ZnMPyTPPW}(\text{CO})_5$  in dichloromethane ( $6.7 \times 10^{-5} \text{ mol dm}^{-3}$ ) were subjected to steady state photolysis ( $\lambda_{\text{exc}} > 500 \text{ nm}$  or  $400 \text{ nm}$ ) (Figure 4.5). Samples were degassed using the freeze pump thaw method before being placed under 1 atmosphere of CO. Irradiation of the sample at  $\lambda_{\text{exc}} > 500 \text{ nm}$  resulted in very little change in the UV-vis spectrum, other than a small grow-in at  $290 \text{ nm}$  (Figure 4.6) attributed to the formation of  $\text{W}(\text{CO})_6$ . More noticeable was the shift of the Q bands to lower energy, together with a change in their relative intensities.

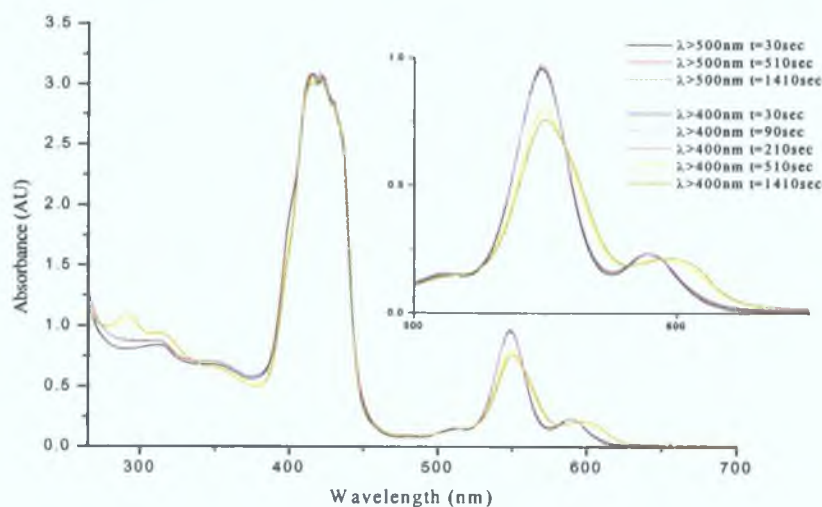


**Figure 4.5** Changes observed in the UV-vis spectrum of  $\text{ZnMPyTPPW}(\text{CO})_5$  ( $6.7 \times 10^{-5} \text{ mol dm}^{-3}$ ) following steady state photolysis ( $\lambda > 400 \text{ nm}$  and  $500 \text{ nm}$ ) in dichloromethane under 1 atmosphere of CO

When the irradiation wavelength was increased to  $\lambda_{\text{exc}} > 400 \text{ nm}$  the effects of photolysis were more obvious. The grow in at  $290 \text{ nm}$  due to the formation of  $\text{W}(\text{CO})_6$  was larger and the Q bands were shifted towards the red. The red shift in the Q band was assigned to

the formation of the ZnMPyTPP polymer formed as a result of the cleavage of the N-W(CO)<sub>5</sub> bond

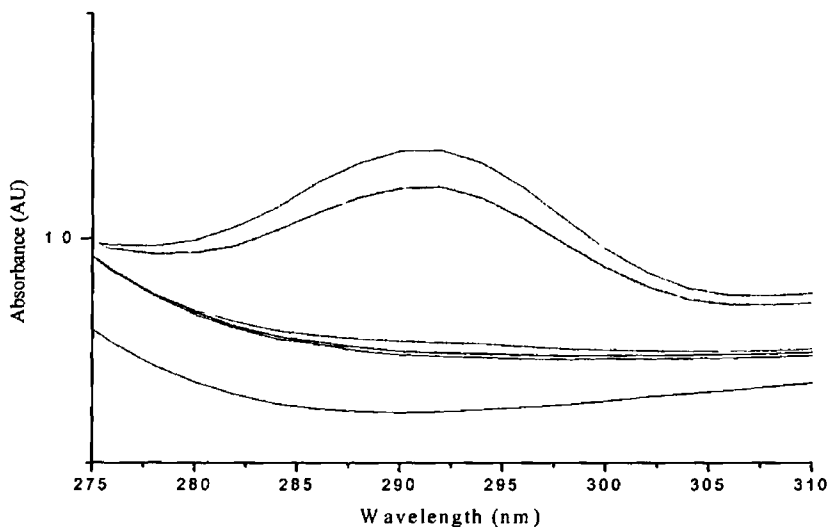


**Figure 4 6 Changes observed between 275 – 310 nm in the UV-vis spectrum following steady state photolysis ( $\lambda > 400$  nm and 500 nm) of ZnMPyTPPW(CO)<sub>5</sub> ( $6.7 \times 10^{-5}$  mol dm<sup>-3</sup>) in dichloromethane under 1 atmosphere of CO**

Photolysis of ZnMPyTPPW(CO)<sub>5</sub> resulted in loss of the W(CO)<sub>5</sub> moiety which allowed formation of the polymer. As the experiment progressed the Q bands shifted further towards the red due to the increasing concentration of the porphyrin polymer in solution. It has been previously observed that increasing the concentrations of a solution of ZnMPyTPP also shifts the Q bands in the same way, this was attributed to increasing polymer length.<sup>6</sup> The intensity of the Q(0,0) band relative to the Q(1,0) band in the porphyrin metal carbonyl complexes is significantly lower than for the uncomplexed metalloporphyrin, ZnMPyTPP.

#### 4.5.2 Steady state photolysis of ZnMPyTPPW(CO)<sub>5</sub> under 1 atmosphere of Ar

Steady state photolysis of ZnMPyTPPW(CO)<sub>5</sub> in dichloromethane ( $5.2 \times 10^{-5} \text{ mol dm}^{-3}$ ), under an atmosphere of argon was also carried out at both  $\lambda_{\text{exc}} > 400 \text{ nm}$  and  $500 \text{ nm}$ . Samples were initially irradiated at  $\lambda_{\text{exc}} > 500 \text{ nm}$ . The changes observed in the UV-vis spectrum for the same photolysis time were not as significant as those observed under 1 atmosphere of CO. Under these conditions formation of W(CO)<sub>6</sub> is less efficient than when experiments are conducted in CO saturated solution (see Figure 4.6 and Figure 4.8). The yield of W(CO)<sub>6</sub> is limited by the ability of the “W(CO)<sub>5</sub>” fragment to co-ordinate CO *via* bimolecular reactions.

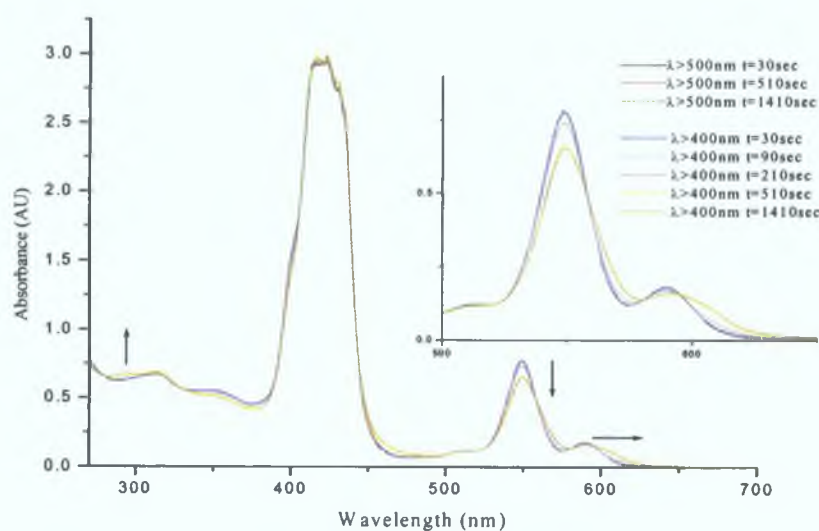


**Figure 4.7** Changes observed in the UV-vis spectrum following irradiation of ZnMPyTPPW(CO)<sub>5</sub> ( $5.2 \times 10^{-5} \text{ mol dm}^{-3}$ ) ( $\lambda > 400 \text{ nm}$  or  $500 \text{ nm}$ ) in dichloromethane under 1 atmosphere of argon

When the irradiation wavelength was increased to  $\lambda_{\text{exc}} > 400 \text{ nm}$  there was some evidence for the formation of W(CO)<sub>6</sub> at  $290 \text{ nm}$  (see Figure 4.8). Tungsten hexacarbonyl continued to form and the reaction was stopped when no further changes were observed in the UV-vis spectrum.

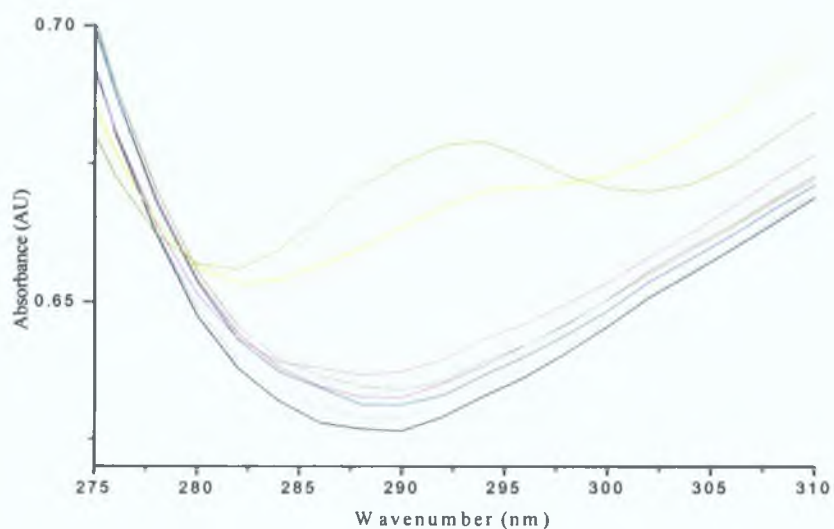


**Figure 4.8** Changes observed between 275 – 310 nm in the UV-vis spectrum following steady state photolysis ( $\lambda > 400$  nm and 500 nm) of  $\text{ZnMPyTPPW}(\text{CO})_5$  ( $5.2 \times 10^{-5}$  mol  $\text{dm}^{-3}$ ) in dichloromethane under 1 atmosphere of Argon

A red shift in the Q bands was noted as the experiment progressed which indicated formation of ZnMPyTPP polymer. No isosbestic points were observed under these conditions for the formation of tungsten hexacarbonyl.

### 4.5.3 Steady state photolysis of ZnMPyTPPCr(CO)<sub>5</sub> under 1 atmosphere of CO

Solutions of ZnMPyTPPCr(CO)<sub>5</sub> in CO saturated dichloromethane (conc.  $5.0 \times 10^{-5}$  mol dm<sup>-3</sup>) were subjected to steady state photolysis ( $\lambda_{\text{exc}} > 400$  nm or 500 nm) and monitored in the UV-vis spectrum as before (see Figure 4.9). Samples were initially irradiated at  $\lambda_{\text{exc}} > 500$  nm and the only noticeable feature in the UV-vis spectrum was a slight increase in absorbance at 290 nm. This increase in absorbance was attributed to the formation of the Cr(CO)<sub>6</sub> (see Figure 4.10). A red shift in the Q bands along with a reduction in their relative intensity was also evident and indicative of N-Cr bond cleavage.

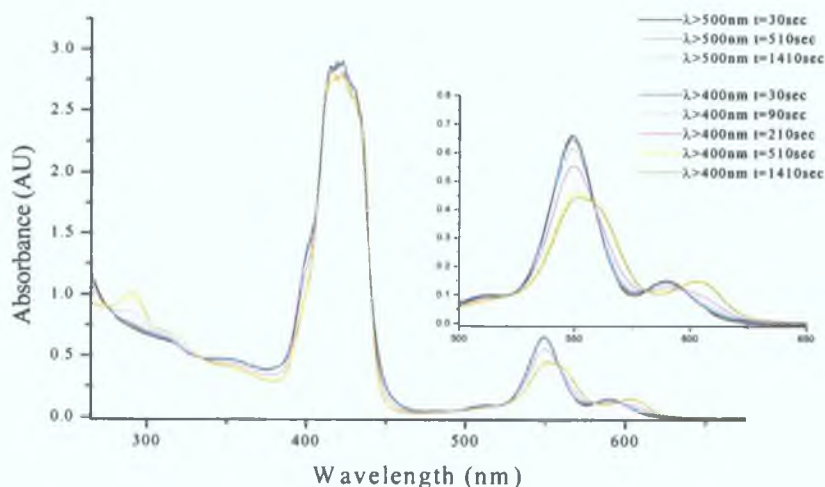


**Figure 4.9** Changes observed in the UV-vis spectrum following irradiation of ZnMPyTPPCr(CO)<sub>5</sub> ( $5.0 \times 10^{-5}$  mol dm<sup>-3</sup>) in dichloromethane under 1 atmosphere of CO

When the irradiation wavelength was increased to higher energy ( $\lambda_{\text{exc}} > 400$  nm) the changes in the UV-vis spectrum became more pronounced. Photolysis was continued until such a point that no further changes were evident.

Photolysis of  $\text{ZnMPyTPPCr(CO)}_5$  results in the loss of the  $\text{Cr(CO)}_5$  moiety and formation of uncomplexed metalloporphyrin. The presence of this metalloporphyrin results in the formation of the polymer in low concentrations. As photolysis time increased the bands shifted further towards the red because of the increasing concentration of polymer present in solution. Previously it has been reported that as the concentration of ZnMPyTPP polymer in solution increases the same effect on the Q bands was reported as is observed in this study.<sup>11</sup> Additionally a change in absorbance of the Q bands was observed as the photolysis progressed. The relative intensity of the Q(0,0) band relative to the Q(1,0) band in the zinc porphyrin metal carbonyl complexes is significantly lower than for the uncomplexed metalloporphyrin, ZnMPyTPP. This has again been attributed to the polymer formation.<sup>11</sup>

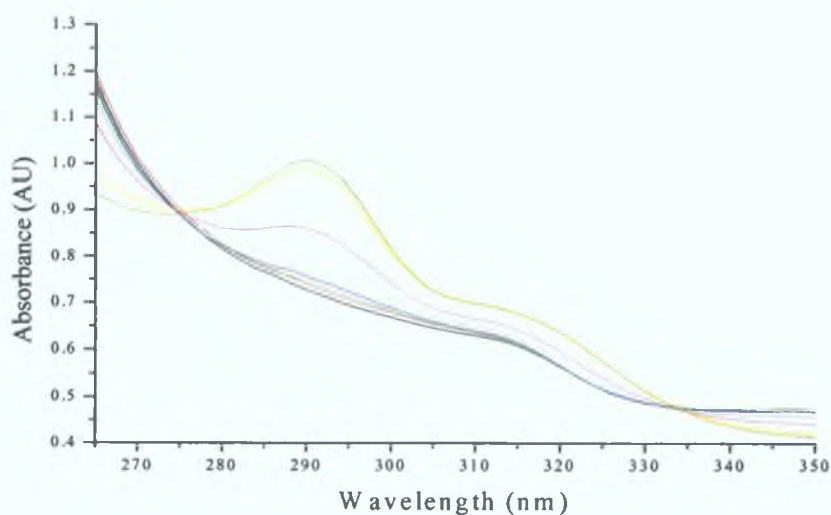


**Figure 4.10** Changes observed between 275 – 350 nm in the UV-vis spectrum of  $\text{ZnMPyTPPCr(CO)}_5$  ( $5.0 \times 10^5 \text{ mol dm}^{-3}$ ) following steady state photolysis ( $\lambda > 400 \text{ nm}$  or  $500 \text{ nm}$ ) under 1 atm of CO in dichloromethane

#### 4.5.4 Steady state photolysis of $\text{ZnMPyTPPCr(CO)}_5$ under 1 atmosphere of Ar

Steady state photolysis ( $\lambda_{\text{exc}} > 400 \text{ nm}$  or  $500 \text{ nm}$ ) of a solution of  $\text{ZnMPyTPPCr(CO)}_5$  in dichloromethane ( $4.9 \times 10^{-5} \text{ mol dm}^{-3}$ ) produced the UV-vis spectral changes presented in Figure 4.11. Initially the sample was irradiated at  $\lambda_{\text{exc}} > 500 \text{ nm}$  and the changes observed during photolysis were not as noticeable as those discussed previously under 1 atmosphere of CO (see Figure 4.9). This difference in the UV-vis absorption is because of the absence of added CO, therefore the formation of  $\text{Cr(CO)}_6$  is not quantitative, and relies on the ability of the photogenerated  $\text{Cr(CO)}_5$  unit to scavenge CO from the parent molecules or another photogenerated metal pentacarbonyl fragment (see Figure 4.12). A red shift in the Q bands together with a reduction in their relative intensity was also evident, using this irradiation wavelength.

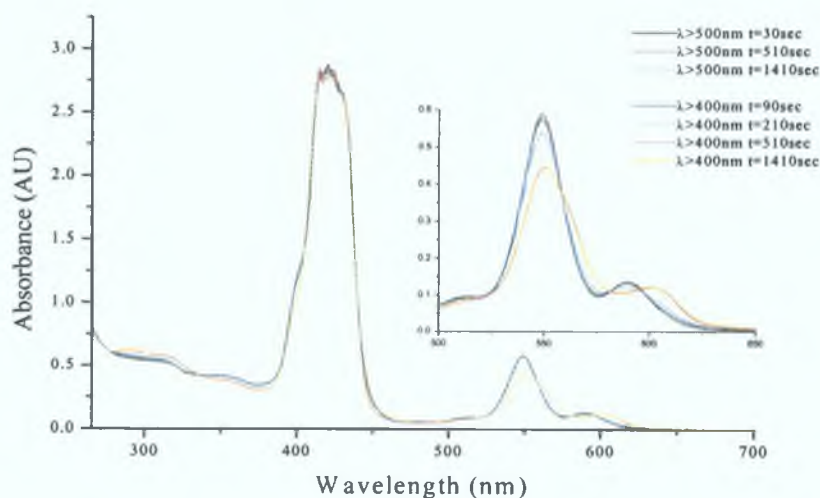


**Figure 4.11** Changes observed in the UV-vis spectrum following irradiation of  $\text{ZnMPyTPPCr(CO)}_5$  ( $4.9 \times 10^{-5} \text{ mol dm}^{-3}$ ) ( $\lambda > 400 \text{ nm}$  or  $500 \text{ nm}$ ) in dichloromethane under 1 atmosphere of Ar

When the irradiation wavelength was increased ( $\lambda_{\text{exc}} > 400 \text{ nm}$ ) the changes in the UV-vis spectrum became much more obvious as there was an increase in absorbance at 290

nm and a red shift in the Q bands, together with a reduction in their relative intensity. Photolysis was continued until no further changes were evident.

As in the previous experiment conducted in the presence of CO, photolysis of ZnMPyTPPCr(CO)<sub>5</sub> results in the loss of Cr(CO)<sub>5</sub> and this allows the formation of the porphyrin polymer. As the length of photolysis progressed, the Q bands were further red shifted due to the increasing concentration of polymer. Additionally a change in absorbance of the Q bands was observed during photolysis. The intensity of the Q(0,0) band relative to the Q(1,0) band in the porphyrin metal carbonyl complexes is significantly lower than for the uncomplexed metalloporphyrin, ZnMPyTPP, which is typical of polymer formation.<sup>11</sup>

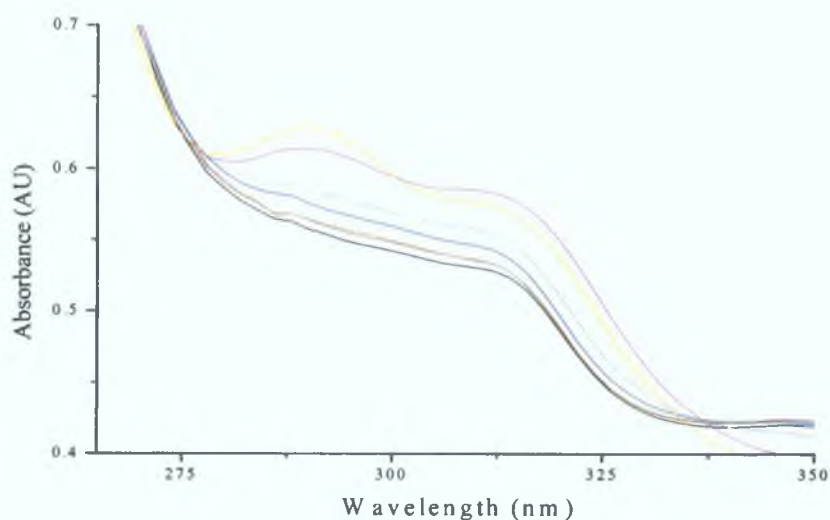


**Figure 4.12** Changes observed between 275 – 350 nm following irradiation of ZnMPyTPPCr(CO)<sub>5</sub> ( $4.9 \times 10^{-5} \text{ mol dm}^{-3}$ ) at  $\lambda_{\text{exc}} > 400 \text{ nm}$  or  $500 \text{ nm}$  in dichloromethane

#### 4.5.5 Discussion of results

Steady state photolysis of the zinc metalloporphyrin metal pentacarbonyl complexes was carried out in dichloromethane solution due to the limited solubility of these complexes in hydrocarbon solvents such as cyclohexane (all samples were prepared as described in Section 6.5.1). Photolysis of the zinc polymer did not cause any changes in the UV-vis spectrum.

The metal carbonyl metalloporphyrin complexes were irradiated using two cut off filters,  $\lambda_{exc} > 400$  nm or  $\lambda_{exc} > 500$  nm, and in the presence and absence of CO (see Section 6.5.2 for details). When the samples were irradiated initially with  $\lambda_{exc} > 500$  nm, the changes observed in the UV-vis spectra were small. However, a slight increase in absorbance was observed at 290 nm for both the Cr and W pentacarbonyl metalloporphyrin complexes following irradiation. This was indicative of the formation of  $M(CO)_6$  for each complex and was confirmed by IR spectroscopy. In addition a red shift of 2-3 nm of the Q bands was also observed. This shift was relatively small when compared to that observed at  $\lambda_{exc} > 400$  nm. The Q bands also underwent a change in their relative absorbances (see Table 4.4). When the samples are irradiated at  $\lambda_{exc} > 500$  nm most of the light is absorbed by the Q bands of the complex (see Figure 4.2). The Q bands are less intense than the Soret band (extinction coefficient for the Soret band is in the region of 100 times higher than that of the Q bands at the same concentration)<sup>20</sup>. When the filter was changed and the sample was irradiated ( $\lambda_{exc} > 400$  nm) the changes in the absorption spectrum became much more pronounced. At this wavelength the Soret band of the porphyrin is absorbing strongly (Soret  $\lambda_{max} = 420$  nm). The increase in absorbed light should lead to an increase in the rate of spectral changes previously monitored at  $\lambda_{exc} > 500$  nm.

When monitored under an atmosphere of Ar the spectral changes were small, even at  $\lambda_{exc} > 400$  nm. However the process is still occurring. This was because the formation of  $M(CO)_6$  was not the only significant process occurring. Cleavage of the M-N bond to form  $M(CO)_6$  does occur but so does the formation of ZnMPyTPP polymer. Formation of

the polymer occurs irrespective of the environment of the sample and is further evidence that the N-M bond breaks during photolysis

As the N-M bond is broken the ZnMPyTPP polymer forms. The UV-vis spectrum of this polymer is different to that of the metalloporphyrin complex. The difference in the UV-vis spectrum, in particular the Q bands are brought about by a change in electron density at the *meso* position of the porphyrin as discussed in Section 4.2. The relative intensity and position of the Q(1,0) and Q(0,0) band are also affected by this change in electron density. The Q bands of the polymer appear at 562 and 604 nm while the corresponding bands of the complexes appear at 548 and 588 nm in the UV-vis spectrum. This is a shift of 14 nm and 16 nm to lower energy respectively for these Q bands. The relative intensity of these bands is 0.55 for the polymer but decreases to 0.24 for the complex (see Table 4.1 and Table 4.4 pg. 134). As the photolysis continues the maximum of the Q bands are continually shifting towards the  $\lambda_{\max}$  of the polymer. The final position of the bands and their relative intensity does not correspond to the polymer exactly. This is because the concentration of the starting materials was very low (between  $4.9 \times 10^{-5}$  -  $6.7 \times 10^{-5}$  mol dm<sup>-3</sup>) hence the concentration of polymer (higher the concentration of the polymer leads to an increase in the polymer chain length) will also be low.<sup>21</sup> Figure 4.24 shows a UV-vis spectrum of ZnMPyTPPCr(CO)<sub>5</sub> at high molar mass and concentration ( $2.0 \times 10^{-4}$  mol dm<sup>-3</sup>) and the Q bands have shifted to the position of the polymer after extensive laser flash photolysis. The increase in intensity and shift in Q bands is greater for the experiments carried out under CO although this should not really matter as the formation of the polymer is independent of CO unlike the formation of M(CO)<sub>6</sub>.

To summarise, the main photochemical process taking place in the metalloporphyrin pentacarbonyl complex during photolysis is the cleavage of the N-M bond. This occurred during irradiation at both  $\lambda_{\text{exc}} > 500$  nm and  $\lambda_{\text{exc}} > 400$  nm. The photosensitivity of these compounds is unusual as almost all the light is being absorbed by the porphyrin moiety at these wavelengths. Aspley *et al* obtained similar results during photolysis of a metalloporphyrin system and their results were tentatively explained by population of tungsten excited states by energy transfer from the porphyrin.<sup>16</sup> The presence of a

pyridine ligand in the *meso* position of the porphyrin and its use as a linker between the porphyrin and metal pentacarbonyl allows comparison of the porphyrin complex with  $M(CO)_5C_5H_4N$ . As was the case with the free base porphyrin complex there is no evidence of the MLCT band or LF band due to  $M(CO)_5C_5H_4N$  as the UV-vis spectrum is dominated by metalloporphyrin absorptions. As  $M(CO)_5C_5H_4N$  only absorbs out as far as 440 nm, excitation at  $\lambda > 500$  nm cannot lead to photosubstitution caused by population of energy levels on this moiety<sup>22,23</sup>. However hexacarbonyl and the ZnMPyTPP polymer are observed following irradiation. Once more cleavage of the N-M bond occurs because of electronic communication between the porphyrin and  $M(CO)_5$ . Loss of the  $M(CO)_5$  moiety arises from population of  $^3LF$  which could occur from singlet to triplet energy transfer from the porphyrin singlet excited state<sup>24</sup>. Figure 4.26 (see Section 4.7) describes a potential energy pathway for the loss of  $M(CO)_5$  from a metalloporphyrin. Previous work on rhenium metalloporphyrin carbonyl complexes showed no evidence of light sensitivity<sup>25</sup>.

**Table 4.4 UV bands (nm) and relative intensities following photolysis**

| <i>Porphyrin</i>                                     | <i>Wavelength of Q bands</i> |                             | <i>Relative intensity of Q bands</i> |                             |
|------------------------------------------------------|------------------------------|-----------------------------|--------------------------------------|-----------------------------|
|                                                      | <i>Before<br/>Photolysis</i> | <i>After<br/>Photolysis</i> | <i>Before<br/>Photolysis</i>         | <i>After<br/>Photolysis</i> |
| ZnMPyTPPW(CO) <sub>5</sub> under 1 atmosphere of CO  | 548/588                      | 550/600                     | 0.23                                 | 0.28                        |
| ZnMPyTPPCr(CO) <sub>5</sub> under 1 atmosphere of CO | 548/588                      | 551/604                     | 0.23                                 | 0.31                        |
| ZnMPyTPPW(CO) <sub>5</sub> under 1 atmosphere of Ar  | 548/588                      | 550/590                     | 0.24                                 | 0.25                        |
| ZnMPyTPPCr(CO) <sub>5</sub> under 1 atmosphere of Ar | 548/588                      | 551/603                     | 0.24                                 | 0.27                        |

Further photophysical and photochemical measurements were carried out in order to fully understand the mechanism involved in the loss of the  $M(CO)_5$  moiety from the porphyrin.

#### 4.6 Fluorescence studies of (5-*mono*-4-pyridyl 10, 15, 20-triphenyl porphyrinato) zinc(II) and its metal pentacarbonyl complexes (M = Cr or W)

##### 4.6.1 Emission spectra and quantum yields for ZnMPyTPP polymer, ZnMPyTPPW(CO)<sub>5</sub> and ZnMPyTPPCr(CO)<sub>5</sub>

Fluorescence spectra were obtained for both metal carbonyl metalloporphyrin complexes and the uncomplexed metalloporphyrin polymer, ZnMPyTPP. The fluorescence spectrum of ZnTPP was also compared to that of the pentacarbonyl complexes (as the fluorescence spectrum of the ZnMPyTPP polymer is very different to that of the pentacarbonyl complexes) as is shown in Figure 4.13. The difference is once again due to the different electronic environment at the *meso* position of the porphyrin in the polymer.

**Table 4.5 Emission bands of Zinc polymer compared to the pentacarbonyl complexes**

| <i>Porphyrin</i>            | <i>Emission Maxima (nm)</i> |            | <i>Relative <math>\phi_f</math></i> |
|-----------------------------|-----------------------------|------------|-------------------------------------|
| ZnMPyTPP polymer            | 619 (1.0)                   | 647 (0.86) | 1.00                                |
| ZnMPyTPPCr(CO) <sub>5</sub> | 608 (1.0)                   | 648 (1.01) | 0.84                                |
| ZnMPyTPPW(CO) <sub>5</sub>  | 609 (1.0)                   | 648 (1.11) | 0.99                                |

**Table 4.6 Emission bands of ZnTPP compared to the pentacarbonyl complexes**

| <i>Porphyrin</i>            | <i>Emission Maxima (nm)</i> |            | <i>Relative <math>\phi_f</math></i> |
|-----------------------------|-----------------------------|------------|-------------------------------------|
| ZnTPP                       | 600 (1.0)                   | 645 (1.49) | 1.00                                |
| ZnMPyTPPCr(CO) <sub>5</sub> | 608 (1.0)                   | 648 (1.01) | 0.69                                |
| ZnMPyTPPW(CO) <sub>5</sub>  | 609 (1.0)                   | 648 (1.11) | 0.81                                |

Table 4.5 and 4.6 above presents the emission maxima and relative intensity of the Q bands of the complexes with respect to ZnMPyTPP polymer and ZnTPP. The maxima in the fluorescence spectrum of ZnMPyTPP are red shifted compared to that of the free base porphyrin.<sup>26</sup> This observation is as expected for metal insertion into free base porphyrins. Another notable feature in the fluorescence spectra on metallation of porphyrins is the change in the relative intensities of the Q bands.<sup>27</sup> The relative intensity of the emission

bands for free base porphyrins (discussed in Section 3.7) are all less than one. For metalloporphyrins the relative intensity of the emission bands has increased to over one (see Table 4.5 and 4.6). These results are consistent with those in the literature.<sup>11</sup> It has been shown that at low concentration, solutions of the ZnMPyTPP polymer have emission spectra similar to that of ZnTPP. However at higher concentrations the emission spectrum is similar to ZnTPP-pyridine (pyridine coordinates to the zinc through the N atom). The ligation of pyridine to ZnTPP produces a red shift in the emission spectrum similar to that caused by ZnMPyTPP polymer formation.<sup>11</sup>

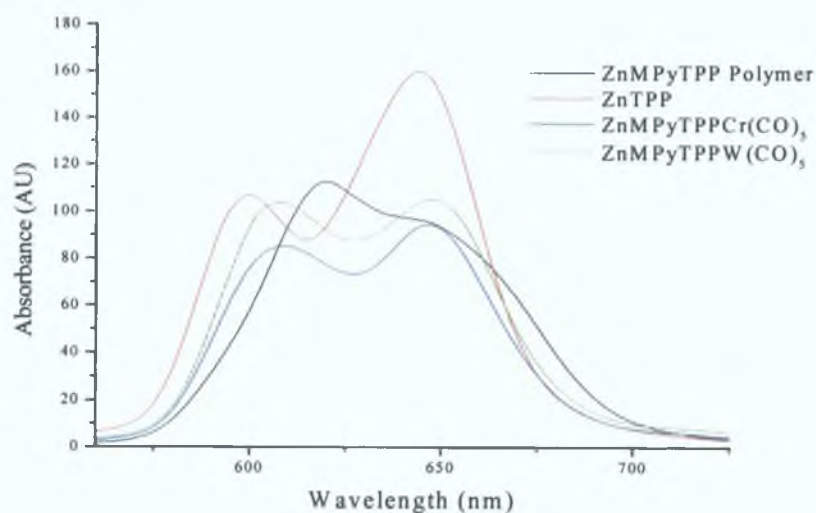


**Figure 4.13 Emission spectra of isoabsorptive samples of ZnTPP, ZnMPyTPP polymer, ZnMPyTPPW(CO)<sub>5</sub> and ZnMPyTPPCr(CO)<sub>5</sub> at 293 K ( $\lambda_{\text{exc}}$  532 nm) in dichloromethane**

A series of solutions were made up which had identical absorbances at the excitation wavelength ( $\lambda_{\text{exc}} = 532 \text{ nm}$ ), so as to determine the fluorescence quantum yields.<sup>28</sup> A reduction in the fluorescence yield of the pentacarbonyl complexes was observed when compared to the uncomplexed metalloporphyrin (see Figure 4.13, Table 4.5 and 4.6). Equation 3.4 was used to calculate the relative yield values for all solutions. While the value of  $\Phi_f$  for the ZnMPyTPP polymer is similar to that of the pentacarbonyl complexes, the profile and position of the bands has changed to such an extent that

comparisons are difficult. What is obvious from this set of data is that the fluorescence quantum yield of the Cr complex is reduced to a greater extent than that of the W complex. When comparing the data for ZnTPP with that of the pentacarbonyl complexes other factors have to be taken into account. ZnTPP does not contain a pyridine ring and also it has been shown that the presence of an N atom affects the fluorescence quantum yield of porphyrins.<sup>29</sup> However, the fluorescence quantum yield of both complexes is reduced when compared to ZnTPP. The reductions in the quantum yields of the complexes are of the order ZnMPyTPP > ZnMPyTPPW(CO)<sub>5</sub> > ZnMPyTPPCr(CO)<sub>5</sub> and ZnTPP > ZnMPyTPPW(CO)<sub>5</sub> > ZnMPyTPPCr(CO)<sub>5</sub>. Previously, fluorescence quenching in Ru porphyrin systems has been attributed to the heavy atom effect,<sup>30</sup> however it is not possible in this instance as Cr is not a heavy atom therefore the heavy atom effect cannot be responsible for any reductions in the fluorescence quantum yield of the pentacarbonyl analogues.

#### 4.6 2 Fluorescence lifetimes of ZnMPyTPPW(CO)<sub>5</sub> and ZnMPyTPPCr(CO)<sub>5</sub>

The fluorescence lifetimes were obtained for the following porphyrins ZnTPP, ZnMPyTPP, ZnMPyTPPW(CO)<sub>5</sub> and ZnMPyTPPCr(CO)<sub>5</sub>. From Table 4.7 it is apparent that the decrease in the relative quantum yields discussed previously is accompanied by a slight decrease in the singlet state lifetimes which is consistent in all solvents. The decrease in lifetimes is in the order ZnTPP > ZnMPyTPP > ZnMPyTPPW(CO)<sub>5</sub> > ZnMPyTPPCr(CO)<sub>5</sub>. This decrease in lifetimes cannot be attributed to the heavy atom effect, as Cr is a lighter element than W. If the heavy atom effect was a factor in the reduction in the singlet lifetimes of the complexes, the W complex would be expected to be shorter lived than the Cr analogue. However, the lifetime obtained for the Cr(CO)<sub>5</sub> derivatives is marginally shorter than the W analogues.

**Table 4.7 Singlet state lifetime values of metallated porphyrins and pentacarbonyl complexes**

| <i>Porphyrin</i>            | <i>RAL (DCM) <math>\tau_{fl}(ns)</math></i> | <i>RAL (EtOH) <math>\tau_{fl}(ns)</math></i> | <i>RAL (Pentane) <math>\tau_{fl}(ns)</math></i> |
|-----------------------------|---------------------------------------------|----------------------------------------------|-------------------------------------------------|
| ZnTPP                       | 2.21                                        | -                                            | -                                               |
| ZnMPyTPP                    | 1.48                                        | -                                            | -                                               |
| ZnMPyTPPCr(CO) <sub>5</sub> | 1.42                                        | 1.89                                         | 1.73                                            |
| ZnMPyTPPW(CO) <sub>5</sub>  | 1.44                                        | 1.91                                         | 1.79                                            |

\* Results obtained at RAL (Rutherford Appleton Laboratories) which were carried out by Jonathon Rochford using the experimental method referenced.<sup>31</sup>

ZnTPP was used as the standard for comparing singlet state lifetimes of the complexes because ZnMPyTPP forms a polymer and is structurally very different to that of the pentacarbonyl complexes. The value for the singlet state lifetime of ZnTPP determined in this study agrees well with that quoted in the literature i.e. 2.3 ns.<sup>32</sup> In Section 4.8 two schemes have been proposed to explain the process occurring during excitation of the metalloporphyrin complex. In Figure 4.26 population of <sup>3</sup>LF state from the metalloporphyrin S<sub>1</sub> state results in loss of the M(CO)<sub>5</sub> moiety and a reduction in the singlet lifetime of the metalloporphyrin complex. However, Figure 4.27 shows that a

reordering of the energy levels has occurred. This is possible, as upon complexation the fluorescence maxima of the pentacarbonyl complexes have shifted to lower energy relative to ZnTPP. The change in lifetimes is therefore caused by a reduction of the energy of the singlet state. As with the free base porphyrin complexes, the metalloporphyrins follow the same order in the lifetime of the excited state. The tungsten complex is longer lived than the chromium complex and this follows for all solvents used. The lifetime of the complexes differ little from one solvent to the next showing that the formation of the excited states are not solvent dependent.

Figure 4.13 represents a typical trace obtained following excitation of ZnMPyTPPW(CO)<sub>5</sub> at 438 nm. All samples were monitored at 605 nm.

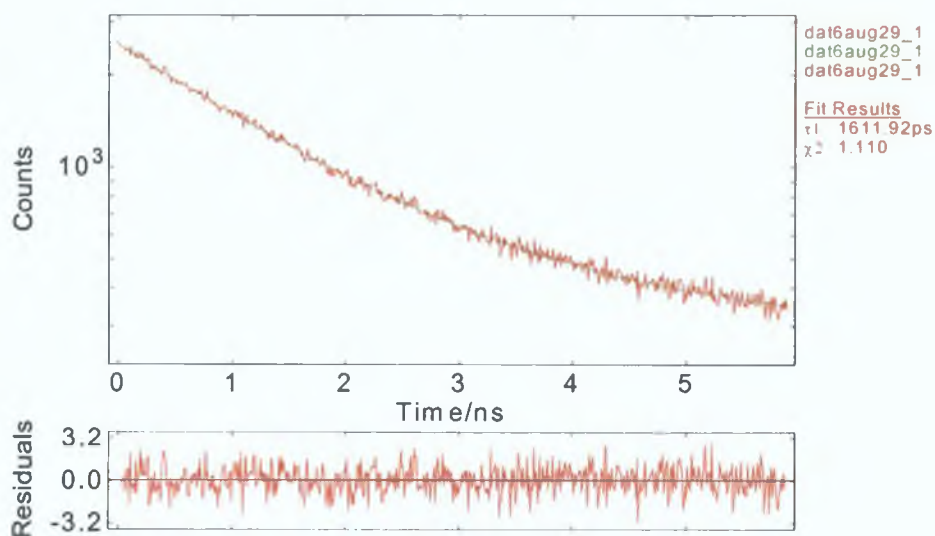


**Figure 4.14** A typical trace obtained at 605 nm following excitation of MPyTPPW(CO)<sub>5</sub> ( $\lambda_{exc}$  438 nm) in dichloromethane at 293 K

### 4 6 3 Discussion of results

As with free base porphyrins, zinc metalloporphyrins also emit from the lower excited singlet state ( $S^1 \rightarrow S^0$  relaxation), which is  $\pi^* - \pi$  in character. Similarly to free base porphyrins, metalloporphyrins exhibit dual emission due to excitation centred on the lowest singlet excited state transition (0-0 and 0-1 transitions) and emit at  $\sim 605$  (Q(0,0)) and 655 nm (Q(0,1))<sup>10</sup>. The profile of the fluorescent emission spectra of metalloporphyrins is somewhat different from free base porphyrins with the Q(0,1) band being more intense than the Q(0,0) band. The lifetimes of metalloporphyrins are shorter than those of free base porphyrins due to the internal heavy atom effect of the metal. In this study the metalloporphyrins studied are all zinc derivatives. Changing the excitation wavelength from higher to lower energy or vice versa leads only to a change in the relative intensity of the bands and does not affect the overall position of the  $\lambda_{\text{max}}$  or lead to the formation of new emission bands. The quantum yield of fluorescence formation for zinc porphyrin is similar in all solvents at 4%<sup>10</sup>.

When the emission spectra of the porphyrin metal carbonyl complexes are compared to those of ZnTPP and the ZnMPyTPP polymer some differences are evident (see Table 4 5 and 4 6). The electron environment at the *meso* position of the ZnMPyTPP polymer is very different from that of ZnTPP. This difference is responsible for the shifts in the UV-vis spectra (see Section 4 2) and the differences in the emission spectra. The polymer has emission bands at 619 and 647 nm while the ZnTPP has emission bands at 600 and 645 nm. Upon complexation to a metal pentacarbonyl unit the emission bands of ZnMPyTPP polymer shift to 608 and 648 nm as ZnMPyTPPM(CO)<sub>5</sub> is formed (M= Cr or W). These are more like ZnTPP, which suggests the environment of the *meso* position of the porphyrin ring of the pentacarbonyl complex, is more like that of ZnTPP. A change is expected as a M(CO)<sub>5</sub> moiety is now at this position but the electronic effect of these metal centres does not radically effect the structure of the porphyrin ring.

There is also a change in the relative intensity of the Q(0,0) band compared to the Q(0,1) band in the UV-vis spectrum when comparing the pentacarbonyl complexes to both

ZnTPP and the ZnMPyTPP polymer. This is also an indicator that the electronic conditions experienced at the *meso* position of ZnMPyTPP polymer differ from that of ZnTPP and the ZnMPyTPPM(CO)<sub>5</sub> complexes. The relative intensity of the Q(0,0) band compared to the Q(0,1) band for the polymer is less than one while the relative intensity of ZnTPP and both the pentacarbonyl complexes are greater than one. The profile of the polymer differs from the other zinc porphyrin complexes where the 0-1 transition is stronger than the 0-0 transition. Also the emission bands of the ZnMPyTPP polymer are not fully resolved as is the case for the other zinc porphyrins.

Singlet lifetimes of the pentacarbonyl complexes were compared with that of ZnTPP. This was because the singlet lifetime of the polymer could not be determined due to limitations of the equipment. A lifetime of 2.3 ns for the singlet excited state of ZnTPP was obtained in this study, which is in good agreement with the literature.<sup>12</sup> A reduction in lifetime upon formation of the pentacarbonyl complex was observed for both pentacarbonyl free base porphyrin complexes (see Section 3.7.2). Previously this reduction in singlet state lifetimes was attributed to the heavy atom effect.<sup>33</sup> As Cr is one of the metals involved in the formation of the complexes the heavy atom effect is excluded. In Figure 4.26 (Section 4.8) it is shown that population of the <sup>3</sup>LF state of M(CO)<sub>5</sub>C<sub>5</sub>H<sub>4</sub>N may result from singlet to triplet intercomponent energy transfer, from the singlet excited state of the porphyrin. Again this would make sense as cleavage of the N-M bond occurs from population of the <sup>3</sup>LF in pyridyl pentacarbonyl complexes.<sup>5</sup> However there is no evidence of a MLCT band or a <sup>3</sup>LF band in the UV-vis spectra, however such bands could be masked by the intensity of the porphyrin bands. Reduction of the singlet lifetime could occur through another process (see Figure 4.27). The emission studies shown in this section suggest that upon complexation a red shift in the emission bands of the pentacarbonyl complexes compared to ZnTPP occurs.

#### 4.7 Laser Flash Photolysis of ZnMPyTPP M(CO)<sub>5</sub> complexes (M = Cr or W)

##### 4.7.1 Laser flash photolysis of ZnMPyTPPW(CO)<sub>5</sub> at 532 nm excitation under 1 atmosphere of CO

The transient absorption difference spectrum for ZnMPyTPPW(CO)<sub>5</sub> (Figure 4.15) was collected between 430 and 800 nm following excitation at 532 nm in dichloromethane. The transient absorption difference spectra for this organometallic porphyrin also has similar characteristics to those previously assigned to the  $^3(\pi-\pi^*)$  excited state of the uncomplexed metalloporphyrin. Similarly to ZnTPP, the transient absorption difference spectrum for ZnMPyTPPW(CO)<sub>5</sub> absorbs strongly between 440 nm and 500 nm having a maximum at approximately 465 nm. Bleaching was observed at 530 nm following flash photolysis for this complex, and less intense transient absorptions in the Q-band region.

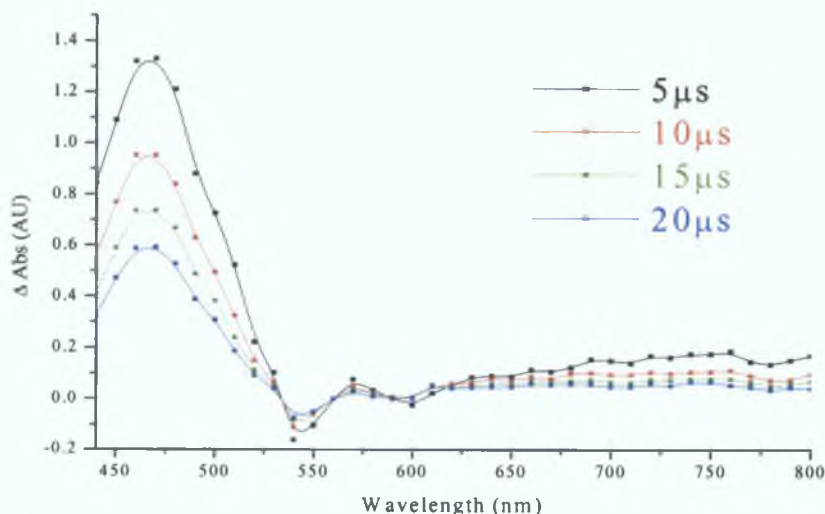


**Figure 4.15** Transient absorption difference spectra obtained following  $\lambda_{exc} = 532$  nm of ZnMPyTPPW(CO)<sub>5</sub> in dichloromethane under 1 atmosphere of CO at 293 K

There is no significant difference in the overall profile of the transient absorption difference spectra of ZnMPyTPPW(CO)<sub>5</sub> once complexation with the carbonyl moiety has occurred. However when the transient absorption difference spectra of ZnTPP and

ZnMPyTPPW(CO)<sub>5</sub> are directly compared in the region of 440 to 500 nm, small differences can be observed (see Figure 4 16) The samples had identical absorbance at the excitation wavelength yet two absorbance maxima are clearly evident for ZnMPyTPPW(CO)<sub>5</sub> but in the case of ZnTPP there is only one Both do show absorbance maxima at ~ 460 nm which is a shorter wavelength maximum than that of free base porphyrins

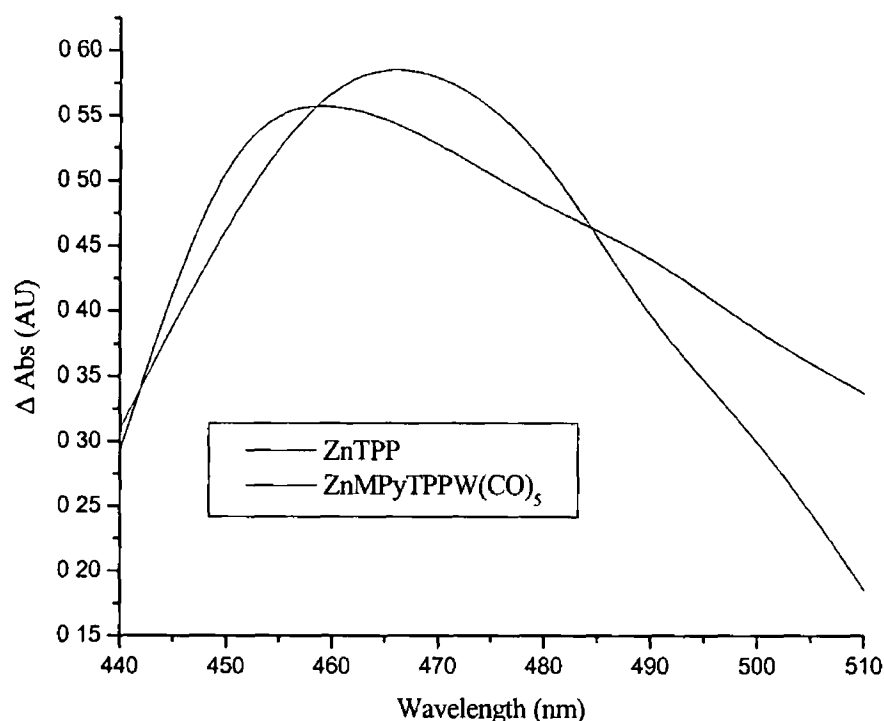


**Figure 4 16 Transient absorption difference spectra obtained following laser flash photolysis at 532 nm for solutions of ZnTPP and ZnMPyTPPW(CO)<sub>5</sub> with identical absorbance at  $\lambda_{exc} = 532$  nm at 293 K**

Metalloporphyrins absorb intensely in the region of 400 - 500 nm and because of this ZnMPyTPPW(CO)<sub>5</sub> is prone to photodissociation when irradiated in this region. In these experiments laser flash photolysis leads to rapid dissociation of the W(CO)<sub>5</sub> moiety. Triplet lifetime measurements were recorded at 490 nm (see Table 4 8), because these systems are prone to photodissociation upon excitation in the Soret band region large

amounts of photosubstitution would take place. The triplet lifetime of the pentacarbonyl complex differs little from that of ZnTPP.

**Table 4.8**

| 490 nm                     |                      |                    |
|----------------------------|----------------------|--------------------|
| <i>Porphyrin</i>           | $\tau_{trip}(\mu s)$ | $k_{obs} (s^{-1})$ |
| ZnTPP                      | 14                   | $70782 \pm 7078$   |
| ZnMPyTPPW(CO) <sub>5</sub> | 19                   | $50574 \pm 5057$   |

The difference is not as significant as would have been expected for the heavy atom effect associated with the W atom. This would suggest that the W(CO)<sub>5</sub> has little effect upon the triplet excited state of the metalloporphyrin. Given that there was a significant reduction in the quantum yield for the fluorescence emission of the pentacarbonyl complex when compared to the metalloporphyrin, some significant changes would have been expected in the triplet lifetimes. Some authors have suggested a heavy atom effect caused the reduction in the singlet lifetimes and fluorescence quantum yields,<sup>30</sup> but the heavy atom effect would have made a considerable difference to the transient absorption spectrum of the pentacarbonyl complex compared to ZnTPP.

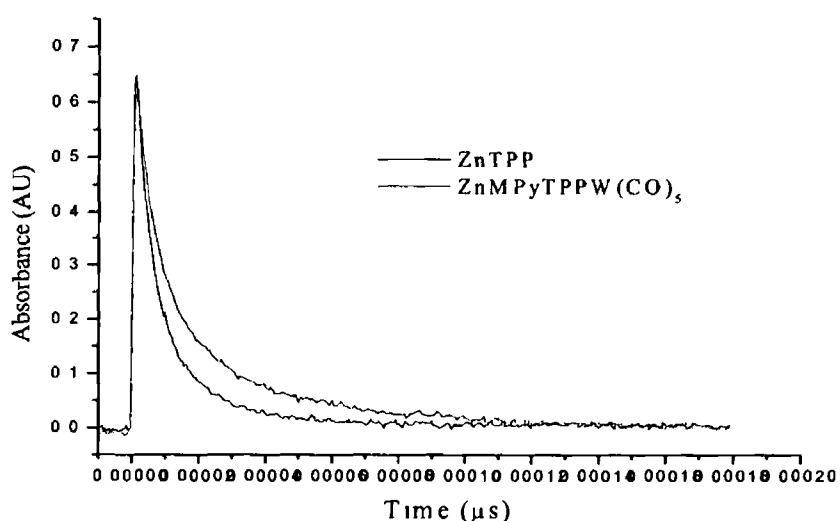


**Figure 4.17** Transient signals obtained at 490 nm following laser flash photolysis of ZnTPP and ZnMPyTPPW(CO)<sub>5</sub> at 532 nm in dichloromethane at 293 K

Figures 4.26 and 4.27 are used to help explain the results obtained in this study (see Section 4.8). Outlined in Figure 4.26 is the suggestion that population of the  $^3\text{LF}$  state of  $\text{W}(\text{CO})_5\text{C}_5\text{H}_4\text{N}$  competes with ISC from the singlet excited state to the triplet excited state. As with free base porphyrins, the predominant route for radiationless deactivation of metalloporphyrins is population of  $^3\text{Zn}$ ,<sup>34</sup> which has a quantum yield of 90%. A reduction in the ISC would be noticeable with a reduction in the intensity of the transient absorption spectrum and transients, as the heavy atom effect causes a mixing of the singlet and triplet states. This should cause an overall reduction in the population of the triplet state.

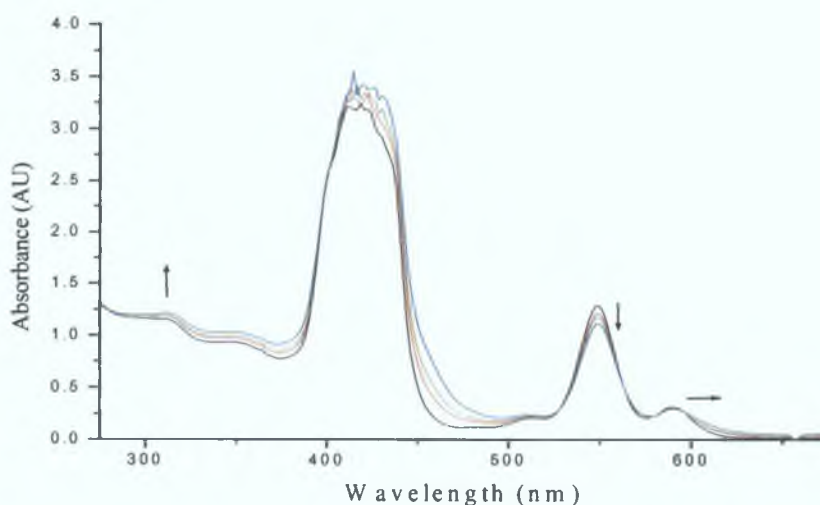


**Figure 4.18** UV-vis spectra of  $\text{ZnMPyTPPW}(\text{CO})_5$  recorded during a laser flash photolysis experiment ( $\lambda_{\text{exc}} = 532 \text{ nm}$ ) in dichloromethane under 1 atmosphere of CO

Figure 4.27 (see Section 4.8) is an alternative explanation of the process. In this diagram loss of the  $\text{M}(\text{CO})_5$  unit follows population of the singlet state. Hence the triplet excited state produced is actually the triplet excited state of the uncoordinated porphyrin.

When the UV-vis spectra are monitored during laser flash photolysis experiments an increase in the absorbance at 290 nm suggests formation of  $\text{W}(\text{CO})_6$  (see Figure 4.18). In addition there is also a shift in the Q bands, which is attributed to formation of the ZnMPyTPP polymer. When an IR spectrum of this sample solution was obtained, in

addition to the parent bands of the complex at 2070, 1930 and 1916  $\text{cm}^{-1}$  an additional band at 1975  $\text{cm}^{-1}$  is obtained in dichloromethane, indicating the presence of  $\text{W}(\text{CO})_6$  (see Figure 4.19) It is undoubtedly the case that photolysis of the  $\text{ZnMPyTPPW}(\text{CO})_5$  complex in the presence of CO ultimately produces  $\text{W}(\text{CO})_6$

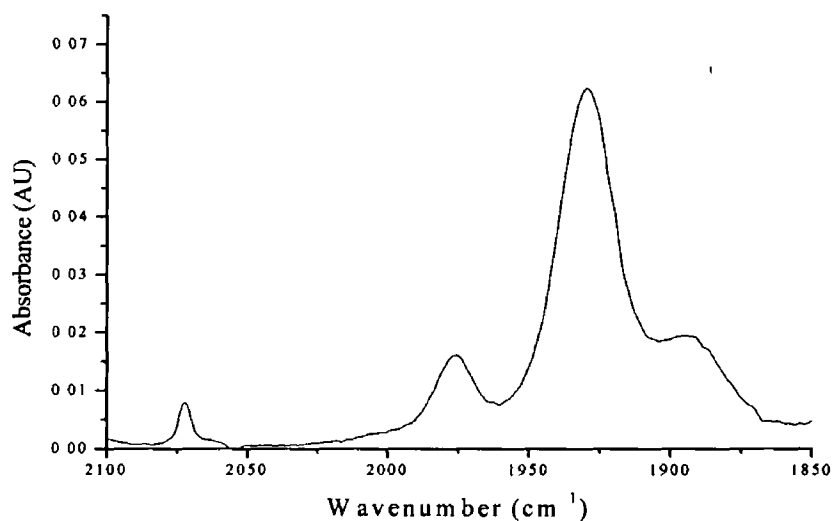


**Figure 4.19 Spectrum obtained following a laser flash photolysis of  $\text{ZnMPyTPPW}(\text{CO})_5$  ( $\lambda_{\text{exc}} = 532 \text{ nm}$ ) in dichloromethane under 1 atmosphere of CO**

#### 4.7.2 Laser flash photolysis of ZnMPyTPPCr(CO)<sub>5</sub> at 532 nm under 1 atmosphere of CO

The transient absorption difference spectrum of ZnMPyTPPCr(CO)<sub>5</sub> (Figure 4.20) was also measured between 430 and 800 nm in the presence of CO. The spectrum was found to have similar characteristics to those previously assigned to the  $^3(\pi-\pi^*)$  excited state relaxation of the uncomplexed metalloporphyrin. Similarly to ZnTPP, the difference spectrum of ZnMPyTPPCr(CO)<sub>5</sub> obtained following laser flash photolysis absorbs strongly between 440 nm and 500 nm. Once again the maximum of the complexed metalloporphyrin occurred at approximately 465 nm but the transient absorption spectrum of the complex has a sharper profile than that of ZnTPP. Both systems exhibit bleaching at *ca.*  $\approx$ 550 nm and less intense transient absorption in the Q-band region, which extends into the near infrared.

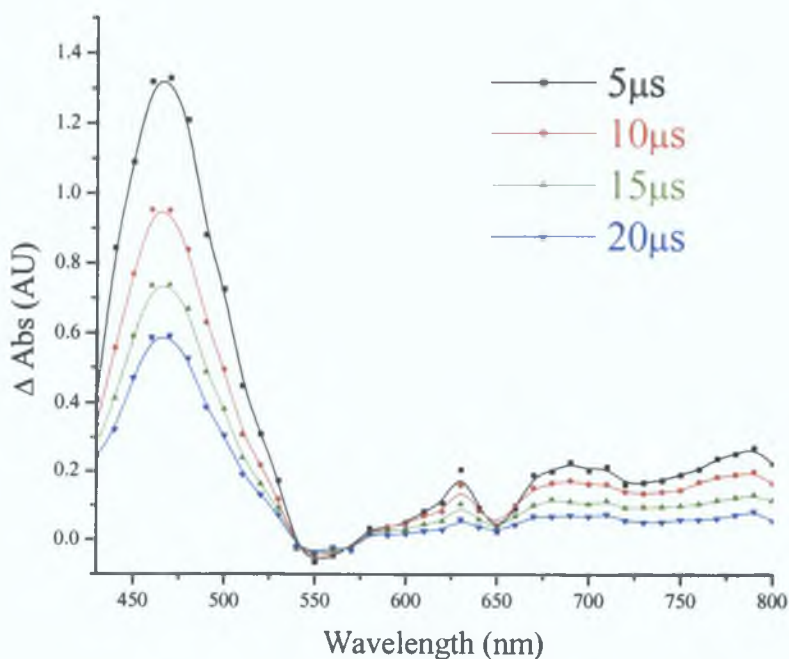


**Figure 4.20** Transient absorption difference spectra of ZnMPyTPPCr(CO)<sub>5</sub> obtained following laser flash photolysis ( $\lambda_{exc} = 532$  nm) under 1 atmosphere of CO in dichloromethane at 293 K

However, upon closer inspection of the transient absorption spectra of ZnMPyTPPCr(CO)<sub>5</sub> and ZnTPP in the region 430 – 500 nm changes in the  $\lambda_{\text{max}}$  were apparent. Both samples had the same absorbance at the excitation wavelength, 532 nm. There is a shift of ~ 10 nm to lower energy in the maxima of both.

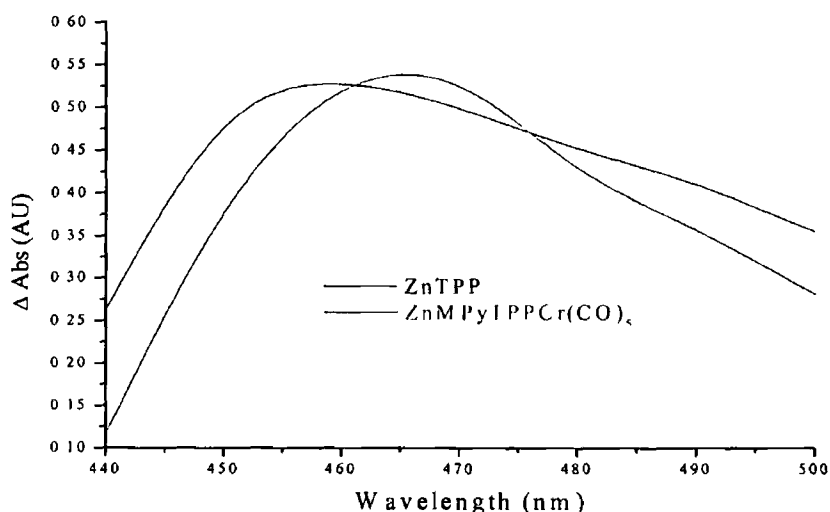


**Figure 4 21** Transient absorption difference spectra collected following laser flash photolysis of solutions of ZnTPP and ZnMPyTPPCr(CO)<sub>5</sub> with identical absorbance at  $\lambda_{\text{exc}} = 532 \text{ nm}$  at 293 K

Since there are changes in the singlet excited state lifetimes and emission spectra the changes in the triplet excited state lifetimes and transient absorption spectrum should be greater.

This is not the case. In Scheme 4 2 population of the singlet excited state of the pentacarbonyl complex causes cleavage of the N-Cr bond. Therefore, excitation of the pentacarbonyl metalloporphyrin cleaves the N-Cr bond and this leads to the formation of the triplet excited state of the uncomplexed metalloporphyrin. This explains why the differences in the lifetimes (see Figure 4 22) or the transient absorption spectrum of the pentacarbonyl complex compared to the uncomplexed metalloporphyrin are not as prominent as would have been expected.

**Table 4 9**

| 490 nm                      |                      |                   |
|-----------------------------|----------------------|-------------------|
| <i>Porphyrin</i>            | $\tau_{trip}(\mu s)$ | $k_{obs}(s^{-1})$ |
| ZnTPP                       | 14                   | $70782 \pm 7078$  |
| ZnMPyTPPCr(CO) <sub>5</sub> | 19                   | $51004 \pm 5100$  |

Figure 4 26 proposes that the metalloporphyrin and the Cr(CO)<sub>5</sub>C<sub>5</sub>H<sub>4</sub>N moiety can be treated as a supramolecular molecule i e they are weakly interacting and that the energy levels of each molecular component are substantially unperturbed As can be seen from the diagram once the singlet excited state of the porphyrin has been populated three pathways are possible Radiationless deactivation back to the ground state is known to have 4% efficiency for the uncomplexed porphyrin<sup>24</sup> ISC to the triplet state has a 90% quantum yield<sup>12</sup> Population of the <sup>3</sup>LF state must compete with these pathways Changes in the population of the triplet state would have to be dramatic to observe an increase/decrease in the quantum yield as it is already 90%

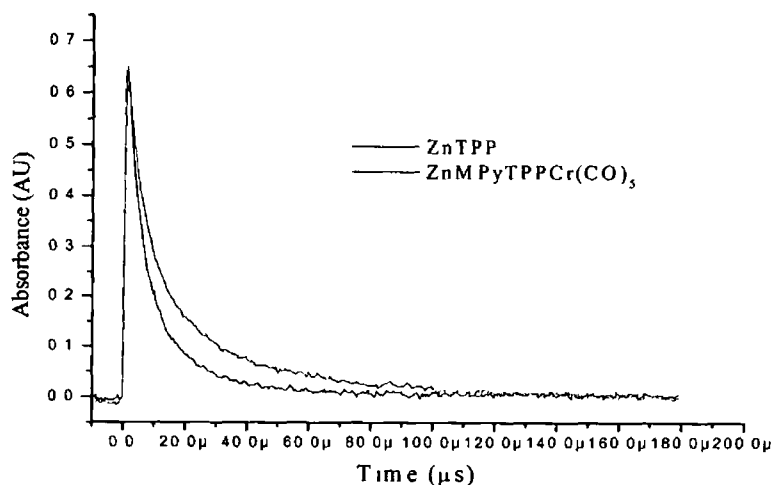


**Figure 4 22 Transient signals at 490 nm following laser flash photolysis of solutions of ZnTPP and ZnMPyTPPCr(CO)<sub>5</sub> with identical absorbance at  $\lambda_{exc} = 532$  nm at 293 K**

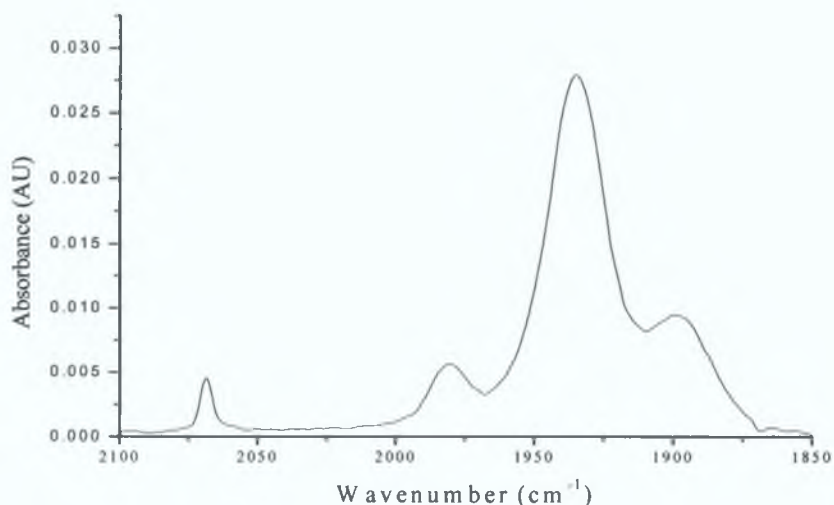


**Figure 4.23 IR spectrum collected following laser flash photolysis of a solution of  $\text{ZnMPyTPPCr(CO)}_5$  at  $\lambda_{\text{exc}} = 532 \text{ nm}$  at 293 K under 1 atmosphere of CO**

IR spectra were recorded for all samples following laser flash photolysis. Shown in Figure 4.23 is the IR spectrum obtained following laser flash photolysis of  $\text{ZnMPyTPPCr(CO)}_5$ . In addition to the pentacarbonyl peaks an additional band is observed at  $1980 \text{ cm}^{-1}$ , indicating the formation of  $\text{Cr(CO)}_6$ .

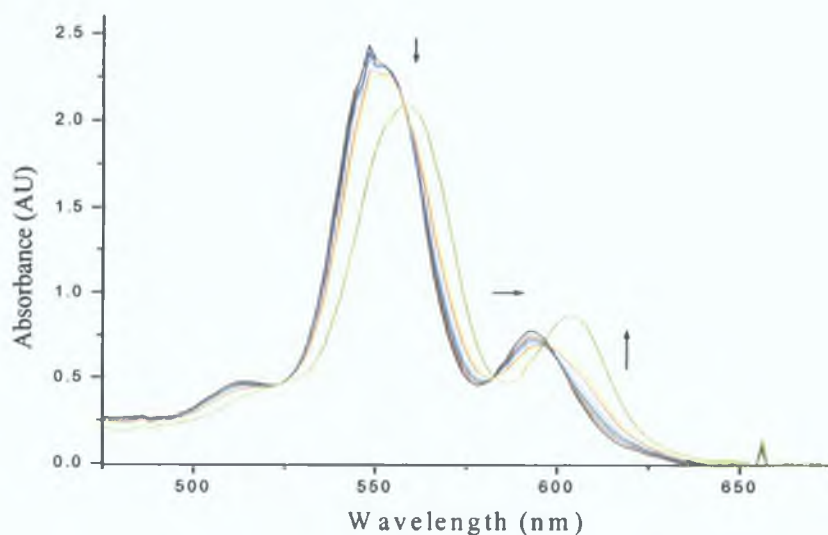


**Figure 4.24 Changes observed in the UV-vis spectrum during laser flash photolysis of a solution of  $\text{ZnMPyTPPCr(CO)}_5$  at  $\lambda_{\text{exc}} = 532 \text{ nm}$ , at 293 K**

The UV-vis spectral changes are shown in Figure 4.24. The Q bands of the complex are red shifted as the experiment proceeds and their relative intensity changed to that expected for the formation of the polymer, ZnMPyTPP. At the end of the experiment the relative intensity of the Q bands has increased to 0.41. This is indicative that the N-Cr bond has been cleaved and ZnMPyTPP has undergone self-coordination to form the polymeric porphyrin.

### 4 7.3 Discussion of results

Laser flash photolysis ( $\lambda_{\text{exc}} = 532 \text{ nm}$ ) was carried out on the uncomplexed metalloporphyrin (ZnTPP) and the metal carbonyl complexes ZnMPyTPPW(CO)<sub>5</sub> and ZnMPyTPPCr(CO)<sub>5</sub> in deoxygenated dichloromethane under one atmosphere of CO

The time-resolved absorbance of the triplet state of a typical metalloporphyrin has a lifetime of *ca* 20  $\mu\text{s}$  at room temperature<sup>16</sup> Metalloporphyrins exhibit strong transient signals from 440 nm to 510 nm, with fewer absorbances in the Q band region when compared to the free base porphyrins The transient signals observed in these experiments are typical of <sup>3</sup>( $\pi\text{-}\pi^*$ ) excited states of metalloporphyrins (see Figure 4 25)<sup>35,36</sup> Previous attempts to obtain transient absorption spectra of a pentacarbonyl metalloporphyrin were unsuccessful as the complex was too photosensitive<sup>16</sup> In this study a number of samples were required to obtain transient absorption difference spectra for both pentacarbonyl complexes

The systems in this study were chosen to investigate the efficiency at which a porphyrin and a metal moiety can communicate across orthogonal  $\pi$ -substituents on the *meso* position of a metalloporphyrin for comparison to free base porphyrins The features of the UV-vis spectrum of M(CO)<sub>5</sub>(C<sub>5</sub>H<sub>4</sub>N) were discussed in Section 4 2 and it was shown that this compound has no significant absorbances at wavelengths longer than 420 nm The photochemistry of M(CO)<sub>5</sub>(C<sub>5</sub>H<sub>4</sub>N) has been discussed in Section 3 2 and Section 3 8 This complex undergoes ligand loss with a quantum yield approaching 1 0 from the population of a metal-centred LF excited state<sup>37</sup> Like the free base porphyrin laser flash photolysis ( $\lambda_{\text{exc}} = 532 \text{ nm}$ ) of ZnMPyTPPM(CO)<sub>5</sub> in deoxygenated dichloromethane populates the excited states associated with the metalloporphyrin moiety rather than the M(CO)<sub>5</sub> pyridyl unit as the porphyrin is the only species with strong absorbances at this wavelength The transient absorption difference spectrum has similar spectral features to that of triplet states of the uncoordinated metalloporphyrin, ZnTPP (see Figure 4 25) with strong absorbances from 440 nm to 510 nm For the metal carbonyl metalloporphyrin the lifetimes of the triplet excited state were slightly shorter than that of the uncoordinated

metalloporphyrin with lifetimes of approximately  $\sim 15 \mu\text{s}$ . Measurements using various concentrations of CO confirmed that the lifetime of the triplet state is unaffected.

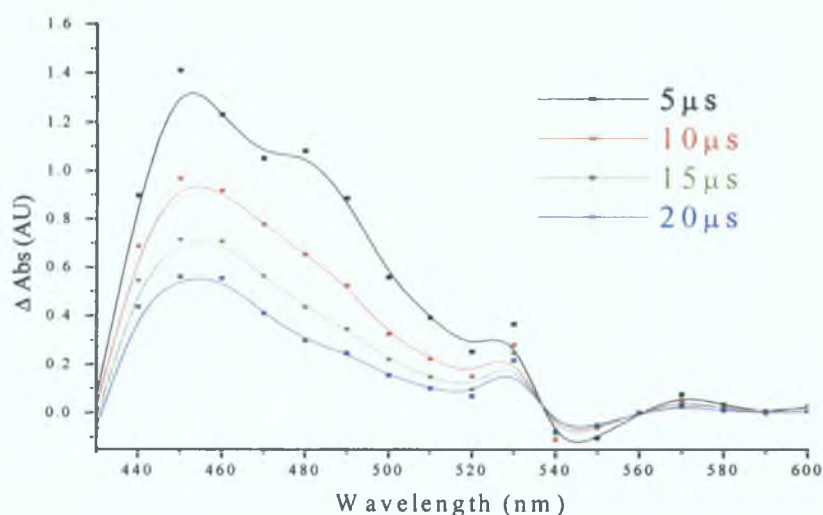
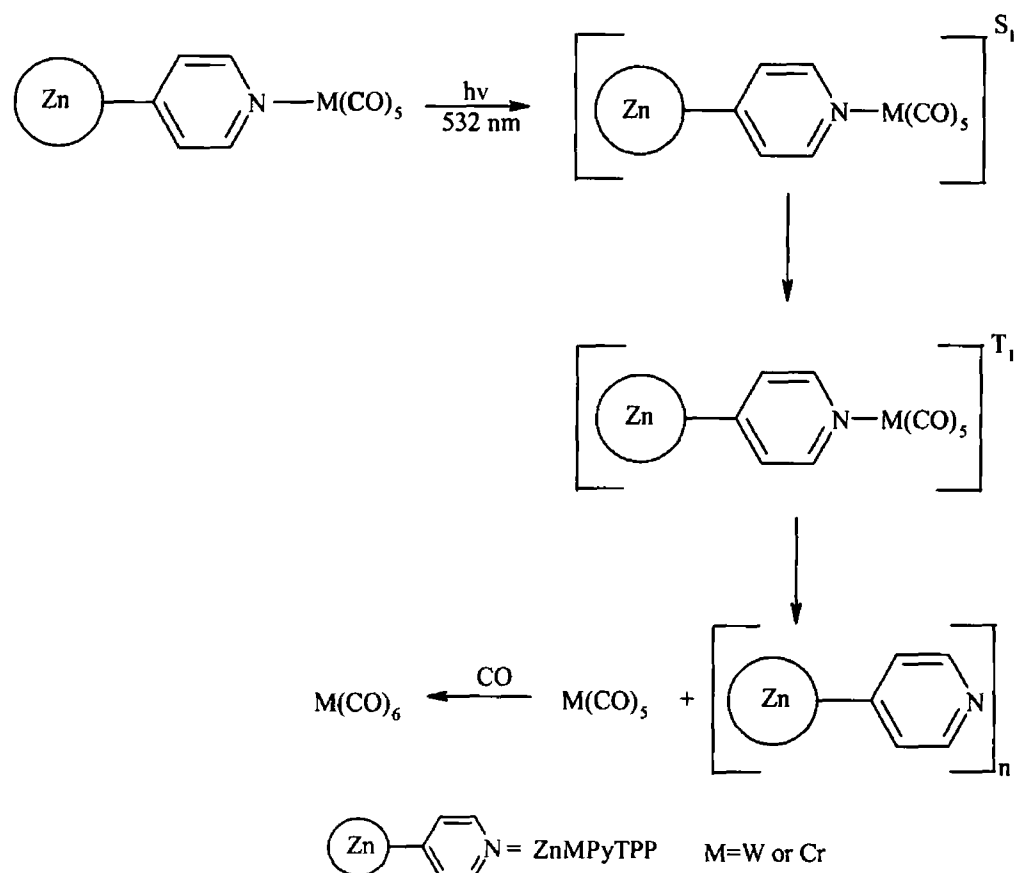


**Figure 4.25** Transient absorption difference spectra collected following laser flash photolysis ( $\lambda_{\text{exc}} = 532 \text{ nm}$ ) of ZnTPP in dichloromethane at 293 K

The changes that occurred during laser flash photolysis were monitored in the UV-vis with the formation of  $\text{M}(\text{CO})_6$  confirmed by IR spectroscopy (see Figure 4.19 and 4.23). In each case formation of the hexacarbonyl species is the end result. Formation of the metal hexacarbonyl at 290 nm was not as obvious using UV-vis spectroscopy because the concentration of the metalloporphyrin complexes used in the experiments masked this region to a certain degree. The major changes in the UV-vis spectra occurred in the Q band region. As the sample undergoes loss of  $\text{M}(\text{CO})_5$  during the experiment the Q bands shift in intensity and position. This is indicative of the formation of ZnMPyTPP polymer. In Figure 4.24 the sample was extensively photolysed after the experiment had been completed. It is possible to see that the relative intensity of the Q bands and their position have changed dramatically as the experiment proceeds. This is because as the N-M bond breaks, and results in the formation of the polymer. As the sample is photolysed the concentration of the polymer increases as is evident from Figure 4.19 and 4.23.

Two possible suggestions for the observed photochemistry are outlined in the following schemes

**Scheme 4 1**



In the above scheme loss of the  $\text{M(CO)}_5$  moiety and formation of the polymer is a consequence of the primary reaction. This involves the initial formation of the singlet excited state of the porphyrin following photolysis followed by intersystem crossing to the triplet state of the complex. Loss of  $\text{M(CO)}_5$  occurs from this excited state to leave the free base porphyrin and the carbonyl moiety. Formation of both the polymer and  $\text{M(CO)}_6$  can be identified from UV-vis spectra with the changes in intensity and position of the Q bands (Figure 4 18 and 4 24). The IR spectra in Figure 4 19 and 4 23 show the formation of  $\text{W(CO)}_6$  and  $\text{Cr(CO)}_6$ , with a M-CO absorption at 1975 and 1980  $\text{cm}^{-1}$  respectively. If the N-M bond is broken from population of the triplet excited state on the

complex a more significant change in the lifetime and transient absorption spectra of the complexed metalloporphyrins as expected, in comparison to the uncomplexed metalloporphyrin. The fact that ZnTPP was used instead of ZnMPyTPP could account for any small changes observed. Another pathway is postulated (see Scheme 4.2)

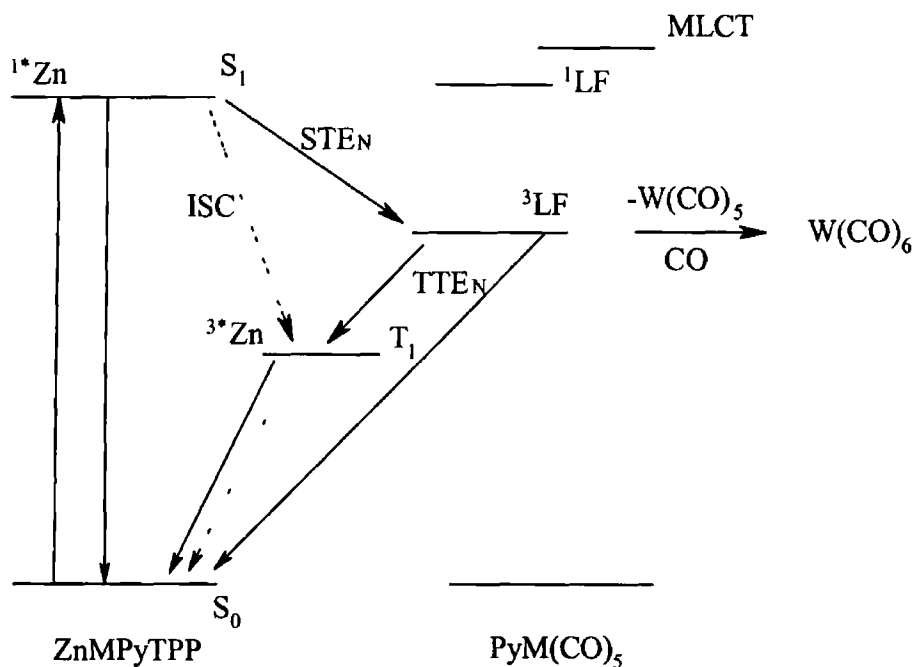


**Figure 4.26** Diagrammatical representation of the deactivation pathway following population of the singlet excited state in ZnMPyTPPM(CO)<sub>5</sub> ( $\lambda_{exc} = 532 \text{ nm}$ )

In the process proposed in Scheme 4.2, excitation of the complex causes population of the singlet state of ZnMPyTPPM(CO)<sub>5</sub>. Loss of the M(CO)<sub>5</sub> component, subsequently occurs from this excited singlet state and ISC leads to population of an excited triplet state of the uncomplexed metalloporphyrin (see Figure 4.27). The transient absorption difference spectra of both the W and Cr porphyrin complexes have the characteristics of a metalloporphyrin.

Even when the photolysis was conducted in the absence of CO in a carefully deaerated solution of ZnMPyTPPM(CO)<sub>5</sub> in dichloromethane and placed under an atmosphere of Ar, formation of the triplet state due to the metalloporphyrin was observed as indicated by the lifetimes of the transient signals. For pyridine metal pentacarbonyl

photodissociation of the pyridine ligand and not CO is the most efficient photochemical process<sup>38</sup>

**Scheme 4.2**

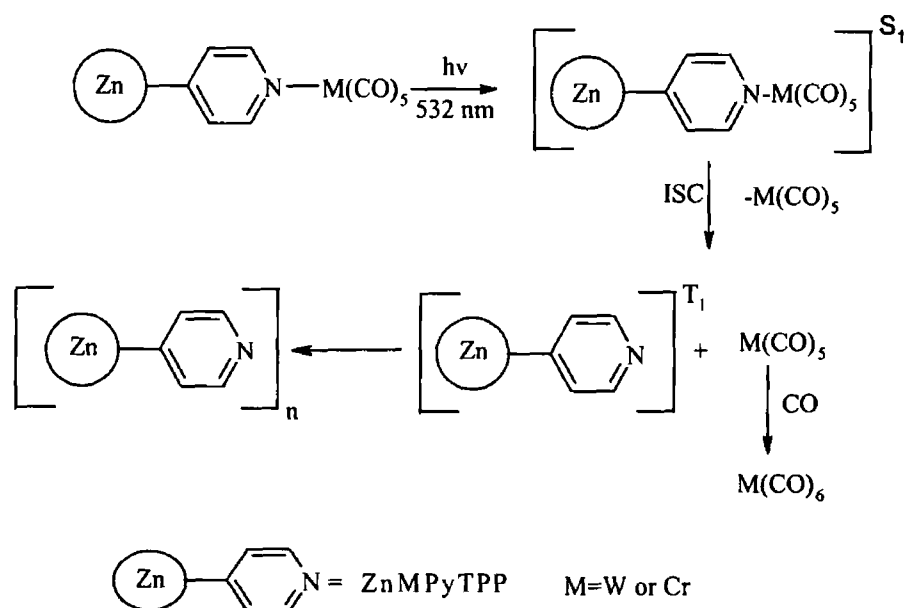
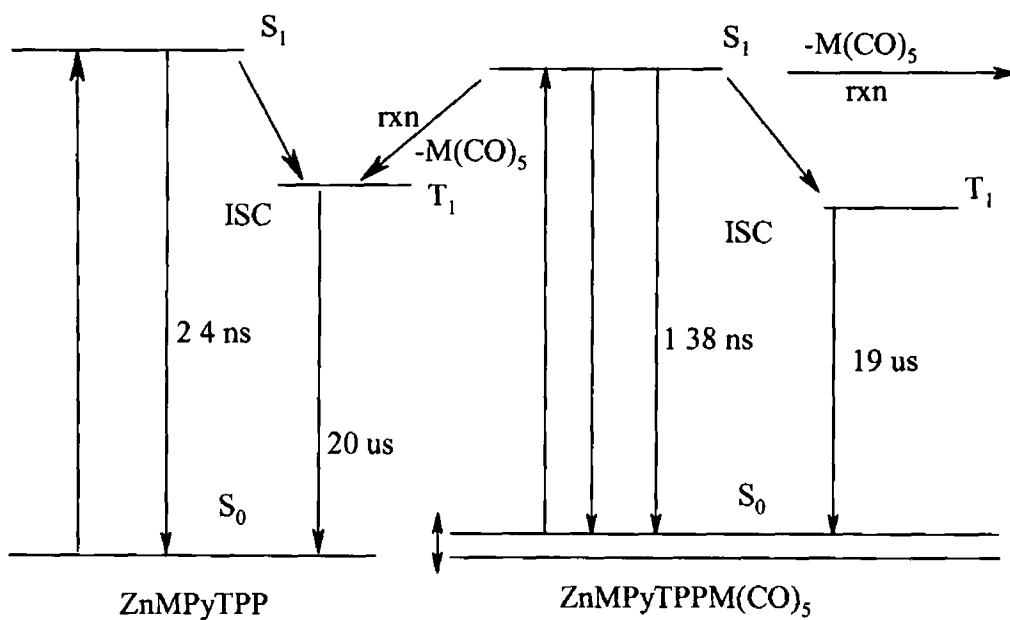


Figure 4 27 gives a representation of the lifetimes and energy levels involved if Scheme 4 2 is followed In Figure 4 27 the lifetimes of the triplet state are similar only differing by 5  $\mu\text{s}$  while the singlet lifetimes of the complexes are almost half that of the uncomplexed porphyrin Scheme 4 2 best describes this as it shows loss of the pentacarbonyl moiety from the singlet excited state of the metalloporphyrin complex Laser flash photolysis of the metalloporphyrin pentacarbonyl complex causes the cleavage of the N-M bond leaving  $\text{M(CO)}_5$  which is scavenged by CO to form  $\text{M(CO)}_6$  The metalloporphyrin is now in the triplet state but as there is no pentacarbonyl unit attached it is simply the triplet state of the uncomplexed porphyrin Following relaxation to the ground state self co-ordination of the metalloporphyrin takes place to give the polymer Hence we see the shift in the UV-vis spectra during laser flash photolysis



**Figure 4.27** Diagrammatical representation of the deactivation pathway from the singlet excited state in ZnMPyTPPM(CO)<sub>5</sub> ( $\lambda_{exc} = 532 \text{ nm}$ )

## 4 8 Conclusion

The photochemistry and photophysics of metalloporphyrin metal carbonyl adducts have been discussed in this chapter. Both tungsten and chromium analogues ( $M(CO)_5L$ ) have been synthesised and characterised ( $L =$  pyridyl porphyrin and  $M = W$  or  $Cr$ ). The spectroscopic data of both complexes were compared to those of the porphyrin polymer (MPyTPP) and a model compound (ZnTPP). Investigation into the electron transfer or energy transfer processes between the metal moiety and the porphyrin chromophore was undertaken using a number of photochemical (time resolved and steady state spectroscopy) and photophysical (emission spectra and singlet state lifetimes) techniques. Given what is known of the photochemistry and photophysical properties of metalloporphyrins, two possible reaction schemes have been proposed for the cleavage of the  $M(CO)_5$  fragment (see Figure 4.26 and 4.27).

A possible consequence of complexation of  $M(CO)_5$  at the N atom in the pyridyl moiety of the porphyrin, is the heavy atom effect, which has been extensively used to explain changes in lifetimes and shifts in spectral bands of porphyrins<sup>39,40</sup>. However as Cr is one of the metals used it is unlikely that the heavy atom effect is causing the changes. Overall there is complexation of a pentacarbonyl unit to the metalloporphyrin which caused a reduction in the lifetimes of the singlet state together with a shift in the emission bands and a reduction in the fluorescence intensity. The overall profile of the transient absorption spectra and lifetimes obtained for the complexes showed no significant changes when compared to both the transient absorption difference spectrum and the lifetimes of the uncomplexed metalloporphyrin<sup>12,16</sup>.

The most important observation from these experiments is that by using excitation wavelengths where only the porphyrin absorbs, loss of the  $M(CO)_5$  moiety from the porphyrin complex results. As has been discussed, loss of  $M(CO)_5$  from the pyridyl unit occurs following population of the  $^3LF$  of the  $M(CO)_5(C_5H_4N)$ . In the porphyrin systems electron/energy transfer from the porphyrin to the metal moiety must result in cleavage of the N-M bond. The photochemical product,  $M(CO)_5$ , is then efficiently scavenged by CO.

to yield  $M(CO)_6$  and the metalloporphyrin polymer (see Figure 4.26). This scheme implies that the heavy atom quenches the singlet excited state and enhances two spin forbidden processes<sup>41,42</sup>. The first is ISC within the porphyrin chromophore to the porphyrin triplet excited state and the second is singlet – triplet energy transfer ( $STE_N$ ) to the attached unit. ISC caused by an external tungsten metal could be competing with the internal zinc atom, which has reduced fluorescence formation from 10% to 4% upon coordination<sup>10</sup>. The zinc atom does not appreciably change the quantum yield of triplet formation, which remains at *ca.* 90%. However if the  $STE_N$  process was the pathway followed the reduction in triplet formation would be substantial. This is not the case as the lifetimes and transient absorption spectra (except for the shift of 10 nm) of the complexes are like that of the uncomplexed metalloporphyrin. This explanation also fails on the grounds that Cr is not a heavy atom and will not affect ISC.

In Section 4.5 it was observed that the shift to lower energy of the various electronic absorption spectra of the complexes could lead to the formation of singlet energy levels, which are lower in energy than that of the uncomplexed free base porphyrin. Figure 4.27 is used to diagrammatically represent this. In this diagram the metalloporphyrin and the  $M(CO)_5C_5H_4N$  unit cannot be treated as a supramolecular system. The components of the system are interacting to such an extent that their energy levels are substantially changed by their intercomponent interaction (see Figure 4.27).

Upon co-ordination of the metal moiety to the porphyrin a shift in energy levels takes place. The fluorescence spectra of the complexes are shifted when compared to both ZnTPP and ZnMPyTPP polymer (see Figure 4.13). As ZnMPyTPP has a tendency to self-associate, ZnTPP is used as the model for comparison. In both cases the emission maxima have shifted to lower energy with respect to the free base porphyrin. The relative quantum yield of the metal carbonyl complexes (see Table 4.5 and 4.6) and the lifetimes of the complexes have also been reduced from 2.4 ns to 1.6 ns. If the heavy atom effect were responsible for causing these changes the reductions in lifetimes expected would be far greater as was the case of the reduction in lifetimes when a metal (zinc) is inserted into the centre of a free base porphyrin ( $\sim 10$  ns to  $\sim 2.0$  ns). Upon complexation of a

tungsten pentacarbonyl moiety to the periphery of the porphyrin the reduction is only ~ 10 ns to ~ 8.6 ns. Therefore the heavy atom effect can be ruled out. Complexation might have caused a change in the energy levels of the new complex in comparison to the uncomplexed metalloporphyrin. This would seem to be the most logical explanation of the two. In Figure 4.27 it can be seen that once the new metal pentacarbonyl complex has been excited into the singlet excited state the N-M bond is broken and the metal pentacarbonyl moiety is lost. Therefore when measuring the triplet state lifetimes there are only minor changes when compared to an uncomplexed metalloporphyrin. Once the pentacarbonyl unit is lost the energy levels return to that of the uncomplexed metalloporphyrin.

In conclusion two possible mechanisms were proposed following excitation of the metalloporphyrin pentacarbonyl complexes. The first scheme involved the heavy atom effect, which could have worked well when discussing the W analogue. However while the singlet lifetime was reduced the presence of the carbonyl moiety had no effect on the triplet lifetimes and therefore did not affect intersystem crossing. It was also inadequate in explaining the same changes observed for the Cr analogue.

In the other scheme it was assumed that the energy levels of the components of the porphyrin pentacarbonyl complex interact to such an extent that the energy levels of the new molecule are changed. This is confirmed by red shifts in the UV-vis absorption spectra and emission spectra of the complexes compared to the uncomplexed metalloporphyrin. Also a change in lifetimes of the singlet state of the pentacarbonyl complexes compared to the uncomplexed metalloporphyrin while the similarity of the triplet lifetime of both the uncomplexed metalloporphyrin and the pentacarbonyl complexes shows that the pentacarbonyl moiety does not affect the triplet state of the complex. Therefore the pentacarbonyl moiety must be removed prior to the formation of the triplet state hence this is the most likely scheme in the excitation of the complexes.

## 4.9 Bibliography

---

- 1 K Kalyanasundaram, M Gratzel, *Photosensitisation and Photocatalysis using Inorganic and Organometallic compounds*, Kluwar Academic Publications, London, 1993
- 2 V Balzani, F Scandola, *Supramolecular Photochemistry*, Horwood, Chichester, UK, 1991
- 3 M R Wasielewski, *Chem Rev* , 1992, 92, 435
- 4 E S Schmidt, T S Calderwood, T C Bruice, *Inorg Chem* , 1986, 25, 3718
- 5 M Wrighton, *Chem Rev* , 1974, 74, 401
- 6 A M Shachter, E B Fleischer, R C Haltiwanger, *J Chem Soc, Chem Commun* , 1988, 960
- 7 D M Collins, J L Hoard, *J Am Chem Soc* , 1970, 92, 3761
- 8 G J B Williams, L C Andrews, L D Spalding, *J Am Chem Soc* , 1977, 99, 6918
- 9 D J Quimby, F R Longo, *J Am Chem Soc* , 1975, 97, 5111
- 10 K Kalyanasundaram, *Photochemistry of Polypyridyl and Porphyrin Complexes*, Academic Press, London, 1992
- 11 F B Fleischer, A M Shachter, *Inorg Chem* , 1991, 30, 3763
- 12 K Kalyanasundaram, *Inorg Chem* , 1984, 23, 2453
- 13 M Moet-Ner, A D Alder, *J Am Chem Soc* , 1975, 97, 5107
- 14 M S Wrighton, H B Abrahamson, D L Morse, *J Am Chem Soc* , 1976, 98, 4105
- 15 C Maralejo, C H Langford, D K Sharma, *Inorg Chem*, 1989, 28, 2205
- 16 C J Aspley, J R Lindsey Smith, R N Perutz, *J Chem Soc Dalton Trans*, 1999, 2273
- 17 P Glyn, F P A Johnson, M W George, A J Lees, J J Turner, *Inorg Chem* , 1991, 30, 3543
- 18 A J Lees, A W Adamson, *J Am Chem Soc* , 1982, 104, 3804
- 19 L T Cheng, W Tam, D F Eaton, *Organometallics*, 1990, 9, 2856
- 20 J B Kim, J J Leonard, F R Longo, *J Am Chem Soc* , 1972, 84, 3986

- 
- 21 R K Kumar, I Goldberg, *Angew Chem Ed Int* , 1998, 37, 3027
- 22 M Wrighton, *Inorg Chem* , 1974, 13, 905
- 23 M S Wrighton, K R Pope, *Inorg Chem* , 1985, 24, 2792
- 24 A Prodi, M T Indelli, C J Kleverlaan, F Scandola, E Alessio, T Gianferrara, L G Marzilli, *Chem Eur J* , 1999, 5, 2668
- 25 C J Aspley, J R Lindsey Smith, R N Perutz, *J Chem Soc, Dalton Trans*, 1999, 2269
- 26 A J Harrison, *J Chem Soc, Faraday Trans 1*, 1980, 31, 1978
- 27 R Humphrey-Baker, K Kalyanasundaran, *J Photochem* , 1985, 31, 105
- 28 M Sirish, B G Marya, *J Photochem Photobiol A Chem* , 1994, 77, 189
- 29 J M Zaleski, C K Chang, G E Leroi, R I Cukier, D G Nocera, *J Am Chem Soc* , 1992, 114, 3564
- 30 A Prodi, C J Kleverlaan, M T Indelli, F Scandola, E Alessio, E Iengo, *Inorg Chem* , 2001, 40, 3498
- 31 R H Bisby, M Arvanitidis, S W Botchway, I R Clark, A W Parker, D Tobin, *Photochem and Photobiol Science* 2, 2003, 2, 157
- 32 C Turro, C K Chang, G E Leroi, R I Cukier, D G Nocera, *J Am Chem Soc* , 1994, 114, 4013
- 33 J S Hsiao, B P Krueger, R W Wagner, T E Johnson, J K Delaney, D C Mauzerall, G R Fleming, J S Lindsey, D F Bocian, R J Donohoe, *J Am Chem Soc* , 1996, 118, 11181
- 34 D J Quimby, F R Longo, *J Am Chem Soc* , 1975, 97, 5111
- 35 M Linke, N Fujita, J C Chambron, V Heitz, J P Sauvage, *New J Chem* , 2001, 25, 790
- 36 L Flamigni, F Barigelletti, N Armaroli, J P Collin, J P Sauvage, J A Gareth Williams, *Chem Eur J* , 1998, 4, 1744
- 37 G Malouf, P C Ford, *J Am Chem Soc* , 1974, 96, 601
- 38 R M Dahlgren, J I Zink, *J Am Chem Soc* , 1979, 101, 1448
- 39 E J Shin, D Kim, *J Photochem and Photobiol A*, 2002, 91, 25
- 40 K Araki, H E Toma, *J Coord Chem* , 1993, 30, 9

- 
- 41 J Fan, J A Whiteford, B Olenyuk, M D Levin, P J Stang, E B Fleischer, *J Am Chem Soc* , **1999**, *121*, 2741
- 42 C M Drain, J M Lehn, *J Chem Soc Chem Commun* , **1994**, 2313

## **Chapter 5**

**5, 10 - *cis* 4 – Dipyridyl - 15, 20 -  
diphenylporphyrin and its tungsten and  
chromium pentacarbonyl complexes -  
Results and discussion**

## 5.1 Introduction

Multicomponent systems involving porphyrins are similar in structure to the natural occurring photosynthetic reaction centre and therefore would make the most useful artificial light harvesting molecular modules<sup>1</sup> For the light harvesting function carried out by a large number of chlorophyll (porphyrin) molecules in the antenna system of the reaction centre several models have been developed<sup>2</sup> These include several types of covalently linked donor – acceptor systems, including dyads and triads and more complex systems which have been designed to mimic the photoinduced charge separation of the reaction centre<sup>3</sup>

Having carried out work on the mono-substituted porphyrin ligand and the mono-substituted metalloporphyrin the next step in this study involved examining the communication process between the porphyrin and the metal moiety attached to the peripheral of the chromophore, in a multicomplexed porphyrin system Pyridyl porphyrins are considered an attractive building block for the synthesis of these supramolecular systems as they provide a convenient method for the coordination of various metal centres Adducts formed by the coordination pyridyl porphyrins to these metal centres have shown new and interesting photophysical and photochemical properties<sup>4</sup> Any changes to the excited state spectra of porphyrins, reductions in fluorescence quantum yield and singlet excited state lifetimes, have been attributed to the heavy atom effect induced by the metal centre<sup>5</sup> But the use of Cr metal in this work has suggested something other than the heavy atom effect is influencing these changes

The use of 5, 15 – dipyrityl 10, 20 – diphenylporphyrin (*cis*-D1PyD1PP) was an obvious choice because of the fact that it provides two available donor nitrogen for complexation and allows direct comparison with MPyTPP complexes previously studied The photochemistry and photophysical properties of *cis*-D1PyD1PP, should be typical of tetra aryl free base porphyrins, which have been extensively researched<sup>6</sup> *Trans*- D1PyD1PP was also synthesised, but it was not possible to isolate the metal pentacarbonyl complex

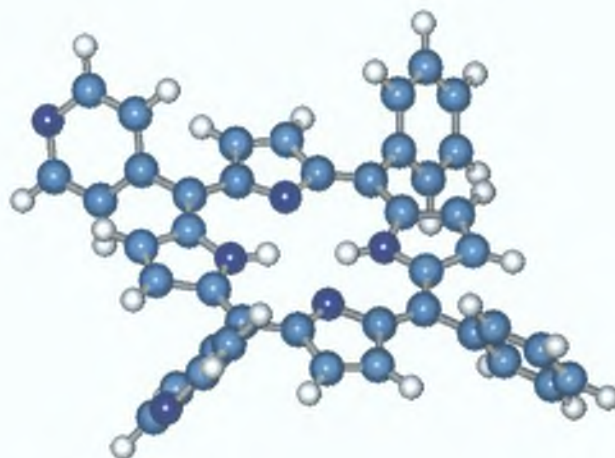


*Figure 5.1 Molecular model representation of cis 5, 10-di- 4-pyridyl - 15,20-diphenylporphyrin (cis-DiPyDiPP) showing the plane of the aryl groups in the meso position are orthogonal to the plane of the porphyrin ring and the two sites of metal coordination (dark blue atoms are nitrogen atoms while the lightest are hydrogen)*

Like all porphyrin pentacarbonyl complexes studied the presence of intense  $\nu_{\text{CO}}$  absorptions in the IR spectrum provides a useful additional spectroscopic handle. The interaction between the porphyrin chromophore and the metal carbonyl moiety was also investigated in the ground state by UV-vis and  $^1\text{H}$  NMR spectroscopies as well as in the excited state by using photochemical studies, fluorescence spectroscopy, singlet and triplet lifetimes and quantum yield determinations.

**5.2 UV-vis studies of *cis* 5, 10-*di*-4, pyridyl-15, 20-diphenyl porphyrin and its pentacarbonyl complexes  $M(CO)_5$  ( $M = Cr$  or  $W$ )**

**Table 5.1 UV bands of free base porphyrin and *di*-pentacarbonyl complexes (nm)**

| <i>Porphyrin</i>                                | $B(0,0)$ | $Q_y(1,0)$ | $Q_y(0,0)$ | $Q_x(1,0)$ | $Q_x(0,0)$ | $A[Q(0,0)]/$<br>$A[Q(1,0)]$ |
|-------------------------------------------------|----------|------------|------------|------------|------------|-----------------------------|
| <i>cis</i> -D1PyD1PP                            | 416      | 513        | 547        | 588        | 643        | 0.41                        |
| <i>cis</i> -D1PyD1PP( $Cr(CO)_5$ ) <sub>2</sub> | 420      | 516        | 552        | 590        | 646        | 0.59                        |
| <i>cis</i> -D1PyD1PP( $W(CO)_5$ ) <sub>2</sub>  | 421      | 517        | 553        | 590        | 646        | 0.53                        |

Table 5.1 summarises the important features of the electronic spectra of *cis* dipyrindyl-diphenylporphyrin (*cis*-D1PyD1PP), *cis*-D1PyD1PP( $W(CO)_5$ )<sub>2</sub> and *cis*-D1PyD1PP( $Cr(CO)_5$ )<sub>2</sub> complexes. The absorption spectrum of the uncomplexed free base porphyrin (*cis*-D1PyD1PP) has previously been reported in the literature<sup>7</sup> and it is typical of tetra-aryl free base porphyrins<sup>8</sup>. The absorption spectra of these metal carbonyl complexes have a similar profile to that of the uncomplexed free base porphyrin. The spectra of free base porphyrins are characterised by a strong Soret band at 420 nm and four Q bands of decreasing intensity between 510 nm and 650 nm (see Figure 5.2). However, the spectra of the adducts differ slightly in that their band maxima are red shifted by 3 – 6 nm compared to those of the parent pyridyl porphyrin. These shifts are greater than those observed for the *mono* substituted series. This has been observed previously for pyridyl porphyrins when complexed to Ru centres<sup>9</sup>. As the number of Ru centres attached to the porphyrin is increased so too is the extent of the observed shift. As previously mentioned this was attributed to the heavy atom effect throughout most of the literature<sup>10</sup>. The case could be applied here but for the fact that the shifts are observed in the Cr based analogues. Cr does not induce the heavy atom effect in complexes so it cannot be responsible for the changes. Although the shifts are small they are indicative of an interaction of the metal carbonyl moieties with the porphyrin macrocycle.

Complexation of the metal carbonyl moieties to the porphyrin macrocycle also causes a change in the relative intensities of the Q bands. The Q bands of a free base porphyrin are

divided into two sets  $Q(0,0)$  and  $Q(1,0)$   $Q(0,0)$  is the electronic origin of the lowest excited singlet state and  $Q(1,0)$  is its vibrational satellite. Due to the symmetry of the free base porphyrin  $Q(0,0)$  is split into  $Q_x$  and  $Q_y$ , both with their own vibrational satellite. The relative intensity of the  $Q(0,0)$  bands to the  $Q(1,0)$  bands shows the extent of the interaction of the porphyrin and the peripheral component<sup>8</sup>

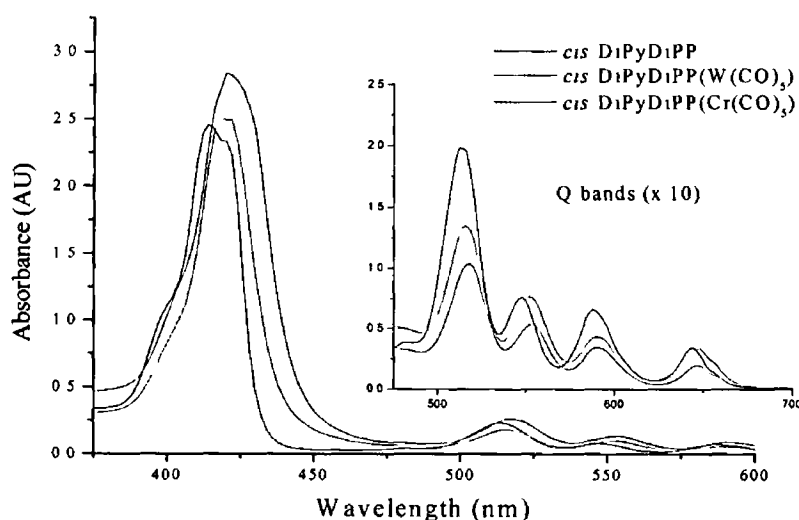


**Figure 5.2** UV-vis spectra of *cis*-DiPyDiPP ( $2.2 \times 10^{-5} \text{ mol dm}^{-3}$  at 532 nm), *cis*-DiPyDiPP(W(CO)<sub>5</sub>)<sub>2</sub> and *cis*-DiPyDiPP(Cr(CO)<sub>5</sub>)<sub>2</sub> ( $8.2 \times 10^{-5} \text{ mol dm}^{-3}$  at 532 nm)

An increase in this ratio is observed after complexation to the peripheral position of the porphyrin. It has been shown that the electron donating character of a substituent in *meso*-tetra phenyl porphyrins increases the absorption intensities of the  $Q_y(0,0)$  transitions while the presence of electron withdrawing substituents results in a decrease in the absorption intensities of the  $Q_y(0,0)$  transitions<sup>11,12</sup>. Both the Cr(CO)<sub>5</sub> and W(CO)<sub>5</sub> moieties should have the effect of decreasing the intensities of  $Q_y(0,0)$  band relative to the  $Q_y(1,0)$  band but the opposite is observed.

**5.3 Infrared studies of *cis*-5, 10-*di*-4, pyridyl 15, 20-diphenyl porphyrin and its metal pentacarbonyl complexes  $M(CO)_5$  ( $M = Cr$  or  $W$ )**

The spectroscopic IR data (in the  $\nu_{CO}$ ) region for the *cis*-DiPyDiPP complexes are presented in Table 5.2. The three carbonyl absorptions observed for each metal carbonyl complex are consistent with the local  $C_{4v}$  symmetry of each metal pentacarbonyl centre (see Figure 5.3).<sup>13</sup> According to Kolodziej *et al.*,<sup>14</sup> the spectral data in Figure 5.3 confirm that the metal atom is bound to the nitrogen atom in the porphyrin macrocycle.

**Table 5.2**

| <i>Porphyrin</i>                                        | <i>IR Bands (cm<sup>-1</sup>)</i> |      |      |
|---------------------------------------------------------|-----------------------------------|------|------|
| <i>cis</i> -DiPyDiPP(Cr(CO) <sub>5</sub> ) <sub>2</sub> | 2069                              | 1936 | 1899 |
| <i>cis</i> -DiPyDiPP(W(CO) <sub>5</sub> ) <sub>2</sub>  | 2073                              | 1929 | 1897 |

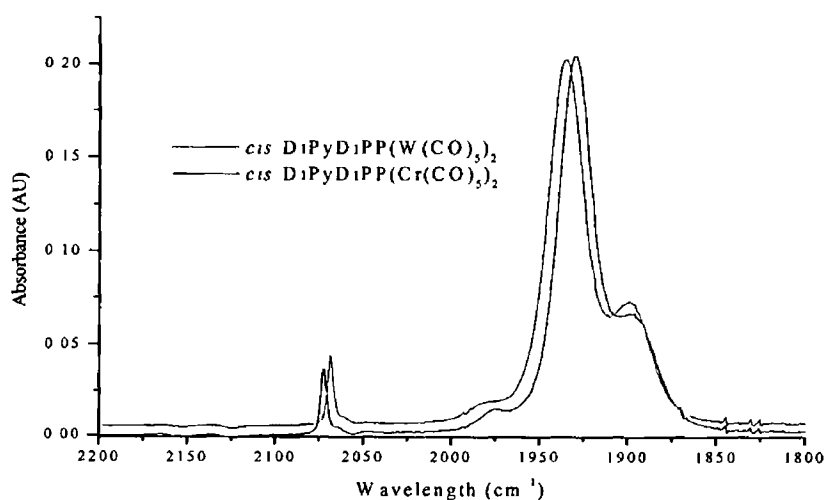


**Figure 5.3 IR spectra of *cis*-DiPyDiPP(W(CO)<sub>5</sub>)<sub>2</sub> and *cis*-DiPyDiPP(Cr(CO)<sub>5</sub>)<sub>2</sub> (recorded in dichloromethane)**

5.4 <sup>1</sup>H NMR spectrum of 5, 10-*di*-4, pyridyl 15, 20-diphenyl porphyrin and its pentacarbonyl complexes M(CO)<sub>5</sub> (M = Cr or W)

Table 5 3

| <i>Porphyrin</i>                                                                  | <i>4 H, 2, 6 dipyridyl, δ ppm</i> | <i>2 H, internal pyrrole, δ ppm</i> |
|-----------------------------------------------------------------------------------|-----------------------------------|-------------------------------------|
| <i>cis</i> -D <sub>1</sub> PyD <sub>1</sub> PP                                    | 9 06                              | - 2 84                              |
| <i>cis</i> -D <sub>1</sub> PyD <sub>1</sub> PP(Cr(CO) <sub>5</sub> ) <sub>2</sub> | 9 22                              | - 2 84                              |
| <i>cis</i> -D <sub>1</sub> PyD <sub>1</sub> PP(W(CO) <sub>5</sub> ) <sub>2</sub>  | 9 20                              | - 2 86                              |

The <sup>1</sup>H NMR data for *cis*-D<sub>1</sub>PyD<sub>1</sub>PP, *cis*-D<sub>1</sub>PyD<sub>1</sub>PP(Cr(CO)<sub>5</sub>)<sub>2</sub> and *cis*-D<sub>1</sub>PyD<sub>1</sub>PP(W(CO)<sub>5</sub>)<sub>2</sub> are presented in Table 5 3 The presence of a singlet at ≈ -2 84 ppm arising from the internal pyrrole protons at the centre of the porphyrin molecule are exclusive to free base porphyrins and are absent in metalloporphyrins (see Table 4 3) As in the *mono* pyridyl porphyrins the internal protons experience this high field shift because of the internal ring current of the porphyrin molecule <sup>15</sup> The presence of this proton signal confirms the absence of a metal at the centre of the porphyrin ring

When comparing the <sup>1</sup>H NMR spectra of the free base porphyrin to either the Cr or W adducts a small shift of ~ δ 0 15 ppm in the position of the 2,6 pyridyl proton resonance is observed This shift confirms that the metal pentacarbonyl unit is co-ordinated through the N of the pyridine site The fact that only one set of proton signals is present confirms that both pyridine sites have undergone coordination to the metal pentacarbonyl moiety The protons are shifted downfield because of the donation of electron density from the pyridine nitrogen lone pair to the metal centre <sup>16</sup> The shifts are slightly greater than that of the MPyTPP complexes due to the double effect of two pentacarbonyl moieties The remaining resonances are unaffected by complexation and are omitted in the above table

## 5.5 Steady state photolysis experiments monitored in the UV-vis

### 5.5.1 Steady state photolysis of *cis*-DiPyDiPP(W(CO)<sub>5</sub>)<sub>2</sub> under 1 atmosphere of CO

A solution of *cis*-DiPyDiPP(W(CO)<sub>5</sub>)<sub>2</sub> in dichloromethane (conc.  $5.8 \times 10^{-5}$  mol dm<sup>-3</sup>) was exposed to steady state photolysis ( $\lambda_{\text{exc}} > 400$  nm or 500 nm). Initially the sample was irradiated at  $\lambda_{\text{exc}} > 500$  nm, and was previously described for the *mono* pyridyl system. Very little change was observed in the UV-vis spectrum other than a small growth in at 290 nm (see Figure 5.4). This was attributed to the formation of W(CO)<sub>6</sub>. Isosbestic points were apparent at 305 and 270 nm. As the process was inefficient and the changes were small, the radiation energy was increased to  $\lambda > 400$  nm.

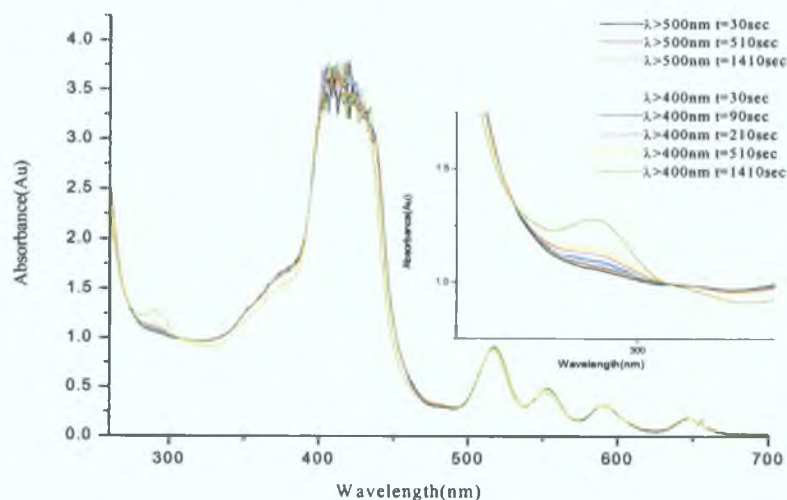


**Figure 5.4** UV-vis spectral changes observed following steady state photolysis ( $\lambda > 400$  nm and 500 nm) of *cis*-DiPyDiPP(W(CO)<sub>5</sub>)<sub>2</sub> ( $5.8 \times 10^{-5}$  mol dm<sup>-3</sup>) in dichloromethane under 1 atmosphere of CO

When the irradiation wavelength was increased to  $\lambda_{\text{exc}} > 400$  nm there was an increase in formation of W(CO)<sub>6</sub> at 290 nm (see Figure 5.4) due to the increased rate of N-W bond cleavage. The photolysis was stopped when no further changes were observed in the UV-

vis spectrum Again a shift of 4 - 6 nm in the Q bands was noted, indicating the formation of the uncomplexed porphyrin It was shown earlier that the presence of a metal carbonyl unit at the peripheral region of a porphyrin causes a red shift in the UV-vis spectrum <sup>17</sup> The formation of the isosbestic points indicates that the formation of  $W(CO)_6$  was a concerted process under these conditions

### 5.5.2 Steady state photolysis of *cis*-DiPyDiPP(W(CO)<sub>5</sub>)<sub>2</sub> under 1 atmosphere of Ar

A solution of *cis*-DiPyDiPP(W(CO)<sub>5</sub>)<sub>2</sub> in dichloromethane (conc.  $3.5 \times 10^{-5}$  mol dm<sup>-3</sup>) was subjected to steady state photolysis ( $\lambda_{\text{exc}} > 400$  nm or 500 nm) under an atmosphere of argon. Samples were initially irradiated at  $\lambda_{\text{exc}} > 500$  nm. The changes observed in the UV-vis spectrum for the same photolysis time were not as significant as those observed under 1 atmosphere of CO. Obviously under these conditions formation of W(CO)<sub>6</sub> is less efficient (see Figure 5.5). The yield of W(CO)<sub>6</sub> is limited by the ability of the “W(CO)<sub>5</sub>” fragment to coordinate CO *via* bimolecular reactions.

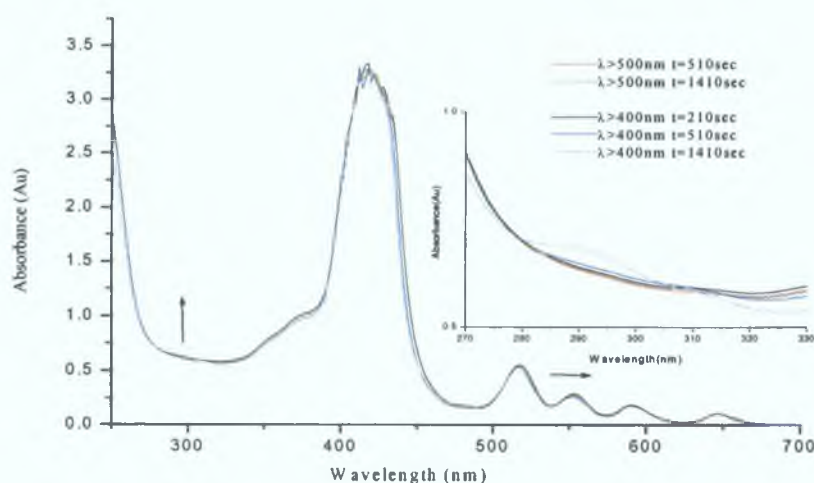


**Figure 5.5** UV-vis spectr of *cis*-DiPyDiPP(W(CO)<sub>5</sub>)<sub>2</sub> ( $3.5 \times 10^{-5}$  mol dm<sup>-3</sup>) observed following steady state photolysis ( $\lambda > 400$  nm or 500 nm) in dichloromethane under 1 atmosphere of Ar

When the irradiation wavelength was decreased to  $\lambda_{\text{exc}} > 400$  nm there was some evidence for the formation of W(CO)<sub>6</sub> at 290 nm (see Figure 5.5). After prolonged photolysis (~ 20 mins) the photolysis was stopped as no further changes were observed in the UV-vis spectrum. Again a red shift in the Q bands was observed indicating the formation of free porphyrin.

### 5.5.3 Steady state photolysis of *cis*-DiPyDiPP(Cr(CO)<sub>5</sub>)<sub>2</sub> under 1 atmosphere of CO

A solution of *cis*-DiPyDiPP(Cr(CO)<sub>5</sub>)<sub>2</sub> in dichloromethane (conc.  $3.9 \times 10^{-5}$  mol dm<sup>-3</sup>) was subjected to steady state photolysis ( $\lambda_{\text{exc}} > 400$  nm or 500 nm) under 1 atm of CO. The same conditions were employed as in the case of the tungsten analogue. The sample was initially irradiated at  $\lambda_{\text{exc}} > 500$  nm, where a slight increase in absorbance at 290 nm was observed (see Figure 5.6). This was attributed to the formation of Cr(CO)<sub>6</sub>. This was subsequently confirmed by IR spectroscopy at the end of the photolysis experiment.

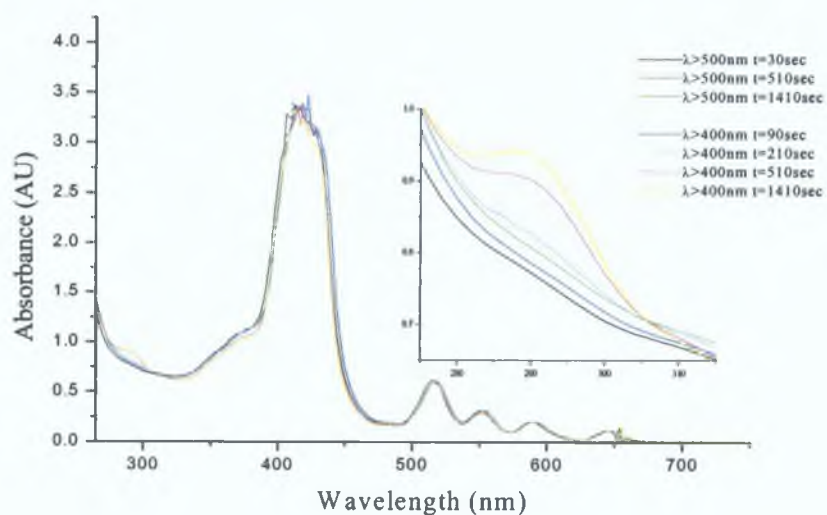


**Figure 5.6** UV-vis spectral changes observed following steady state photolysis ( $\lambda > 400$  nm and 500 nm) of *cis*-DiPyDiPP(Cr(CO)<sub>5</sub>)<sub>2</sub> ( $3.9 \times 10^{-5}$  mol dm<sup>-3</sup>) in dichloromethane under 1 atmosphere of CO

When the irradiation wavelength was changed to ( $\lambda_{\text{exc}} > 400$  nm) the changes in the UV-vis spectrum became more pronounced. Photolysis was continued until such a point that no further changes were evident.

#### 5.5.4 Steady state photolysis of *cis*-DiPyDiPP(Cr(CO)<sub>5</sub>)<sub>2</sub> under 1 atmosphere of Ar

Steady state photolysis ( $\lambda_{\text{exc}} > 400$  nm or 500 nm) of a solution of *cis*-DiPyDiPP(Cr(CO)<sub>5</sub>)<sub>2</sub> in dichloromethane ( $1.5 \times 10^{-5}$  mol dm<sup>-3</sup>) under 1 atm of argon produced the spectral changes presented in Figure 5.7. Initially the sample was irradiated at  $\lambda_{\text{exc}} > 500$  nm and the changes observed during photolysis were not as noticeable as those discussed previously under 1 atmosphere of CO (see Figure 5.6). This is because the formation of Cr(CO)<sub>6</sub> is not quantitative, and relies on the ability of the photogenerated Cr(CO)<sub>5</sub> unit to scavenge CO from the parent molecules or another photogenerated metal pentacarbonyl fragment. A red shift in the Q bands together with a change in their relative intensity was also evident.

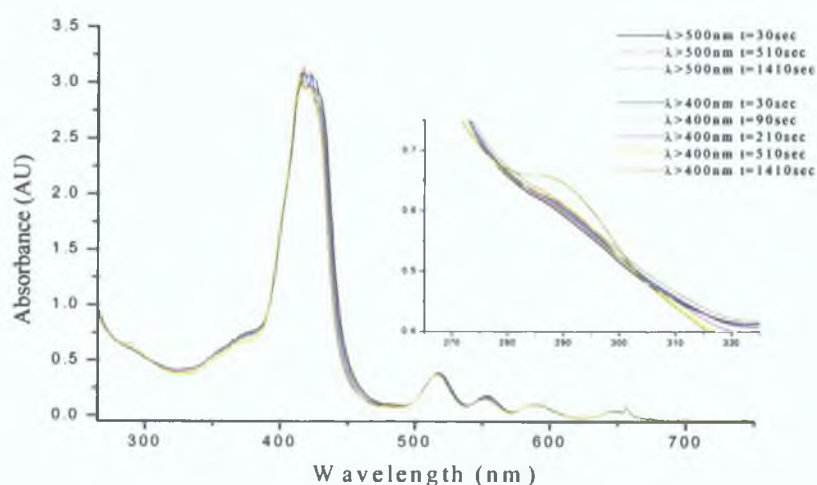


**Figure 5.7** UV-vis spectra of *cis*-DiPyDiPP(Cr(CO)<sub>5</sub>)<sub>2</sub> ( $1.5 \times 10^{-5}$  mol dm<sup>-3</sup>) recorded following steady state photolysis ( $\lambda > 400$  nm or 500 nm) in dichloromethane under 1 atmosphere of argon

When the irradiation wavelength was decreased ( $\lambda_{\text{exc}} > 400$  nm) the changes in the UV-vis spectrum, became much more obvious. Photolysis was again continued until such a stage that no further changes were observed

### 5.5.5 Discussion of results

Steady state photolysis was carried out in dichloromethane, as opposed to a hydrocarbon solution because of the limited solubility of the free base porphyrin and its metal carbonyl complexes (all samples were prepared as described in Section 6.5.1)

Photolysis carried out on the uncomplexed free base porphyrin yielded no changes in the UV-vis spectrum. For all systems studied steady state photolysis was carried out using two cut off filters with a  $\lambda_{exc} > 500$  nm followed by a  $\lambda_{exc} > 400$  nm. Initially samples were irradiated using an  $\lambda_{exc} > 500$  nm. As described in the previous sections only small changes were observed in the UV-vis spectra of the complexes following irradiation at this wavelength. As for all free base porphyrins the Q bands are the only bands absorbing at  $> 500$  nm (see Figure 5.8). As the Q bands are less intense than the Soret band and changes brought about here are less than those brought about by excitation into the Soret band. Although reduced considerably, some cleavage of the N-M bond takes place. A grow in at 290 nm is evident for all the spectrum due to the formation of the corresponding  $M(CO)_6$

When the irradiation wavelength was increased to  $\lambda_{exc} > 400$  nm the changes in the UV-vis spectrum became much more pronounced. At this irradiating wavelength the light is absorbed by the highly intense Soret band of the porphyrin, and the changes in the UV-vis spectrum were more obvious. The increase in absorbance at 290 nm became much more noticeable. This was due to the increased rate of N-M bond cleavage and formation of  $M(CO)_6$ . Such porphyrin to metal interaction had only been observed once before by Aspley *et al* and it was attributed to population of tungsten based excited states by energy transfer from the porphyrin<sup>18</sup>. Along with the increase in the absorbance at 290 nm there is also a blue shift in the Q bands. After complexation took place the Q bands of the *cis*-DiPyDiPP were absorbing 3 - 6 nm lower in energy than the uncomplexed porphyrin. As the N-M bond is broken the Q bands shift back towards the higher energy of the uncomplexed porphyrin.

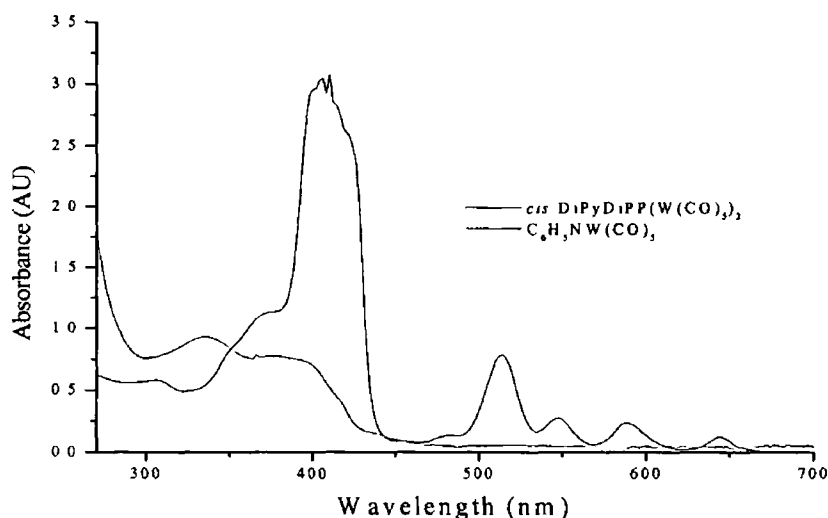


**Figure 5.8** UV-vis absorption spectra of *cis*-D<sub>1</sub>PyD<sub>1</sub>PP(W(CO)<sub>5</sub>)<sub>2</sub> ( $3.76 \times 10^{-5} \text{ mol dm}^{-3}$ ) and C<sub>5</sub>H<sub>5</sub>NW(CO)<sub>5</sub> ( $1.0 \times 10^{-4} \text{ mol dm}^{-3}$ ) in dichloromethane

Despite the intense porphyrin bands dominating the spectra there is loss of the carbonyl moiety. Communication between the porphyrin and the metal carbonyl unit is obviously taking place through excitation of the porphyrin. The extinction coefficient of *cis*-D<sub>1</sub>PyD<sub>1</sub>PP is much greater than that of C<sub>5</sub>H<sub>4</sub>NM(CO)<sub>5</sub> and any MLCT or LF bands due to this component would be masked. As was the case with MPyTPP free base porphyrin, this can occur through electron/energy transfer from the porphyrin.<sup>18, 19</sup> The argument can again be put forward that population of the <sup>3</sup>LF state is required for the cleavage of N-M bond on a pyridyl entity (discussed in Section 3.5.5) but in this case it must occur through interaction with the porphyrin.

Further photophysical and photochemical measurements were carried out in order to fully understand the mechanism involved in the loss of the M(CO)<sub>5</sub> moiety from the porphyrin.

## 5.6 Fluorescence studies of 5, 10 *cis*-4-dipyridyl-15, 20-diphenylporphyrin and its *di*-M(CO)<sub>5</sub> complexes (M = W or Cr)

### 5.6.1 Emission spectra and quantum yields of 5, 10 *cis* 4-dipyridyl 15, 20-diphenyl porphyrin and its M(CO)<sub>5</sub> complexes (M = W or Cr)

Fluorescence spectra were obtained for both metal carbonyl complexes and the uncomplexed free base porphyrin ligand. The spectra are similar as can be seen from Figure 5.9, these porphyrins emit from the porphyrin unit of the molecule. The overall fluorescence profiles of the free base porphyrin and the metal carbonyl complexes are essentially the same but with slight shifts in the maxima of the complexes. The most significant difference between the complexes and the free base porphyrin is the dramatic decrease in emission lifetimes.

**Table 5.4** Emission maxima and relative intensities of free base porphyrin and pentacarbonyl complexes

| <i>Porphyrin</i>                                        | <i>Emission Maxima (nm)</i> |            | <i>Relative <math>\phi_f</math></i> |
|---------------------------------------------------------|-----------------------------|------------|-------------------------------------|
| <i>cis</i> -D1PyD1PP                                    | 652                         | 715 (0.51) | 1.0                                 |
| <i>cis</i> -D1PyD1PP(Cr(CO) <sub>5</sub> ) <sub>2</sub> | 656                         | 717 (0.36) | 0.34                                |
| <i>cis</i> -D1PyD1PP(W(CO) <sub>5</sub> ) <sub>2</sub>  | 656                         | 718 (0.41) | 0.57                                |

The 2-4 nm red shift of the bands is indicative of a metal entity attached to the periphery of the porphyrin ring (see Table 5.4).<sup>20</sup> The shifts in the emission maxima are greater than those of the mono substituted complexes due to the presence of two metal moieties, now attached to the macrocycle.

There is a clear reduction in the intensity of the emission maxima of the complexes compared to that of the uncomplexed free base porphyrin (see Figure 5.9). This reduction is accompanied by a reduction in the fluorescence yield, which was calculated in the same way as that for the MPyTPP (using Equation 3.4). Again these are relative yields. A series of solutions were made that had identical absorbances at the excitation wavelength,

$\lambda_{exc} = 532 \text{ nm}$  The reduction in the fluorescence yield has increased significantly when compared to the MPyTPP porphyrin and pentacarbonyl analogues. The overall reduction in the fluorescence yield is over twice that experienced for the MPyTPP complexes but the difference between the Cr and W complexes is still the same.

As outlined in the previous chapters the reduction in emission quantum yield cannot be attributed to the heavy atom effect as the reduction is observed for both the chromium and tungsten analogues.<sup>20</sup> There is also a small reduction in the relative intensities of the emission peaks (Table 5.4) with the greatest decrease seen in the intensity of the band of the W complex. The intensity of the fluorescence bands falls with the relative order  $cis\text{-DiPyDiPP} > cis\text{-DiPyDiPP(W(CO)}_5)_2 > cis\text{-DiPyDiPP(Cr(CO)}_5)_2$ .

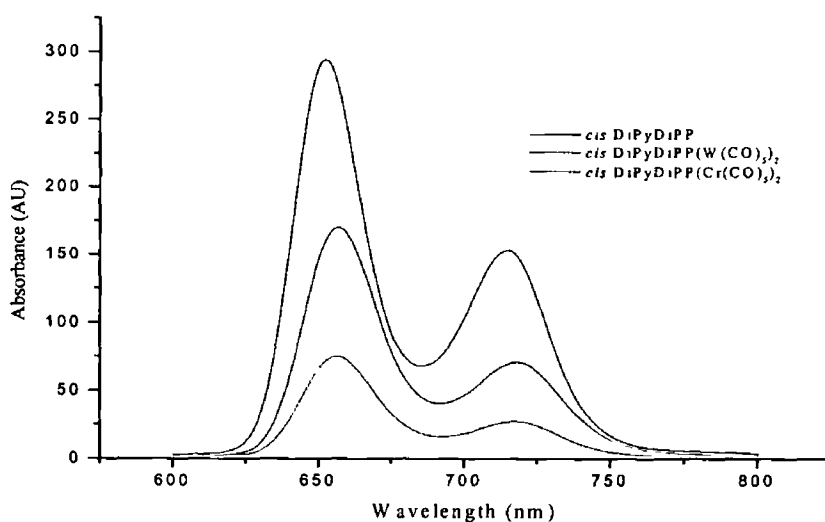


**Figure 5.9** Emission spectra of isoabsorptive samples of *cis*-DiPyDiPP, *cis*-DiPyDiPP(W(CO)<sub>5</sub>)<sub>2</sub> and *cis*-DiPyDiPP(Cr(CO)<sub>5</sub>)<sub>2</sub> at 293 K ( $\lambda_{exc}$  532 nm) in dichloromethane

### 5.6.2 Fluorescence lifetimes of *cis*-D<sub>1</sub>PyD<sub>1</sub>PP(W(CO)<sub>5</sub>)<sub>2</sub> and *cis*-D<sub>1</sub>PyD<sub>1</sub>PP(Cr(CO)<sub>5</sub>)<sub>2</sub>

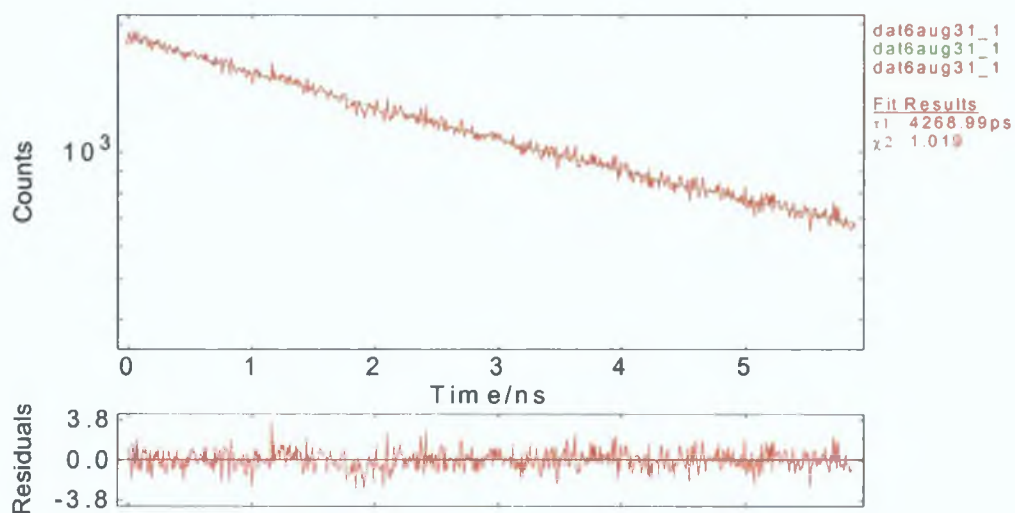
The fluorescence lifetimes were measured for the *cis*-D<sub>1</sub>PyD<sub>1</sub>PP uncomplexed free base porphyrin, *cis*-D<sub>1</sub>PyD<sub>1</sub>PP(W(CO)<sub>5</sub>)<sub>2</sub> and *cis*-D<sub>1</sub>PyD<sub>1</sub>PP(Cr(CO)<sub>5</sub>)<sub>2</sub> complexes. From Table 5.5 it is clear that the decrease in the singlet state lifetimes corresponds to the difference in emission intensities. The larger decrease in the fluorescence yield observed in the previous section compared to the MPyTPP complexes are accompanied by an equally larger decrease in singlet state lifetimes. The decrease in lifetimes is in the order *cis*-D<sub>1</sub>PyD<sub>1</sub>PP > *cis*-D<sub>1</sub>PyD<sub>1</sub>PP(W(CO)<sub>5</sub>)<sub>2</sub> > *cis*-D<sub>1</sub>PyD<sub>1</sub>PP(Cr(CO)<sub>5</sub>)<sub>2</sub>.

**Table 5.5**

| <i>Porphyrin</i>                                                                  | $\tau_f(ns)$ |
|-----------------------------------------------------------------------------------|--------------|
| <i>cis</i> -D <sub>1</sub> PyD <sub>1</sub> PP                                    | 9.92         |
| <i>cis</i> -D <sub>1</sub> PyD <sub>1</sub> PP(Cr(CO) <sub>5</sub> ) <sub>2</sub> | 4.32         |
| <i>cis</i> -D <sub>1</sub> PyD <sub>1</sub> PP(W(CO) <sub>5</sub> ) <sub>2</sub>  | 5.82         |

Reductions in lifetimes are not double those of the MPyTPP complexes (Table 3.5) but they do show a significant decrease. This adds to the theory proposed by previous authors that the number of units attached to the porphyrin increase the reduction in lifetimes on the chromophore.<sup>21</sup> The lifetime of the *cis*-D<sub>1</sub>PyD<sub>1</sub>PP is less than that of MPyTPP due to the fact that pyridyl porphyrins are more acidic than the tetra phenyl porphyrins and some reports have shown that as the number of pyridine groups increases, the lifetimes of the porphyrin decrease.<sup>22</sup>

Shown in Figure 5.10 is a typical transient signal obtained for *cis*-D<sub>1</sub>PyD<sub>1</sub>PP(Cr(CO)<sub>5</sub>)<sub>2</sub> monitored at 655 nm and is representative of a typical signal obtained for lifetime measurements. All samples were monitored at 655 nm, as this is the maximum absorbance of the emission spectrum. Samples were prepared as described in section 6.5.1.



**5.10 Single photon counting signal of *cis*-DiPyDiPP(Cr(CO)<sub>5</sub>)<sub>2</sub> at 293 K ( $\lambda_{exc}$  438 nm) in dichloromethane**

Upon complexation the ground state absorbance and emission spectrum of the complexes are shifted to lower energy when compared to the uncomplexed free base porphyrin. There is a shift in energy of the order *cis*-DiPyDiPP > *cis*-DiPyDiPP(W(CO)<sub>5</sub>)<sub>2</sub> > *cis*-DiPyDiPP(Cr(CO)<sub>5</sub>)<sub>2</sub> which is the same as the reduction in lifetimes observed. Complexation therefore has caused a reordering of the energy levels of the subunits of the complex compared to the individual component. This was explained in section 5.8 using Figure 5.20 and will be discussed in relation to the disubstituted complexes in the next section.

### 5.6.3 Discussion of results

As for all tetra aryl free base porphyrins, *cis*-D<sub>1</sub>PyD<sub>1</sub>PP emits from the lowest excited singlet state ( $S^1 \rightarrow S^0$  relaxation), which is  $\pi^* - \pi$  in character and is independent of the substituent in the *meso* position. The emission maxima for these disubstituted porphyrins occurs at 652 and 715 nm and are centred on the lowest singlet excited state transition (0-0 and 0-1 transitions). There is a slight change between the relative intensities of the Q(1,0), (652 nm) band and the Q(0,0), (715 nm) band. For *cis*-D<sub>1</sub>PyD<sub>1</sub>PP the intensity of Q(0,0) band has increased relative to Q(1,0) band when compared to MPyTPP, the intensity changes from 0.41 to 0.51 (see Table 3.4 and 5.4). This is a trend followed for all pyridyl porphyrins. As the number of pyridyl groups on a porphyrin increases the intensity of Q(1,0) band increases relative to the Q(0,0) band.<sup>23</sup> The quantum yield for fluorescence is approximately 10% for TPP and varies slightly by changing the number of pyridine ligands in the *meso* position of the porphyrin. The fluorescence quantum yield for *cis*-D<sub>1</sub>PyD<sub>1</sub>PP is about 1% less than that for TPP.<sup>22</sup> The decrease in quantum yield with extra pyridyl units is thought to be the result of interaction of the N on the pyridyl and the solvents.<sup>24</sup>

Upon complexation of the porphyrins with a  $M(CO)_5$  moiety there is a significant change in the emission spectra of the complexes studied compared to the uncomplexed porphyrin. Although the emission maxima are shifted by 2 – 4 nm, the intensity of the spectra is reduced dramatically. The shifts in the emission maxima of the complexes are approximately double that of the mono substituted complexes where a red shift to the red of 1 – 2 nm was observed for the complexes versus the free base porphyrin. The drop in  $\phi_f$  of the organometallic porphyrin compared to the free base porphyrins, is greater in the *di*-substituted complexes than the *mono* substituted analogues. This reduction is also accompanied by a decrease in the singlet excited state lifetimes of the complexes. This is in good agreement with work carried out previously on ruthenium porphyrin complexes where there was a correlation between the lifetime shortening and the number of metal centres attached to the porphyrin.<sup>21</sup> In other work carried out on Pd/Re based porphyrin systems the change in emission intensity and reduction in lifetimes was attributed to the

presence of heavy atoms<sup>25,26</sup> This argument cannot be used to explain the reduction in the lifetimes for both disubstituted porphyrin pentacarbonyl complexes, as the photophysics for both the Cr and W adducts probed were similar The observed red shifts in the UV-vis absorption spectra and the emission spectra of the metal carbonyl porphyrins compared to the uncomplexed porphyrin indicate intramolecular interactions between the two chromophores These shifts are larger than those of the mono substituted complexes and would therefore explain why the changes are also greater This is the theory that was put forward using Figure 5 20 in section 5 8 The only differences are that the changes in the energy levels would be larger than those of the mono substituted complexes

## 5.7 Laser Flash Photolysis of *cis*-DiPyDiPP(M(CO)<sub>5</sub>)<sub>2</sub> complexes (M = Cr or W)

### 5.7.1 Laser flash photolysis of *cis*-DiPyDiPP(W(CO)<sub>5</sub>)<sub>2</sub> at 532 nm under 1 atmosphere of CO

The transient absorption spectrum of *cis*-DiPyDiPP(W(CO)<sub>5</sub>)<sub>2</sub> (Figure 5.11) was measured in the 430 to 800 nm range, and was found to have similar characteristics to those assigned to the <sup>3</sup>( $\pi$ - $\pi^*$ ) excited state relaxation of the uncomplexed free base porphyrin. Similarly to the uncomplexed free porphyrin *cis*-DiPyDiPP(W(CO)<sub>5</sub>)<sub>2</sub> absorbs strongly between 440 nm and 490 nm, with a maximum at approximately 450 nm. Both systems contributed bleaching at *ca.* 520 nm and less intense transient absorption in the Q-band region. The difference spectrum of the complex rises sharply to a maximum peak while the uncomplexed free base porphyrin increases gradually to a maximum before decreasing in intensity slowly (see Figure 5.19).

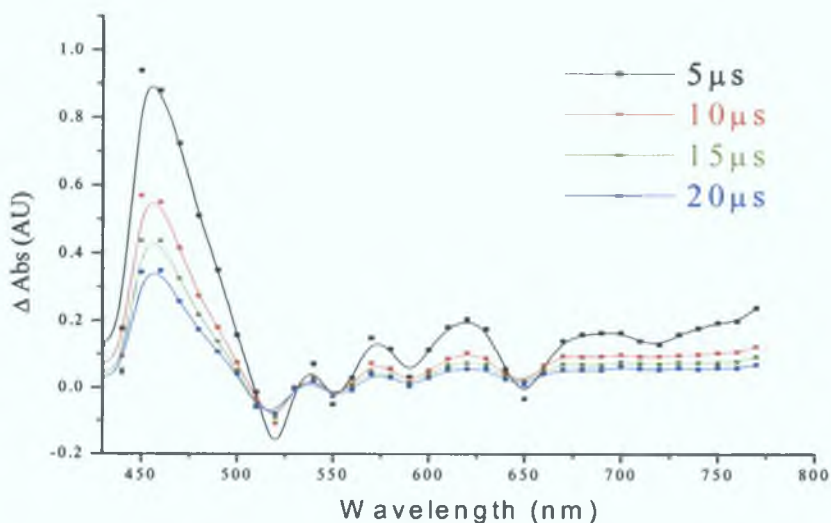


**Figure 5.11** Transient absorption spectrum of *cis*-DiPyDiPP(W(CO)<sub>5</sub>)<sub>2</sub> at  $\lambda_{exc} = 532$  nm under 1 atmosphere of CO in dichloromethane at 293 K

When the transient absorption spectrum of *cis*-DiPyDiPP is directly compared to the transient absorption spectrum of *cis*-DiPyDiPP(W(CO)<sub>5</sub>)<sub>2</sub> in the 450 – 530 nm region,

there is little evidence that complexation has changed the triplet excited state profile of the system (see Figure 5.12). The samples used in this experiment had identical absorbance at the excitation wavelength. The maximum of the complexed porphyrin does occur at approximately 10 nm lower in energy than the free base porphyrin. This was also the case for the mono substituted derivatives.

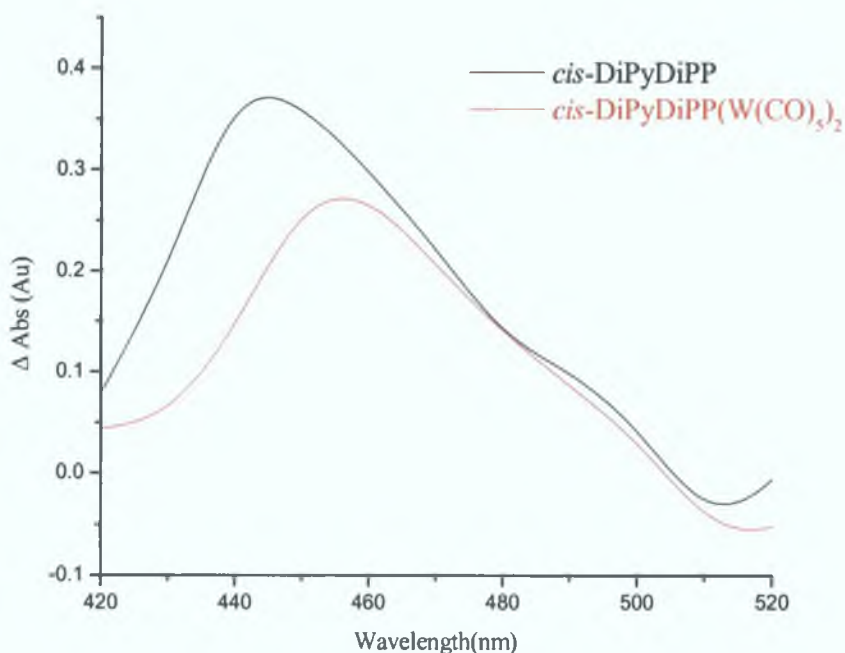


**Figure 5.12** Transient absorption spectrum of solutions of *cis*-DiPyDiPP and *cis*-DiPyDiPP(W(CO)<sub>5</sub>)<sub>2</sub> with identical absorbance at  $\lambda_{exc} = 532 \text{ nm}$  at 293 K

The heavy atom effect can be ruled out, as this would have a dramatic effect on the lifetime of the triplet state, the intensity of the signals and profile of the transient absorption spectrum, despite the fact that S → T formation is 90% for tetra aryl porphyrins.<sup>27</sup> The lifetime of both the tungsten complex and the uncomplexed free base porphyrins are similar (see Table 5.6) and the intensity of the transient signals are marginally different (see Figure 5.13). This suggests that coordination of the metal moiety to the porphyrin chromophore has no effect on the triplet state properties. Given that the fluorescence measurements were changed so dramatically and the triplet state

measurements are similar, loss of the metal moiety from the singlet excited state would seem a logical explanation to the similarities between the triplet characteristics of the free base porphyrin and the complexed analogue. Scheme 3.2 (Section 3.8) has been used to explain the possible cause of this in the mono substituted derivatives and the same reasoning could apply for the disubstituted analogues (see Figure 5.20, section 5.8).

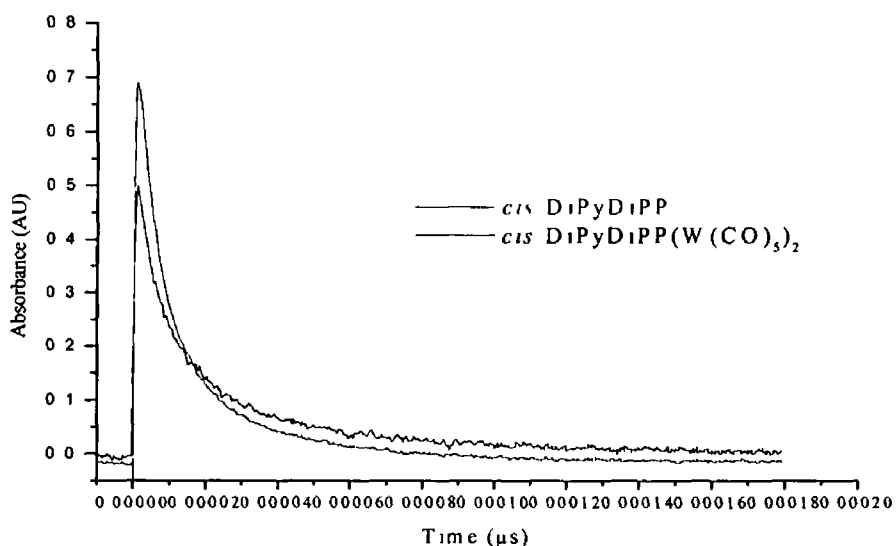


**Figure 5.13** Transient signals obtained at 490 nm following excitation of *cis*-DiPyDiPP and *cis*-DiPyDiPP(W(CO)<sub>5</sub>)<sub>2</sub>  $\lambda_{exc} = 532\text{nm}$  in dichloromethane solution at 293 K

As for all porphyrins the triplet state decays with mixed first/second order kinetics (Figure 5.13), this is attributed to competition between unimolecular decay and triplet-triplet annihilation processes and is typical for all porphyrins.<sup>6</sup> The lifetime obtained for the free base porphyrin, *cis*-DiPyDiPP is in good agreement for those obtained for tetra aryl free base porphyrins in the literature.<sup>8</sup> The lifetime of *cis*-DiPyDiPP(W(CO)<sub>5</sub>)<sub>2</sub> was also found to be in the range of the tetra aryl free base porphyrin (see Table 5.6). This indicates that the metal units had no influence over the triplet state of the porphyrin even though there are two units present.

**Table 5 6**

| 450 nm                                                                           |                      |                   |
|----------------------------------------------------------------------------------|----------------------|-------------------|
| <i>Porphyrin</i>                                                                 | $\tau_{trip}(\mu s)$ | $k_{obs}(s^{-1})$ |
| <i>cis</i> -D <sub>1</sub> PyD <sub>1</sub> PP                                   | 30                   | 32748 ± 3275      |
| <i>cis</i> -D <sub>1</sub> PyD <sub>1</sub> PP(W(CO) <sub>5</sub> ) <sub>2</sub> | 26                   | 37989 ± 3799      |

An IR spectrum of the photolysed solution indicated the formation of a band at 1981  $cm^{-1}$  which is assigned as  $W(CO)_6$ . Once more the pentacarbonyl bands of the complex had are joined by the hexacarbonyl peak (see Figure 5 14). These changes have been attributed to the formation of the singlet excited state of the porphyrin pentacarbonyl complex which leads to cleavage of the N-M bond

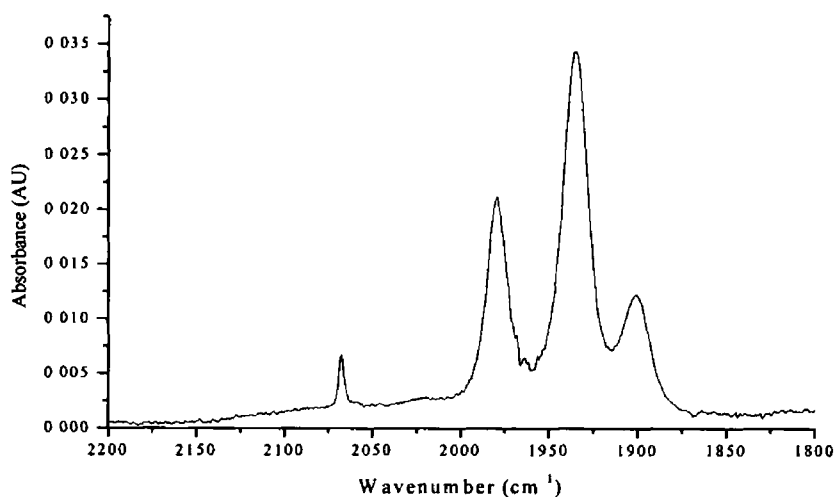


**Figure 5.14 IR spectrum of *cis*-D<sub>1</sub>PyD<sub>1</sub>PP(W(CO)<sub>5</sub>)<sub>2</sub> after laser flash photolysis ( $\lambda_{exc} = 532\text{ nm}$ ) in dichloromethane under 1 atmosphere of CO**

### 5.7.2 Laser flash photolysis of *cis*-DiPyDiPP(Cr(CO)<sub>5</sub>)<sub>2</sub> at 532 nm under 1 atmosphere of CO

The transient absorption spectrum of *cis*-DiPyDiPP(Cr(CO)<sub>5</sub>)<sub>2</sub> (Figure 3.19) was recorded between 430 nm and 800 nm and as was found with *cis*-DiPyDiPP(W(CO)<sub>5</sub>)<sub>2</sub> had similar characteristics of the <sup>3</sup>( $\pi$ - $\pi^*$ ) excited states of the uncomplexed free base porphyrin. Both the free base porphyrin and *cis*-DiPyDiPP(Cr(CO)<sub>5</sub>)<sub>2</sub> absorbs strongly between 440 and 490 nm with the maxima again at  $\sim$  440-460 nm. *cis*-DiPyDiPP(Cr(CO)<sub>5</sub>)<sub>2</sub> showed bleaching at 520 nm and less intense absorption in the Q-band region which is typical of tetra aryl porphyrins such as *cis*-DiPyDiPP. The difference spectrum of the complex has a rises sharply to maximum peak while the uncomplexed free base porphyrin increases gradually to a maximum before decreasing in intensity slowly.

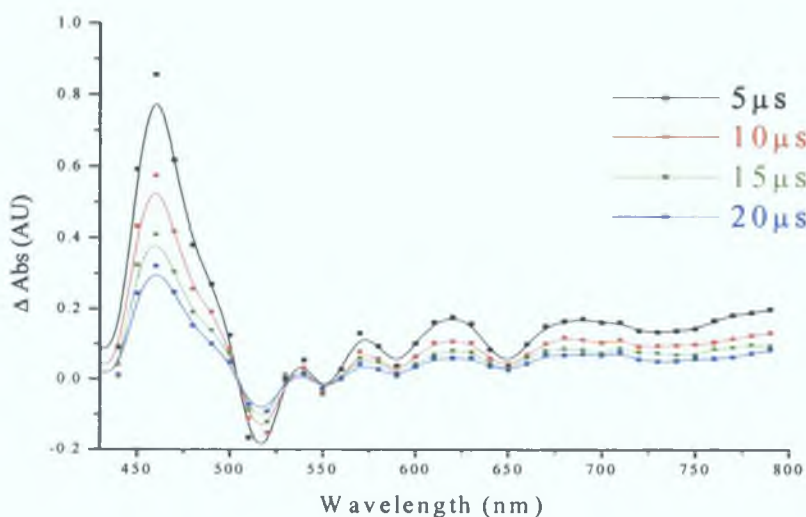


**Figure 5.15** Transient absorption spectrum of *cis*-DiPyDiPP(Cr(CO)<sub>5</sub>)<sub>2</sub> at  $\lambda_{exc} = 532$  nm under 1 atmosphere of CO in dichloromethane at 293 K

The transient absorbance spectrum of the disubstituted Cr(CO)<sub>5</sub> porphyrin is typical of a transient absorption spectrum of a tetra aryl free base porphyrin and there is little difference between the spectrum of uncomplexed *cis*-DiPyDiPP and the complexed

porphyrin. A direct comparison was made between the transient absorption spectrum of the uncomplexed porphyrin and the pentacarbonyl complex (see Figure 5.16) in the region 450 to 530 nm. The samples had identical absorbance at the excitation wavelength yet the profile of both spectra was noticeably similar apart from a red shift of 10 nm in the  $\lambda_{\text{max}}$  of the complex compared to the free base porphyrin. This was also the case for the mono substituted  $\text{Cr}(\text{CO})_5$  complex. The zinc derivative has a maxima at  $\sim 460$  nm which is a shorter wavelength maximum than that of free base porphyrins.

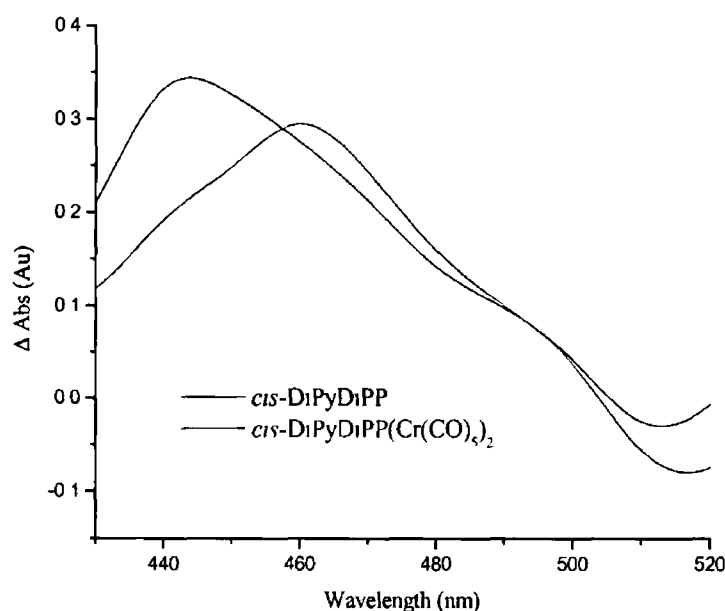


**Figure 5.16** Transient absorption spectrum of solutions of *cis*-DiPyDiPP and *cis*-DiPyDiPP( $\text{W}(\text{CO})_5$ )<sub>2</sub> with identical absorbance at  $\lambda_{\text{exc}} = 532$  nm at 293 K

Once again the fact that there is no great change in the spectrum of the complex compared to the free base porphyrin suggests that the coordination of the metal pentacarbonyl units to the porphyrin has no effect on the triplet state. As mentioned for the W analogue, the changes observed for the fluorescence work and the reduction in lifetimes of the singlet excited state suggest that the N-M bond could be cleaved before the triplet excited state is formed.

Lifetime measurements for the Cr pentacarbonyl porphyrin complex and the uncomplexed porphyrin were recorded at 450 nm using samples with the same absorbance at the excitation wavelength, 532 nm. The transient signals for both are slightly different (see Figure 5.17) but have lifetimes, which occur, in the same region providing further evidence that the pentacarbonyl moiety does not affect the triplet excited state of the porphyrin. Previously it was thought that a metal coordinated to a porphyrin would induce the heavy atom effect. Given that Cr is not a heavy atom this can be ruled out.

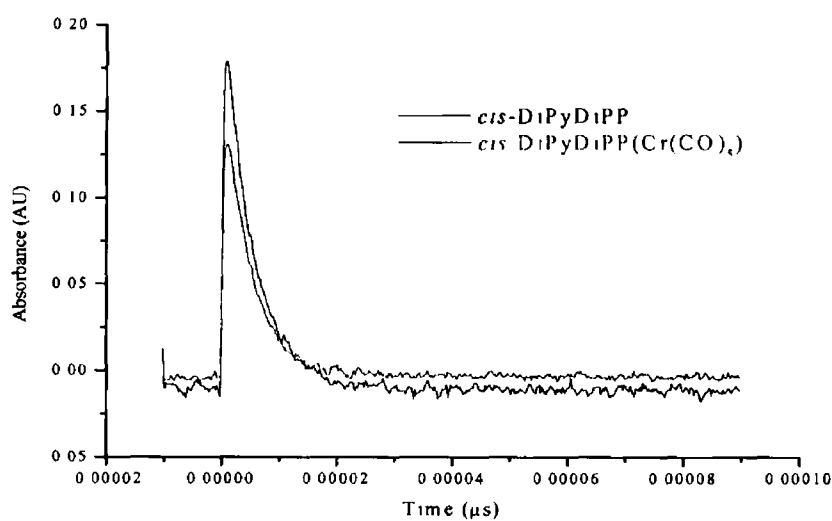
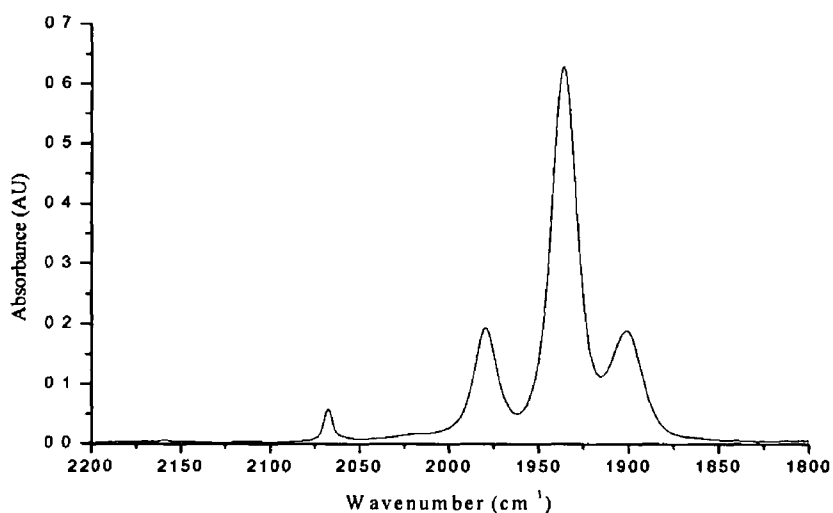


**Figure 5.17** Transient signals obtained at 490 nm following excitation of *cis*-DiPyDiPP and *cis*-DiPyDiPP(Cr(CO)<sub>5</sub>)<sub>2</sub> at  $\lambda_{exc} = 532\text{nm}$  in dichloromethane solution at 293 K

The triplet state decays with mixed first/second order kinetics (Figure 3.21). As previously stated this is attributed to competition between unimolecular decay and triplet-triplet annihilation processes and is typical for all porphyrins.<sup>6</sup>

**Table 5.7**

| Porphyrin                 | 450 nm                     |                   |
|---------------------------|----------------------------|-------------------|
|                           | $\tau_{trip}(\mu\text{s})$ | $k_{obs}(s^{-1})$ |
| MPyTPP                    | 30                         | $32748 \pm 3275$  |
| MPyTPPCr(CO) <sub>5</sub> | 27                         | $36797 \pm 3680$  |



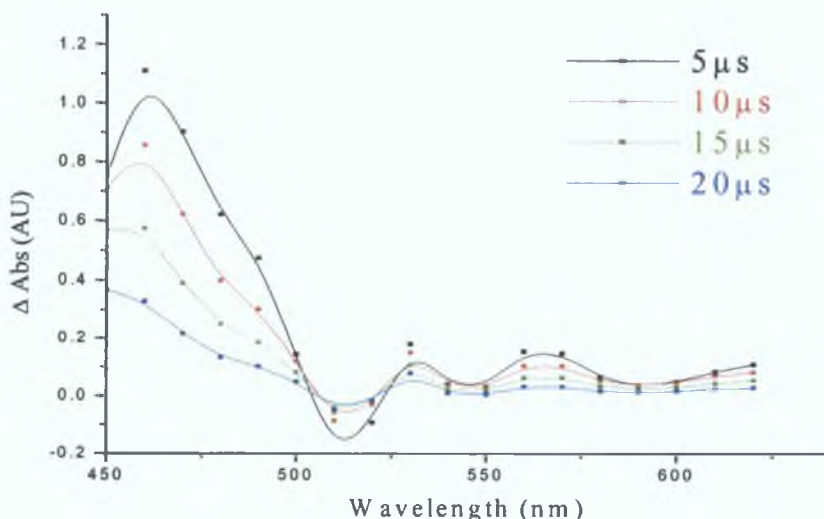
**Figure 5.18 IR spectrum of *cis*-D<sub>1</sub>PyD<sub>1</sub>PP(Cr(CO)<sub>5</sub>)<sub>2</sub> after laser flash photolysis ( $\lambda_{exc} = 532$  nm) in dichloromethane under 1 atmosphere of CO**

Figure 5 18 shows the IR spectrum of *cis*-D<sub>1</sub>PyD<sub>1</sub>PP(Cr(CO)<sub>5</sub>)<sub>2</sub> measured after the transient absorption spectrum had been obtained. As the N-Cr bond was cleaved and a grow in due to the formation of Cr(CO)<sub>6</sub> is seen at 1980 cm<sup>-1</sup>. It is undoubtedly the case that irradiation at 532 nm of the *cis*-D<sub>1</sub>PyD<sub>1</sub>PP(Cr(CO)<sub>5</sub>)<sub>2</sub> complex in the presence of CO produces the Cr(CO)<sub>6</sub> species.

### 5.7.3 Discussion of results

Laser flash photolysis was carried out on the uncomplexed free base aryl porphyrin (*cis*-DiPyDiPP) and its metal carbonyl complexes (*cis*-DiPyDiPP(M(CO)<sub>5</sub>)<sub>2</sub> where M = W or Cr) in deoxygenated dichloromethane under one atmosphere of CO. The solutions were degassed using the freeze pump thaw method. All the transient absorption difference spectra were recorded using pulsed laser excitation at 532 nm.

The time-resolved absorbance of the triplet state of a typical tetraphenyl or tetrapyrrolyl porphyrins have a lifetime of *ca.* 30  $\mu$ s at room temperature.<sup>6</sup> Free base porphyrins exhibit strong transient signals from 430 nm to 480 nm and there is also bleaching at 520 nm with less intense absorption in the Q-band region extending into the IR region. The transient signals obtained were typical of <sup>3</sup>( $\pi$ - $\pi^*$ ) excited states of aryl porphyrins (see Figure 5.19).<sup>28,29</sup> Like all free base porphyrins the triplet excited state was efficiently quenched by the addition of O<sub>2</sub>.



**Figure 5.19** Transient absorption spectrum of *cis*-DiPyDiPP at  $\lambda_{exc} = 532$  nm under 1 atmosphere of CO in dichloromethane at 293 K

Two metal carbonyl moieties were attached to the porphyrin *via* pyridyl linkers in a method described in see Section 6.6. These disubstituted systems were chosen to investigate the efficiency at which electron transfer or energy transfer process can occur across orthogonal  $\pi$ -substituents on the *meso* position of the porphyrin for comparison with the mono substituted free base porphyrin analogues.

The UV-vis spectrum of  $M(CO)_5(C_5H_5N)$  has been discussed previously and it was shown that this compound has no significant absorbances at wavelengths longer than 420 nm.<sup>30</sup> Therefore any excitation of the complex above 420 nm would populate triplet excited state associated with the porphyrin only. This is shown in the transient absorption difference spectra in Figure 5.11 and 5.15. The formation of a new band in the UV-vis spectrum at 290 nm represents the formation of  $M(CO)_6$ . This was confirmed by IR analysis of the sample after photolysis was complete (see Figure 5.18).

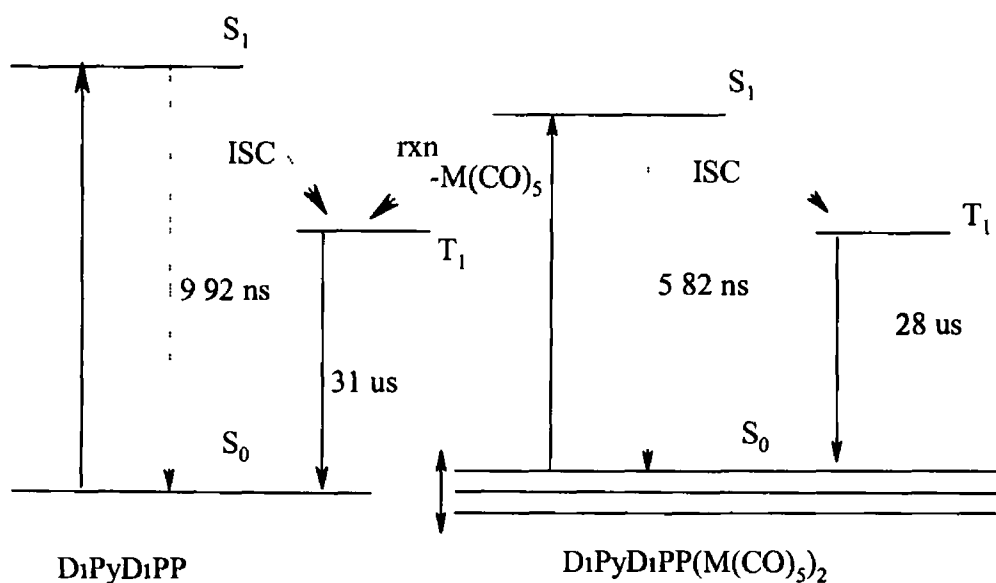


**Figure 5.20. Schematic representation of the deactivation pathway from  $DiPyDiPP(M(CO)_5)_2$  singlet excited state. ( $\lambda_{exc} = 532$  nm)**

Based on evidence from the *mono* substituted and zinc analogues in chapter 3 and 4 a figure representing the deactivation pathway from the singlet excited state was proposed (see Figure 5.20). As the electronic communication is like that observed in chapter three

and four a diagram based on Figure 3 26, Chapter 3 and Figure 4 27 Chapter 4 is presented here. The theories put forward in the previous chapters can be used again to explain the results for the *di* substituted complexes. In Figure 5 20 the *cis* complexes are not treated as a supramolecular molecule but the components of the molecule act on their own. In the ground state absorbance spectra of the porphyrin complexes the complexes are shifted to lower energy compared to the uncomplexed porphyrin. The reduction in singlet lifetime can be explained by the formation of a lower energy singlet state of the complex relative to the singlet state of the free base porphyrin. This can be clarified by the red shift of the emission spectra and ground state spectra of the complexes relative to the uncomplexed chromophore. In the triplet excited state there are no changes related to population of a complex based triplet excited state, the lifetimes are very similar for both the free base porphyrin and the metal complexes.

This shows that upon formation of the singlet excited state of the complexes the carbonyl moiety is lost and the triplet state of the free base porphyrin is formed. The spin forbidden process of singlet to triplet intersystem crossing is the predominant route for radiationless deactivation of  $S_1$  in porphyrins with  $S \rightarrow T$  formation about 90%<sup>12</sup>. With little room for increase in triplet formation it is unlikely that the metal fragment affects the triplet state of the complex greatly. This would make it difficult to observe any reduction or increase in intensity of the transient absorption spectra. The pyridine and phenyl rings of the porphyrin are twisted out of the molecular plane so that they are isolated from the conjugated system of the macro ring (see Figure 5 1). Therefore the interaction of the metal entity and the porphyrin are not as strong as would be expected but the presence of two of these units does enhance the effects.

## 5.8 Conclusion

*Cis*-D<sub>1</sub>PyD<sub>1</sub>PP, *cis*-D<sub>1</sub>PyD<sub>1</sub>PP(W(CO)<sub>5</sub>)<sub>2</sub> and *cis*-D<sub>1</sub>PyD<sub>1</sub>PP(Cr(CO)<sub>5</sub>)<sub>2</sub> were prepared as discussed in chapter six. The metal complexes were used to investigate the electronic properties of the porphyrin and to compare these with the free base porphyrin and the *mono* substituted species discussed in chapter three. The techniques used were similar to those used previously such as photophysical (emission spectra and singlet lifetimes) and photochemical (time resolved and steady state spectroscopy).

The UV-vis spectra of the complexes were shifted to lower energy by 2 - 6 nm compared to the free base porphyrin. The increased red shift is due to the presence of the two metals at the periphery of the porphyrin and the net removal of electron density from the porphyrin  $\pi$  system upon metal-pyridine bond formation.<sup>26</sup> For both complexes laser flash photolysis resulted in the loss of the M(CO)<sub>5</sub> moiety from the porphyrin macrocycle. This was confirmed by the IR and UV-vis spectra obtained following photolysis experiments (see Section 5.7). As photolysis was carried out at  $\lambda > 500$  or  $> 400$  nm the porphyrin chromophore was the dominant absorbing species. Therefore there is the same electronic communication between the chromophore and the metal moiety as discussed for the *mono* substituted complex and the zinc analogue.

As with the previous systems the interaction of the metal moiety and the porphyrin only appears to take place in the singlet state. There is a shift in the transient absorption maxima for the two complexes when compared to the free base porphyrin but the lifetimes remain in the same region. Without any real change in the lifetimes of the triplet excited state of the porphyrin complexes compared to the free base porphyrin it was concluded that the metal moiety did not affect the electronic make up of the porphyrin in the triplet state. In the singlet excited state, lifetimes are reduced by almost 50% showing that the metal moiety had a substantial effect on the porphyrin. Therefore like the complexes discussed in previous chapters the results would indicate that the electronic communication takes place in the singlet excited state of the complexes.

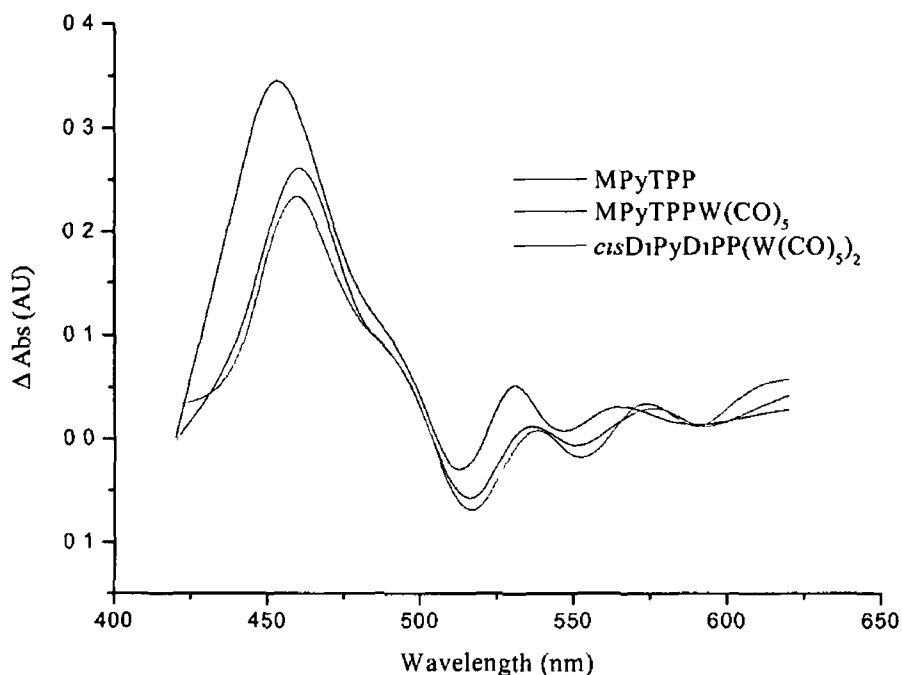


**Figure 5.21 Comparison of the transient absorption spectrum of MPyTPP, MPyTPPW(CO)<sub>5</sub> and cis-DiPyDiPP(W(CO)<sub>5</sub>)<sub>2</sub> after 20 μs**

An overlap of the transient absorption spectra of MPyTPP, MPyTPPW(CO)<sub>5</sub> and cis-DiPyDiPP(W(CO)<sub>5</sub>)<sub>2</sub> are given in Figure 5.21. The differences between the triplet excited state of the three compounds is shown and confirms the slight differences between the complexes and the free base porphyrin in the triplet state. The shift of ~ 10 nm is obvious from this spectrum as is the reduction in intensity.

## 5.9 Bibliography

---

- 1 N Aratani, A Osuka, H S Cho, D Kim, *J of Photochem And Photobiol , C Photochem Rev* , **2002**, 3, 25
- 2 G Dermott, S M Prince, A A Freer, A M Hawthornwaite-Lawless, M Z Papiz, R J Cogdell, N W Isaacs, *Nature*, **1995**, 374, 517.
- 3 M R Wasielewski, *Chem Rev* **1992**, 92,435
- 4 H E Toma, K Araki, *J Photochem Photobiol A Chem* , **1994**, 83, 245
- 5 A Prodi, M T Indelli, C, J, Cornelis, J Kleverlaan, E Alessio, F Scandola, *Coord Chem Rev* , **2002**, 229, 51
- 6 K Kalyanasundaram, *Photochemistry of Polypyridyl and Porphyrin Complexes*, Academic Press, London, 1992
- 7 E B Fleicher, A M Shachter, *Inorg Chem* , **1991**, 30, 3763
- 8 K Kalyanasundaram, *Inorg Chem* , **1984**, 23, 2453
- 9 H E Toma, K Araki, *J Photochem Photobiol , A*, **1994**, 83, 245
- 10 H Yaun, L Thomas, L K Woo, *Inorg Chem* , **1996**, 35, 2808
- 11 J B Kim, J J Leonard, F R Longo, *J Am Chem Soc* , **1972**, 94, 3986
- 12 D J Quimby, F R Longo, *J Am Chem Soc* , **1975**, 97, 5111
- 13 P Glyn, F P A Johnson, M W George, A J Lees, J J Turner, *Inorg Chem* , **1991**, 30, 3543
- 14 R M Kolodziej, A J Lees, *Organometallics*, **1986**, 5, 450
- 15 E B Fleicher, A M Shachter, *Inorg Chem* , **1991**, 30, 3763
- 16 L T Cheng, W Tam, D F Eaton, *Organometallics*, **1990**, 9, 2856
- 17 N M Rowley, S S Kurek, P R Ashton, T A Hamor, C J Jones, N Spencer, J A McCleverty, G S Beddard, T E Feehan, N T H White, E J L McInnes, N N Paynes, L J Yellowlees, *Inorg Chem* , **1996**, 35, 7526
- 18 C J Aspley, J R Lindsay Smith, R N Perutz, D Pursche, *J Chem Soc , Dalton Trans* , **2002**, 170
- 19 A Prodi, C J Kleverlaan, M T Indelli, F Scandola, E Alessio, E Iengo, *Inorg Chem* , **2001**, 40, 3498

- 
- 20 C M Drain, F Nifiatis, A Vasenko, J D Batteas, *Angew Chem Int Ed* , **1998**, 37, 2344
- 21 A Prodi, M T Indelli, C J Kleverlaan, F Scandola, E Alessio, T Gianferrara, L G Marzilli, *Chem Eur J* , **1999**, 5, 2668
- 22 F M Engelmann, P Losco, H Winnischofer, K Araki, H E Toma, *J Porph and Phthalo* , **2002**, 6, 33
- 23 B Steiger, C Shi, F C Anson, *Inorg Chem* , **1993**, 32, 2107
- 24 J M Zaleski, C K Chang, G E Leroi, R I Cukier D G Nocera, *J Am Chem Soc* , **1992**, 114, 3564
- 25 C M Drain, J M Lehn, *J Chem Soc Chem Commun* , **1994**, 2313
- 26 R V Slone, J T Hupp, *Inorg Chem* , **1997**, 36, 5422
- 27 D J Quimby, F R Longo, *J Am Chem Soc* , **1975**, 97, 5111
- 28 M Linke, N Fujita, J C Chambron, V Heitz, J P Sauvage, *New J Chem* , **2001**, 25, 790
- 29 H Shiratori, T Ono, K Nozaki, A Osuka, *Chem Commun* , **1999**, 2181
- 30 M S Wrighton, H B Abrahamson, D L Morse, *J Am Chem Soc* , **1976**, 98, 4105

## **Chapter 6**

### **Experimental**

## 6.1 Reagents

All solvents used in laser flash photolysis and steady state photolysis experiments were of spectroscopic grade (Aldrich Chemical Company) and these solvents included dichloromethane, toluene and cyclohexane (all were used without further purification )

Tetrahydrofuran (THF) was dried over sodium metal using benzophenone as an indicator, prior to use

All gases used (Argon and CO) were supplied by Air products and IIG respectively

All organic synthetic reagents were of commercial grade and used without further purification unless otherwise stated

Pyrolle (Aldrich Chemical Company) was distilled over KOH under reduced pressure. It was stored over KOH under Argon and kept in the fridge at 4 °C

The hexacarbonyls,  $W(CO)_6$  and  $Cr(CO)_6$  (Aldrich Chemical Company) were used without further purification

Silica Gel used for column chromatography was used as received. All solvents used for chromatography were bench top solvents and dried using  $MgSO_4$

## **6.2 Equipment**

### **6.2.1 Infrared spectroscopy**

Infrared spectra were carried out on a Perkin Elmer 2000 FT-IR spectrometer using 0.1 mm sodium chloride liquid solution cells

### **6.2.2 Absorption spectroscopy**

UV-vis spectra were recorded on a Hewlett Packard 8452A photodiode Array spectrometer. Samples were held in a 1 cm pathlength quartz cell.

### **6.2.3 Nuclear Magnetic Resonance spectroscopy**

<sup>1</sup>H NMR spectroscopy was the main tool used in the identification of compounds throughout this thesis.

All <sup>1</sup>H (400 MHz) experiments were recorded on a Bruker Avance AC 400 NMR spectrometer and the free induction decay (FID) profiles processed using a XWIN-NMR software package. All measurements for both the ligands and the pentacarbonyl complexes were carried out in CD<sub>3</sub>Cl. Peak positions are relative to the residual peak position or TMS.

### **6.2.4 Emission spectroscopy**

Emission spectra were obtained at room temperature using a Perkin-Elmer LS50 or LS50-B luminescence spectrophotometer equipped with a red sensitive Hamamatsu R928 detector, interfaced to an Elonex PC466 personal computer employing Perkin-Elmer FL WinLab custom built software. Emission and excitation slit widths of 10 nm were used for all the measurements. The spectra were corrected for the photomultiplier response.

Emission quantum yield measurements were carried out by using the optically dilute method<sup>1</sup>. The quantum yield of each complex is determined relative to the uncomplexed porphyrin. Emission spectra were obtained at a wavelength where the absorbance of the uncomplexed porphyrin and the pentacarbonyl complexes being examined were identical. The area under the emission spectrum of each sample was calculated using the spectrometer software supplied and the quantum yield was calculated using Equation 3.4. All measurements were carried out in dichloromethane.

**Equation 3.4**

$$\frac{\Phi_c}{\Phi_L} = \frac{A_L I_c}{A_c I_L}$$

### 6.3 Determination of extinction coefficients

Extinction coefficients were calculated for each compound at the laser excitation wavelength (532 nm). These values were used to determine the concentration of the samples. Using the Beer-Lambert law (see equation 6.1) and knowing the absorbance at a particular wavelength, the concentration of the sample can be determined. The Beer-Lambert law is given by the equation

#### *Equation 6.1*

$$A = \epsilon cl$$

Where  $A$  = absorbance at a particular wavelength

$c$  = concentration of sample ( $\text{moles dm}^{-3}$ )

$l$  = pathlength of cell (1 cm)

$\epsilon$  = molar extinction coefficient of the sample ( $\text{dm}^3 \text{ moles cm}^{-1}$ )

#### 6.4 Time Correlated Single Photon counting (TCSPC) techniques – nanosecond time resolved emission spectroscopy

All singlet state lifetimes measurements were obtained using TCSPC (an Edinburgh Instruments nf900 ns flashlamp and CD900 time to amplitude converter (TAC)) Lifetimes were measured using spectroscopic grade solvents Samples were degassed by three cycles of the freeze thaw procedure to  $10^{-2}$  torr using specially designed degassing bulb attached to a fluorescence cell Deconvolution of the lamp profile was carried out for each sample, as emission lifetimes were  $< 11$  ns The lamp profile was obtained using a colloidal suspension of silica in water as a scattering agent

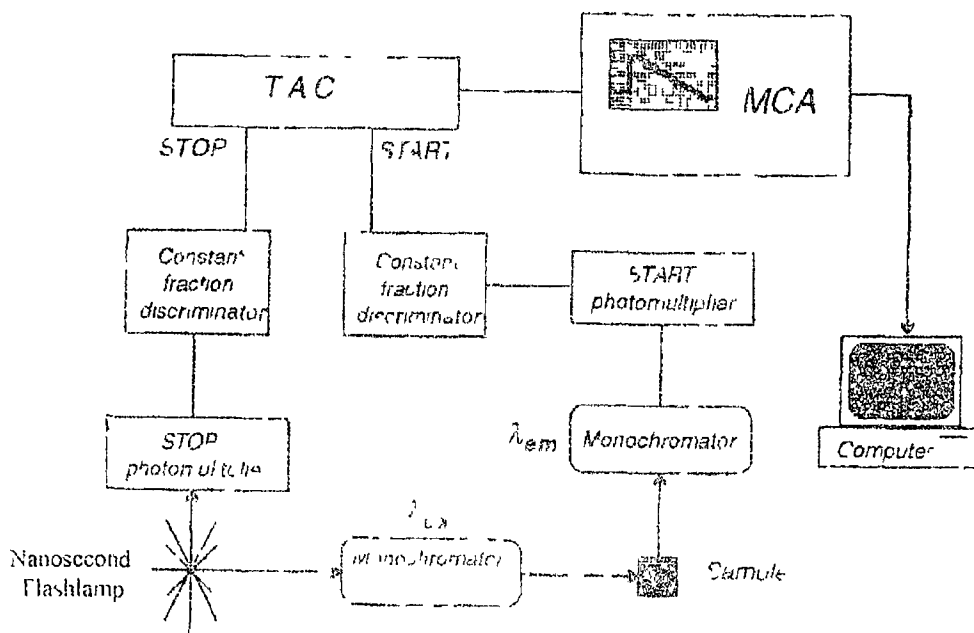


Figure 6.1 A schematic diagram of the TCSPC apparatus

When the Start photomultiplier detects a photon of emitted light it triggers the TAC to initiate a voltage ramp. The ramp is halted when the STOP photomultiplier detects a photon from the reference beam (i.e. the nanosecond flashlamp pulse). The multi channel analyser (MCA) records the number of times a specific voltage is obtained depending on the settings used. A spectrum of voltages, and hence time differences, is produced by the

MCA memory and the experiment is terminated when a sufficient number of counts are collected (typically 1000 in the peak channel) The spectrum of voltages is directly related to the emission decay allowing for the measurement of the emission The quality of the lifetime data obtained is judged primarily by two criteria the  $\chi^2$ , and the random nature of the residuals plot A  $\chi^2$  as close to one but not below it is ideal

## **6 5 Laser flash photolysis**

### **6 5.1 Preparation of degassed samples for laser flash photolysis**

Samples were prepared in a specially designed degassing bulb attached to a fluorescence cell. This cell was cleaned thoroughly by steeping in base for 24 hours prior to use. All samples were prepared in the dark room to ensure decomposition did not take place. They were prepared using only spectroscopic grade solvent. Absorbance of the samples at the desired wavelength (532 nm) was between 0.65 and 1.0 AU. The samples were then degassed by three cycles of the freeze thaw procedure to  $10^{-2}$  torr. Liquid pump phase was then carried out to remove any trace impurities such as water if necessary.

An atmosphere of CO or argon was then placed over the sample to prevent boiling of the solvent or investigate different properties of the process. The pressure of CO admitted to the cell after degassing process determined the concentration of CO. The solubility of the CO in cyclohexane was taken to be  $9.0 \times 10^{-3}$  M under 1 atmosphere of CO. Spectral changes were monitored at regular intervals in the UV-vis or IR spectroscopy during the photolysis experiment.

### **6 5.2 Laser Flash Photolysis with UV-Vis Detector Apparatus**

The excitation source was a neodymium yttrium aluminium garnet (Nd-YAG) laser, which operates at 1064 nm. Nd atoms are implanted in the host YAG crystals of approximately one per hundred. The YAG host material has the advantage of having a relatively high thermal conductivity to remove the wasted heat, thus allowing these crystals to operate at high repetitions rates of the order of many pulses per second. The frequency can be doubled, tripled or quadrupled with non-linear optical techniques to generate a second, third or fourth-harmonic frequency at 532, 355 or 266 nm respectively. This allows certain atomic processes to be preferentially selected. The power of the laser can be amplified by applying different voltages across the amplifier flash tube. The pulse time is approximately 10 ns, the energy generated for 266, 355 and 532 nm frequencies is typically 25, 45 and 55 mJ per pulse respectively.

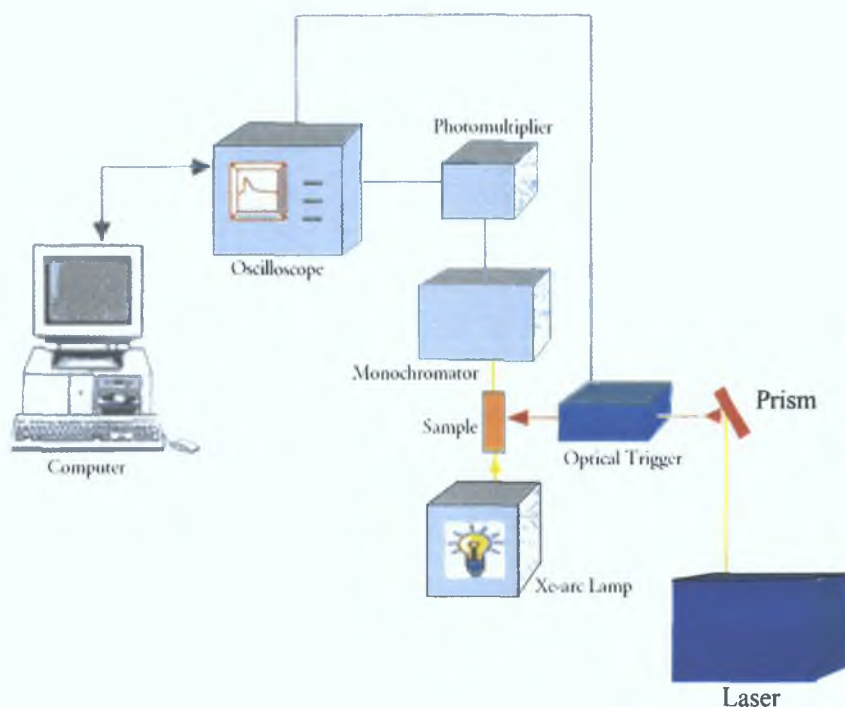


*Figure 6.2 A schematic diagram of the instrumentation used in the laser flash photolysis experiments*

The circular laser pulse is diverted *via* a Pellin Broca prism onto the sample cuvette. When the pulse passes through the power meter situated after the prism, but before the sample cuvette, the oscilloscope is triggered. The monitoring light source is an air-cooled 275-watt xenon arc lamp arranged at right angles to the laser beam. The monitoring beam passes through the sample and is directed to the entrance slit of an Applied Photophysics  $f/3$  monochromator *via* a circular lens. UV-vis filters were employed between monitoring source and sample to prevent excessive sample photo-degradation. A hamatsu 5 stage photomultiplier operating at 850 V was placed at the exit slit of the monochromator. The absorbance changes were measured by a transient digitiser (oscilloscope) *via* a variable load resistor. The digitiser, a Hewlett Packard HP 54510A oscilloscope was interfaced to a PC. All signals were recorded on floppy discs.

A typical transient signal was obtained as follows the amount of monitoring light being transmitted through the solution before the laser flash,  $I_0$ , is recorded initially This is the voltage corresponding to the amount of light detected by the photomultiplier tube when the source (Xe arc lamp) shutter opens, less the voltage generated by stray light When the monitoring source is opened while simultaneously firing the laser pulse through the sample cuvette and the amount of light transmitted through is recorded ( $I_t$ ) Since  $I_0/I_t =$  absorbance, the change in intensity of the probe beam transmitted is measured as a function of time and/or wavelength

By recording transient signals sequentially over a range of wavelengths, absorbance readings can be calculated at any time after the flash to generate a difference absorption spectrum of the transient species Spectra are obtained as a result of point by point build-up by optically changing the wavelength of the monochromator It is necessary that the solution is optically transparent for the monitoring light beam and hence solvents of spectroscopic transparency are required A schematic diagram of the laser flash photolysis instrumentation is presented in Figure 6 2

## 6.6 Structures of compounds synthesised in this study

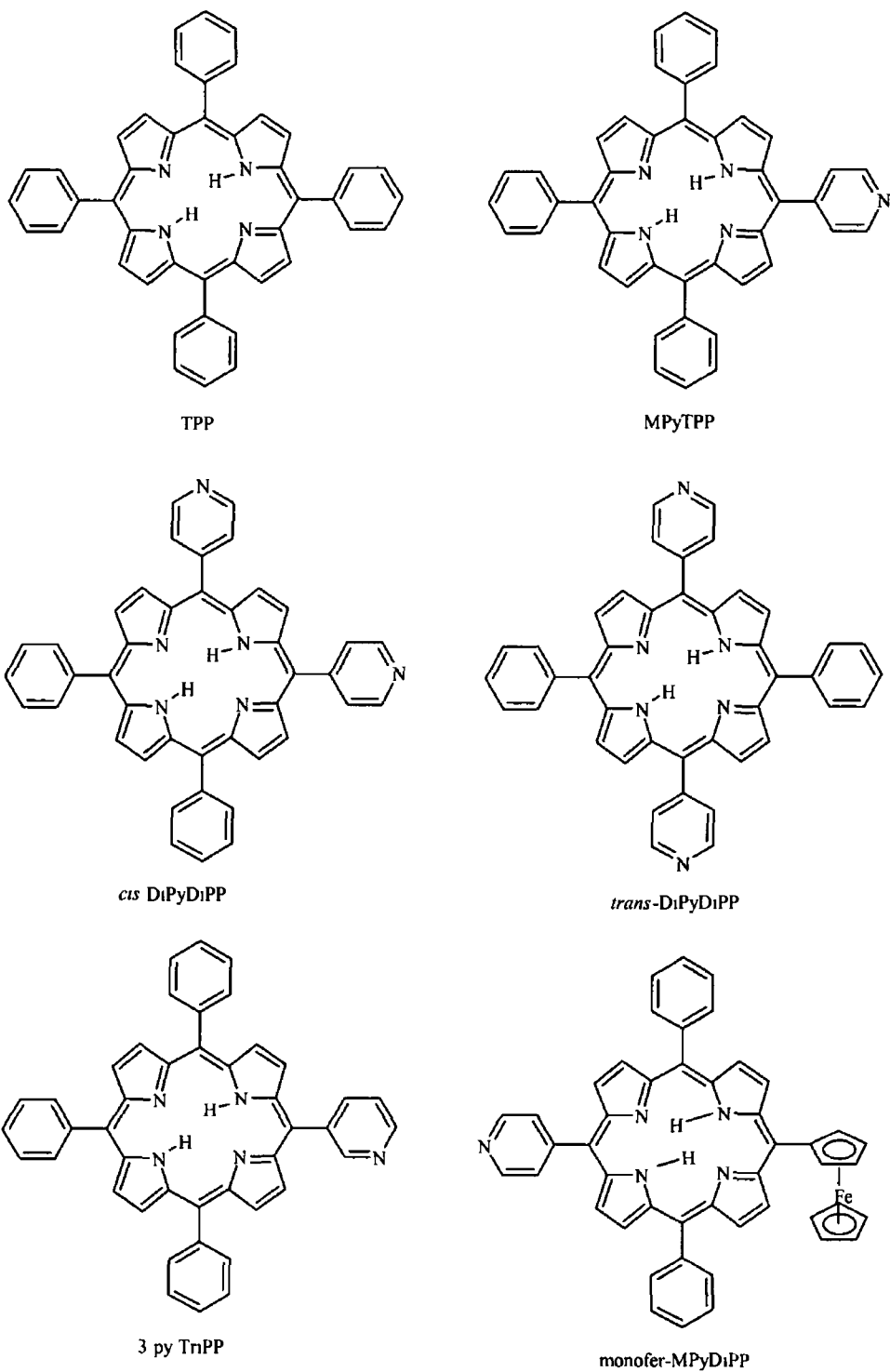
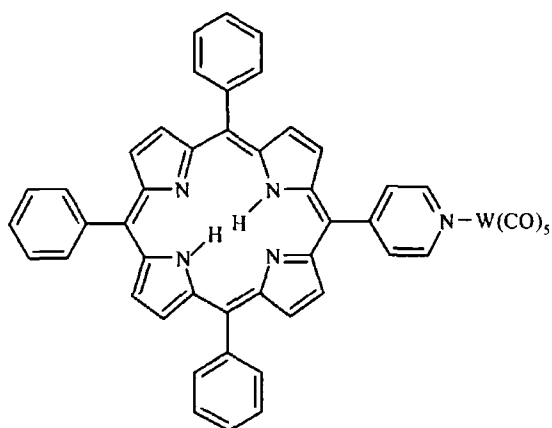
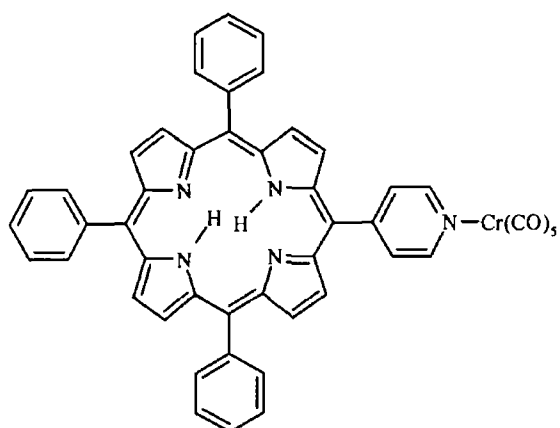


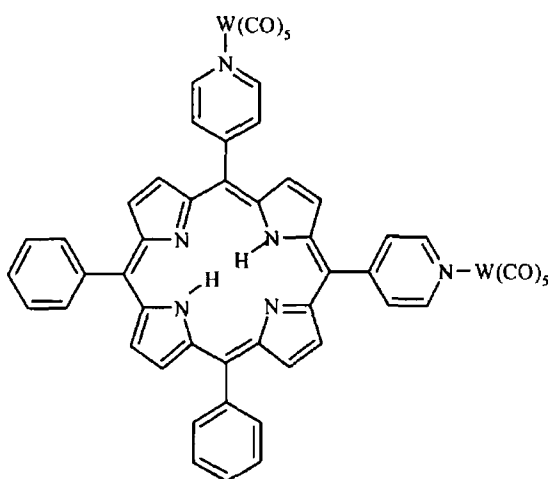
**Figure 6 3 Free base porphyrins ligands**



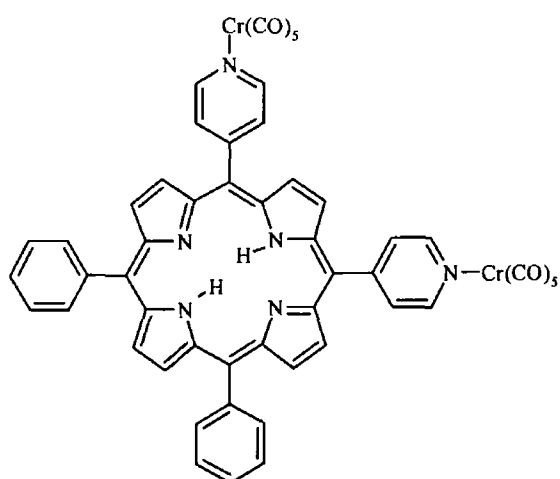
MPyTPPW(CO)<sub>5</sub>



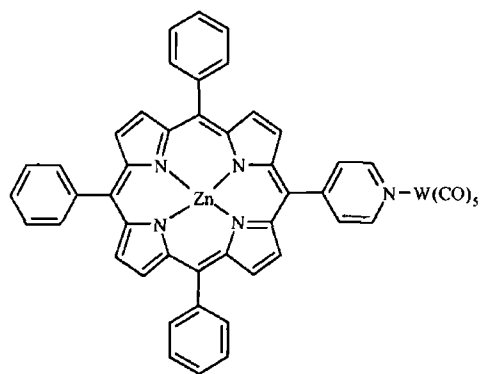
MPyTPPCr(CO)<sub>5</sub>



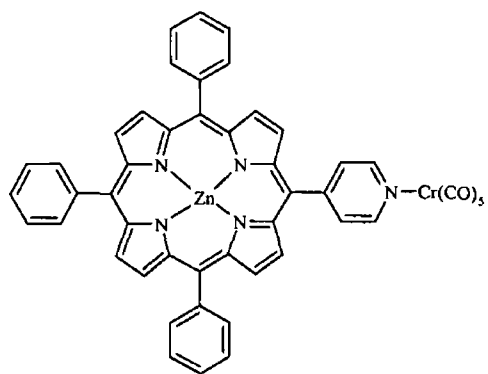
cis DiPyDiPP(W(CO)<sub>5</sub>)<sub>2</sub>



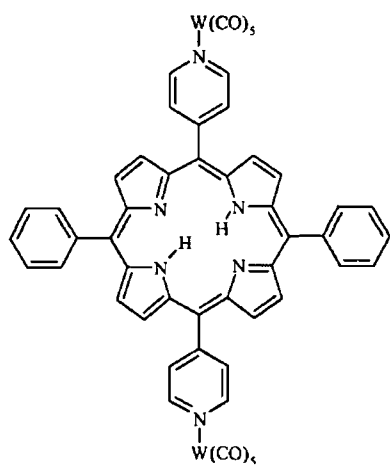
cis DiPyDiPP(Cr(CO)<sub>5</sub>)<sub>2</sub>



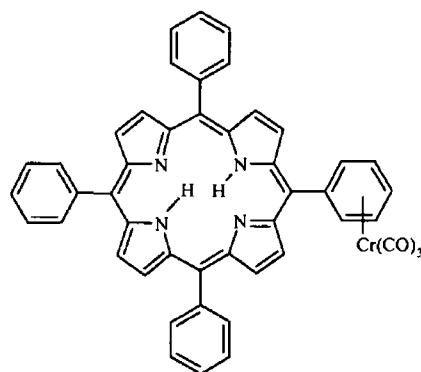
ZnMPyTPPW(CO)<sub>5</sub>



ZnMPyTPPCr(CO)<sub>5</sub>



trans DiPyDiPP(W(CO)<sub>5</sub>)<sub>2</sub>



TPPCr(CO)<sub>3</sub>

**Figure 6.4 Free base and metalloporphyrin complexes**

**Table 6.1**

| <b>Abbreviation</b>                                                               | <b>Full Name</b>                                                                      |
|-----------------------------------------------------------------------------------|---------------------------------------------------------------------------------------|
| TPP                                                                               | 5, 10, 15, 20-tetra phenyl porphyrin                                                  |
| MPyTPP                                                                            | 5-Mono 4-pyridyl 10, 15, 20-triphenyl porphyrin                                       |
| <i>cis</i> -D <sub>1</sub> PyD <sub>1</sub> PP                                    | 5,10 - <i>cis</i> 4 - Dipyridyl 15,20 - Diphenyl porphyrin                            |
| <i>trans</i> -D <sub>1</sub> PyD <sub>1</sub> PP                                  | 5,15 - <i>trans</i> 4 - Dipyridyl 10,20 - Diphenyl porphyrin                          |
| 3-Py-TriPP                                                                        | 5-Mono 4-pyridyl 10, 15, 20-triphenyl porphyrin                                       |
| Monofer-MPyD <sub>1</sub> PP                                                      | 5-Mono ferrocene 15-mono 4-pyridyl 10, 20-triphenyl porphyrin                         |
| MPyTPPW(CO) <sub>5</sub>                                                          | 5-Mono 4-pyridyl 10, 15, 20-triphenyl porphyrin tungsten pentacarbonyl                |
| MPyTPPCr(CO) <sub>5</sub>                                                         | 5-Mono 4-pyridyl 10, 15, 20-triphenyl porphyrin chromium pentacarbonyl                |
| <i>cis</i> -D <sub>1</sub> PyD <sub>1</sub> PP(W(CO) <sub>5</sub> ) <sub>2</sub>  | 5,10 - <i>cis</i> 4 - Dipyridyl 15,20 - Diphenyl porphyrin ditungsten pentacarbonyl   |
| <i>cis</i> -D <sub>1</sub> PyD <sub>1</sub> PP(Cr(CO) <sub>5</sub> ) <sub>2</sub> | 5, 10 - <i>cis</i> 4 - Dipyridyl 15, 20 - Diphenyl porphyrin dichromium pentacarbonyl |

| Abbreviation                                                                       | Full Name                                                                             |
|------------------------------------------------------------------------------------|---------------------------------------------------------------------------------------|
| ZnMPyTPPW(CO) <sub>5</sub>                                                         | 5-Mono 4-pyridyl 10, 15, 20-triphenyl porphyrinato zinc(II) tungsten pentacarbonyl    |
| ZnMPyTPPCr(CO) <sub>5</sub>                                                        | 5-Mono 4-pyridyl 10, 15, 20-triphenyl porphyrinato zinc(II) chromium pentacarbonyl    |
| <i>trans</i> -D <sub>1</sub> PyD <sub>1</sub> PP(W(CO) <sub>5</sub> ) <sub>2</sub> | 5, 15 - <i>trans</i> 4-Dipyridyl 10, 20 - Diphenyl porphyrin ditungsten pentacarbonyl |
| TPPCr(CO) <sub>3</sub>                                                             | 5, 10, 15, 20-tetra phenyl porphyrin chromium tricarbonyl                             |

While the synthesis of these compounds was carried out not all complexes were successfully isolated and characterised

## 6 6 1 Synthesis of free base tetra aryl porphyrins

All synthesis was carried out using conventional glassware under a nitrogen or argon atmosphere. All samples used for laser flash photolysis and steady state photolysis were degassed for 15 – 20 mins prior to measurements.

All free base porphyrins were synthesised by a method described by Alder *et al*<sup>2</sup>

7.0 mL (100 mmol) of freshly distilled pyrrole, 7.5 mL (74 mmol) of benzaldehyde and 5.0 mL (52 mmol) of 4-pyridine carboxaldehyde were added to 250 mL of 99% propionic acid and brought to reflux temperature. The acidic solution gradually turned black on addition of the reagents. The mixture was left at reflux temperature for 2 hrs, allowed to cool and left to stand overnight at room temperature. The black solution was filtered and the purple crystals formed were collected and washed several times with methanol to give a bright purple crystalline solid. This method typically gives a yield of 2.5 g (15%) of crude porphyrin.

TLC using chloroform/ethanol (98/2) indicated the presence of a mixture of six products which formed during the reaction. The six compounds formed were 5, 10, 15, 20-tetraphenylporphyrin (TPP), 5-pyridyl-10, 15, 20-triphenylporphyrin (MPyTPP), *cis*-5,10-dipyridyl-15,20-diphenylporphyrin (*cis*-DPyDPP), 5,15-dipyridyl-10, 20-diphenylporphyrin (*trans*-DPyDPP), 5,10,15-pyridyl-20-phenylporphyrin (TPyMPP) and 5,10,15,20-tetrapyrrolylporphyrin.

The crude porphyrin was purified on a silica gel column. The initial eluent was 98% chloroform and 2% ethanol which elutes the TPP. Subsequent columns of increasing polarity (chloroform/ethanol (97/3) and chloroform/ethanol (96/4)) separated out the remaining porphyrins.

### Porphyrin Spectroscopy.

**TPP** UV-vis spectrum [ $\lambda$ , nm, CH<sub>2</sub>Cl<sub>2</sub>] 418, 516, 550, 590, 648

$^1\text{H NMR}$  [400MHz  $\text{CDCl}_3$ ]  $\delta$  8.86 (8 H, m, pyrrole  $\beta$ ), 8.22 (8 H, m, o-phenyl), 7.77 (12 H m, m- and p- phenyl), -2.95 (2 H, s, internal pyrrole)

**MPyTPP** UV-vis spectrum [ $\lambda$ , nm,  $\text{CH}_2\text{Cl}_2$ ] 418, 514, 548, 588, 644

$^1\text{H NMR}$  [400MHz  $\text{CDCl}_3$ ]  $\delta$  9.04 (2 H, d, 2,6-pyridyl), 8.86 (8 H, m, pyrrole  $\beta$ ), 8.22 (8 H, m, o-phenyl and 3,5 pyridyl), 7.77 (9 H m, m- and p- phenyl), -2.83 (2 H, s, internal pyrrole)

**cis-DiPyDiPP** UV-vis spectrum [ $\lambda$ , nm,  $\text{CH}_2\text{Cl}_2$ ] 416, 513, 547, 588, 643

$^1\text{H NMR}$  [400MHz  $\text{CDCl}_3$ ]  $\delta$  9.06 (4 H, d, 2,6-pyridyl), 8.86 (8 H, h, pyrrole  $\beta$ ), 8.20 (8 H, m, o-phenyl and 3,5 pyridyl), 7.77 (6 H m, m- and p- phenyl), -2.84 (2 H, s, internal pyrrole)

**trans-DiPyDiPP** UV-vis spectrum [ $\lambda$ , nm,  $\text{CH}_2\text{Cl}_2$ ] 416, 514, 548, 588, 643

$^1\text{H NMR}$  [400MHz  $\text{CDCl}_3$ ]  $\delta$  9.06 (4 H, d, 2,6-pyridyl), 8.90 (8 H, d, pyrrole  $\beta$ ), 8.18 (8 H, m, o-phenyl and 3,5 pyridyl), 7.79 (6 H m, m- and p- phenyl), -2.86 (2 H, s, internal pyrrole)

### 6.6.2 Synthesis of ZnTPP

The following is the procedure for metallation of all porphyrins in this study. Zinc was inserted into the porphyrin using a standard method.<sup>3,4</sup> An excess of zinc acetate (0.03 g) in 5 mL of methanol was added to a deep purple solution of the free base porphyrin for example, TPP (0.05 g) in 50 mL of chloroform. The chloroform had previously been dried over  $\text{MgSO}_4$ . The reaction mixture was allowed to stir overnight at room temperature under a  $\text{N}_2$  atmosphere.

UV-vis spectroscopy was used to measure the completion of the reaction. Metal insertion was confirmed by the collapse of the four Q bands of TPP free base porphyrin ( $\lambda = 516$ ,

550, 590 and 646 nm) and the formation of two peaks ( $\lambda = 543$  and 578 nm) of the zinc metalloporphyrin monomer

The solvents were removed by rotary evaporation at room temperature and the crude ZnTPP was purified using a silica column and chloroform to give a bright pink crystalline product Yield 47mg (86% yield)

**ZnTPP** UV-vis spectrum [ $\lambda$ , nm, CH<sub>2</sub>Cl<sub>2</sub>] 418, 543,578  
<sup>1</sup>H NMR [400MHz CDCl<sub>3</sub>]  $\delta$  8.86 (8 H, m, pyrrole  $\beta$ ), 8.22 (8 H, m, o-phenyl), 7.77 (12 H m, m- and p- phenyl)

Note Zinc pyridyl porphyrins aggregate in non-co-ordinating solvents and are a darker blue colour compared to the bright pink colour of ZnTPP<sup>5,6</sup> The <sup>1</sup>H NMR gives evidence for this aggregation Yield 50 mg (83% yield)

**ZnMPyTPP** UV-vis spectrum [ $\lambda$ , nm, CH<sub>2</sub>Cl<sub>2</sub>] 418, 562, 604  
<sup>1</sup>H NMR [400MHz CDCl<sub>3</sub>]  $\delta$  8.86 (m, pyrrole  $\beta$ ), 8.51 (m, pyrrole  $\beta$ ), 8.10 (m, o-phenyl), 7.67 (m, m- and p- phenyl), 7.41 (m, pyrrole), 6.23 (3,5 pyridyl), 2.60 (2,6-pyridyl)

### 6 6 3 Synthesis of 5-(4-pyridyl)-10,15,20 triphenyl porphyrin tungsten pentacarbonyl

All pentacarbonyl complexes were synthesised using a method described by Strohmeier <sup>7</sup>

0.15 g (0.43 mmol) of  $W(CO)_6$  was dissolved in 150 mLs of dry THF which was previously degassed for 15 minutes with nitrogen. The solution was photolysed with a 200 W medium pressure Hg lamp in a photolysis well. The solution was continually purged with nitrogen. After about 60 minutes the solution had turned a strong yellow colour. Completion of photolysis and the formation of  $W(CO)_5THF$  was determined by IR spectroscopy. Depletion of the hexacarbonyl peak at  $1891\text{ cm}^{-1}$  and the growth of the pentacarbonyl peaks indicated completion of the reaction.

The  $W(CO)_5THF$  solution was then stirred overnight with 0.2 g (0.33 mmol) of 5-(4-pyridyl)-10, 15, 20 – triphenyl porphyrin under a nitrogen atmosphere. THF was removed under reduced pressure on the rotary evaporator. The complex was redissolved in chloroform and purified on a silica column using a chloroform/pentane (90/10) solvent system. Most of the unreacted hexacarbonyl was eluted initially on the column with any further hexacarbonyl impurities removed by sublimation under reduced pressure. The complex was recrystallised from cold pentane to yield pure  $MPyTPPW(CO)_5$  which was an appreciably browner colour than the parent porphyrin. The yield was 246 mg (78%).

**$MPyTPPW(CO)_5$**  UV-vis spectrum [ $\lambda$ , nm,  $CH_2Cl_2$ ] 422, 516, 552, 590, 646  
IR ( $CH_2Cl_2$ )  $\nu_{CO}$  2072, 1929 and  $1895\text{ cm}^{-1}$   
 $^1H$  NMR [400 MHz  $CDCl_3$ ]  $\delta$  9.13 (2 H, d, 2,6-pyridyl), 8.86 (8 H, m, pyrrole  $\beta$ ), 8.22 (8 H, m, o-phenyl and 3,5 pyridyl), 7.77 (9 H m, m- and p- phenyl), -2.83 (2 H, s, internal pyrrole)  
FAB 938 ( $C_{48}H_{29}N_5O_5W$ ), 617 ( $-W(CO)_5$ )

#### 6.6.4 Synthesis of 5-(4-pyridyl)-10,15,20 triphenylporphyrin chromium pentacarbonyl

The chromium pentacarbonyl analogue was synthesised by the method described previously<sup>7</sup>

0.15 g (0.68 mmol) of the  $\text{Cr}(\text{CO})_6$  was photolysed in 150 mLs of dry THF that was previously degassed for 15 minutes with nitrogen. The solution was photolysed with a 200 W medium pressure Hg lamp in a photolysis well. The solution was continually purged with nitrogen and after about 60 minutes the solution had turned a strong orange colour. Completion of photolysis and the formation of  $\text{Cr}(\text{CO})_5\text{THF}$  was determined by IR spectroscopy. Depletion of the hexacarbonyl peak at  $1971\text{ cm}^{-1}$  and the growth of the pentacarbonyl peaks indicated completion of the reaction.

0.2 g (0.32 mmol) of 5-(4-pyridyl)-10,15,20-triphenylporphyrin was stirred with the  $\text{THFCr}(\text{CO})_5$  under an atmosphere of nitrogen overnight. THF was then removed under reduced pressure on the rotary evaporator. The complex was then redissolved in chloroform and purified on a silica column using a chloroform-pentane (90/10) solvent system. Unreacted hexacarbonyl was eluted initially on the column with any further hexacarbonyl impurities removed by sublimation under reduced pressure. The complex was recrystallised from cold pentane to yield pure  $\text{MPyTPPCr}(\text{CO})_5$  which had a strong orange tinge compared to the parent. The yield was 165 mg (64%).

**$\text{MPyTPPCr}(\text{CO})_5$**  UV-vis spectrum [ $\lambda$ , nm,  $\text{CH}_2\text{Cl}_2$ ] 420, 516, 552, 590, 646  
IR ( $\text{CH}_2\text{Cl}_2$ )  $\nu_{\text{CO}}$  2069, 1935 and  $1899\text{ cm}^{-1}$   
 $^1\text{H NMR}$  [400 MHz  $\text{CDCl}_3$ ]  $\delta$  9.17 (2 H, d, 2,6-pyridyl), 8.81 (8 H, m, pyrrole  $\beta$ ), 8.20 (8 H, m, o-phenyl and 3,5-pyridyl), 7.75 (9 H, m, m- and p-phenyl), -2.83 (2 H, s, internal pyrrole)  
FAB 806 ( $\text{C}_{48}\text{H}_{29}\text{N}_5\text{O}_5\text{Cr}$ ), 617 ( $-\text{Cr}(\text{CO})_5$ )

### 6.6.5 Synthesis of *cis*-5,10-(4-dipyridyl)-15,20 diphenylporphyrin ditungsten pentacarbonyl

The di-tungsten pentacarbonyl complex was synthesised as described previously <sup>2</sup>

0.30 g (0.85 mmol) of the  $W(CO)_6$  was photolysed in 200 mLs of dry THF which had been previously purged with nitrogen for 15 minutes. The solution was continually purged with nitrogen to avoid any oxidation effects. After about 60 minutes the solution had turned a strong yellow colour. Completion of photolysis and the formation of  $W(CO)_5THF$  was determined by IR spectroscopy. The solution was photolysed with a 200-W medium pressure Hg lamp in a photolysis well. A two fold excess of hexacarbonyl was needed because there were now two sites on the porphyrin for the pentacarbonyl moiety to bind. The depletion of the hexacarbonyl peak at  $1971\text{ cm}^{-1}$  and the growth of the pentacarbonyl peaks indicated that the reaction was finished.

0.2 g (0.32 mmol) of 5,10-di-(4-pyridyl)-15,20-diphenylporphyrin was stirred with the  $THFW(CO)_5$  under an atmosphere of nitrogen overnight. THF was then removed under reduced pressure on the rotary evaporator. The complex was then redissolved in chloroform and purified on a silica column using a chloroform/pentane (90/10) solvent system. Most of the unreacted hexacarbonyl was eluted initially on the column with any further hexacarbonyl impurities removed by sublimation under reduced pressure. The complex was recrystallised from cold pentane to yield pure *cis*-DiPyDiPP( $W(CO)_5$ )<sub>2</sub> which was an appreciably browner colour than the parent porphyrin and the mono-substituted porphyrin due to the presence of two metal units. The yield was 215 mg (53%).

*cis*-DiPyDiPP( $W(CO)_5$ )<sub>2</sub>    UV-vis spectrum [ $\lambda$ , nm,  $CH_2Cl_2$ ] 421, 517, 552, 590, 646  
IR ( $CH_2Cl_2$ )  $\nu_{CO}$  2073, 1929 and  $1897\text{ cm}^{-1}$   
<sup>1</sup>H NMR [400MHz  $CDCl_3$ ]  $\delta$  9.20 (4 H, d, 2,6-pyridyl),  
8.82 (8 h, m, pyrrole  $\beta$ ), 8.10 (8 H, m, o-phenyl and 3,5

pyridyl), 7 73 (6 H m, m- and p- phenyl), -2 86 (2 H, s, internal pyrrole)

FAB 1263 (C<sub>52</sub>H<sub>28</sub>N<sub>6</sub>O<sub>10</sub>W<sub>2</sub>), 617 ((-W(CO)<sub>5</sub>)<sub>2</sub>)

#### 6.6.6 Synthesis of *cis*-5,10-(4-dipyridyl)-15,20 diphenylporphyrin dichromium pentacarbonyl

The di-chromium pentacarbonyl complex was synthesised as outlined before <sup>2</sup>

0 30 g (1 36 mmol) of the Cr(CO)<sub>6</sub> was photolysed in 200 mLs of dry THF having previously been degassed for 15 minutes with nitrogen The solution was photolysed with a 200-W medium pressure Hg lamp in a photolysis well The solution was continually purged with nitrogen After about 60 minutes the solution had turned a strong orange colour Completion of photolysis and the formation of Cr(CO)<sub>5</sub>THF was determined by IR spectroscopy The depletion of the hexacarbonyl peak at 1971 cm<sup>-1</sup> and the grow in of the pentacarbonyl peaks indicated completion of the reaction A large two fold excess of hexacarbonyl was needed because there were two sites on the porphyrin for the pentacarbonyl to bind

0 2 g (0 32 mmol) of 5,10-di-(4-pyridyl)-15,20-diphenylporphyrin was stirred with the THFCr(CO)<sub>5</sub> under an atmosphere of nitrogen overnight THF was then removed under reduced pressure on the rotary evaporator The complex was then redissolved in chloroform and purified on a silica column using a chloroform pentane (90 10) solvent system Most of the unreacted hexacarbonyl was eluted initially during column chromatography with any further hexacarbonyl impurities removed by sublimation under reduced pressure The complex was recrystallised from cold pentane to yield pure *cis*-DiPyDiPP(Cr(CO)<sub>5</sub>)<sub>2</sub> which was had a strong tinge compared to the parent porphyrin and the mono-substituted complex Yield 141 mg (44%)

*cis*-DiPyDiPP(Cr(CO)<sub>5</sub>)<sub>2</sub> UV-vis spectrum [ $\lambda$ , nm, CH<sub>2</sub>Cl<sub>2</sub>] 420, 516, 552, 590, 646

IR (CH<sub>2</sub>Cl<sub>2</sub>)  $\nu_{\text{CO}}$  2069, 1936 and 1899 cm<sup>-1</sup>

<sup>1</sup>H NMR [400MHz CDCl<sub>3</sub>]  $\delta$  9.22 (4 H, d, 2,6-pyridyl),  
8.83 (8 h, m, pyrrole  $\beta$ ), 8.12 (8 H, m, o-phenyl and 3,5  
pyridyl), 7.74 (6 H m, m- and p- phenyl), -2.84 (2 H, s,  
internal pyrrole)

FAB 1001 (C<sub>52</sub>H<sub>28</sub>N<sub>6</sub>O<sub>10</sub>Cr<sub>2</sub>), 617 ((-Cr(CO)<sub>5</sub>)<sub>2</sub>)

#### 6.6.8 Synthesis of ZnMPyTPPW(CO)<sub>5</sub>

The zinc porphyrin pentacarbonyl complexes were made using two different methods. The first method involved photolysis of the zinc porphyrin in a solution of the desired THF pentacarbonyl complex. The Zn-N bond is so intrinsically weak that stable polymers are difficult to form,<sup>8,9</sup> therefore formation of a M-N bond can usually take place in the presence of the polymer. The second method involved the reaction of MPyTPPW(CO)<sub>5</sub> with zinc acetate as described in section 6.5.2. This method involved stirring the pentacarbonyl in solution overnight. The yields for both reactions were lower than those obtained for the uncomplexed porphyrin. The first method was chosen above the other as its yield was slightly higher.

0.10 g (0.28 mmol) of W(CO)<sub>6</sub> was dissolved in 100 mLs of dry THF and degassed for 15 minutes with nitrogen. The solution was photolysed with a 200 W medium pressure Hg lamp in a photolysis well. The solution was continually purged with nitrogen to avoid any oxidation effects. After about 60 minutes the solution had turned a strong yellow colour. Completion of photolysis and the formation of W(CO)<sub>5</sub>THF was determined by IR spectroscopy. The depletion of the hexacarbonyl peak at 1891 cm<sup>-1</sup> and the growth of the pentacarbonyl peaks indicated that the reaction was complete.

The W(CO)<sub>5</sub>THF solution and 0.05 g (0.073 mmol) of ZnMPyTPPW porphyrin was stirred overnight under an atmosphere of nitrogen. THF was then removed under reduced pressure on the rotary evaporator. The complex was then redissolved in chloroform and

purified on a silica column using a chloroform pentane (90/10) as the solvent system. The unreacted hexacarbonyl was eluted initially on the column or removed by sublimation under reduced pressure. The solvent was removed under reduced pressure to yield pure  $\text{ZnMPyTPPW}(\text{CO})_5$  which was pink in colour compared to the brown/purple colour of the porphyrin pentacarbonyl complex and the blue/purple colour of  $\text{ZnMPyTPP}$  polymer. The yield was 43 mg (57%).

**$\text{ZnMPyTPPW}(\text{CO})_5$**       UV-vis spectrum [ $\lambda$ , nm,  $\text{CH}_2\text{Cl}_2$ ] 422, 548, 588  
 IR ( $\text{CH}_2\text{Cl}_2$ )  $\nu_{\text{CO}}$  2070, 1931 and 1916  $\text{cm}^{-1}$   
 $^1\text{H}$  NMR [400MHz  $\text{CDCl}_3$ ]  $\delta$  9.22 (2 H, d, 2,6-pyridyl),  
 8.86 (8 h, m, pyrrole  $\beta$ ), 8.18 (8 H, m, o-phenyl and 3,5  
 pyridyl), 7.76 (9 H m, m- and p- phenyl)  
 FAB 1002 ( $\text{C}_{48}\text{H}_{27}\text{N}_5\text{O}_5\text{WZn}$ ), 681 ( $-\text{W}(\text{CO})_5$ )

### 6.6.9 Synthesis of $\text{ZnMPyTPPCr}(\text{CO})_5$

0.10 g (0.45 mmol) of  $\text{Cr}(\text{CO})_6$  was dissolved in 100 mLs of dry THF and degassed for 15 minutes with nitrogen. The solution was photolysed with a 200-W medium pressure Hg lamp in a photolysis well. The solution was continually purged with nitrogen to avoid any oxidation effects. After about 60 minutes the solution had turned a strong yellow colour. Completion of photolysis and the formation of  $\text{Cr}(\text{CO})_5\text{THF}$  was determined by IR spectroscopy. Depletion of the hexacarbonyl peak at 1891  $\text{cm}^{-1}$  and the growth of the pentacarbonyl peaks indicated that the reaction was complete.

The  $\text{Cr}(\text{CO})_5\text{THF}$  solution and 0.05 g (0.073 mmol) of  $\text{ZnMPyTPP}$  porphyrin was stirred overnight with under an atmosphere of nitrogen. THF was then removed under reduced pressure on the rotary evaporator. The complex was then redissolved in chloroform and purified on a silica column using a chloroform pentane (90/10) as the solvent system. Most of the unreacted hexacarbonyl was eluted initially on the column with any further hexacarbonyl impurities removed by sublimation under reduced pressure. The solvent

was removed under reduced pressure to yield pure ZnMPyTPPCr(CO)<sub>5</sub> which was pink in colour compared to the orange/purple colour of the porphyrin pentacarbonyl complex and the blue/purple colour of ZnMPyTPP polymer. The yield was 38 mg (59%)

**ZnMPyTPPCr(CO)<sub>5</sub>**      UV-vis spectrum [ $\lambda$ , nm, CH<sub>2</sub>Cl<sub>2</sub>] 420, 548, 588  
IR (CH<sub>2</sub>Cl<sub>2</sub>)  $\nu_{CO}$  2067, 1937 and 1917 cm<sup>-1</sup>  
<sup>1</sup>H NMR [400MHz CDCl<sub>3</sub>]  $\delta$  9.20 (2 H, d, 2,6-pyridyl),  
8.85 (8 h, m, pyrrole  $\beta$ ), 8.19 (8 H, m, o-phenyl and 3,5  
pyridyl), 7.75 (9 H m, m- and p- phenyl)  
FAB 871 (C<sub>48</sub>H<sub>27</sub>N<sub>5</sub>O<sub>5</sub>W), 681 (-W(CO)<sub>5</sub>)

#### 6.6.10 Synthesis of *trans*-D<sub>1</sub>PyD<sub>1</sub>PP(W(CO)<sub>5</sub>)<sub>2</sub>

The *trans* di-tungsten pentacarbonyl was synthesised as described previously <sup>2</sup>

0.20 g (0.56 mmol) of the W(CO)<sub>6</sub> was photolysed in 150 mLs of dry THF and having been degassed for 15 minutes with nitrogen. The solution was photolysed with a 200-W medium pressure Hg lamp in a photolysis well. The solution was continually purged with nitrogen to avoid any oxidation effects. After about 60 minutes the solution had turned a strong orange colour. Completion of photolysis and the formation of W(CO)<sub>5</sub>THF was determined by IR spectroscopy. Depletion of the hexacarbonyl peak at 1971.17 cm<sup>-1</sup> and the growth of the pentacarbonyl peaks indicated that the reaction was completed. A two fold excess of hexacarbonyl was needed because there were now two sites on the porphyrin for the pentacarbonyl to bind.

0.1 g (0.16 mmol) of 5,15-di-(4-pyridyl)-10,20-diphenylporphyrin was stirred with the THFW(CO)<sub>5</sub> overnight under an atmosphere of nitrogen. The product could not be purified as it was insoluble in all solvents except THF.

## 6.6.11 Synthesis of 3-pyridyl porphyrin

Synthesis of 5-Mono 3-pyridyl 10, 15, 20-triphenyl porphyrin (3-Py-TriPP) was achieved using a combination of two methods described previously<sup>10,11</sup>

1.5 mL (21 mmol) of freshly distilled pyrrole, 1.8 mL (18 mmol) of benzaldehyde and 1.2 mL (12 mmol) of 3-pyridine carboxaldehyde were added to 250 mL of CH<sub>2</sub>Cl<sub>2</sub> with 0.2 mL of trifluoroacetic acid and stirred overnight under an atmosphere of nitrogen. The acidic solution gradually turned brown before eventually turning black. An excess of 3-dichloro-5,6-dicyano-1,4-benzoquinone (DDQ), 0.68 g (30 mmol), was added to the reaction mixture and the sample allowed to stir overnight. Finally an excess of triethylamine, 0.5 mL (35 mmol), was added and the mixture stirred for 1 hr. The solvent was then removed under reduced pressure. Yield 660 mg (9%)

TLC using chloroform/ethanol (98/2) indicated the presence of a mixture of six products which formed during the reaction. The six compounds formed were similar to those formed in section 6.5.1 but the nitrogen of the pyridine ring was now in the 3-position. The crude porphyrin was purified on a silica gel column. The initial elution was 98% chloroform and 2% ethanol which elutes the TPP. Subsequent columns of increasing polarity (chloroform/ethanol (97/3) and chloroform/ethanol (96/4)) separated out the remaining porphyrins. Only 3-Py-TriPP was of interest.

### Porphyrin Spectroscopy

3-Py-TriPP                      UV-vis spectrum [ $\lambda$ , nm, CH<sub>2</sub>Cl<sub>2</sub>] 418, 516, 550, 590, 648  
                                          <sup>1</sup>H NMR [400MHz CDCl<sub>3</sub>]  $\delta$  9.03 (1 H, d, 4 pyridyl), 8.96 (1 H, s  
                                          2 pyridyl), 8.86 (8 H, m, pyrrole  $\beta$ ), 8.22 (8 H, m, o-phenyl), 7.77  
                                          (12 H m, m- and p- phenyl), -2.95 (2 H, s, internal pyrrole)

### 6.6.12 Attempted synthesis of ferrocene-pyridine porphyrin

The synthesis of 5-Mono ferrocene 15 – mono 4-pyridyl 10, 20-diphenyl porphyrin (*mono-fer-MPyDiPP*) was attempted using both of the methods described previously<sup>10 11</sup>

1.5 mL (21 mmol) of freshly distilled pyrrole, 1.2 mL (12 mmol) of benzaldehyde, 1.3 g (6 mmol) of ferrocene carboxaldehyde and 0.6 mL (6 mmol) of 4-pyridine carboxaldehyde were added to 250 mL of CH<sub>2</sub>Cl<sub>2</sub> followed by 0.2 mL of trifluoroacetic acid. The reaction mixture was allowed to stir overnight under an atmosphere of nitrogen. The acidic solution gradually turned brown before eventually turning black in colour. An excess of 3-dichloro-5,6-dicyano-1,4-benzo-quinone (DDQ), 0.68 g (30 mmol), was added to the reaction mixture and the sample stirred overnight. Finally an excess of triethylamine, 0.5 mL (35 mmol), was added and the mixture stirred for 1 hr. The solvent was then removed under reduced pressure. Yield 113 mg.

TLC using chloroform/ethanol (95/5) showed that there were up to 15 compounds present in the reaction mixture. No attempt was made to purify the mixture any further.

### 6.6.13 Attempted synthesis of tetraphenyl Cr(CO)<sub>3</sub> porphyrin

The synthesis of a series of tetraphenyl and zinc tetraphenyl chromium tricarbonyl complexes was also attempted using a method that had previously been reported in the literature<sup>12 13</sup>

The TPP porphyrin used was synthesised as described in section 6.5.1.

TPP (0.1 g, 16 mmol) and an excess of Cr(CO)<sub>6</sub> (0.1 g, 45 mmol) were refluxed in dry di-*n*-butyl ether for 10 hrs under a nitrogen atmosphere. A sample was removed from the reaction at regular intervals to monitor the formation of the tricarbonyl complex using IR spectroscopy. Once the reaction was complete the solvent was removed *in vacuo* to leave

a green solid TLC showed the presence of three compounds Only the mono substituted porphyrin tricarbonyl complex was isolated The stability of the complex was poor and no  $^1\text{H}$  NMR were obtained Due to this no further photochemical or photophysical studies were carried out

#### **Porphyrin Spectroscopy.**

**TPPCr(CO)<sub>3</sub>**            UV-vis spectrum [ $\lambda$ , nm, CH<sub>2</sub>Cl<sub>2</sub>] 425, 517, 566, 603, 637  
                                 IR (CH<sub>2</sub>Cl<sub>2</sub>)  $\nu_{\text{CO}}$  1972 and 1896 cm<sup>-1</sup>

#### **6.6.14 Attempted synthesis of zinc tetraphenyl Cr(CO)<sub>3</sub> porphyrin**

ZnTPP porphyrin used was synthesised as described in section 6.5.2

ZnTPP (0.1 g 14  $\mu\text{mol}$ ) and an excess of Cr(CO)<sub>6</sub> (0.1 g 45  $\mu\text{mol}$ ) were brought to reflux in dry di-*n*-butyl ether for 10 hrs under a nitrogen atmosphere Samples were removed from the reaction flask at regular intervals to monitor the formation of the tricarbonyl complex using IR spectroscopy Once the peaks representing the tricarbonyl complex formed the solvent was removed *in vacuo* to leave a green solid TLC showed the presence of three compounds Only the mono substituted porphyrin tricarbonyl complex was isolated Again the stability of the complex was poor and no  $^1\text{H}$  NMR was obtained Due to this no further photochemical or photophysical studies were carried out

**ZnTPPCr(CO)<sub>3</sub>**            UV-vis spectrum [ $\lambda$ , nm, CH<sub>2</sub>Cl<sub>2</sub>] 419, 550, 587  
                                 IR (CH<sub>2</sub>Cl<sub>2</sub>)  $\nu_{\text{CO}}$  1972.26 and 1903.22 cm<sup>-1</sup>

## 6.7 Bibliography

---

- 1 J N Demas, G A Crosby, *J Phys Chem* 1971, 75, 991
- 2 A D Alder, F R Longo, J D Finarelli, J Goldmacher, J Assour, L Korsalioff, *J Org Chem* , 1967, 32, 476
- 3 A D Alder, F R Longo, F Kampas, J Kim, *J Inorg Nucl Chem* , 1970, 2, 2443
- 4 Fleicher, E B , Shachter, A M *Inorg Chem* , 1991, 30, 3763
- 5 A K Burrell, D L Officer, D C W Reid, K Y Wild, *Angew Chem Int Ed* , 1998, 37, 114
- 6 C A Hunter, R K Hyde, *Angew Chem , Int Ed Engl* , 1996, 35, 1936
- 7 W Strohmeier, *Angew Chem , Int Ed Engl* , 1964, 3, 730
- 8 R K Kumar, I Goldberg, *Angew Chem Ed Int* , 1998, 37, 3027
- 9 R V Slone, J T Hupp, *Inorg Chem* , 1997, 36, 5422
- 10 C H Lee, J S Lindsey, *Tetrahedron*, 1994, 50, 11427
- 11 M S Vollmer, F Wurthner, F Effenberg, P Emele, D U Meyer, T StumpFigure, H Port, H C Wolf, *Chem Eur J* , 1998, 4, 260
- 12 N J Gogan, Z U Siddiqui, *Chem Commun* , 1970, 284
- 13 N J Gogan, Z U Siddiqui, *Can J Chem* 1972, 50, 720

# Appendix A

## Extinction Coefficients

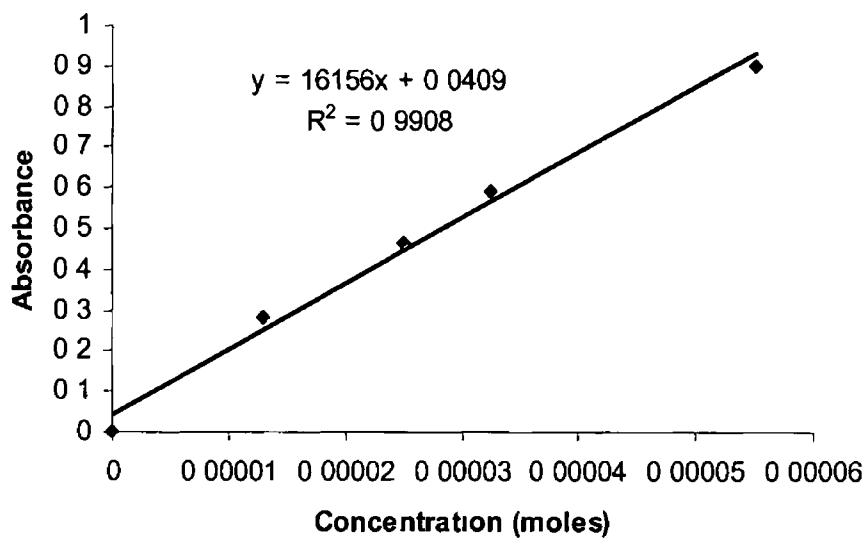


**Figure 1 1 Graph used to determine the extinction coefficient for MPyTPP at 355 nm in dichloromethane**

**Extinction coefficient =  $16156 \text{ dm}^3 \text{ mol}^{-1} \text{ cm}^{-1}$**

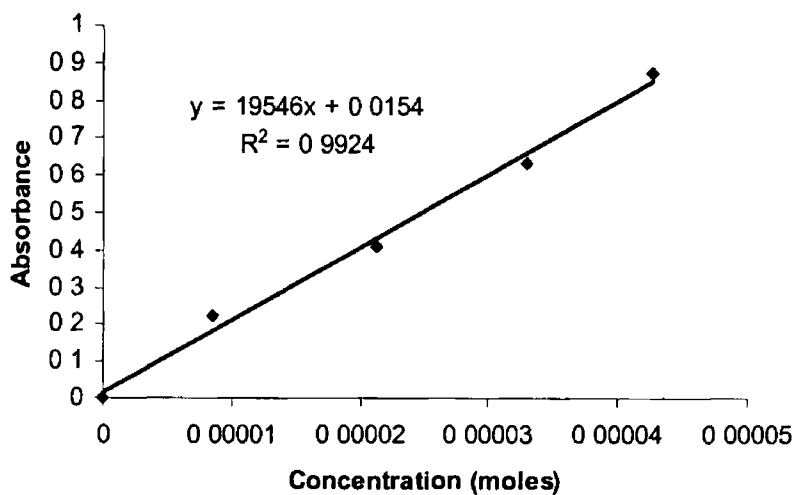


**Figure 1 2 Graph used to determine the extinction coefficient for MPyTPPW(CO)<sub>5</sub> at 355 nm in dichloromethane**

**Extinction coefficient =  $19546 \text{ dm}^3 \text{ mol}^{-1} \text{ cm}^{-1}$**

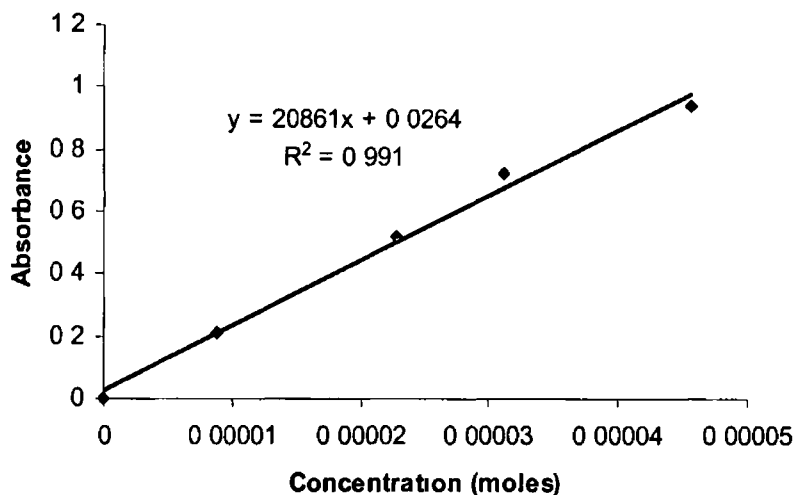


**Figure 1 3 1 Graph used to determine the extinction coefficient for MPyTPPCr(CO)<sub>5</sub> at 355 nm in dichloromethane**  
**Extinction coefficient = 20861 dm<sup>3</sup> mol<sup>-1</sup> cm<sup>-1</sup>**

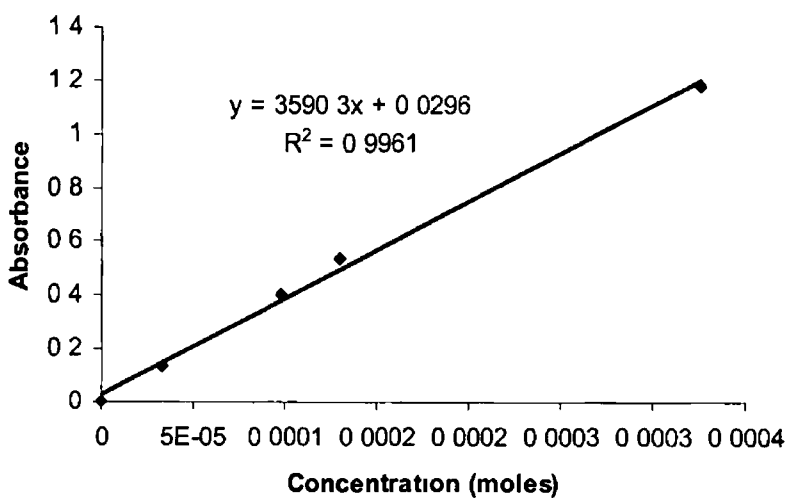


**Figure 1 4 Graph used to determine the extinction coefficient for MPyTPP at 532 nm in dichloromethane**  
**Extinction coefficient = 3590 dm<sup>3</sup> mol<sup>-1</sup> cm<sup>-1</sup>**

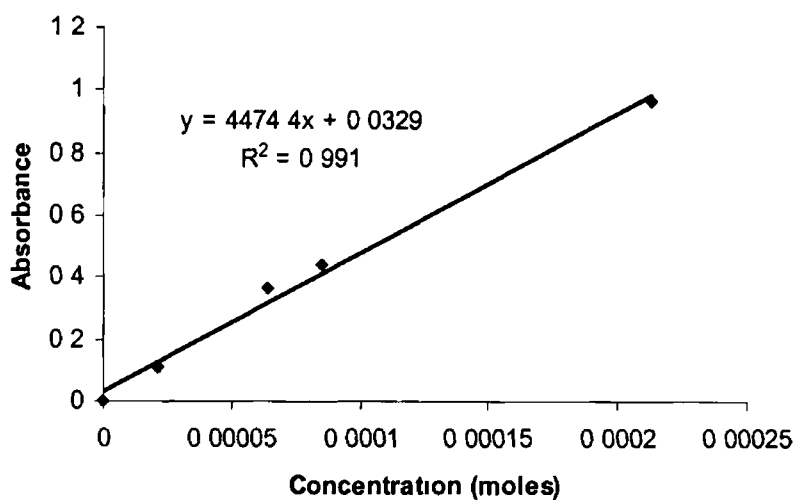


**Figure 1.5** Graph used to determine the extinction coefficient for  $\text{MPyTPPW}(\text{CO})_5$  at 532 nm in dichloromethane

**Extinction coefficient =  $4474 \text{ dm}^3 \text{ mol}^{-1} \text{ cm}^{-1}$**

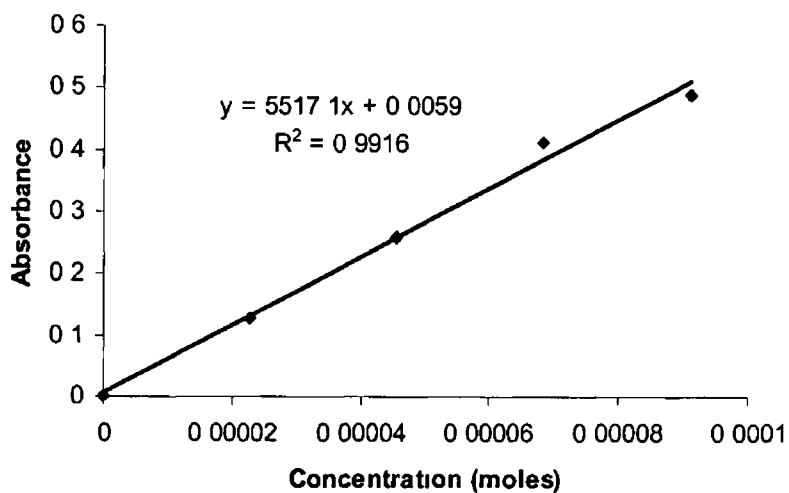


**Figure 1.6** Graph used to determine the extinction coefficient for  $\text{MPyTPPCr}(\text{CO})_5$  at 532 nm in dichloromethane

**Extinction coefficient =  $5517 \text{ dm}^3 \text{ mol}^{-1} \text{ cm}^{-1}$**

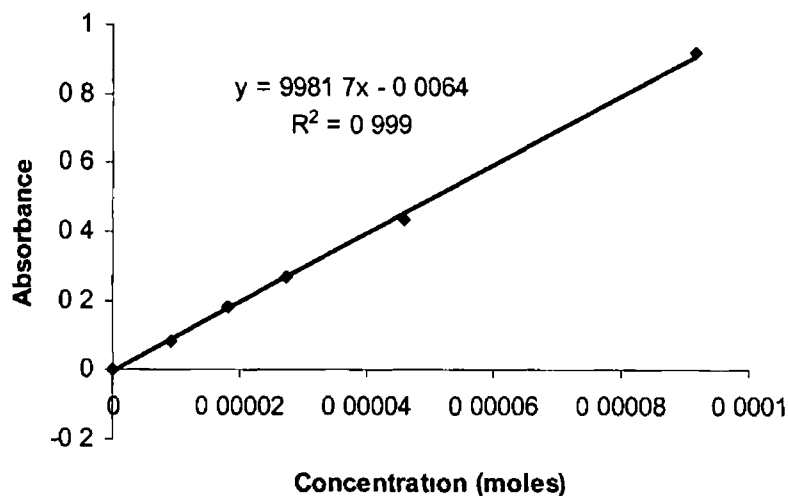


**Figure 1 7 Graph used to determine the extinction coefficient for ZnMPyTPPW(CO)<sub>5</sub> at 355 nm in dichloromethane**

**Extinction coefficient =  $9982 \text{ dm}^3 \text{ mol}^{-1} \text{ cm}^{-1}$**

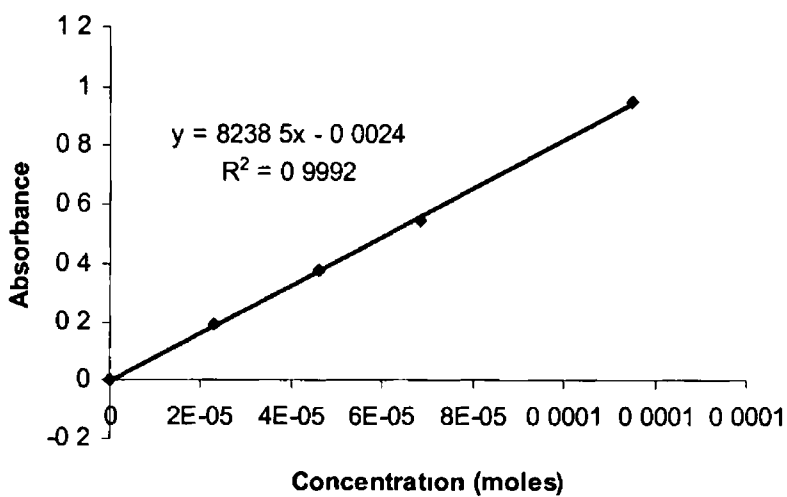


**Figure 1 8 Graph used to determine the extinction coefficient for ZnMPyTPPCr(CO)<sub>5</sub> at 355 nm in dichloromethane**

**Extinction coefficient =  $8239 \text{ dm}^3 \text{ mol}^{-1} \text{ cm}^{-1}$**

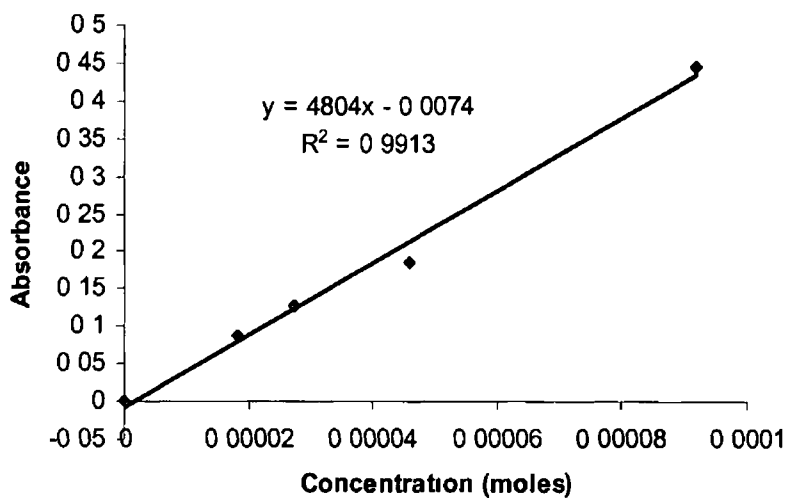


**Figure 1 9 Graph used to determine the extinction coefficient for ZnMPyTPPW(CO)<sub>5</sub> at 532 nm in dichloromethane**

**Extinction coefficient =  $4804 \text{ dm}^3 \text{ mol}^{-1} \text{ cm}^{-1}$**

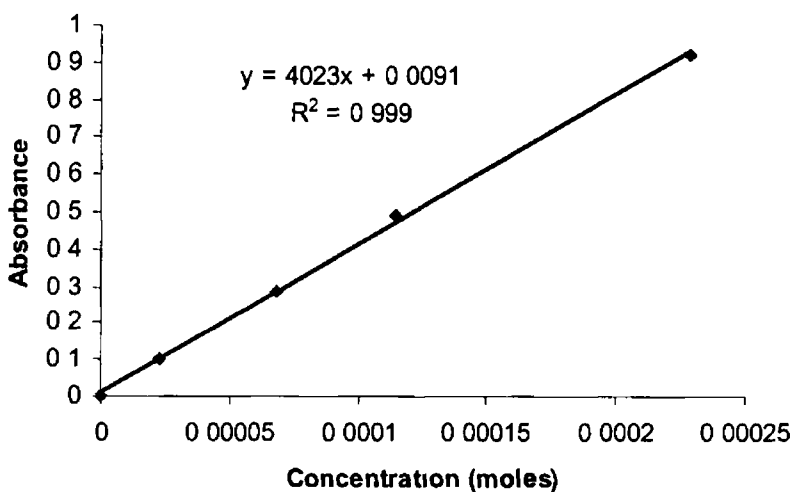


**Figure 1 10 Graph used to determine the extinction coefficient for ZnMPyTPPCr(CO)<sub>5</sub> at 532 nm in dichloromethane**

**Extinction coefficient =  $4023 \text{ dm}^3 \text{ mol}^{-1} \text{ cm}^{-1}$**

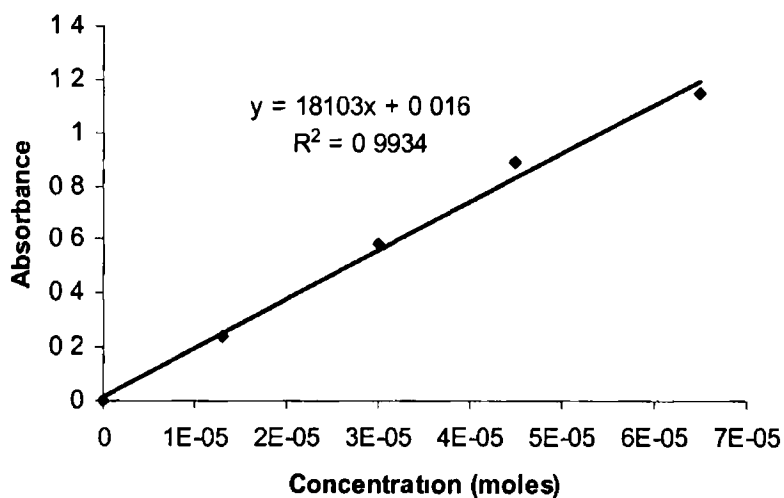


**Figure 1.11 Graph used to determine the extinction coefficient of cis-DiPyDiPP at 355 nm in dichloromethane**

**Extinction coefficient =  $18103 \text{ dm}^3 \text{ mol}^{-1} \text{ cm}^{-1}$**

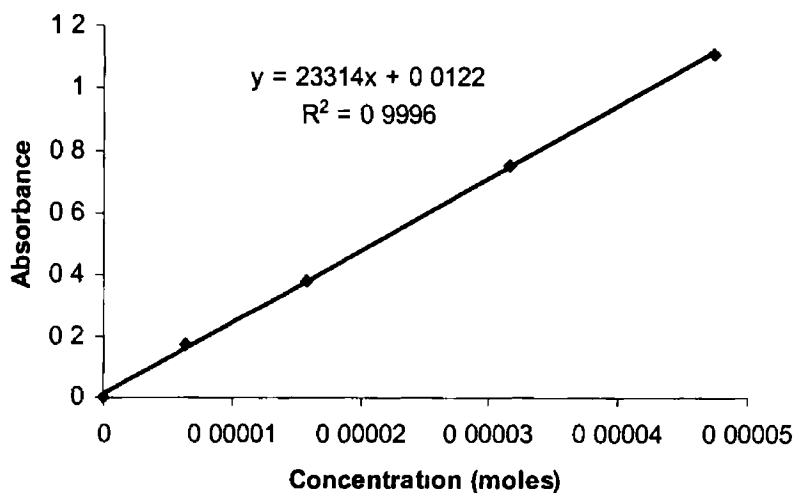


**Figure 1.12 Graph used to determine the extinction coefficient of cis-DiPyDiPPW(CO)<sub>5</sub><sub>2</sub> at 355 nm in dichloromethane**

**Extinction coefficient =  $23314 \text{ dm}^3 \text{ mol}^{-1} \text{ cm}^{-1}$**

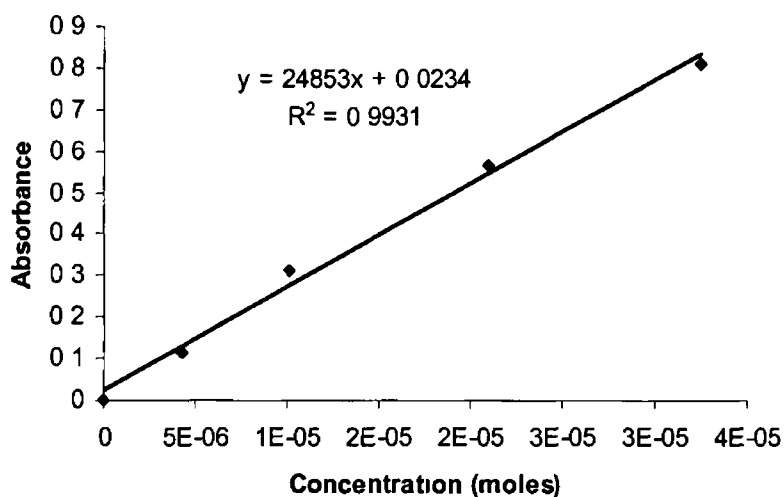


**Figure 1 13 Graph used to determine the extinction coefficient of cis-DiPyDiPP(Cr(CO)<sub>5</sub>)<sub>2</sub> at 355 nm in dichloromethane**  
**Extinction coefficient = 24853 dm<sup>3</sup> mol<sup>-1</sup> cm<sup>-1</sup>**

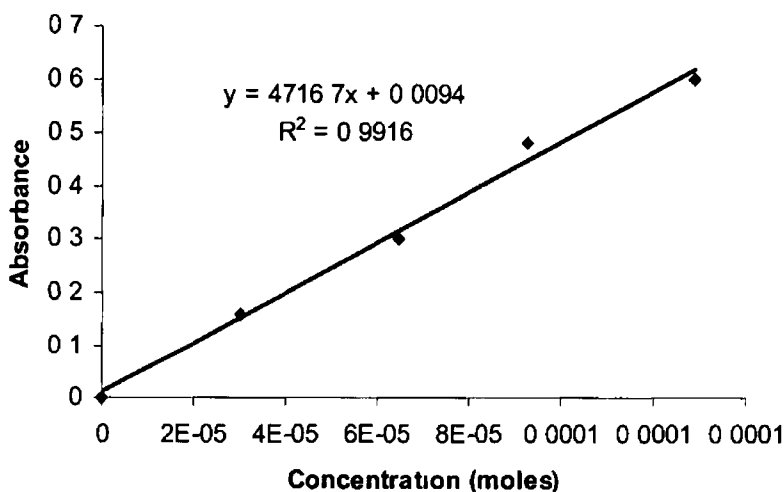


**Figure 1 14 Graph used to determine the extinction coefficient of cis-DiPyDiPP at 532 nm in dichloromethane**  
**Extinction coefficient = 4717 dm<sup>3</sup> mol<sup>-1</sup> cm<sup>-1</sup>**

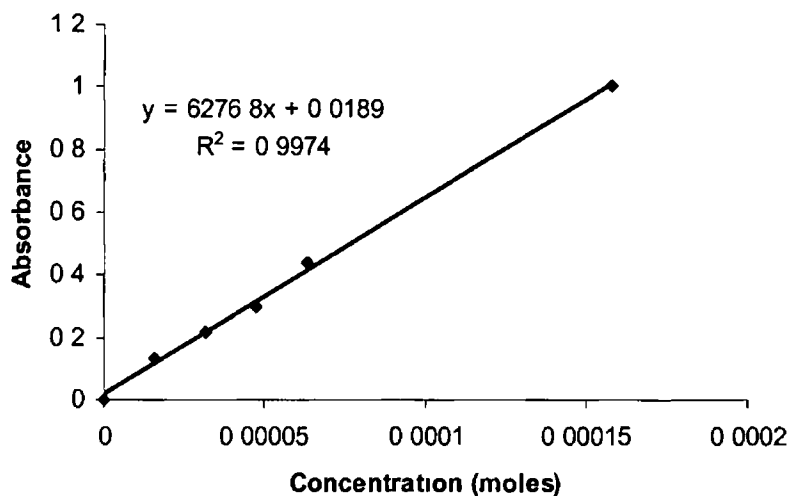


**Figure 1 15 Graph used to determine the extinction coefficient of cis-DiPyDiPP(W(CO)<sub>5</sub>)<sub>2</sub> at 532 nm in dichloromethane**  
**Extinction coefficient = 6277 dm<sup>3</sup> mol<sup>-1</sup> cm<sup>-1</sup>**

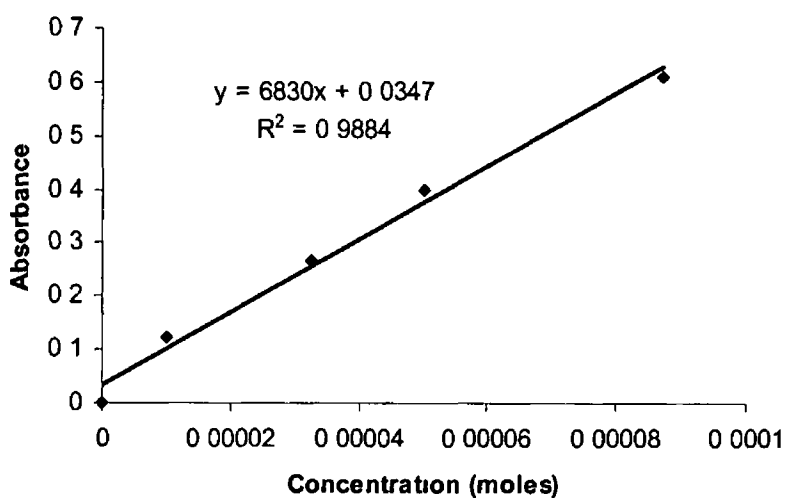


**Figure 1 16 Graph used to determine the extinction coefficient of cis-DiPyDiP(Cr(CO)<sub>5</sub>)<sub>2</sub> at 532 nm in dichloromethane**  
**Extinction coefficient = 6830 dm<sup>3</sup> mol<sup>-1</sup> cm<sup>-1</sup>**